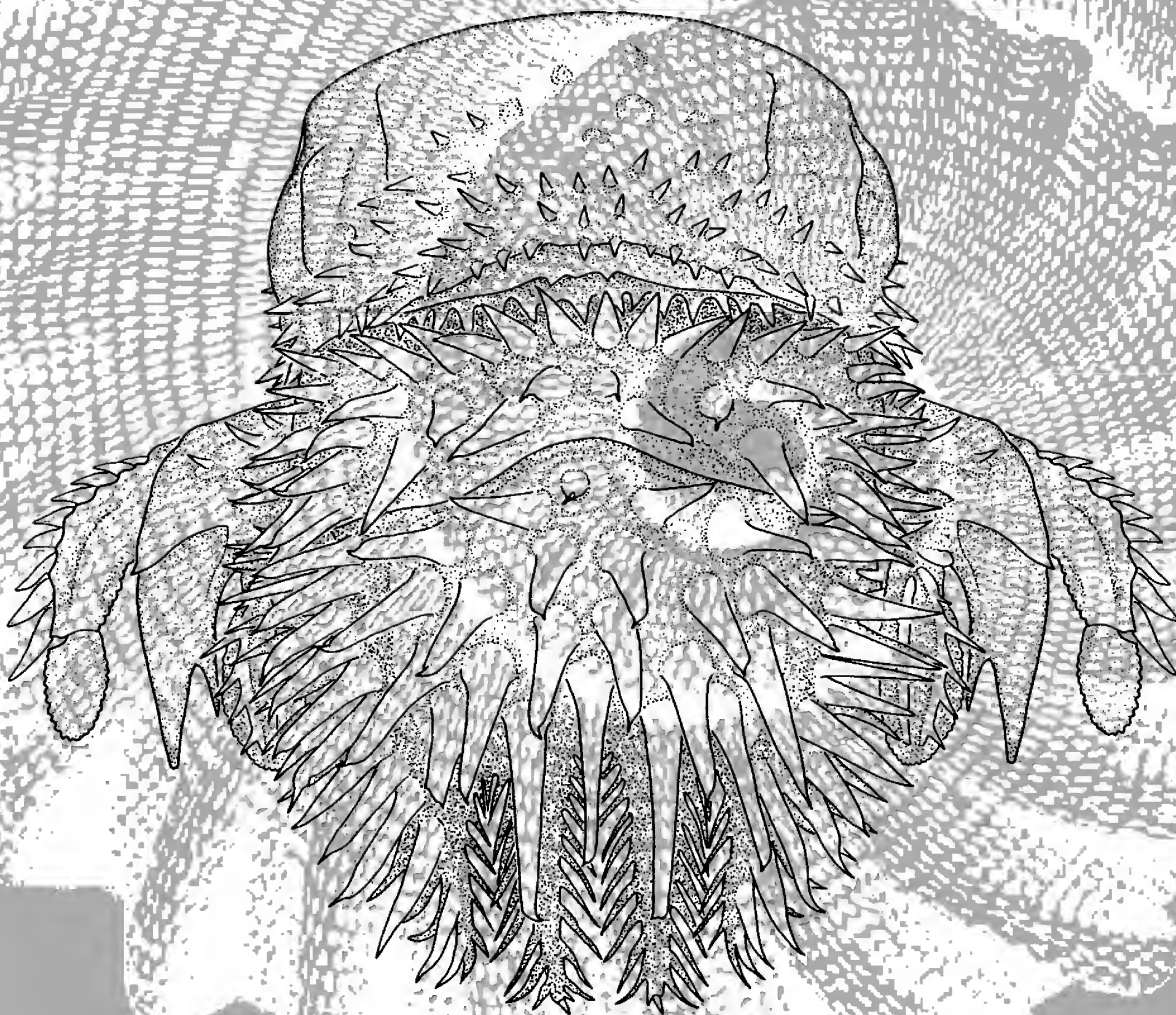


RECORDS OF THE AUSTRALIAN MUSEUM



RECORDS OF THE AUSTRALIAN MUSEUM

Director: M. Archer

Editor: S.F. McEvey

Editorial Committee:

S.T. Ahyong (INVERTEBRATE ZOOLOGY)
V.J. Attenbrow (ANTHROPOLOGY)
D.J. Bickel (INVERTEBRATE ZOOLOGY)
G.D. Edgecombe (PALAEOONTOLOGY)
A.E. Greer (VERTEBRATE ZOOLOGY)

Chair: J.M. Leis (VERTEBRATE ZOOLOGY)
S.F. McEvey (INVERTEBRATE ZOOLOGY)
F.L. Sutherland (GEOLOGY)
G.D.F. Wilson (INVERTEBRATE ZOOLOGY)

The Australian Museum's mission is to increase understanding of, and influence public debate on, the natural environment, human societies and human interaction with the environment. The Museum has maintained the highest standards of scholarship in these fields for more than 100 years, and is one of Australia's foremost publishers of original research in anthropology, geology and zoology.

The *Records of the Australian Museum* (ISSN 0067-1975) publishes the results of research on Australian Museum collections and of studies that relate in other ways to the Museum's mission. There is an emphasis on Australasian, southwest Pacific and Indian Ocean research. The *Records* is released annually as three issues of one volume, volume 53 was published in 2001. Monographs are published about once a year as *Records of the Australian Museum, Supplements*. Supplement 27 (ISBN 0-7347-2305-9) was published in November 2001. Catalogues, lists and databases have been published since 1988 as numbered *Technical Reports of the Australian Museum* (ISSN 1031-8062). *Technical Report* number 16 was published in May 2002. *Australian Museum Memoirs* (ISSN 0067-1967) ceased in 1983.

These three publications—*Records*, *Supplements* and *Technical Reports*—are distributed to libraries throughout the world and are now uploaded at our website six months after they are published. Librarians are invited to propose exchange agreements with the *Australian Museum Research Library*. Back issues are available for purchase direct from the *Australian Museum Shop*.

Authors are invited to submit manuscripts presenting results of their original research. Manuscripts meeting subject and stylistic requirements outlined in the *Instructions to Authors* are assessed by external referees.

www.amonline.net.au/publications/

Back issues may be purchased at the Australian Museum Shop or online at

www.amonline.net.au/shop/

© Copyright Australian Museum, 2002

No part of this publication may be reproduced without permission of the Editor.

Printed 10 July 2002

Price: AU\$50.00

Printed by RodenPrint Pty Ltd, Sydney

ISSN 0067-1975

Cover illustration (by Shane Ahyong): The telson (barely 6 mm wide) and uropods of the posterior end of the stomatopod crustacean *Echinosquilla guerinii* (White, 1861)—an inhabitant of reefs and level muddy sand from the western Indian Ocean to the central Pacific. This species is one of many dealt with in a major taxonomic revision of the Australian stomatopod fauna by Australian Museum carcinologist: Dr Shane Ahyong (*Rec. Aust. Mus., Suppl.* 26 [2001], 326 pp).

Australian Museum Scientific Publications are released as Adobe Acrobat PDF files, at our website, free of charge and six months after publication. For example, the above monograph on Australian Stomatopoda can now be viewed at www.amonline.net.au/pdf/publications/1333_complete.pdf or purchased as a bound volume (AU\$97.00) from the Australian Museum Shop.

The Amaryllididae of Australia (Crustacea: Amphipoda: Lysianassoidea)

J.K. LOWRY AND H.E. STODDART

Division of Invertebrate Zoology,
Australian Museum, 6 College Street, Sydney NSW 2010, Australia
jimlowry@crustacea.net
helenst@austmus.gov.au

ABSTRACT. Lowry & Stoddart (in press) established the lysianassoid amphipod family Amaryllididae. In the following paper the systematics of the diverse Australian amaryllidid fauna is presented. All amaryllidid genera are revised and rediagnosed and a key to genera is provided. Five genera and 23 species are recorded from Australian waters. *Bathyamaryllis* is recorded from Australia for the first time and new evidence indicates that *Amaryllis* is confined to Australia and possibly the New Zealand area. Two subfamilies (Amaryllidinae and Vijayiinae), three genera (*Bamarooka*, *Devo* and *Wonga*) and 20 species are new. The new species are *Amaryllis carrascoi*, *A. croca*, *A. dianae*, *A. kamata*, *A. keablei*, *A. migo*, *A. moona*, *A. olinda*, *A. philatelica*, *A. quokka*, *A. spencerensis*, *Bamarooka anomala*, *B. dinjerra*, *B. endota*, *B. kimbla*, *B. tropicalis*, *Bathyamaryllis kapala*, *Devo dubuc*, *D. grahami* and *Wonga wonga*. Distribution, depth and habitat notes are given for all species. Amaryllidids form two natural groups: a presumed free-living deep-water group with a subquadrate mouthpart bundle (Vijayiinae) and a presumed commensal shallow-water group with a subconical mouthpart bundle (Amaryllidinae). Except for *Vijaya tenuipes* the vijayiines are exclusively found in the deep seas of the North and South Atlantic and South Pacific Oceans. The amaryllidines are found in shallow temperate and tropical seas of the southern hemisphere. The largest diversity of genera and species is currently known from Australian waters, but the African and South American faunas have not been adequately described.

LOWRY, J.K., & H.E. STODDART, 2002. The Amaryllididae of Australia (Crustacea: Amphipoda: Lysianassoidea). *Records of the Australian Museum* 54(2): 129–214.

The amaryllidids have a long taxonomic history. Haswell (1879: 253) originally described the genus *Amaryllis* (in the “sub-family Stegocephalides”) for two species, *A. macrophthalma* and *A. brevicornis*, from southeastern Australia. Neither species was well described. Stebbing (1888) synonymised *A. brevicornis* with *A. macrophthalma*, transferred *Amaryllis* to the Lysianassidae and described two new species: *A. bathycephala* from southeastern Australia and *A. haswelli* from the North Atlantic.

Bonnier (1896) described *A. pulchellus* from the Bay of Biscay in the North Atlantic Ocean. Walker (1904) described

Vijaya tenuipes, a new genus and species of amaryllidid amphipod from Sri Lanka. He based the genus on the fact that the male had a callynophore on antenna 1. Stebbing (1910a) synonymised *Vijaya* with *Amaryllis* because males of that genus also have callynophores. However, Lowry & Stoddart (in press) have redescribed *Vijaya tenuipes* and shown that *Vijaya* is a valid genus more closely related to *Pseudamaryllis* and *Bathyamaryllis* than to *Amaryllis*. Chevreux (1911) described *A. rostrata* from the deep sea of the North Atlantic Ocean and K.H. Barnard (1925) described *A. conocephalus* from southern Africa.

While studying material from the *Siboga* Expedition, Pirlot (1933) realised that there were two groups within the accumulated species of *Amaryllis*. One group, *Amaryllis*, with no rostrum and a short peduncle on antenna 1, included the shallow-water coastal species *A. macrophthalma*, *A. bathycephala* and *V. tenuipes*. The other group, *Bathyamaryllis*, with a prominent rostrum and a long peduncle on antenna 1, included the deep-water species *B. haswelli*, *B. perezii* Pirlot, *B. rostrata* and *B. conocephalus*. This concept is reflected in our present recognition of two subfamilies in the Amaryllididae, but with *Vijaya* included in the otherwise exclusively deep-water group.

Andres (1981) described a fourth amaryllidid genus, *Pseudamaryllis*, from the abyssal zone in the Red Sea. Ledoyer (1986) reduced this genus to a subgenus of *Amaryllis* but Lowry & Stoddart (1994) showed that *Pseudamaryllis* is a distinct genus related to *Bathyamaryllis*. Lowry & Stoddart (1987) described a shallow-water genus, *Erikus*, from southern South America. Ren (1998) described a new genus, *Paravijaya*, from the South China Sea, but we do not consider this genus to be distinct from *Pseudamaryllis*.

There have been only a few subsequent reports of the described deep-water species (Chevreux, 1903; Chevreux, 1935; Stephensen, 1923; Griffiths, 1977; Ledoyer, 1986; Lawson *et al.*, 1993); but shallow-water amaryllidids have been widely reported as *Amaryllis macrophthalma* (Fig. 1).

A major impediment to the development of amaryllid systematics has been the persistent misidentification of *A. macrophthalma* from many areas. These erroneous reports (e.g., Stebbing, 1888; Thomson, 1902; Walker, 1909; Chilton, 1912; K.H. Barnard, 1916; Schellenberg, 1926, 1931; Griffiths, 1973–1977; Ledoyer, 1978–1986; Alonso, 1987; Lyons & Myers, 1991) have hindered the recognition of generic and specific level diversity in the amaryllidine part of this group.

In this paper we describe two new subfamilies, Amaryllidinae and Vijayiinae, three new genera, *Bamarooka*, *Devo* and *Wonga* and 20 new species; we revise, diagnose and provide keys for all genera; we confine the genus *Amaryllis* to the Australasian area and the species *A. macrophthalma* to southeastern Australia.

Materials and methods

Material used in this study comes from a very large collection of Australian lysianassoid amphipods belonging to, or currently on loan to, the Australian Museum. Most of the inshore Australian coastal waters are represented plus continental shelf samples from southeastern and northwestern Australia and slope samples from off New South Wales and the Bass Strait. However, the abundance of samples and thoroughness of sampling is far from balanced. The southeastern coastline is well represented, but we have no samples at all from, for example, the Gulf of Carpentaria.

Major collections include: CSIRO, North West Shelf survey (CSIRO NWS); Victorian Ministry for Conservation, Marine Studies Group, Western Port Bay Environmental Study (WPBES) and Port Phillip Bay Environmental Study (PPBES); Museum of Victoria, Bass Strait Survey (BSS), SLOPE survey, and expeditions to southern and southwestern Australia, South Australia and Tasmania; New South Wales Department of Agriculture, Division of

Fisheries, dredge samples taken by the FRV *Kapala* on the New South Wales continental shelf and slope; Australian Museum expeditions to Cobourg Peninsula, Northern Territory, Western Australia, Kangaroo Island, South Australia, Lizard Island, Queensland, and the New South Wales coast.

Material is deposited in: Australian Museum, Sydney (AM); Museum Victoria, Melbourne, [formerly the National Museum of Victoria] (NMV); South Australian Museum, Adelaide (SAMA); and Western Australian Museum (WAM).

The taxonomic descriptions presented in this paper were generated from a DELTA (Dallwitz *et al.*, 1993; Dallwitz *et al.*, 1998) database of world amaryllidid amphipod species. Italicised phrases in the descriptions indicate diagnostic characters.

Descriptions of setae on the mandibular palp follow the scheme of Lowry & Stoddart (1993). Descriptions of gnathopod palmar angles follow the scheme of Poore & Lowry (1997). Measurements of whole animals are made from the front of the head (including rostrum) to the base of the telson.

Abbreviations used on figures in the text are: A, antenna; C, coxa; E, epistome; EP, epimeron; G, gnathopod; H, head; LL, lower lip; MD, mandible; MDp, mandibular palp; MP, maxilliped; MPIP, maxilliped inner plate; MPOP, maxilliped outer plate; MPp, maxilliped palp; MX, maxilla; MX1IP, maxilla 1 inner plate; MX1OP, maxilla 1 outer plate; P, pereopod; T, telson; U, uropod; UR, urosome; l, left; r, right.

Systematics

Variation, development and sexual dimorphism

Descriptions of species are, wherever possible, based on mature females with dimorphic characters based on mature males. However, within species morphological variation results from age/size and sexual maturity.

Variation resulting from age/size occurs in characters such as: the number of articles in the accessory flagellum of antenna 1 and the flagella of antennae 1 and 2; the number of setae on the propodus of gnathopod 1; the number of robust setae on the palm of gnathopod 2; setation of the distal articles of the pereopods; number of robust setae on the uropods. This variation is much greater in species that grow to a large size (for example *A. macrophthalma*) than in species that are sexually mature at a smaller size (for example *A. moona*).

Many characters differ between mature males and mature females. Some of these differences are because mature males are usually smaller than mature females of the same species. Sexual dimorphism can be expressed in mature males in the following characters: eye slightly enlarged; well-developed callynophore, or in species where a callynophore is present in females, then it is more strongly developed in the mature male; calceoli on antennae 1 and 2 or only on antenna 2; elongation of antenna 2; development of brush setae on peduncular articles 4 and 5 of antenna 2; development of strong setae on the distal half of mandibular palp article 2 and an increase in the number of D-setae on article 3; development of a fringe of setae on the posterior margin of the merus and carpus of pereopods 3 and 4; development of plumose setae on one or both rami of uropod 3.

Not all character states are expressed in all, or even one genus.

Amaryllididae Lowry & Stoddart

Amaryllididae Lowry & Stoddart, 2002: 165.

Diagnosis. Head much deeper than long, with lateral cephalic lobe weak, midanterior notch present or absent. Epistome and upper lip fused. Mandible, left lacinia mobilis a stemmed serrate blade; accessory setal row well developed, usually with intermediate setae, with a large tuft of setae distally; molar a slightly setose flap with setose margins. Maxilla 1, outer plate with setal-teeth in a 6/5 arrangement, palp absent. Maxilliped, outer plate without distal or medial slender or robust setae; palp well developed, article 4 reduced. Gnathopod 1 simple, coxa vestigial, merus and carpus not rotated, posterior margin of propodus serrate, dactylus simple, without subterminal tooth. Gnathopod 2, posterodistal corner of propodus with medial and lateral robust setae. Pereopods 3–7 simple; propodus without

posterodistal spur. Telson with slight to medium cleft.

Type genus. *Amaryllis* Haswell, 1879.

Generic composition. The family contains eight genera in two subfamilies: Amaryllidinae n.subfam. with *Amaryllis* Haswell, 1879; *Bamarooka* n.gen.; *Erikus* Lowry & Stoddart, 1987 and *Wonga* n.gen.; and Vijayiinae n.subfam. with *Bathyamaryllis* Pirlot, 1933; *Devo* n.gen.; *Pseudamaryllis* Andres, 1981 and *Vijaya* Walker, 1904.

Remarks. Amaryllidids are very distinctive amphipods. They are distinguished from other lysianassoid family groups by their head shape; maxilla 1 without a palp; extremely reduced gnathopod 1 coxa; and gnathopod 1 propodus with serrate posterior margin. Most are immediately recognizable by their very deep head shape with midanterior notch.

Key to subfamilies and genera of the Amaryllididae

- 1 Mouthpart bundle subquadrate. Gnathopod 1, posterior margin of propodus with robust setae. Epimeron 3 with notch immediately above acute posteroventral corner (Vijayiinae) 2
- Mouthpart bundle conical or subconical. Gnathopod 1, posterior margin of propodus without robust setae. Epimeron 3 without notch or with notch slightly or well above posteroventral corner (Amaryllidinae) 5
- 2 Antenna 1 peduncular article 1 not ball-shaped proximally, article 2 medium length (about as long as broad). Uropod 3 outer ramus 1-articulate 3
- Antenna 1 peduncular article 1 ball-shaped proximally, article 2 long (length more than 1.5× length). Uropod 3 outer ramus 2-articulate 4
- 3 Head with or without rostrum. Eye reniform. Antenna 1, callynophore present in female. Antenna 2 not elongate in male *Pseudamaryllis*
- Head with rostrum. Eye ventrally tapered. Antenna 1, callynophore absent in female. Antenna 2 elongate in male *Vijaya*
- 4 Rostrum cone-shaped. Pereopods 5 to 7, dactyls long, slender. Pereopod 7 basis rounded posteriorly, posteroventral corner rounded *Devo*
- Rostrum anteriorly rounded or truncated, not cone-shaped. Pereopods 5 to 7, dactyls short, slender. Pereopod 7 basis subrectangular, posteroventral corner subquadrate *Bathyamaryllis*
- 5 Pereopod 4 coxa, anterior and posterior margins subparallel 6
- Pereopod 4 coxa, anterior margin slightly obtuse, posterior margin rounded *Bamarooka*
- 6 Mouthpart bundle subconical. Pereopods 5–7, distal articles elongate, slender. Uropod 3 rami lanceolate 7
- Mouthpart bundle conical. Pereopods 5–7, distal articles short, broad. Uropod 3 rami clasper-like *Wonga*
- 7 Mandibular palp article 3 with proximal A3-seta. Pereopods 3 and 4 in male with fringe of plumose setae on posterior margin of merus and carpus. Uropod 3 outer ramus 2-articulate *Erikus*
- Mandibular palp article 3 without proximal A3-seta. Pereopods 3 and 4 in male without fringe of setae on posterior margin of merus and carpus. Uropod 3 outer ramus 1-articulate *Amaryllis*

Amaryllidinae n.subfam.

Diagnosis. Mouthpart bundle subconical or conical. Gnathopod 1 propodus without robust setae along posterior margin. Epimeron 3 without a notch or with notch slightly or well above posteroventral corner.

Type genus. *Amaryllis* Haswell, 1879.

Generic composition. The subfamily contains four genera: *Amaryllis* Haswell, 1879; *Bamarooka* n.gen.; *Erikus* Lowry & Stoddart, 1987; and *Wonga* n.gen.

Remarks. The amaryllidines are found in shallow temperate and tropical seas of the southern hemisphere. The largest diversity of genera and species is currently known from Australian waters, but the African and South American faunas have not been adequately described.

Amaryllis Haswell

Amaryllis Haswell, 1879: 253.—Haswell, 1880: 31.—Haswell, 1882: 227.—Stebbing, 1888: 698.—Della Valle, 1893: 781.—Stebbing, 1906: 23.—Pirlot, 1933: 122 (in part, part = *Vijaya* Walker, 1904).—J.L. Barnard, 1969: 320.—Ledoyer, 1986: 717 (in part, part = *Pseudamaryllis*).—Barnard & Karaman, 1991: 460.

Diagnosis. Mouthpart bundle subconical. Mandible palp article 3 without A3-seta. Pereopod 4 coxa with anterior and posterior margins subparallel. Pereopods 5–7 with distal articles elongate. Uropod 3 rami lanceolate; without plumose setae in male and female; outer ramus 1-articulate.

Type species. *Amaryllis macrophthalmalma* Haswell, 1879, selected by Pirlot, 1933.

Species composition. *Amaryllis* contains 13 species: *A. brevicornis* Haswell, 1879; *A. carrascoi* n.sp.; *A. croca* n.sp.; *A. dianae* n.sp.; *A. kamata* n.sp.; *A. keablei* n.sp.; *A. macrophthalmalma* Haswell, 1879; *A. migo* n.sp.; *A. moona* n.sp.; *A. olinda* n.sp.; *A. quokka* n.sp.; *A. philatelica* n.sp. and *A. spencerensis* n.sp.

Remarks. The genus *Amaryllis* (almost exclusively as *A. macrophthalmalma*) has been recorded from a wide geograph-

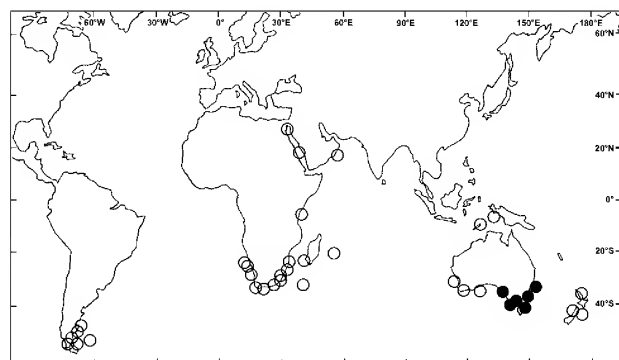


Figure 1. ○ literature records of “*Amaryllis macrophthalmalma*”; ● distribution of *Amaryllis macrophthalmalma*.

ical area: from southeastern South America, through southern and eastern Africa, the Red Sea, Indonesia, New Zealand and all of southern Australia (see Fig. 1). Where the material has been illustrated or described we can, with our current knowledge of the Australian species of *Amaryllis*, exclude the non-Australasian records from *A. macrophthalmalma*. We are also convinced they do not belong to the genus *Amaryllis* (see Remarks for *Erikus*).

Amaryllis apparently occurs only in the Australasian area. Within Australia, it has not been recorded north of 30°S on either the east or west coast (Fig. 2).

Distribution. Currently confirmed only from Australia.

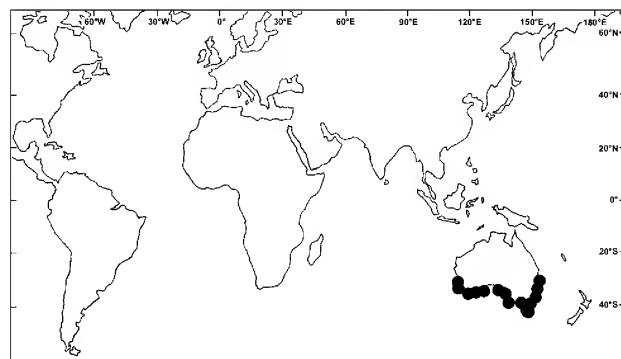


Figure 2. Distribution of the genus *Amaryllis*.

Key to species of *Amaryllis*

1	Epimeron 3 posterior margin with a single notch above posteroventral corner	6
—	Epimeron 3 posterior margin with more than a single notch	2
2	Epimeron 3 posterior margin serrate	3
—	Epimeron 3 posterior margin with a notch plus small or tiny serrations above rounded posteroventral corner	4
3	Antenna 1 peduncular article 1 distal margin with well-developed medial spine. Epistome in lateral view with a mid-anterior hook. Gnathopod 2 of adult female with 1 lateral and 3–4 medial robust setae defining palm	<i>A. croca</i>
—	Antenna 1 peduncular article 1 distal margin with small medial spine. Epistome in lateral view with a strong mid-anterior angle. Gnathopod 2 of adult female with 3–4 lateral and 4 medial robust setae defining palm	<i>A. keablei</i>

4 Antenna 1 peduncular article 1 distal margin with small medial spine; flagellum without callynophore in female. Pereopod 7 basis subrectangular. Uropod 1 outer ramus without cuticular spikes between robust setae 5

— Antenna 1 peduncular article 1 distal margin without medial spine; flagellum with weak callynophore in female. Pereopod 7 basis posteriorly rounded. Uropod 1 outer ramus with cuticular spikes between robust setae *A. migo*

5 Epistome in lateral view slightly angled. Gnathopod 2 of adult female with 3 lateral and 3 medial robust setae defining palm. Pereopod 7 basis posteroventral corner notched *A. carrascoi*

— Epistome in lateral view with slight depression above moderate angle. Gnathopod 2 of adult female with no lateral and 2–3 medial robust setae defining palm. Pereopod 7 basis posteroventral corner subquadrate *A. dianae*

6 Pereopod 7 basis subrectangular 7

— Pereopod 7 basis rounded posteriorly 9

7 Antenna 1 peduncular article 1 distal margin with well-developed medial spine. Epimeron 3 posterior margin with notch well above rounded posteroventral corner 8

— Antenna 1 peduncular article 1 distal margin without medial spine. Epimeron 3 posterior margin with notch slightly above posteroventral corner *A. philatelica*

8 Pereopod 7 basis posteroventral corner with a distinct notch. Gnathopod 2 palm of female with 2 lateral and 1 medial robust setae *A. spencerensis*

— Pereopod 7 basis posteroventral corner right-angled, without a notch. Gnathopod 2 palm of female with 2–4 lateral and 2–3 medial robust setae *A. macrophthalmia*

9 Left lacinia mobilis forming a broad cup distally, teeth reduced to irregular projections. Gnathopod 2 palm of female without lateral robust setae 10

— Left lacinia mobilis forming a flat blade with several strong distal teeth. Gnathopod 2 palm of female with at least 1 lateral robust seta 11

10 Epistome almost straight in lateral view. Mandible accessory setal row without intermediate setae. Maxilliped outer plate with distomedial margin serrate. Gnathopod 2 palm slightly acute *A. moona*

— Epistome with a broad midanterior bulge. Mandible accessory setal row with intermediate setae. Maxilliped outer plate with distomedial margin smooth. Gnathopod 2 palm transverse *A. quokka*

11 Antenna 1 peduncular article 1 distal margin with small medial spine. Pereopod 7 basis posteroventral margin straight 12

— Antenna 1 peduncular article 1 distal margin without medial spine. Pereopod 7 basis posteroventral margin curved *A. olinda*

12 Epistome in lateral view with small depression above moderate mid-anterior angle. Gnathopod 1 carpus subequal to propodus *A. kamata*

— Epistome in lateral view almost straight. Gnathopod 1 carpus shorter than propodus *A. brevicornis*

***Amaryllis brevicornis* Haswell**

Figs. 3, 4

Amaryllis brevicornis Haswell, 1879: 254.—Haswell, 1882: 228.—Whitelegge, 1889: 54.—J.L. Barnard, 1974: 140.—Springthorpe & Lowry, 1994: 11.

Amaryllis sp. 3.—Hutchings *et al.*, 1989: 362.

Type material. LECTOTYPE, female, 11.2 mm, ovigerous (40 eggs), AM G5417; 3 PARALECTOTYPES, female, AM P37181; Port Jackson, New South Wales, Australia, [approx. 33°51'S 151°16'E].

Springthorpe & Lowry (1994:5) have discussed the general problem of Haswell "types". For *Amaryllis brevicornis*, two lots of material in the Australian Museum collection (AM G5417 and P3440) were regarded as syntypes. The first lot (G5417) was registered into the collection and labelled as "Type" by A.R. McCulloch in 1905; the material is from Port Jackson (the type locality and the only locality recorded for this species in Haswell's original publication of 1879). The second lot (P3440), was registered into the collection in 1912 and was not then regarded as type material. It is also from Port Jackson. However, the register entries for P3439 and P3441 are also *A. brevicornis*, from Griffiths Point and Port Stephens. This set of localities—Port Jackson, Port Stephens and Griffiths Point—are the three localities given by Haswell (1882) in his subsequent report of *A. brevicornis* material. It seems to us that the material of AM P3440 should not be regarded as type material.

The syntypes of *A. brevicornis* were mounted with glue onto a glass plate and stored in alcohol for more than 100 years. The specimens were heavily coated with precipitate from the preserving fluid. We have removed one specimen from the glass plate, peeled off the glue, and removed as much as possible of the accumulated deposit. However, many setae (for which insertion points can still be recognized) have been lost and some parts are still not clearly visible. Although we are designating this specimen as a lectotype, we have chosen to describe and illustrate in detail a female not from the type collection. The specimen described (from Clovelly Pool, AM P37116, just south of Port Jackson) agrees extremely well with all characters that can be determined from the lectotype.

One specimen from the original syntype series of 5 specimens is not *A. brevicornis*. It has a serrate epimeron 3 and is a specimen of *A. keablei*. It is now registered as AM P37180.

Additional material. NEW SOUTH WALES: 16 specimens, AM P37217, Sugarloaf Point, 32°26'S 152°32'E, 1–2 m, coralline algae in rock pool, J.K. Lowry, 14 January 1981, stn NSW-135. 8 specimens, AM P37218, N of Fly Point, Port Stephens, 32°43'S 152°09'E, 20 m, sponges, shell and sediment, R.T. Springthorpe & D. Stracey, 8 November 1981, stn NSW-84. 3 specimens, AM P37219, Nelson Head, Port Stephens, 32°43'S 152°09'E, 18 m, bryozoans and hydroids, J. Hall, 27 October 1980, stn NSW-192. 7 specimens, AM P37220, same locality, 15–18 m, sand and shell grit, J. Hall & I. Loch, 27 October 1980, stn NSW-193. 6 specimens, AM P37221, same locality, 20–24 m, rubble on stones, J. Hall, 27 October 1980, stn NSW-197. 1 specimen, AM P5719, off Red Rocks, Port Stephens, [approx. 32°42'S 152°06'E], dredge, A. Musgrave, 30 August 1920. 4 specimens, AM P3441, Port Stephens, [approx. 32°42'S 152°06'E]. 4 specimens, NMV J3331, Port Stephens. 1 specimen, AM P22054, E of North Head, Port Jackson, 33°49'S 151°18'E, 21 m, with sponge *Teichonella labyrinthica*, 27 February 1973, AMSBS, stn 07. 4 specimens, AM P22056, Fairlight Beach, Port Jackson, 33°48'S 151°16'E, 6–9 m, shell rubble, 26 May 1972, AMSBS. 4 specimens, AM P37222,

Fairlight Beach, Port Jackson, 33°48'S 151°16'E, 6–9 m, shell rubble, I. Loch, 28 February 1981, stn NSW-180. 8 specimens, AM P37223, SE of Chinamans Beach, Port Jackson, 33°49'S 151°15'E, 9 m, dead shells and sand, Malacological Society, 8 May 1971, stn NSW-182. 4 specimens, AM P37224, off Sow and Pigs, Port Jackson, 33°50'S 151°15'E, 5 m, shelly sand, J.K. Lowry & A.R. Jones, on FV *Port Jackson*, 30 September 1976, stn NSW-184. 2 specimens, AM P37225, W of Spit Bridge, Port Jackson, 33°48'S 151°15'E, 8 m, *Tethya* sponge and dead mussel shells, J.K. Lowry, 9 June 1981, stn NSW-34. 30 specimens, AM P3440, Port Jackson, 1 specimen, AM P5720, Port Jackson. 2 specimens, AM P5855, Port Jackson. 2 specimens, AM P37116, Clovelly Pool, 33°55'S 151°16'E, 3–6 m, under stones, P.C. Terrill, 12 June 1979, stn NSW-210. 1 specimen, AM P37226, Botany Bay, [approx. 34°00'S 151°13'E], NSW State Fisheries, 1975, stn NSW SF 899. 7 specimens, AM P37227, Botany Bay, [approx. 34°00'S 151°13'E], NSW State Fisheries, 1975, stn NSW SF 901. 2 specimens, AM P37228, off Moona Moona Creek, Jervis Bay, 35°03.5'S 150°41'E, 3 m, encrusting sponge, J.K. Lowry, 19 June 1982, stn NSW-112. 1 specimen, AM P37229, same locality, 8 m, algae and sponge on sandy rocks and mussels, J.K. Lowry, 19 June 1982, stn NSW-113. 8 specimens, AM P37230, same locality, 3 m, *Zonaria* and encrusting ascidian in *Ecklonia* bed, J.K. Lowry, 19 June 1982, stn NSW-114. 2 specimens, AM P37231, same locality, 4 m, *Ecklonia* holdfast, P.B. Berents, 15 October 1981, stn NSW-265. 1 specimen, P37232, same locality, 4 m, *Ecklonia* holdfast, P.B. Berents, September 1981, stn NSW-266. 117 specimens, AM P37233 to P37241, same locality, 4.5 m, epifauna on test of solitary ascidian, *Herdmania momus*, in *Ecklonia* bed, P.B. Berents, October 1981–July 1982. 1 specimen, AM P37242, off Plantation Point, Jervis Bay, 35°04'S 150°42'E, 3 m, red alga, *Liagora*, P.B. Berents, 21 February 1982, stn NSW-246. 169 specimens, AM P35982, P36702 and P37244 to P37248, Munganno Point, Twofold Bay, 37°06.2'S 149°55.7'E, to 7 m, sublittoral rock platform and wharf piles, S. Keable, October 1984–December 1985, stns FIRTA M3-M11. 35 specimens, AM P37249 to P37253, Murrumbulga Point, Twofold Bay, 37°04.7'S 149°53.1'E, to 3 m, sublittoral rock platform and breakwater wall, J. van der Velde & S. Keable, October 1984–September 1985, stns FIRTA Q1–Q13.

Type locality. Port Jackson, New South Wales, Australia, Tasman Sea, [approx. 33°51'S 151°16'E].

Description. Based on female, 11.0 mm, AM P37116. Head much deeper than long, anterior margin with notch extended into a slit; rostrum absent; eye present, elongate, reniform. *Antenna 1* peduncular article 1 not ball-shaped proximally, distal margin with small medial spine; peduncular article 2 medium length; flagellum with or without callynophore, calceoli absent. Antenna 2 flagellum about as long as that of antenna 1, without calceoli. Mouthpart bundle subconical. *Epistome/upper lip* almost straight (lateral view). *Mandible* lacinia mobilis a stemmed, distally-cusped blade; accessory setal row with intermediate setae; palp article 2 with 2 posterodistal setae, article 3 without A3-seta. *Maxilliped* outer plate with distal margin smooth, medial margin without notch.

Gnathopod 1 carpus shorter than propodus (0.8×); propodus, posterior margin without robust setae. *Gnathopod 2* palm slightly acute, with 1–3 lateral robust setae, 1 medial robust seta. Pereopods 3 and 4 merus and carpus without setal fringe. Pereopod 4 coxa with anterior and posterior margins subparallel, anteroventral corner rounded. Pereopods 5–7 with distal articles elongate, dactyls short and stocky. Pereopod 5 basis expanded posteriorly, rounded. *Pereopod 7* basis rounded posteriorly, posteroventral corner rounded, posteroventral margin straight.

Epimeron 3 posterior margin smooth, with notch well above rounded posteroventral corner. *Uropod 1* peduncle dorsolateral margin with 8 robust setae; outer ramus without large spines between robust setae. *Uropod 2* inner ramus slightly constricted. *Uropod 3* rami lanceolate; without plumose setae; outer ramus 1-articulate. *Telson* moderately cleft (about 40%).

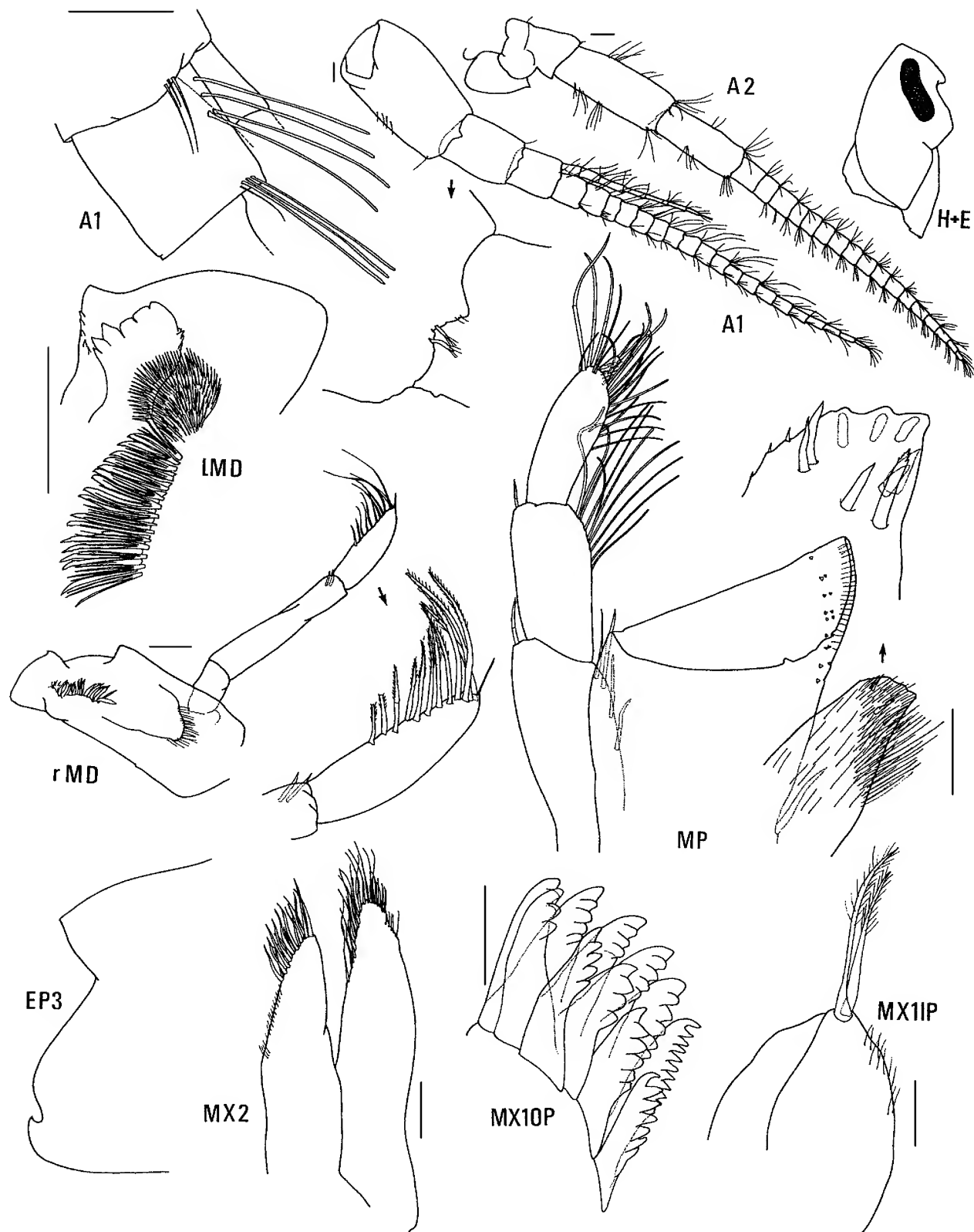


Figure 3. *Amaryllis brevicornis* Haswell, female, 11.0 mm, AM P37116, Clovelly Pool, NSW. Scales for MX1 represent 0.05 mm; remainder represent 0.1 mm.

Variation. *Amaryllis brevicornis*, as we regard it here, shows more variation in the robust setae of gnathopod 2 palm than does any other species of *Amaryllis*. Adult females can be found with from 1 to 4 lateral (but always 1 medial) robust setae on the palm. There is also some variation in the

arrangement of robust setae on the outer ramus of uropod 1. In some specimens, instead of regular spacing of the setae there is a distinct gap between the 1 or 2 proximal robust setae and the 1 or 2 distal robust setae. The variation in these characters does not occur consistently with either size

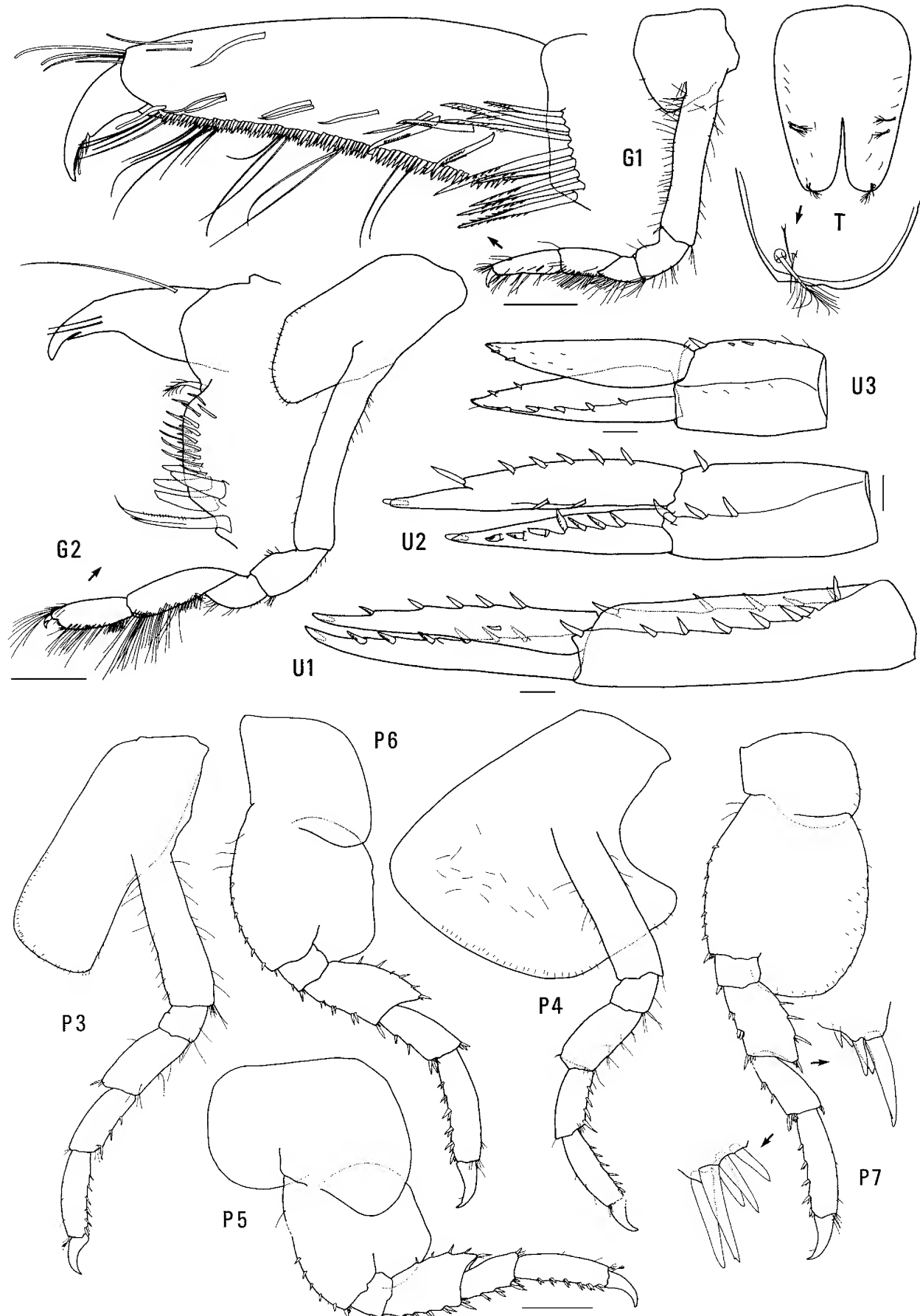


Figure 4. *Amaryllis brevicornis* Haswell, female, 11.0 mm, AM P37116, Clovelly, NSW. Scales for U1–3 and T represent 0.1 mm, remainder represent 0.5 mm.

or geographical distribution, with any other character, or with each other. (A similar gap in the uropod 1 robust setae also occurs in *A. migo*, but in this case it consistently appears with other species characters.)

Remarks. *Amaryllis brevicornis* belongs to the group of species with a smooth posterior margin on epimeron 3 and a rounded posteroventral corner on the basis of pereopod 7. Within this group it is most similar to *A. kamata*, from which it differs in the shape of the epistome and the length of the gnathopod 1 carpus.

Habitat. *Amaryllis brevicornis* has been often collected with sponges; less often with other sessile invertebrates such as bryozoans, hydroids and ascidians, or in algal holdfasts, coralline algae and coarse rubble.

Distribution. Coastal New South Wales, southeastern Australia; to 24 m depth.

Amaryllis carrascoi n.sp.

Figs. 5–8, Plate 1a.

Amaryllis macrophthalma.—Chilton, 1921: 55 (in part).—J.L. Barnard, 1972: 262 (in part, figure of 8.5 mm female).
Amaryllis sp. 2.—Hutchings *et al.*, 1989: 362.

Type material. HOLOTYPE, female, 11.7 mm, ovigerous (9 eggs), NMV J13954; 1 PARATYPE, male, 8.4 mm, NMV J13955; 30 PARATYPES, NMV J13956; 30 PARATYPES, AM P37117; 10 PARATYPES, SAMA C5971; 1 km off bay on north shore of Flinders Island, Investigator Group, South Australia, Southern Ocean, 33°41'S 134°31'E, 20 m, seagrass *Posidonia*, drift on sand, G.C.B. Poore, 19 April 1985, FV *Lemnos*, NMV stn SA-67.

Additional material. NEW SOUTH WALES: 1 specimen, AM P10858, small bay near Kurnell, Botany Bay, 34°00'S 151°12'E, sand and weed, F.A. McNeill, 27 October 1927. 4 specimens, AM P10849, Kurnell, Botany Bay, 34°00'S 151°13'E, F.A. McNeill, 6 October 1927. 1 specimen, AM P37118, Moe's Rock, S of Jervis Bay, 35°09'S 150°45'E, 6 m, coralline algae *Amphiroa anceps*, P.B. Berents, 29 June 1981, stn NSW-58. 35 specimens, AM P37119, N side of Bawley Point, 35°31'S 150°24'E, 11 m, coralline algae, P.B. Berents, 27 April 1981, stn NSW-27. 1 specimen, AM P37120, same locality, 3 m, coralline algae, P.D. Filmer-Sankey, 27 April 1981, stn NSW-26. 21 specimens, AM P36701, Murrumbulga Point, Twofold Bay, 37°04.7'S 149°53.1'E, breakwater wall, 3 m, S. Keable & P. Hutchings, 17 September 1985, stn FIRTA Q8. 1 specimen, AM P37121, Aslings Beach, Calle Calle Bay, Twofold Bay, 37°05'S 149°56'E, 8.5 m, sediment, S. Keable & P. Albertson, 22 February 1985, stn FIRTA EB6. 7 specimens, AM P37122, Quarantine Bay, Twofold Bay, 37°05'S 149°56'E, 2 m, seagrass *Posidonia*, S. Keable, 25 June 1985, stn FIRTA Q8-10. VICTORIA: 36 specimens, NMV J11536, Duck Point, Corner Inlet, 38°49'S 146°16'E, 2 m, seagrass *Zostera* on sand, corer, G.J. Morgan, 20 November 1983, stn CIN 24. 1 specimen, NMV J13957, Bennison Channel, Corner Inlet, 38°49'S 146°23'E, 6 m, sand and shell grit, airlift, G.J. Morgan, 23 November 1983, stn CIN 28E. 13 specimens, NMV J3336, Shoreham, Western Port, [approx. 38°26'S 145°03'E], O.A. Sayce Collection. 1 specimen, NMV J13958, Western Port, O.A. Sayce Collection. 1 specimen, NMV J13959, West Channel, O.A. Sayce Collection. 1 specimen, NMV J3235, Hobsons Bay, Port Phillip Bay, 3 m, sandy shell, grab, stn PPBES 189. 1 specimen, NMV J13960, Port Phillip Bay. 8 specimens, NMV J13961, Port Phillip Bay, W. Williams, stn 25. 1 specimen, NMV J3247, Port Phillip Bay, 9–12 m, W. Williams, 2 April 1959. 1 specimen, NMV J3261, Port Phillip Bay, W. Williams, stn 64. 17 specimens, NMV J3269, Port Phillip Bay, 38°14.0'S 144°39.5'E, 1 m, Venturi sampler, 23 January 1973, stn PPBES 966. 3 specimens, AM P58121, Lawrence Rocks, Portland, Victoria, 38°24'S 141°40.1'E, 23 m, bryozoan, possibly *Orthoscuticella* sp., R.T. Springthorpe & P.B. Berents, 30 April 1988, stn VIC-49. BASS STRAIT: 10 specimens, AM

P58115, eastern Bass Strait, 38°56.5'S 148°19.3'E, 80–85 m, epibenthic sled, P.B. Berents, 27 August 1994, FV *Southern Surveyor*, stn SS 05/95/59. 3 specimens, AM P58118, eastern Bass Strait, 38°59.1'S 148°31.6'E, 125 m, epibenthic sled, P.B. Berents, 27 August 1994, FV *Southern Surveyor*, stn SS 05/95/60. 6 specimens, NMV J13963, 9 km SSW of Cape Adansan, Three Hummock Island, central Bass Strait, 40°30.9'S 144°56'E, 27 m, very coarse sand, epibenthic sled, M. Gomon & G.C.B. Poore, 3 November 1980, FV *Sarda*, stn BSS-109. 6 specimens, NMV J13987, 5 km E of Cape Edie, Robbins Island, Central Bass Strait, 40°41.8'S 145°07'E, 16 m, fine shelly sand, epibenthic sled, M. Gomon & G.C.B. Poore, 3 November 1980, FV *Sarda*, stn BSS-110. TASMANIA: 1 specimen, AM P37123, off St Helens Point, 41°20.6'S 148°30'E, 110 m, fine clayey sand, P.H. Colman, 25 March 1973, MV *Sprightly*, stn BMR S73-2038. 1 specimen, AM P37124, Bicheno, 41°53'S 148°18'E, 20–30 m, bryozoans and *Macrocystis* holdfast, R.H. Kuiter, 8 May 1986, AM stn TAS-26. 4 specimens, NMV J13962, Coles Bay, 42°07'S 148°17'E, 1 m, red algae and invertebrates on rock wall, airlift, R.S. Wilson, 21 April 1985, NMV stn TAS-17. 110 specimens, AM P58120, off rocky point near eastern end of Bryans Beach, Freycinet Peninsula, Tasmania, 42°16'S 148°17.4'E, 12 m, baited trap, probably sandy bottom, J.K. Lowry & S.J. Keable, 30 April–1 May 1991, AM stn TAS-338. 7 specimens, AM P27052, Shouten Passage, 42°17'S 148°18'E, 12 m, coarse sand and coralline algae, van Veen grab, A.J. Dartnall, 8 June 1977, FV *Penghana*, stn 46. 1 specimen, NMV J13984, 5 km NE of Mistaken Cape, Maria Island, 42°37'S 148°12.5'E, 100 m, "fine muddy bryozoans", epibenthic sled, R.S. Wilson, 23 April 1985, RV *Challenger*, NMV stn TAS-31. 1 specimen, AM P37125, Tasmanian coast, FIS *Endeavour* Collection. SOUTH AUSTRALIA: 2 specimens, NMV J13964, NE end of West Island, Encounter Bay, 35°37'S 138°36'E, 12 m, red algae, G.C.B. Poore & H.M. Lew Ton, 20 March 1985, NMV stn SA-39. 1 specimen, NMV J13965, N side of West Island, Encounter Bay, 35°37'S 138°36'E, 5 m, coralline algae, G.C.B. Poore & H.M. Lew Ton, 21 March 1985, NMV stn SA-43. 14 specimens, NMV J13966, same locality, 5 m, sandy sediment, G.C.B. Poore & H.M. Lew Ton, 21 March 1985, NMV stn SA-46. 1 specimen, AM P37126, Marino, Gulf St Vincent, [approx. 35°03'S 138°31'E], W.H. Baker, 1910. 2 specimens, AM P37127, Sellicks Beach, Gulf St Vincent, [approx. 35°20'S 138°27'E], H.M. Hale, 1936. 1 specimen, SAMA C5972, Dangerous Reef, Spencer Gulf, [approx. 34°49'S 136°12'E], dredged, K. Sheard. 2 specimens, SAMA C5973, Marion Bay, Yorke Peninsula, [approx. 35°14'S 137°00'E], 15 m, on bait in craypots, W. Zeidler, 28 January 1980. 2 specimens, NMV J13967, The Hotspot reef, 5 nautical miles W of N end of Flinders Island, 33°40.5'S 134°22.0'E, 17 m, tufted bryozoan on exposed rock face, G.C.B. Poore, 19 April 1985, FV *Lemnos*, NMV stn SA-62. 2 specimens, NMV J13983, same locality, 17 m, tufted red alga on flat exposed rock face, G.C.B. Poore, 19 April 1985, FV *Lemnos*, NMV stn SA-63. 26 specimens, NMV J13968, same locality, 12 m, mixed large forms of brown, red and green algae, S. Shepherd, 19 April 1985, FV *Lemnos*, NMV stn SA-64. 9 specimens, NMV J13969, same locality, 17 m, mixed large forms of brown, red and green algae, S. Shepherd, 19 April 1985, FV *Lemnos*, NMV stn SA-65. 5 specimens, NMV J13970, The Hotspot reef, 5 nautical miles W of N end of Flinders Island, 33°40.8'S 134°22.5'E, 21 m, tufted red alga and soft erect bryozoan, G.C.B. Poore, 29 April 1985, FV *Lemnos*, NMV stn SA-72. 4 specimens, NMV J13971, 1 km off bay on N shore of Flinders Island, 33°41'S 134°31'E, drift algae on sand, hand dredge, G.C.B. Poore, 19 April 1985, NMV stn SA-68. 1 specimen, NMV J13972, NE coast of Topgallant Island, Investigator Group, 33°43.0'S 134°36.6'E, 16 m, brown alga *Cystophora* sp., S. Shepherd & G.C.B. Poore, 22 April 1985, NMV stn SA-84. 7 specimens, NMV J13973, Venus Bay, S side of Germein Island, 33°13.2'S 134°40.1'E, 2 m, shelly sand flat, hand dredge, G.C.B. Poore, 23 April 1985, NMV stn SA-87. 1 specimen, NMV J13974, same data, NMV stn SA-88. 1 specimen, AM P37396, off St Francis Island, [approx. 32°31'S 133°18'E], 11–24 m, J.C. Verco. WESTERN AUSTRALIA: 1 specimen, AM P37128, SE of South Point, Two Peoples Bay, 34°58'S 118°12'E, 12 m, bryozoan *Orthoscuticella* sp., R.T. Springthorpe, 16 December 1983, stn WA-182. 1 specimen, AM P37129, same locality, 12 m, coralline and green algae, sea grasses, R.T. Springthorpe, 16 December 1983, stn WA-183. 1 specimen, AM P37130, Mistaken Island, Vancouver Peninsula, King George Sound, 35°04'S 117°56'E, 3 m, stalked ascidian, J.K. Lowry, 13 December 1983, stn WA-109. 1 specimen, AM P37131, off Possession Point, King George Sound, 35°02.5'S 117°55'E, 10 m, sand and detritus from bases of sea grasses, R.T. Springthorpe & J.K. Lowry, 14 December 1983, stn WA-131. 1 specimen, AM P37132, same locality, 7 m, algae, bryozoan and sponge, R.T. Springthorpe & J.K. Lowry, 14 December 1983, stn WA-133. 1 specimen, NMV J13975, N of False Island, King George Sound, 35°00.7'S 118°10.1'E, 27 m, red algae and bryozoan, G.C.B. Poore & H.M. Lew Ton, 15 April 1985, NMV stn SWA-57.

Type locality. One kilometre off bay on north shore of Flinders Island, Investigator Group, South Australia, 33°41'S 134°31'E, 20 m depth.

Description. Based on holotype female, 11.7 mm, NMV J13954. Head much deeper than long, anterior margin with notch extended into a slit; rostrum absent; eye present, elongate, reniform. *Antenna 1 peduncular article 1* not ball-shaped proximally, *distal margin with small medial spine*; peduncular article 2 medium length; *flagellum without callynophore*, calceoli absent. Antenna 2 flagellum about as long as that of antenna 1, without calceoli. Mouthpart bundle subconical. *Epistome/upper lip almost straight (lateral view)*. *Mandible lacinia mobilis a stemmed, distally-cusped blade; accessory setal row with intermediate setae; palp article 2 with 2 posterodistal setae, article 3 without A3-seta*. *Maxilliped outer plate with distal margin smooth, medial margin without notch*.

Gnathopod 1 carpus subequal in length to propodus (0.9×); propodus, posterior margin without robust setae. Gnathopod 2 palm slightly acute, with 3 lateral robust setae, 3 medial robust setae. Pereopods 3 and 4 merus and carpus without setal fringe. Pereopod 4 coxa with anterior and posterior margins subparallel, anteroventral corner rounded. Pereopods 5–7 with distal articles elongate, dactyls short and stocky. Pereopod 5 basis expanded posteriorly, rounded. *Pereopod 7 basis subrectangular, posteroventral corner notched*, posteroventral margin straight.

Epimeron 3 posterior margin serrate, with notch well above rounded posteroventral corner. Uropod 1 peduncle dorsolateral margin with 9 robust setae; outer ramus without large spines between robust setae. Uropod 2 inner ramus slightly constricted. Uropod 3 rami lanceolate; without plumose setae; outer ramus 1-articulate. Telson moderately cleft (about 40%).

Male (sexually dimorphic characters). Based on paratype male, 8.4 mm, NMV J13955. Antenna 1 flagellum with

callynophore, with calceoli. Antenna 2 flagellum with calceoli. Mandible palp article 2 with 8 posterodistal setae. Gnathopod 2 palm with 1 lateral robust seta and 1 medial robust seta.

Variation. There is some minor variation in the appearance of epimeron 3 in *A. carrascoi*. In small specimens there may be as few as 2 small serrations above the notch on the posterior margin. Although always present, the notch itself is not well developed in some specimens, in which case the margin may appear to be only serrate. However, in *Amaryllis* species with a serrate posterior margin on epimeron 3, the serrations begin at the ventral margin whereas in species with a notch and serrations, the notch is well above the rounded posteroventral corner and the additional small serrations occur above the notch.

Etymology. Named for Jacque Carrasco, a Colombian natural history artist who lived and died in Australia before many of his ideas, integrating art and conservation, were ever realised.

Remarks. *Amaryllis carrascoi* is similar to other *Amaryllis* species with a serrate posterior margin on epimeron 3, such as *A. croca*, *A. dianae*, *A. keablei* and *A. migo*. It differs from all other species in this group in having a notched posteroventral corner on the basis of pereopod 7.

Habitat. *Amaryllis carrascoi* has been most frequently collected in association with coralline algae, but also with other types of algae, sea grasses and bryozoans; or on fine to coarse sands. It has twice been taken in baited traps.

Distribution. Southern Australia; from Botany Bay on the southeastern coast, through Tasmanian, Victorian and South Australian coasts to King George Sound in southern Western Australia. Except for a few records from 80–125 m off eastern Bass Strait and the Tasmanian coast, it occurs in shallow water, 1–30 m depth.

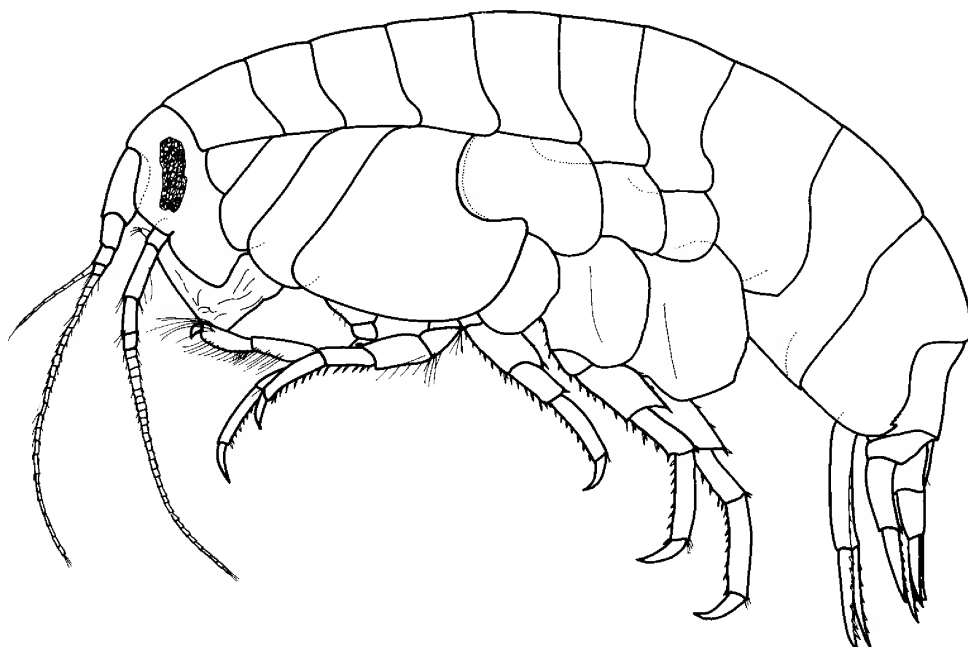


Figure 5. *Amaryllis carrascoi* n.sp., holotype female, 11.7 mm, NMV J13954, Flinders Island, South Australia.

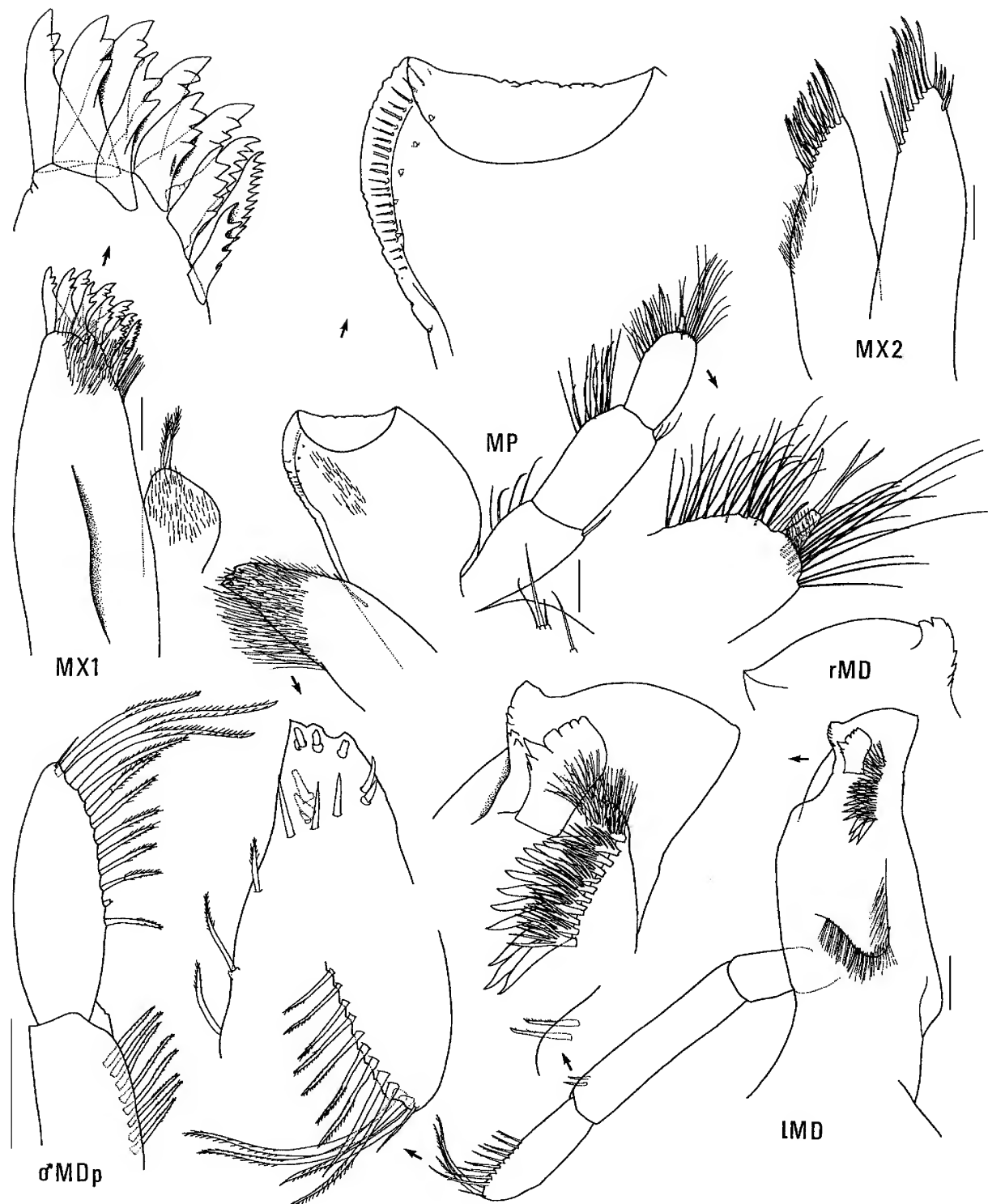


Figure 6. *Amaryllis carrascoi* n.sp., holotype female, 11.7 mm, NMV J13954; paratype male, 8.4 mm, NMV J13955; Flinders Island, South Australia. Scales represent 0.1 mm.

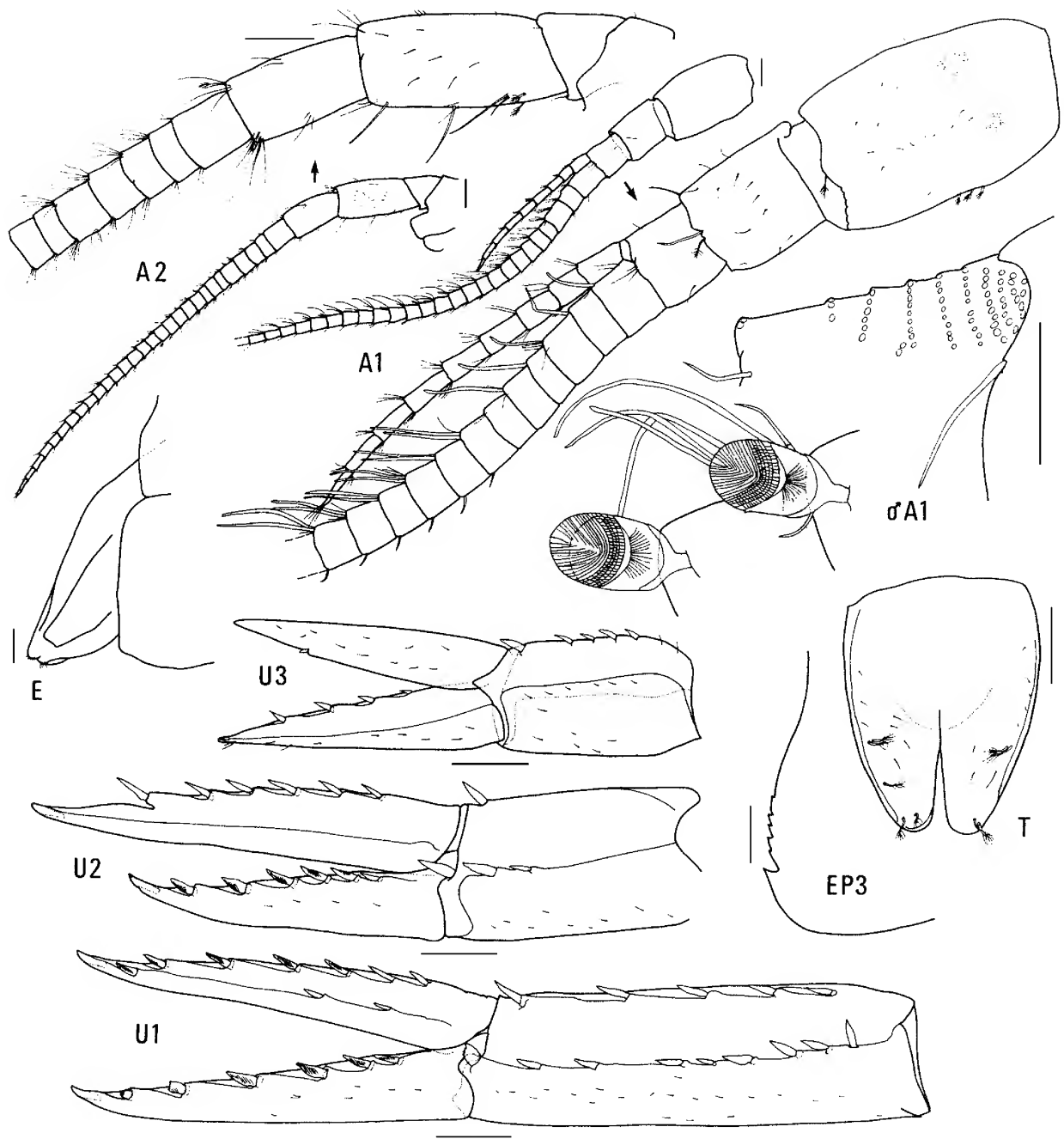


Figure 7. *Amaryllis carrascoi* n.sp., holotype female, 11.7 mm, NMV J13954; paratype male, 8.4 mm, NMV J13955; Flinders Island, South Australia. Scales represent 0.2 mm.

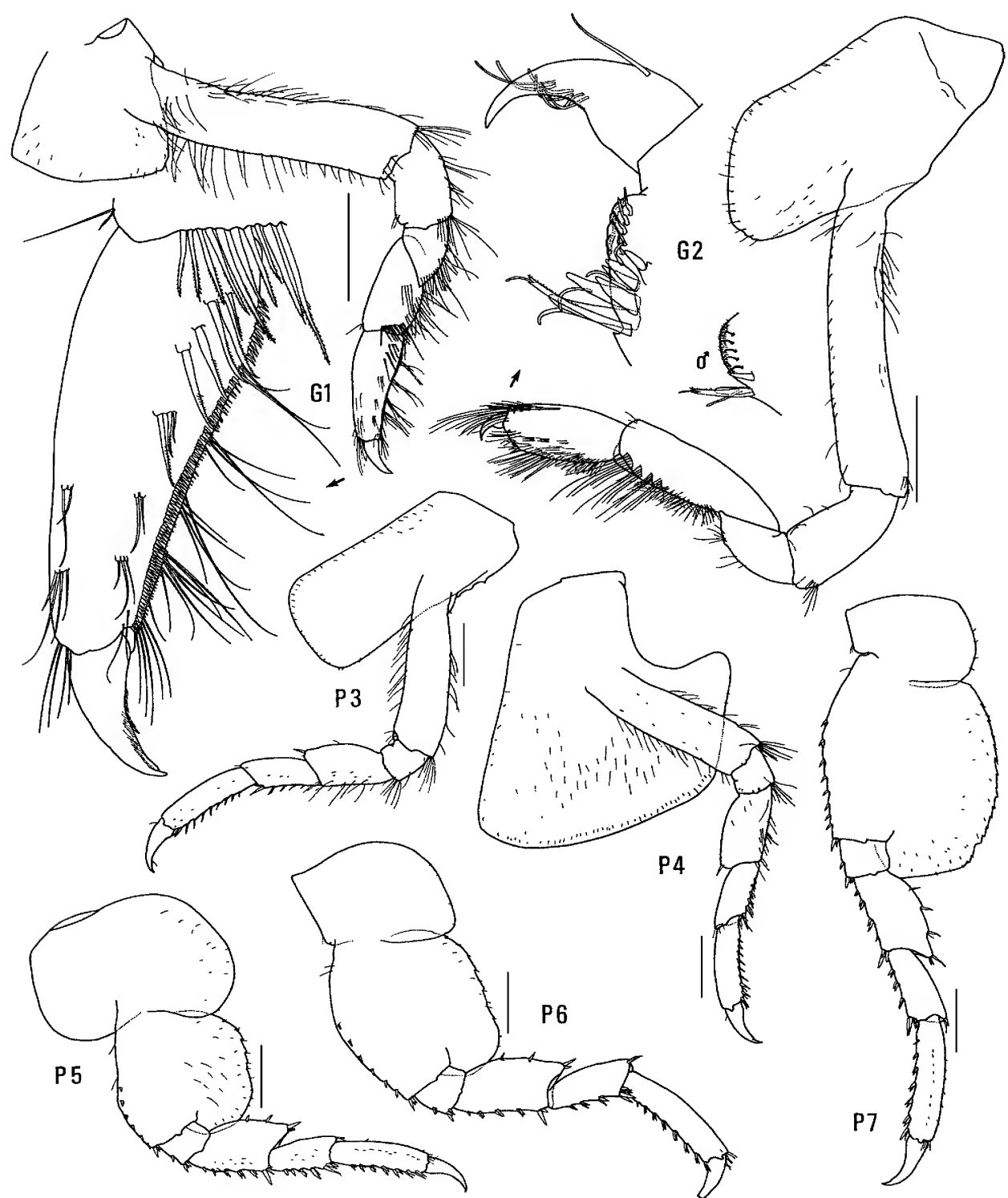
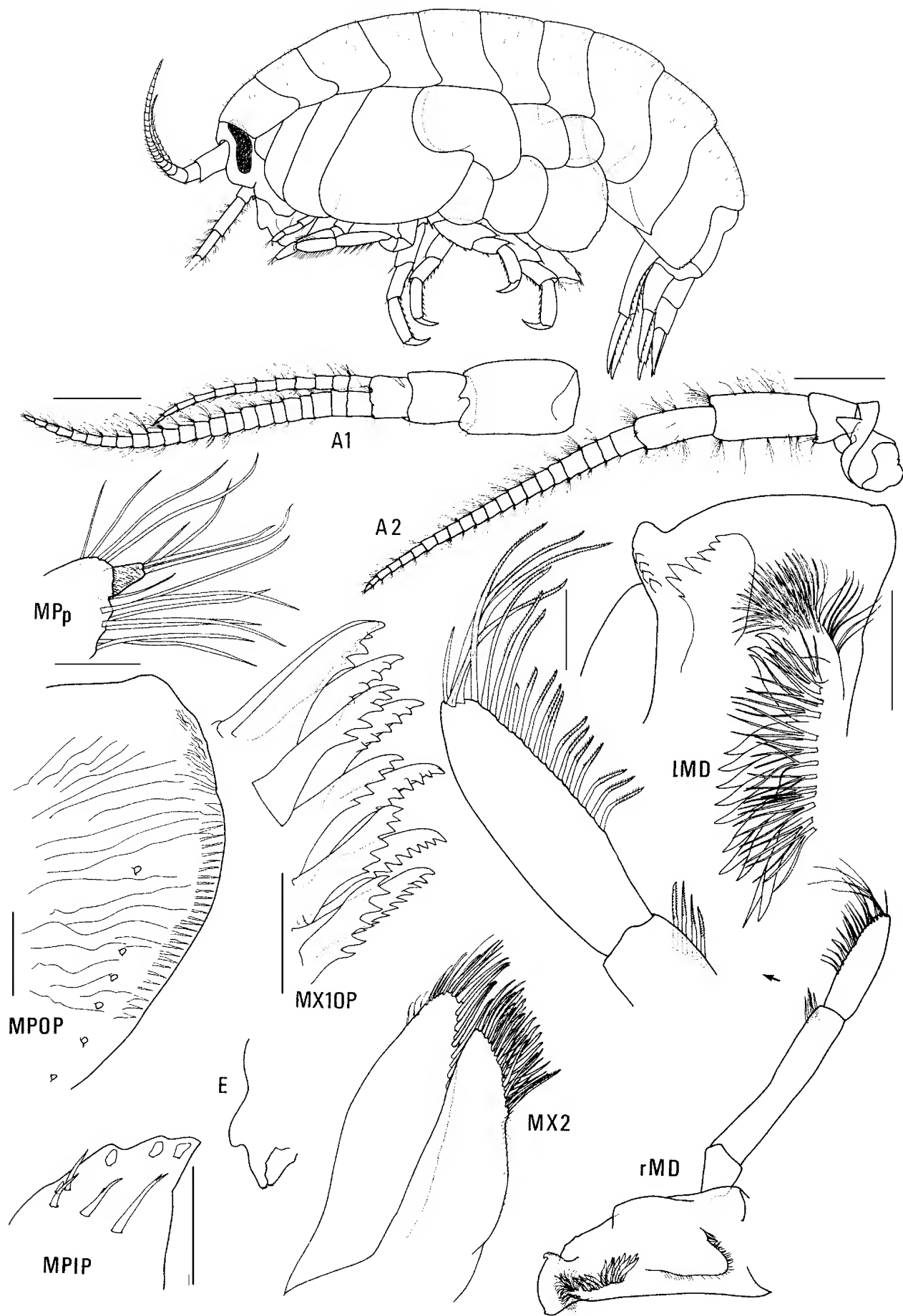


Figure 8. *Amaryllis carrascoi* n.sp., holotype female, 11.7 mm, NMV J13954; paratype male, 8.4 mm, NMV J13955; Flinders Island, South Australia. Scales represent 0.5 mm.



Amaryllis croca n.sp.

Figs. 9, 10

Amaryllis macrophthalma.—Chilton, 1921: 55 (in part).

Type material. HOLOTYPE, female, 16.5 mm, ovigerous (40 eggs), NMV J13976, The Hotspot reef, 5 nautical miles west of Flinders Island, South Australia, Southern Ocean, 33°40.8'S 134°22.5'E, 21 m, erect hard bryozoan on vertical rock face, G.C.B. Poore & H.M. Lew Ton, 20 April 1985, NMV stn SA-71.

Additional material. VICTORIA: 2 females, NMV J3791, Western Port, 11 May 1968, stn B/1/20. 1 female, NMV J13977, Western Port, 7 April 1968, stn B/1/9. SOUTH AUSTRALIA: 1 female, AM E6525, 24 km NW of Cape Jarvis, Gulf St Vincent, [approx. 35°25'S 137°55'E], 31 m, FIS Endeavour collection. 2 specimens, immature, AM P37179, Rapid Bay, Gulf St Vincent, 35°31'S 138°11'E, on jetty piles, P. Hutchings, 7 March 1979.

Type locality. The Hotspot reef, 5 nautical miles west of Flinders Island, South Australia, Southern Ocean, 33°40.8'S 134°22.5'E, 21 m depth.

Description. Based on holotype female, 16.5 mm, NMV J13976. Head much deeper than long, anterior margin with notch extended into a slit; rostrum absent; eye present, elongate, reniform. *Antenna 1 peduncular article 1* not ball-shaped proximally, *distal margin with well-developed medial spine*; peduncular article 2 medium length; *flagellum without callynophore*, calceoli absent. *Antenna 2 flagellum* about as long as that of antenna 1, without calceoli. Mouthpart bundle subconical. *Epistome/upper lip with a mid-anterior hook (lateral view)*. *Mandible lacinia mobilis a stemmed, distally-cusped blade*; *accessory setal row with intermediate setae*; *palp article 2 with 4 posterodistal setae*, article 3 without A3-seta. *Maxilliped outer plate with distal margin smooth*, medial margin without notch.

Gnathopod 1 carpus subequal in length to propodus; propodus, posterior margin without robust setae. *Gnathopod 2 palm slightly acute, with 1 lateral robust seta, 3–4 medial robust setae*. Pereopods 3 and 4 merus and carpus without setal fringe. Pereopod 4 coxa with anterior and posterior margins subparallel, anteroventral corner rounded. Pereopods 5–7 with distal articles elongate, dactyls short and stocky. Pereopod 5 basis expanded posteriorly, rounded. *Pereopod 7 basis subrectangular, posteroventral corner subquadrate*, posteroventral margin straight.

Epimeron 3 posterior margin serrate, without notch. *Uropod 1 peduncle dorsolateral margin with 10 robust setae; outer ramus without large spines between robust setae*. *Uropod 2 inner ramus slightly constricted*. Uropod 3 rami lanceolate; without plumose setae; outer ramus 1-articulate. *Telson moderately cleft (about 45%)*.

Etymology. The specific name *croca* is a Medieval Latin word for a shepherd's crook, an allusion to the hooked epistome of this species.

Remarks. *Amaryllis croca* is similar to other *Amaryllis* species with a serrate posterior margin on epimeron 3, such

as *A. carrascoi*, *A. dianae*, *A. keablei* and *A. migo*. It is most similar to *A. keablei*, in that the serrations extend to the posteroventral corner. *Amaryllis croca* differs from *A. keablei* in having a well-developed medial spine on peduncular article 1 of antenna 1, posterodistal setae on article 2 of the female mandibular palp and one lateral robust seta on the palm of gnathopod 2. *Amaryllis croca* differs from all other *Amaryllis* species in having a midanterior hook on the epistome/upper lip.

Habitat. *Amaryllis croca* is known from bryozoans on a rock face and on wharf pilings.

Distribution. Southeastern coast of Australia; 21–31 m depth.

Amaryllis dianae n.sp.

Figs. 11–13

Amaryllis macrophthalma.—Chilton, 1921: 55 (in part).

Type material. HOLOTYPE, female, 16.5 mm, AM P37378, off South Mole, Arthur Head, Fremantle, Western Australia, eastern Indian Ocean, 32°03'S 115°44'E, 6 m, spirorbid worm tubes, J.K. Lowry, 25 December 1983, stn WA-283. 1 PARATYPE, female, AM P37379, type locality, 6 m, orange gorgonian, R.T. Springthorpe, 25 December 1983, stn WA-286. 2 PARATYPES, male, AM P37380, Cathedral Rock, Rottnest Island, Western Australia, 32°01.5'S 115°27'E, 3 m, orange tunics, J.K. Lowry, 21 December 1983, stn WA-247. 1 PARATYPE, AM P37381, same locality, 3 m, coralline algae, some red algae and sponge, J.K. Lowry, 21 December 1983, stn WA-248. 1 PARATYPE, male, AM P37382 and 3 PARATYPES, female, WAM C28202, same locality, 6 m, mixed algae, R.T. Springthorpe, 21 December 1983, stn WA-251.

Additional material. VICTORIA: 1 specimen, AM P58122, Lawrence Rocks, Portland, 38°24'S 141°40.1'E, 23 m, bryozoan, possibly *Orthoscuticella*, R.T. Springthorpe & P.B. Berents, 30 April 1988, stn VIC-49. SOUTH AUSTRALIA: 1 specimen, NMV J48799, NE end of West Island, Encounter Bay, 35°37'S 138°36'E, 15 m, red algae, sponges and bryozoans, G.C.B. Poore & H.M. Lew Ton, 20 March 1985, NMV stn SA-42. 1 specimen, AM P37383, 8–10 km off Semaphore, Gulf St Vincent, [approx. 34°52'S 138°20'E], 9 m, H.M. Hale, 1925. 2 specimens AM P37384, Marino, Gulf St Vincent, [approx. 35°03'S 138°31'E], W.H. Baker, 1910. 2 specimens, SAMA C5974, 20 km due W of Outer Harbour, Adelaide, [approx. 34°45'S 138°15'E], 23–25 m, quadrat G8, J. McPhailain, 17 April 1975. 2 specimens, SAMA C5975, same locality, quadrat H4, J. McPhailain, 22 April 1975. 1 specimen, SAMA C5976, same locality, quadrat G6, J. McPhailain, 17 April 1975. 1 specimen, SAMA C5977, same locality, quadrat H7, J. McPhailain, 22 April 1975. 1 specimen, SAMA C5978, Tiparra Reef, Spencer Gulf, S.A., [approx. 34°03'S 137°24'E], 5 m, in seagrass *Posidonia*, S.A. Shepherd. 2 specimens, SAMA C5979, The Pages, [approx. 35°47'S 138°17'E], 27 m, dredged, K. Sheard, 12 April 1941. 1 specimen, AM P37385, Nepean Bay, Kangaroo Island, [approx. 35°42'S 137°37'E], F. Moorhouse, May 1938. 1 specimen, AM P37386, unknown locality, Gulf St Vincent. 2 specimens, AM P37387, behind Lowly Point, Spencer Gulf, [approx. 33°00'S 137°46'E], 18 m, K. Sheard on FL Whyalla, 7 March 1938. 1 specimen, AM P37388, Western Shoal, Spencer Gulf, [approx. 33°09'S 137°31'E], 9 m, K. Sheard on FL Whyalla, 10 March 1938. 1 specimen, NMV J13982, The Hotspot Reef, W of Flinders Island, 33°40.8'S 134°22.5'E, 21 m, erect hard bryozoan on vertical rock face, G.C.B. Poore, 20 April 1985,

Figure 9. *Amaryllis croca* n.sp., holotype female, 16.5 mm, NMV J13976, The Hotspot Reef, South Australia. Scales for A1, 2 represent 0.5 mm; remainder represent 0.1 mm.

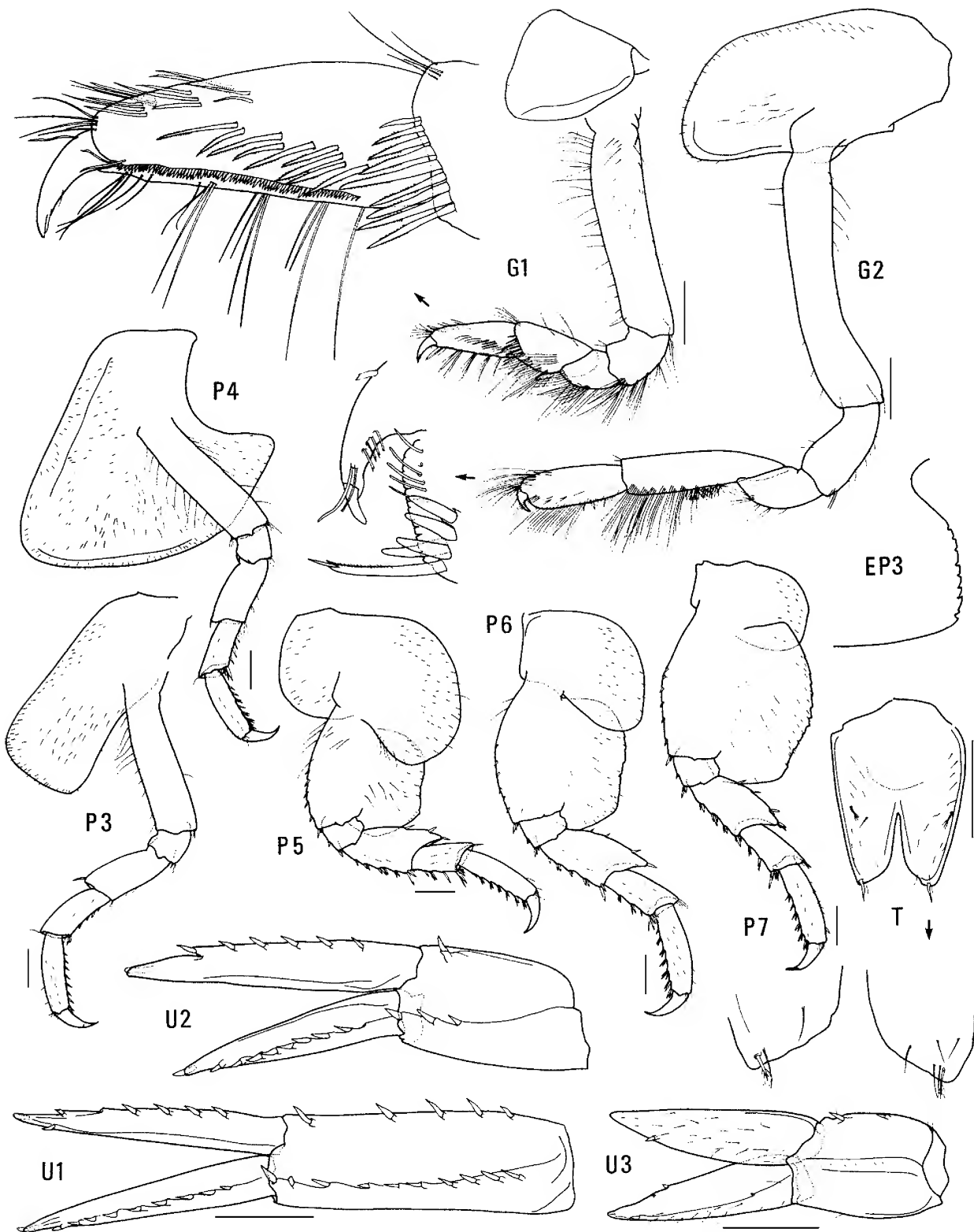


Figure 10. *Amaryllis croca* n.sp., holotype female, 16.5 mm, NMV J13976, The Hotspot Reef, South Australia. Scales represent 0.5 mm.

NMV stn SA-71. WESTERN AUSTRALIA: 1 specimen, AM P18313, SW of Eucla, Great Australian Bight, 146–219 m, FIS *Endeavour*. 3 specimens, AM P37389, 2 km SE of South Point, Two Peoples Bay, 34°58'S 118°12'E, 14 m, among green alga *Caulerpa* bases and fine sand, J.K. Lowry, 16 December 1983, stn WA-178. 5 specimens, AM P37390, rocks near Migo Island, Port Harding, Torbay Bay, 35°04'S 117°39'E, 6–7 m, sponge and algae, R.T. Springthorpe, 15 December 1983, stn WA-

145. 1 specimen, AM P37391, Geographe Bay, [approx. 33°37'S 115°18'E], 27–29 m, J.C. Verco.

Type locality. Off South Mole, Arthur Head, Fremantle, Western Australia, eastern Indian Ocean, 32°03'S 115°44'E, 6 m depth.

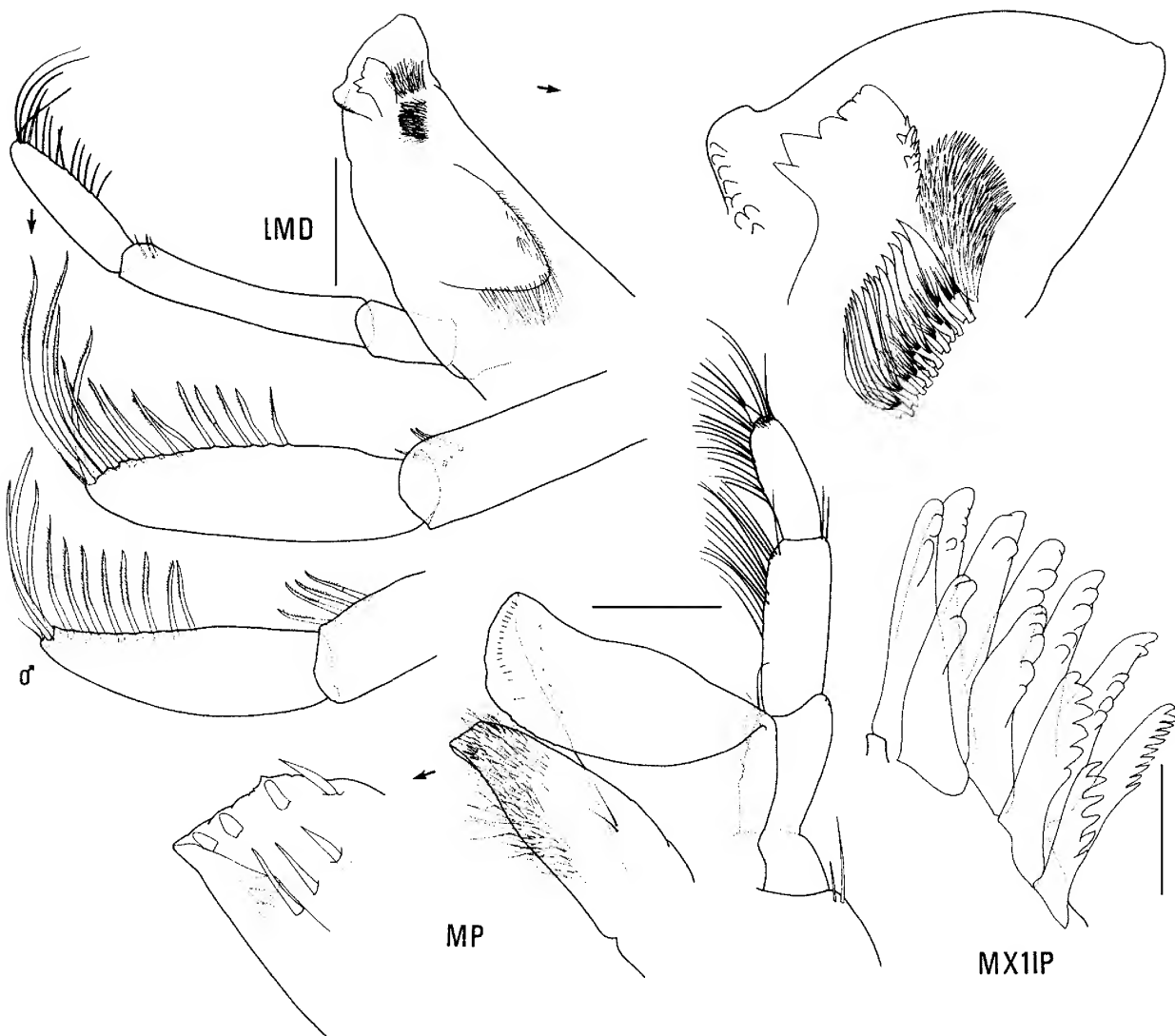


Figure 11. *Amaryllis dianae* n.sp., holotype female, 16.5 mm, AM P37378; paratype immature male, 6.0 mm, AM P37380; Fremantle, Western Australia. Scales represent 0.1 mm.

Description. Based on holotype female, 16.5 mm, AM P37378. Head much deeper than long, anterior margin with notch extended into a slit; rostrum absent; eye present, elongate, reniform. Antenna 1 peduncular article 1 not ball-shaped proximally, distal margin with small medial spine; peduncular article 2 medium length; flagellum without callynophore, calceoli absent. Antenna 2 flagellum about as long as that of antenna 1, without calceoli. Mouthpart bundle subconical. Epistome/upper lip with moderate mid-anterior angle with small depression above angle (lateral view). Mandible lacinia mobilis a stemmed, distally-cusped blade; accessory setal row with intermediate setae; palp article 2 with 3 posterodistal setae, article 3 without A3-seta. Maxilliped outer plate with distal margin smooth, medial margin without notch.

Gnathopod 1 carpus shorter than propodus; propodus, posterior margin without robust setae. Gnathopod 2 palm slightly acute, without lateral robust setae, 2–3 medial robust setae. Pereopods 3 and 4 merus and carpus without setal fringe. Pereopod 4 coxa with anterior and posterior margins subparallel, anteroventral corner rounded. Pereopods 5–7 with distal articles elongate, dactyls short

and stocky. Pereopod 5 basis expanded posteriorly, rounded. Pereopod 7 basis subrectangular, posteroventral corner subquadrate, posteroventral margin straight.

Epimeron 3 posterior margin serrate, with notch well above rounded posteroventral corner. Uropod 1 peduncle dorsolateral margin with 17 robust setae; outer ramus without large spines between robust setae. Uropod 2 inner ramus slightly constricted. Uropod 3 rami lanceolate; without plumose setae; outer ramus 1-articulate. Telson moderately cleft (about 41%).

Male (sexually dimorphic characters). Based on paratype male, 6.0 mm, AM P37380 (probably not fully mature). Antenna 1 flagellum with callynophore. Antenna 2 flagellum with calceoli. Gnathopod 2 palm with 1 lateral robust seta, without medial robust setae.

Etymology. Named for Diana Jones, carcinologist at the Western Australian Museum, in appreciation of her generous help with collections of Western Australian amphipods.

Remarks. *Amaryllis dianae* is most similar to other *Amaryllis* species with a serrate posterior margin on

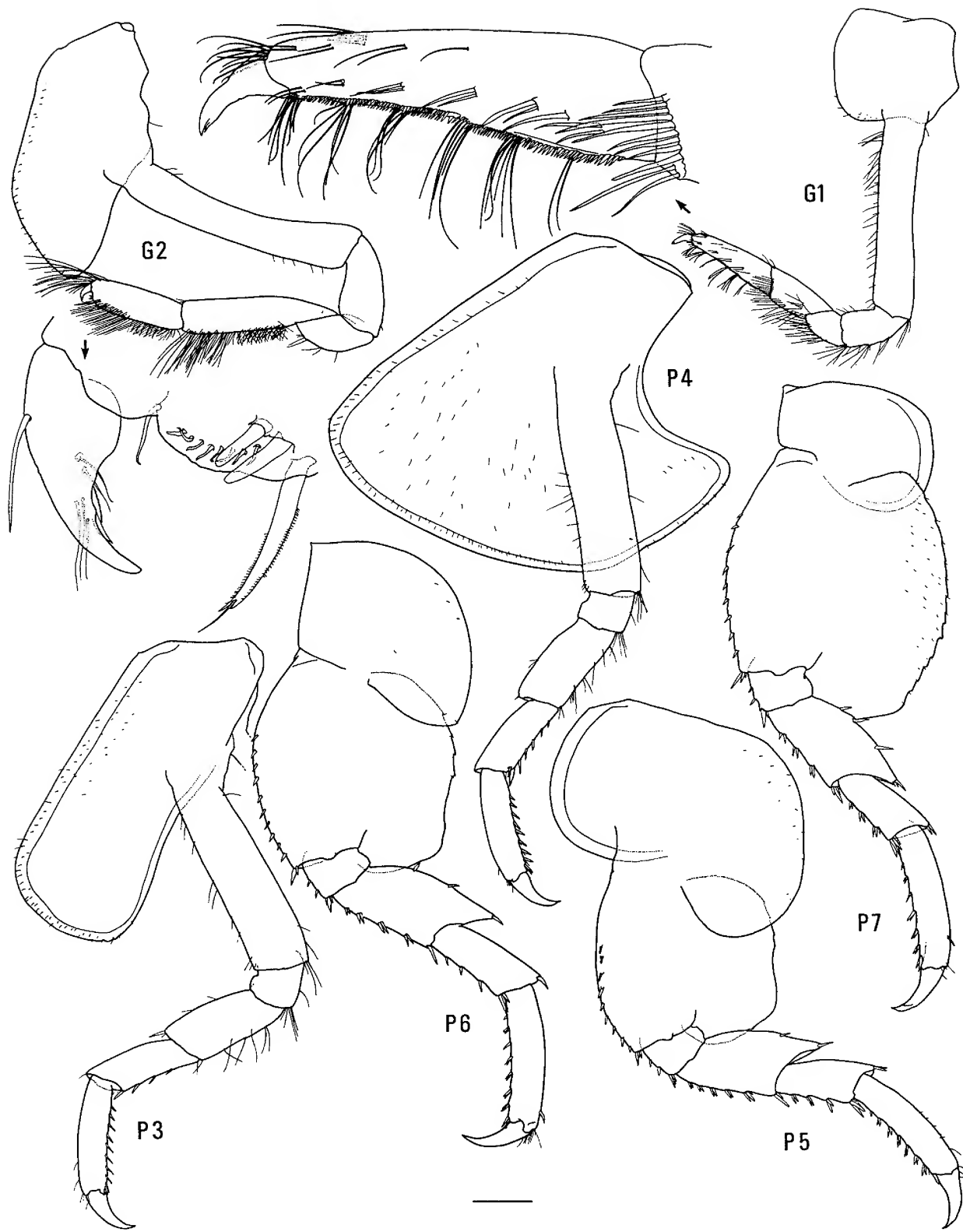


Figure 12. *Amaryllis dianae* n.sp., holotype female, 16.5 mm, AM P37378, Fremantle, Western Australia. Scales represent 0.5 mm.

epimeron 3, such as *A. carrascoi*, *A. croca*, *A. keablei* and *A. migo*. *Amaryllis dianae*, *A. carrascoi* and *A. migo* all have a notch above the posteroventral corner of epimeron 3; in *A. croca* and *A. keablei* the serrations extend to the posteroventral corner. The posteroventral corner of

pereopod 7 is rounded in *A. migo*, subquadrate in *A. dianae* and subquadrate with a distinct notch in *A. carrascoi*.

Distribution. Southern and southwestern Australia; 3–219 m depth.

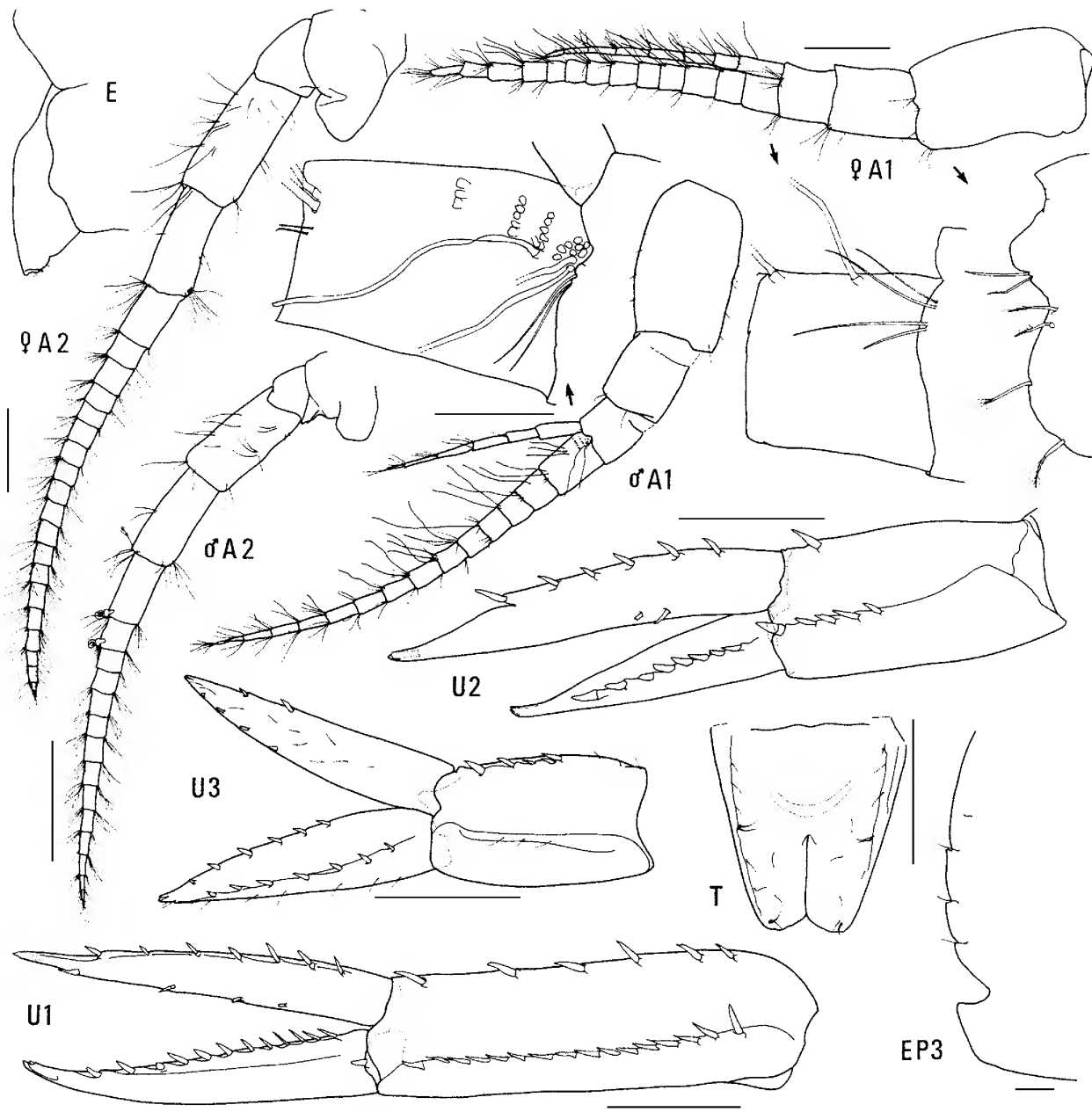


Figure 13. *Amaryllis dianae* n.sp., holotype female, 16.5 mm, AM P37378; paratype immature male, 6.0 mm, AM P37380; Fremantle, Western Australia. Scale for EP3 represents 0.1 mm; remainder represent 0.5 mm.

***Amaryllis kamata* n.sp.**

Figs. 14–16

Amaryllis macrophthalma. Stebbing, 1910a: 569 (in part).

Type material. HOLOTYPE, female, 9.2 mm, ovigerous (14 eggs), AM P37107; 1 PARATYPE, male, 6.2 mm, AM P37108; 44 PARATYPES, AM P37109; E of Long Reef, NSW, Australia, 33°46'S 151°43'E, dredged, 176 m, 5 December 1977, FRV *Kapala*, stn K77-23-01.

Additional material. NEW SOUTH WALES: 11 specimens, AM P2468, 6.5–10.5 km off Manning River, [approx. 31°57'S 152°46'E], 40 m, fine grey sand, trawl, 5 March 1898, HMCS *Thetis*, stn 28. 10 specimens, AM P37110, E of Newcastle, 32°53'S 152°35'E, 165 m, 15 August 1985, FRV *Kapala*, stn K85-12-23. 28 specimens, AM P59045, NE of Broken Bay, 33°22'S 152°04'E to 33°24'S 152°04'E, 181–112 m, benthic trawl, 11 February 1986, FRV *Kapala* stn K86-01-04. 1 specimen, AM P37111,

NE of Broken Bay, 33°29'S 152°06'E to 33°30'S 152°04'E, 492–523 m, trawl, 11 February 1986, FRV *Kapala*, stn K86-01-05. 2 specimens, AM P37395, SE of Broken Bay, 33°36'S 151°30'E to 33°37'S 151°29'E, 71–75 m, 10 February 1986, FRV *Kapala*, stn K86-01-02. 1 specimen, P37112, NE of Long Reef Point, 33°41'S 151°53'E, 366 m, 5 December 1977, FRV *Kapala*, stn K77-23-03. 114 specimens, AM P37113, E of Long Reef Point, 33°43'S 151°46'E to 33°44'S 151°56'E, 174 m, 20 December 1985, FRV *Kapala*, stn K85-21-08. 10 specimens, AM P37114, E of Bondi, 33°52'S 151°23'E, 80 m, 11 December 1980, FRV *Kapala*, stn K80-20-11. 2 specimens, AM P2469, 8–9.5 km off Coogee, [approx. 33°57'S 151°21.5'E], 90–91 m, fine sand, trawl, E.R. Waite, 15 March 1898, HMCS *Thetis*, stn 44. 1 specimen, AM P58759, Cape Banks, 34°00'S 151°16'E, 45–50 m, The Ecology Lab, November 1990, stn S2T3. 2 specimens, AM P5427, 4–6 km E of Botany Bay, [approx. 34°01'S 151°19'E], 60–102 m, trawl, F.A. McNeill & A. Livingstone, August 1921, ST *Goonambee*. 26 specimens, AM P2466, 2–3 km off Port Hacking, [approx. 34°03.5'S 151°12.5'E], 40–69 m, sandy, trawl, E.R. Waite, 10 March 1898, HMCS *Thetis*, stn 35. 34 specimens, AM P2464 and 10 specimens, AM P2465, 3–4 km off Botany Bay, [approx. 34°05'S 151°15'E], 91–95 m, mud, trawl, E.R. Waite, 11 March 1898, HMCS

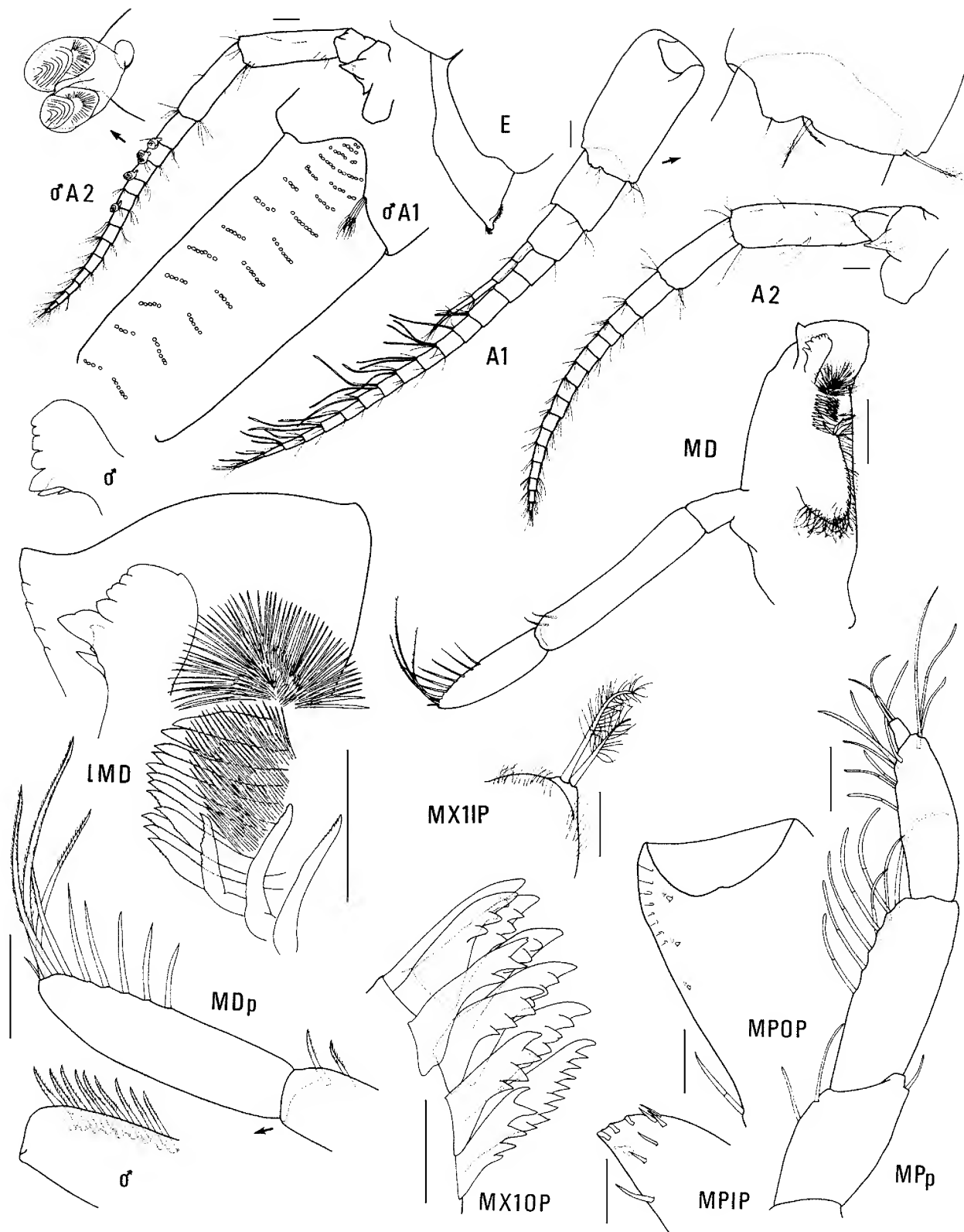


Figure 14. *Amaryllis kamata* n.sp., holotype female, 9.2 mm, AM P37107; paratype male, 6.2 mm, AM P37108; east of Long Reef, NSW. Scales for A1, 2 represent 0.1 mm; remainder represent 0.05 mm.

Thetis, stn 37. 64 specimens, AM P2467, 5.5–6.5 km off Wata Mooli [now Wattamolla], [approx. 34°10'S 151°11'E], 108–99 m, mud, trawl, E.R. Waite, 22 March 1898, HMCS *Thetis*, stn 57. 1 specimen, AM P37115, NE of Montague Island, 35°58'S 150°30'E to 36°03'S 150°27'E, 384 m, 21 November 1979, FRV *Kapala*, stn K79-18-07. BASS STRAIT: 7 specimens, AM P58116, eastern Bass Strait, 38°56.5'S 148°19.3'E, 80–

85 m, benthic sled, P.B. Berents, 27 August 1994, FRV *Southern Surveyor*, stn 05/94/59. 6 specimens, AM P58117, eastern Bass Strait, 38°59.1'S 148°31.6'E, 125 m, benthic sled, P.B. Berents, 27 August 1994, FRV *Southern Surveyor*, stn 05/94/60. TASMANIA: 1 specimen, AM E6526, Tasmanian coast, FIS *Endeavour* Collection.

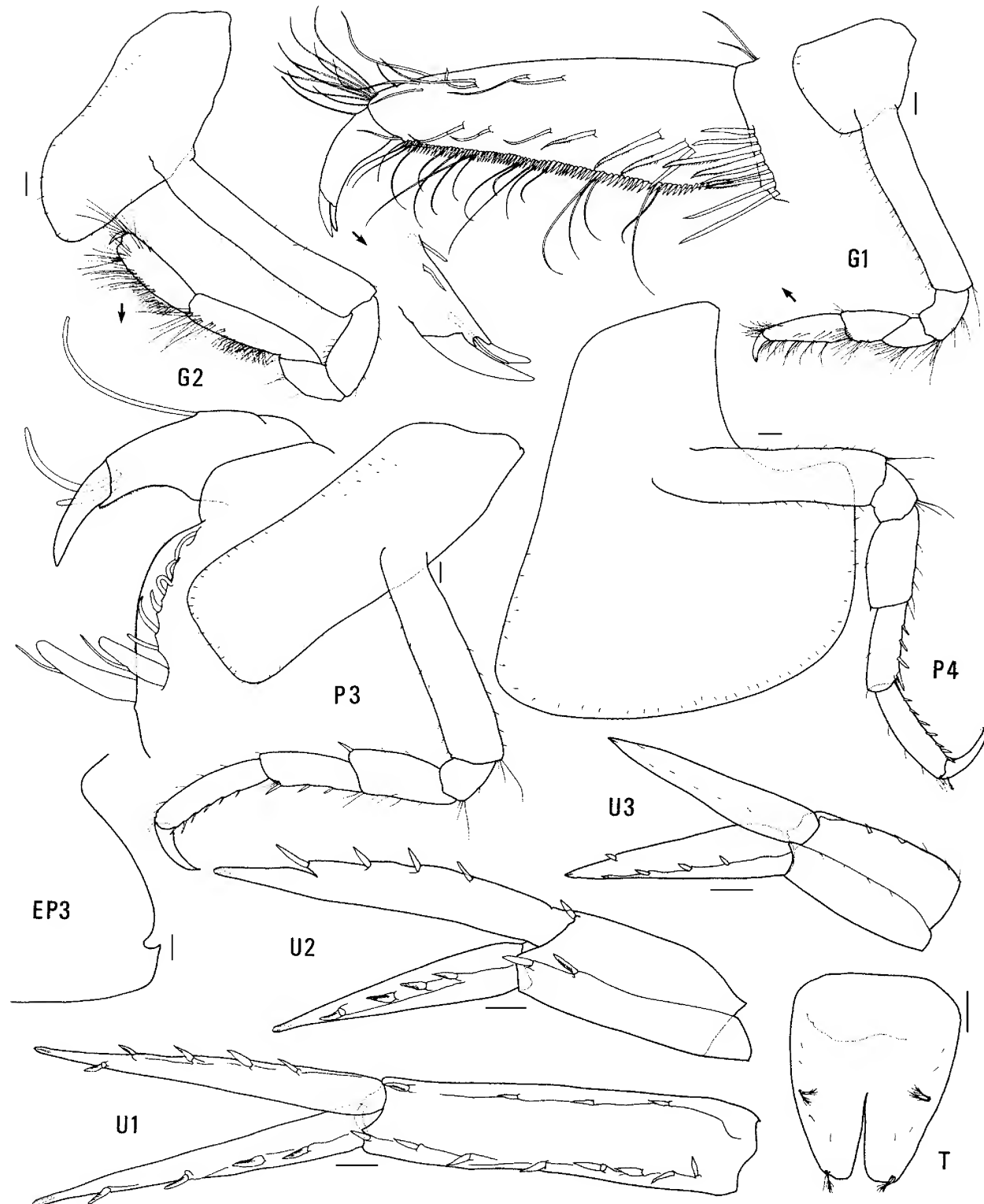


Figure 15. *Amaryllis kamata* n.sp., holotype female, 9.2 mm, AM P37107, east of Long Reef, NSW. Scales represent 0.1 mm.

Type locality. East of Long Reef, NSW, Australia, 33°46'S 151°43'E, 176 m depth.

Description. Based on holotype female, 9.2 mm, AM P37107. Head much deeper than long, anterior margin with notch extended into a slit; rostrum absent; eye present, elongate, reniform. Antenna 1 peduncular article 1 not ball-shaped proximally, distal margin with small medial spine;

peduncular article 2 medium length; flagellum without callynophore, calceoli absent. Antenna 2 flagellum about as long as that of antenna 1, without calceoli. Mouthpart bundle subconical. Epistome/upper lip with moderate mid-anterior angle with small depression above angle (lateral view). Mandible lacinia mobilis a stemmed, distally-cusped blade; accessory setal row with intermediate setae; palp article 2 with 2 posterodistal setae, article 3 without A3-

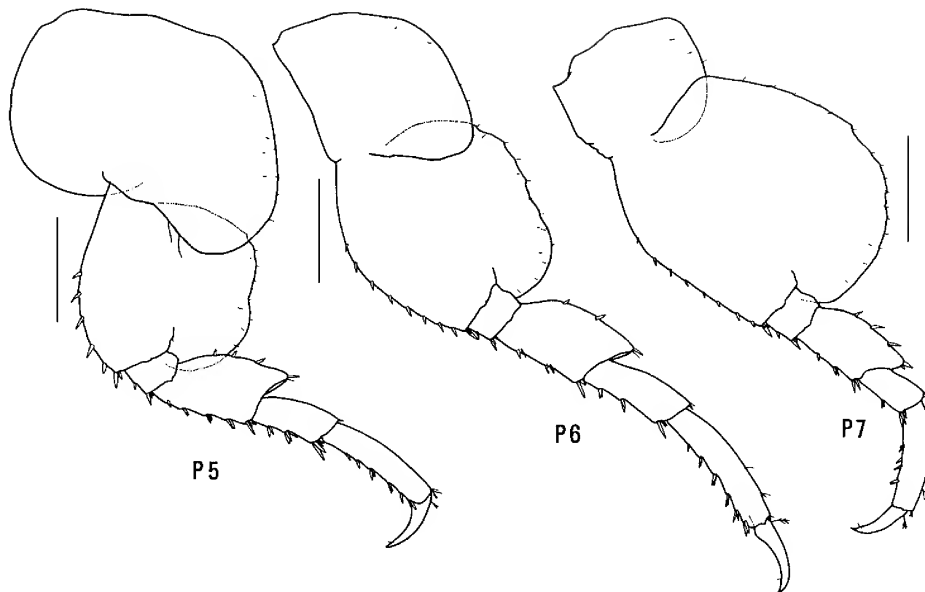


Figure 16. *Amaryllis kamata* n.sp., holotype female, 9.2 mm, AM P37107, east of Long Reef, NSW. Scales represent 0.5 mm.

seta. Maxilliped outer plate with distal margin smooth, medial margin without notch.

Gnathopod 1 carpus subequal in length to propodus (0.9×); propodus, posterior margin without robust setae. Gnathopod 2 palm slightly acute, with 1 lateral robust seta, 1 medial robust seta. Pereopods 3 and 4 merus and carpus without setal fringe. Pereopod 4 coxa with anterior and posterior margins subparallel, anteroventral corner rounded. Pereopods 5–7 with distal articles elongate, dactyls short and stocky. Pereopod 5 basis expanded posteriorly, rounded. Pereopod 7 basis rounded posteriorly, posteroventral corner rounded, posteroventral margin straight.

Epimeron 3 posterior margin smooth, with notch well above rounded posteroventral corner. Uropod 1 peduncle dorsolateral margin with 8 robust setae; outer ramus without large spines between robust setae. Uropod 2 inner ramus slightly constricted. Uropod 3 rami lanceolate; without plumose setae; outer ramus 1-articulate. Telson moderately cleft (about 43%).

Male (sexually dimorphic characters). Based on paratype male, 6.2 mm, AM P37108. Antenna 1 flagellum with callynophore, with calceoli. Antenna 2 flagellum with calceoli. Mandible palp article 2 with 9 posterodistal setae. Gnathopod 2 palm with no lateral robust setae and 1 medial robust seta.

Etymology. The specific name is contrived and has no special meaning.

Remarks. *Amaryllis kamata* belongs to the group of species with a smooth posterior margin on epimeron 3 and a rounded posteroventral corner on the basis of pereopod 7. Within this group it is most similar to *A. brevicornis* but differs in the shape of the epistome/upper lip and the length of the gnathopod 1 carpus.

Habitat. *Amaryllis kamata* is known from sand and mud bottoms off the New South Wales coast. It is the deepest-occurring species (50 to 525 m depth) of *Amaryllis* known from Australian waters.

Distribution. Southeastern Australia; 40–523 m depth.

Amaryllis keablei n.sp.

Figs. 17–19

Amaryllis macrophtalma.—Chilton, 1921: 55 (in part).—J.L. Barnard, 1972: 262, fig. 156 (in part, figs. of female "n"). *Amaryllis* sp. 1.—Hutchings *et al.*, 1989: 362.

Type material. HOLOTYPE, female, 20.5 mm, ovigerous (23 eggs), NMV J3765, 23 km east of Cape Rochon, Three Hummock Island, central Bass Strait, Tasmania, Australia, 40°22.2'S 145°17'E, 40 m, sand, epibenthic sled, M. Gomon & G.C.B. Poore, 3 November 1980, FRV *Sarda*, stn BSS 112. 3 PARATYPES, female, NMV J13946; 3 PARATYPES, female, AM P37100; 9 km SSW of Cape Adansan, Three Hummock Island, central Bass Strait, Tasmania, Australia, 40°30.9'S 144°56'E, 27 m, very coarse sand, epibenthic sled, M. Gomon & G.C.B. Poore, 2 November 1980, FRV *Sarda*, stn BSS 109.

Additional material. NEW SOUTH WALES: 1 specimen, NMV J13947, Port Stephens, [approx. 32°42'S 152°06'E], O.A. Sayce Collection. 2 specimens, AM P37101, Port Jackson. 1 specimen, AM P37180, Port Jackson [was part of *Amaryllis brevicornis* syntype series, AM G5417]. 2 specimens, AM P36700, Quarantine Bay side of Murrumbulga Point, Twofold Bay, 37°04.7'S 149°53.1'E, 3 m, subtidal breakwater wall, S. Keable & P. Hutchings, 17 September 1985, stn FIRTA Q9-Q11. 1 male (illustrated), AM P37102, Munganno Point, Twofold Bay, 37°06.2'S 149°55.7'E, 7 m, sublittoral rock platform, P. Hutchings, 10 October 1984, stn FIRTA M3. VICTORIA: 2 females, NMV J13948, Crawfish Rock, Western Port, 14 m. 4 specimens, NMV J13949, Western Port. 2 females, NMV J3789, Western Port, 28 April 1968, stn D/1/11. 1 specimen, NMV J13950, Crib Point, Western Port, 38°20.83'S 145°13.49'E, 13 m, sandy gravel, 23 March 1965, stn CPBS 32N. 3 females, NMV J3241, Port Phillip Bay, stn 25. 1 ovigerous female, NMV J13951, Port Phillip Bay, stn 26. 1 female, NMV J3262, mouth of Werribee River to centre of Bay, Port Phillip Bay, W. Williams, 20 March 1963, stn 25, area 9 to 19. 1 specimen, AM P38945, Ricketts Point, Port Phillip Bay, [approx. 37°58'S 144°54'E], 2 m, rock shelf, N. Coleman, 21 June 1979, AMPI Crust No. 899. BASS STRAIT: 1 specimen, NMV J13952, 33 km S of Deal Island, Tasmania, Central Bass Strait, 39°47.3'S 147°19.3'E, 60 m, muddy sand, epibenthic sled, R. Wilson, 14 November 1981, RV *Tangaroa*, stn BSS-161. TASMANIA: 1 specimen, AM P37103, Derwent Estuary, D'Entrecasteaux Channel, March 1940, Tasmanian Biological Survey, Fisheries Department, stn OL81. 1 specimen, AM P5913, Tasmanian Coast, FIS *Endeavour*. SOUTH AUSTRALIA: 1 specimen, SAMA C5980, Dangerous

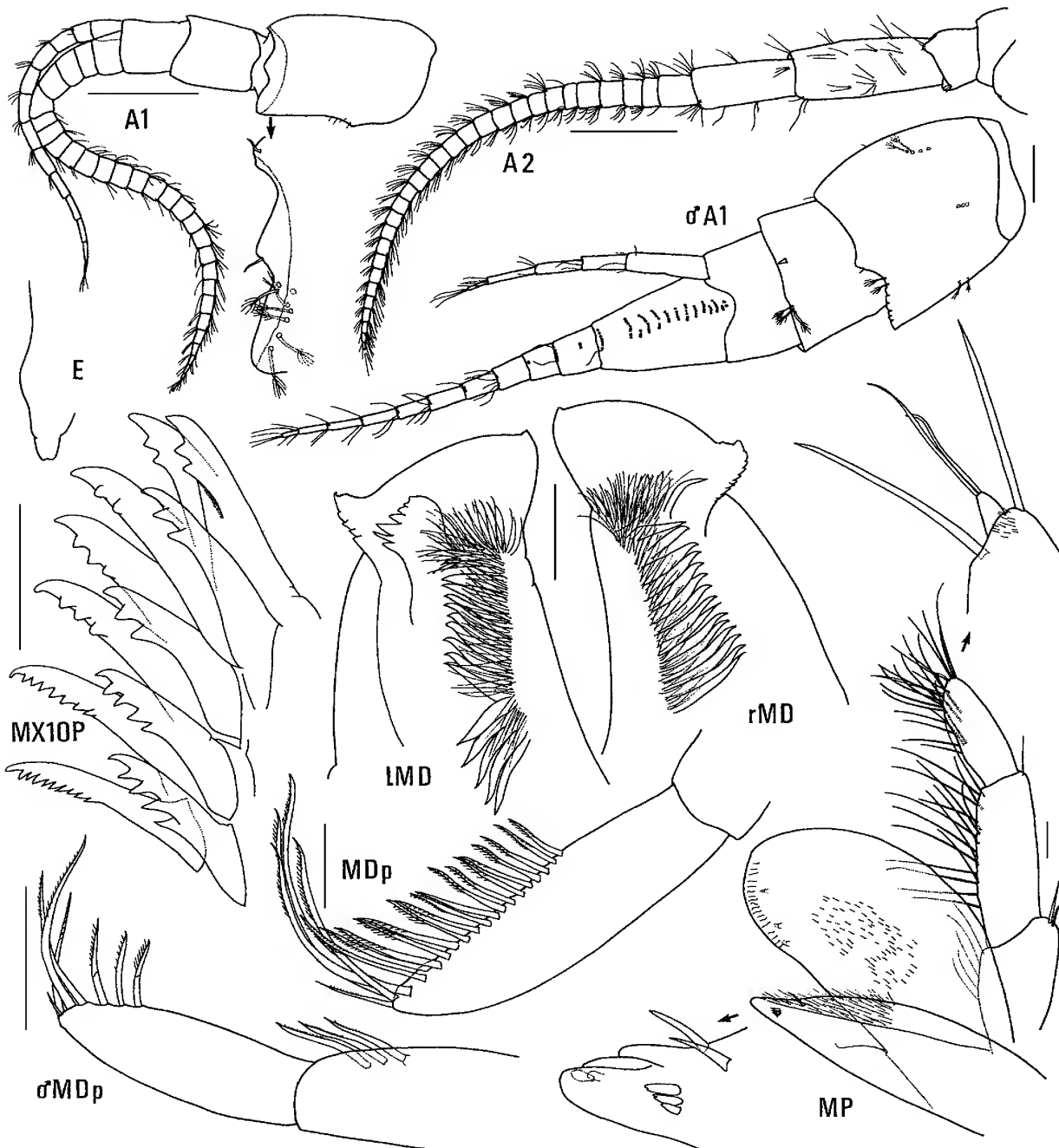


Figure 17. *Amaryllis keablei* n.sp., holotype female, 20.5 mm, NMV J3765, Bass Strait; male, 5.8 mm, AM P37102; Twofold Bay, NSW. Scales for A1, 2 represent 0.5 mm; remainder represent 0.1 mm.

Reef, Spencer Gulf, [approx. 34°49'S 136°12'E], dredged, K. Sheard. 1 specimen, NMV J13953, The Hotspot Reef, W of Flinders Island, 33°40.8'S 134°22.5'E, 21 m, erect hard bryozoan on vertical rock face, G.C.B. Poore, 20 April 1985, stn NMV SA-71. 2 females, AM P37104, Marino, Gulf St Vincent, [approx. 35.03'S 138°30'E], W.H. Baker, 1910. 1 specimen, AM P37105, Port Adelaide, Gulf St Vincent, [approx. 34°50'S 138°30'E], H.M. Hale, 1924. 1 female, AM P37106, 19 km from Mount Young toward Wallaroo, Spencer Gulf, [approx. 33°18'S 137°31'E], 18 m, K. Sheard, 8 March 1938, FL Whyalla.

Type locality. 23 km east of Cape Rochon, Three Hummock Island, central Bass Strait, Tasmania, Australia, 40°22.2'S 145°17'E, 40 m depth.

Description. Based on holotype female, 20.5 mm, NMV J3765. Head much deeper than long, anterior margin with

notch extended into a slit; rostrum absent; eye present, elongate, reniform. Antenna 1 peduncular article 1 not ball-shaped proximally, distal margin with small medial spine; peduncular article 2 medium length; flagellum without callynophore, calceoli absent. Antenna 2 flagellum about as long as that of antenna 1, without calceoli. Mouthpart bundle subconical. Epistome/upper lip with strong mid-anterior angle (lateral view). Mandible lacinia mobilis a stemmed, distally-cusped blade; accessory setal row with intermediate setae; palp article 2 without posterodistal setae, article 3 without A3-seta. Maxilliped outer plate with distal margin smooth, medial margin deeply notched.

Gnathopod 1 carpus subequal in length to propodus; propodus, posterior margin without robust setae. Gnathopod

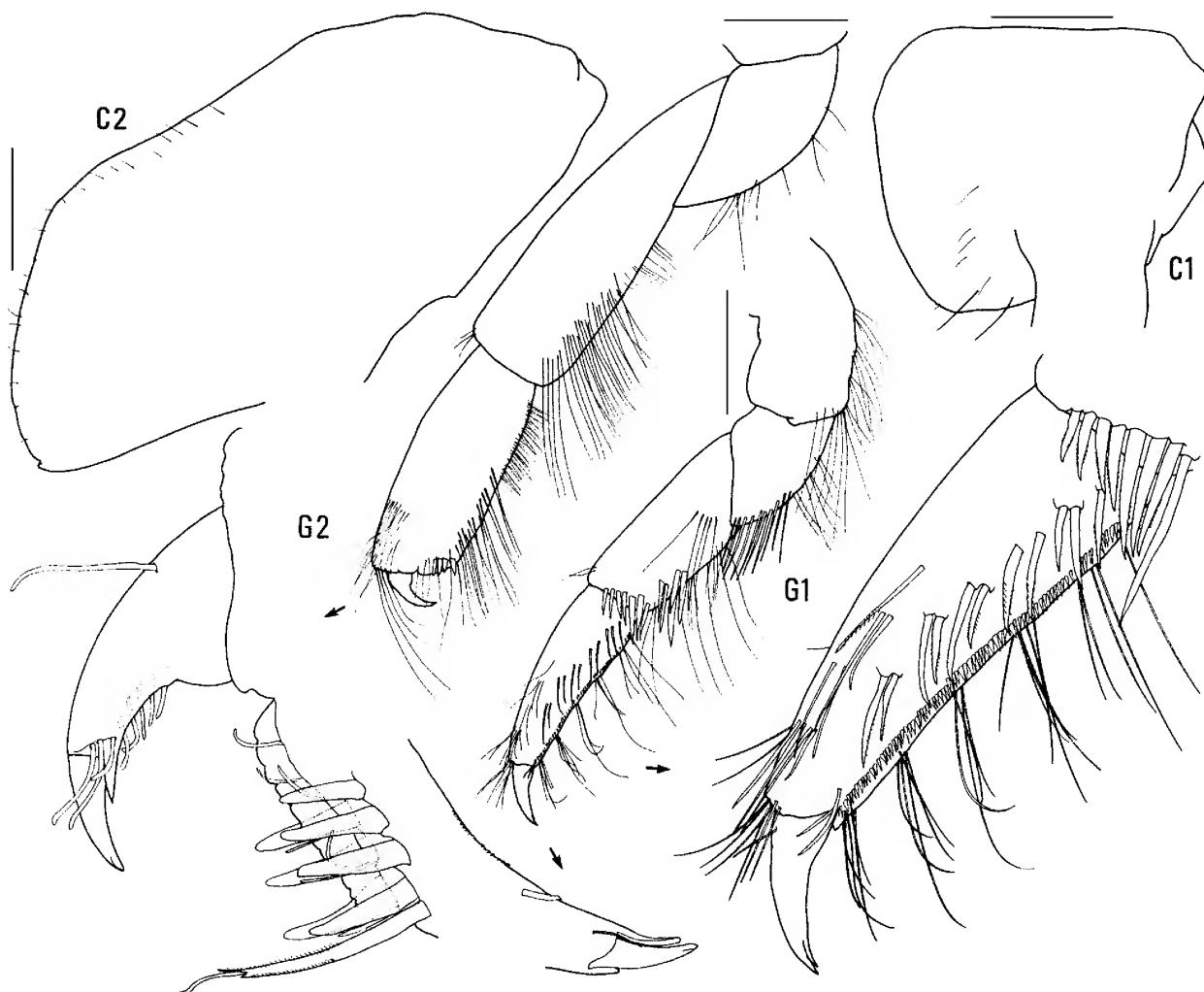


Figure 18. *Amaryllis keablei* n.sp., holotype female, 20.5 mm, NMV J3765, Bass Strait. Scales represent 0.5 mm.

2 palm slightly acute, with 3–4 lateral robust setae, 4 medial robust setae. Pereopods 3 and 4 merus and carpus without setal fringe. Pereopod 4 coxa with anterior and posterior margins subparallel, anteroventral corner rounded. Pereopods 5–7 with distal articles elongate, dactyls short and stocky. Pereopod 5 basis expanded posteriorly, rounded. *Pereopod 7 basis subrectangular, posteroventral corner subquadrate, posteroventral margin straight.*

Epimeron 3 posterior margin serrate, without notch. Uropod 1 peduncle dorsolateral margin with 17 robust setae; outer ramus without large spines between robust setae. Uropod 2 inner ramus slightly constricted. Uropod 3 rami lanceolate; without plumose setae; outer ramus 1-articulate. Telson moderately cleft (about 37%).

Male (sexually dimorphic characters). Based on male, 5.8 mm, AM P37102 (probably not fully mature). Antenna 1 flagellum with callynophore. Antenna 2 flagellum with calceoli. Mandible palp article 2 with 3 posterodistal setae.

Etymology. Named for Stephen Keable in recognition and appreciation of his meticulous work in producing illustrations of amphipods.

Remarks. *Amaryllis keablei* is similar to other *Amaryllis* species with a serrate posterior margin on epimeron 3, such

as *A. carrascoi*, *A. croca*, *A. dianae* and *A. migo*. It is most similar to *A. croca* in that the serrations extend to the posteroventral corner. *Amaryllis keablei* differs from *A. croca* in having a strong mid-anterior angle on the epistome/upper lip, a small medial spine on peduncular article 1 of antenna 1, no posterodistal setae on mandibular palp article 2 of the female and 3 to 4 lateral robust setae on the palm of female gnathopod 2.

Distribution. Southeastern and southern Australia, from Port Stephens on the east coast to the South Australian Gulfs; 2–60 m depth.

Amaryllis macrophthalmus Haswell

Figs. 20–22

Amaryllis macrophthalmus Haswell, 1879: 253, pl. 8 fig. 3.—Haswell, 1882: 227.—Della Valle, 1893: 781 (in part).—J.L. Barnard, 1974: 140.—Barnard & Karaman, 1991: 461.—Springthorpe & Lowry, 1994: 129.

Amaryllis macrophthalmus.—Stebbing, 1906: 24 (in part).—Chilton, 1921: 55 (in part).—Guiler, 1952: 28.—J.L. Barnard, 1958: 88.—J.L. Barnard, 1972: 262, figs. 156–158 (in part).—Poore *et al.*, 1975: 34, 67 (in part).

not *Glycerina affinis* Chilton, 1885: 1036, pl. 47 fig. 1.—Della Valle, 1893: 849.

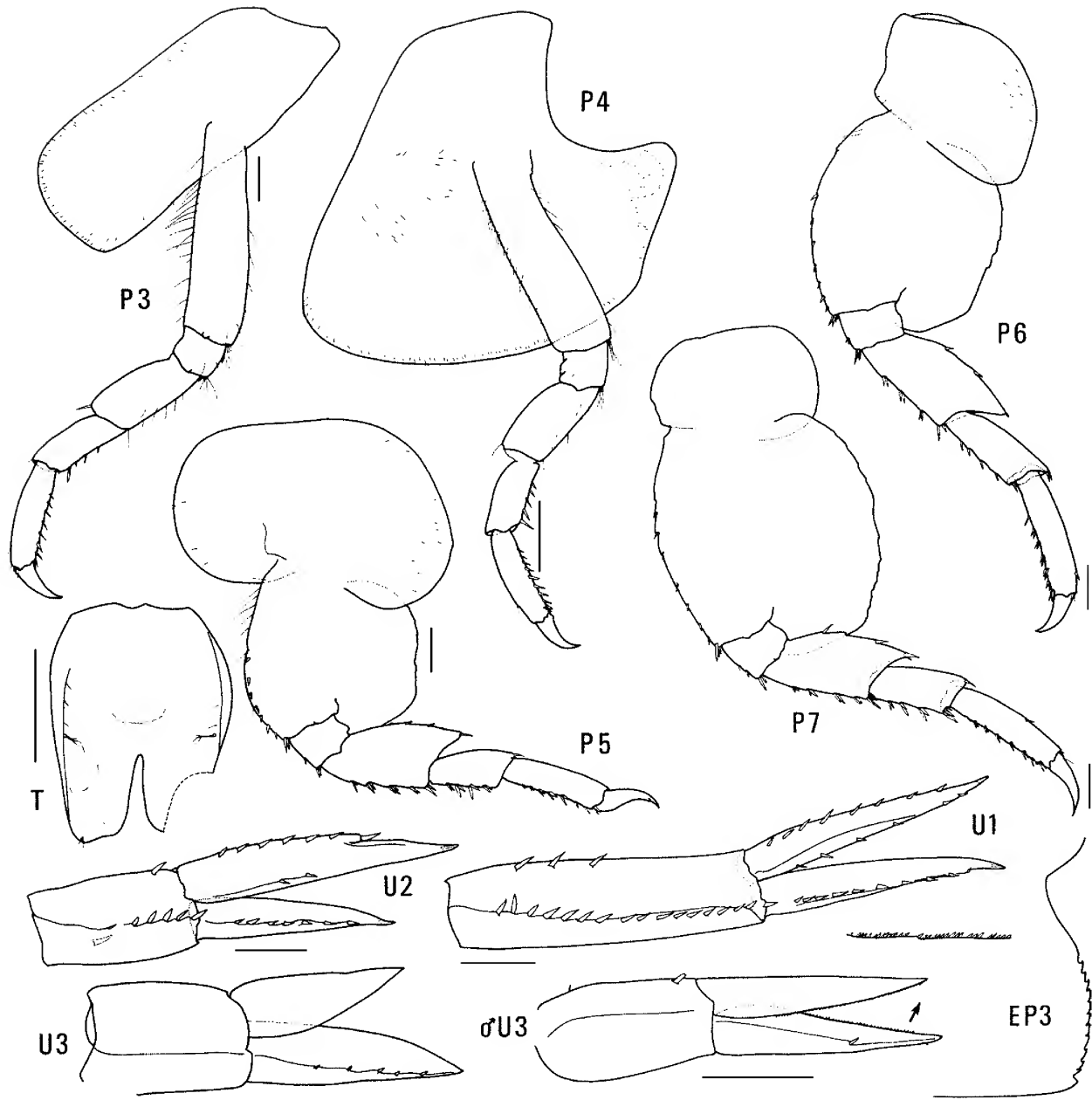


Figure 19. *Amaryllis keablei* n.sp., holotype female, 20.5 mm, NMV J3765, Bass Strait. Scales represent 0.5 mm.

possibly *Amaryllis macrophthalma*.—Hale, 1929: 208.—Sheard, 1937: 18 (list).—Sergeev *et al.*, 1988: 102 (table 1).
 not *Amaryllis macrophthalma*.—Stebbing, 1888: 706, pl. 29.—Thomson, 1902: 463.—Hutton, 1904: 258.—Chilton, 1906: 267.—Stebbing, 1908: 67.—Stebbing, 1910b: 448.
 not *Amaryllis macrophthalma*.—Walker, 1909: 327.—Stebbing, 1910a: 569, 633 (= *A. kamata* and *B. endota*).—Chilton, 1912: 463.—K.H. Barnard, 1916: 114.—Schellenberg, 1926: 243.—Schellenberg, 1931: 10.—K.H. Barnard, 1932: 34.—Pirlot, 1933: 122.—K.H. Barnard, 1937: 141.—Pirlot, 1939: 73.—K.H. Barnard, 1940: 514 (list).—Grindley & Kensley, 1966: 8.—Day *et al.*, 1970: 50.—Griffiths, 1973: 292.—Griffiths, 1974a: 199.—Griffiths, 1974b: 247.—Griffiths, 1974c: 308.—Griffiths, 1975: 144.—Griffiths, 1976: 56, fig. 31A, B.—Lowry & Bullock, 1976: 83.—Griffiths, 1977: 107.—Kensley & Penrith, 1977: 189 (list).—Ledoyer, 1978: 304.—Ledoyer, 1979: 112, fig. 71.—Ledoyer, 1986: 718, fig. 275.—Alonso, 1987: 2, figs. 1–15.—Gonzalez, 1991: 58.
 not *Amaryllis*?*macrophthalma*.—Lyons & Myers, 1991: 614, fig. 13.

Type material. NEOTYPE, female, 21.5 mm, ovigerous (14 eggs), AM P37214, Derwent Estuary, D'Entrecasteaux Channel, Tasmania, Australia, [approx. 42°54'S 147°23'E], Fisheries Department, March 1940, Tasmanian Biological Survey, Station OL 81.

Haswell (1879) did not designate type material for *A. macrophthalma*, but he indicated that material examined by him was held in the Macleay Museum, University of Sydney. This material is now either lost or no longer exists (see J.L. Barnard, 1974: 139–140 and Springthorpe & Lowry, 1994: 129, for further discussion of Haswell's material). We are establishing a neotype for two reasons: *Amaryllis macrophthalma* is the type species of the genus (selected by Pirlot, 1933) and as such must be clearly and adequately established; we now recognize many species in the genus *Amaryllis* and a neotype is needed to clearly

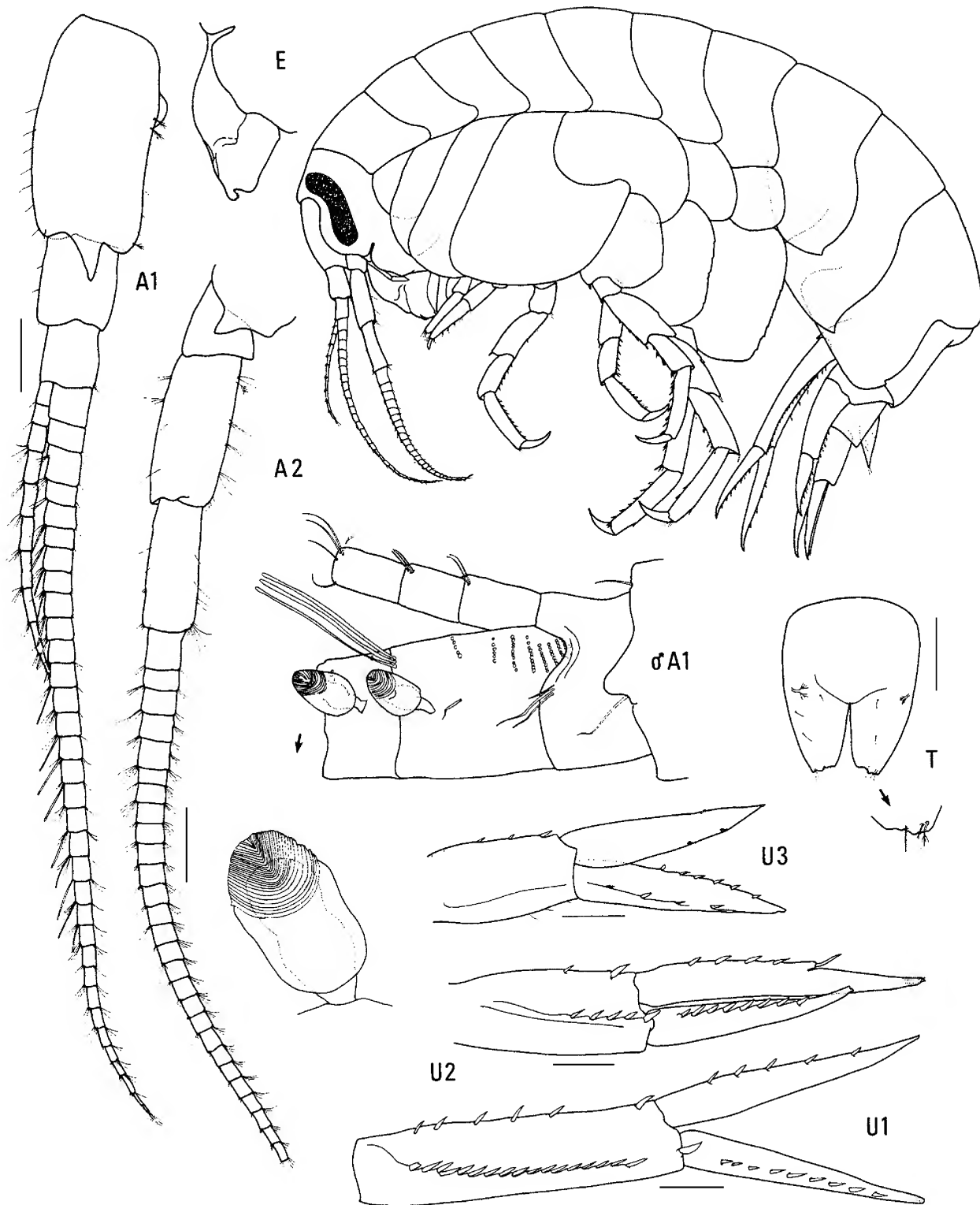


Figure 20. *Amaryllis macrophthalma* Haswell, neotype female, 21.4 mm, AM P37214; male, 17.8 m, AM P37215; Derwent Estuary, Tasmania. Scales represent 0.5 mm.

distinguish *A. macrophthalma* from several closely related species.

The original locality for *A. macrophthalma* was given as "Tasmania". There is no extant material of *A. macrophthalma* from Tasmania in the Macleay Museum or the Australian Museum which could have been examined by

Haswell. We have examined material from Tasmania which includes at least three species. From Haswell's rather poor description and figures two characters, when taken together, are diagnostic: the square (rather than rounded) posterior margin of the basis of pereopod 7 (pl. 8 fig. 3) and the large size of the species ("nine-and-a-half lines" or approx. 20

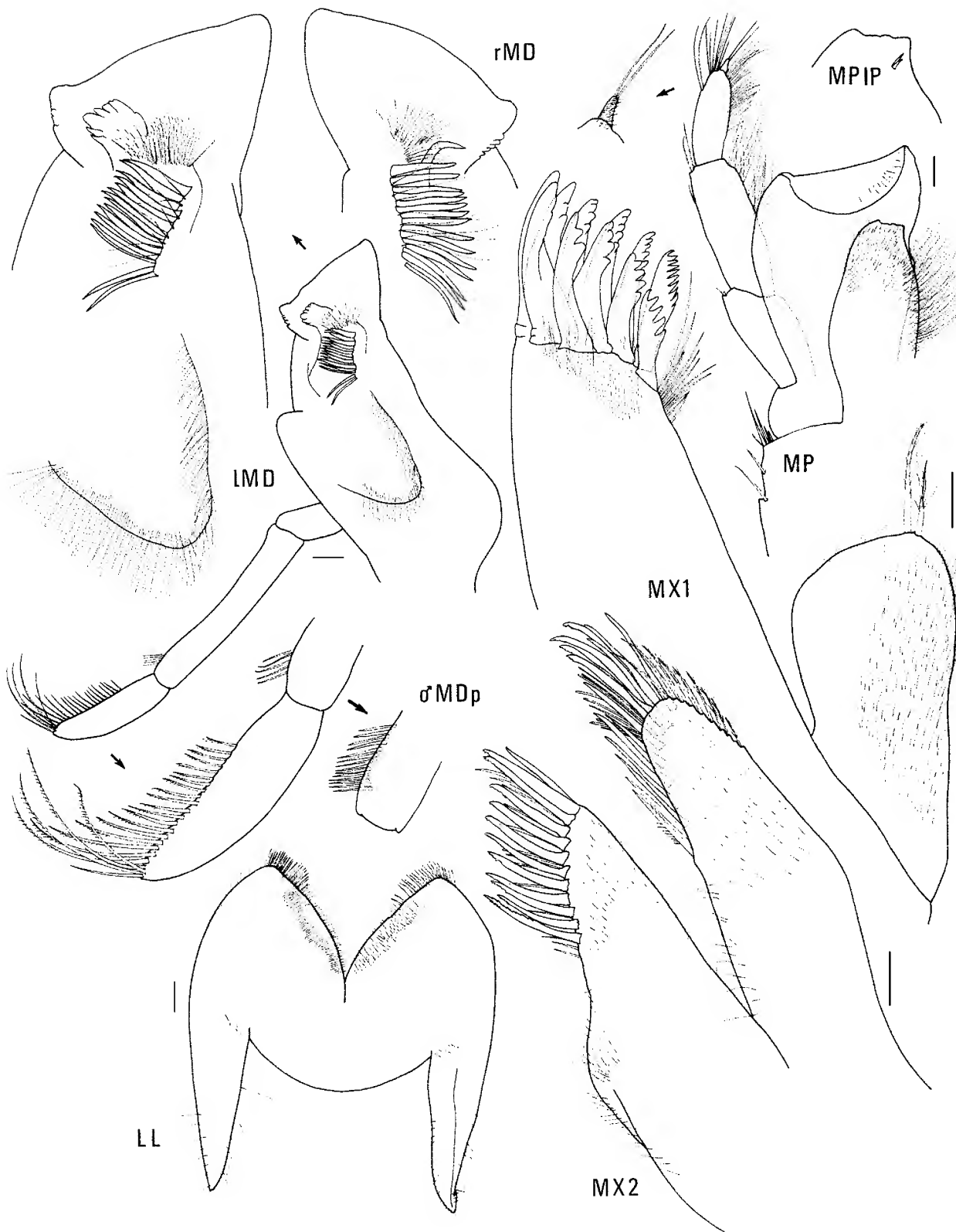


Figure 21. *Amaryllis macrophthalma* Haswell, neotype female, 21.4 mm, AM P37214; male, 17.8 m, AM P37215; Derwent Estuary, Tasmania. Scales represent 0.1 mm.

mm). These characters are the basis for our neotype selection.

Additional material. NEW SOUTH WALES: 3 females and 1 immature male, AM P37211, Port Jackson, [approx. 33°52'S 151°13'E], [from AM Old Collection]. 1 female, AM P18203, 8 km E of Green Cape, [approx. 37°16'S 150°08'E], 82 m, K. Moller, May 1930. 3 females, AM P18332,

19–35 km NE of Green Cape, [approx. 37°00'S 150°08'E], 71–84 m, A.A. Livingstone & H.O. Fletcher, June 1924, *Goonambee*. VICTORIA: 1 female, AM P18268, SW of Point Hicks, 37°55'S 149°00'E, 77 m, R.J. MacIntyre, 20 June 1962, HMAS *Gascoyne*, stn G2/61/6. 13 specimens, NMV J11545, Bennison Channel, Corner Inlet, 38°49'S 146°23'E, 6 m, sand and shell grit, airlift, G.J. Morgan, 23 November 1983, stn CIN 28E. 2 specimens, NMV J3793, Crawfish Rock, Western Port, 14 m. 34

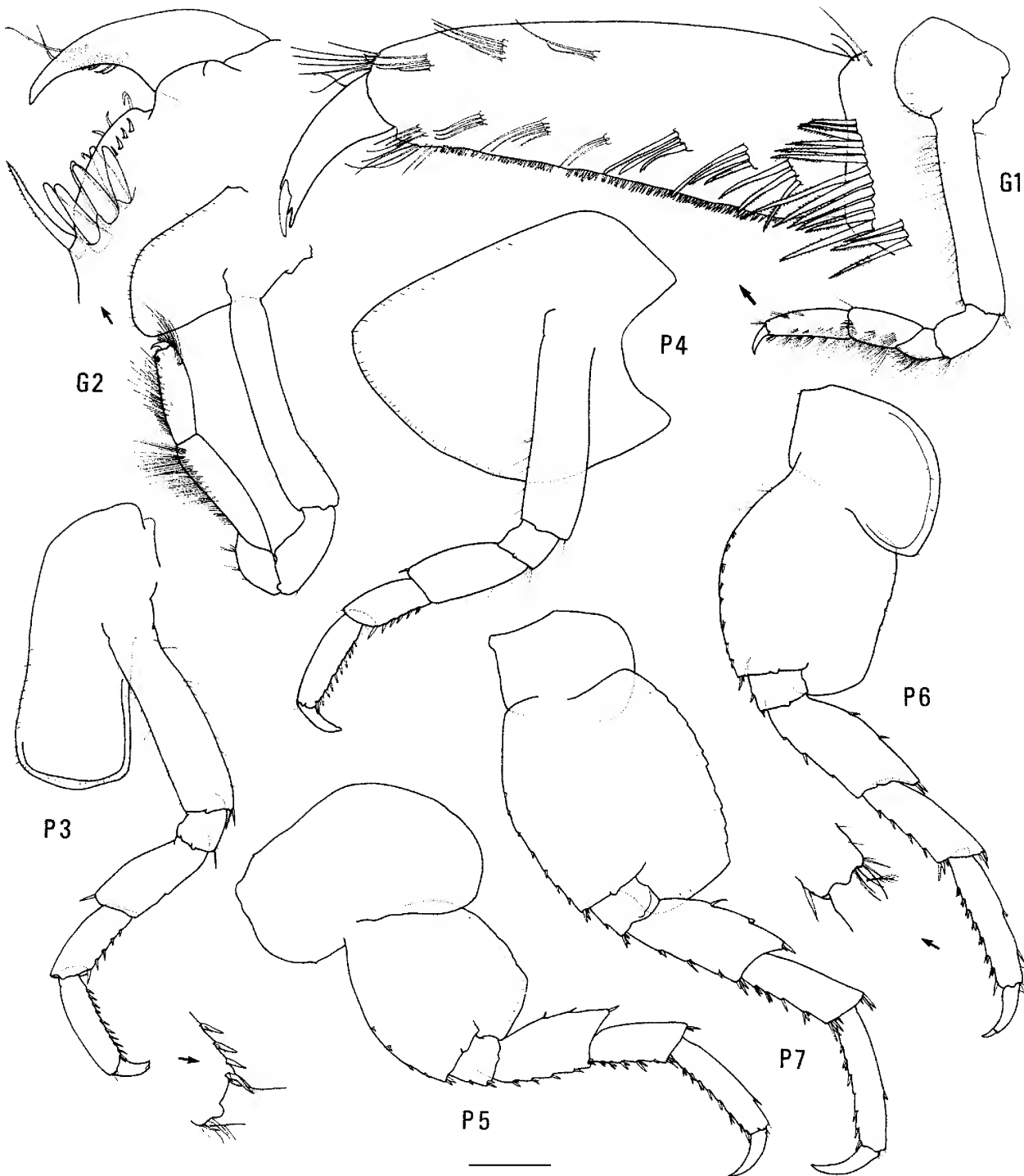


Figure 22. *Amaryllis macrophthalma* Haswell, neotype female, 21.4 mm, AM P37214, Derwent Estuary, Tasmania.
Scales represent 0.5 mm.

specimens, AM P37400, NMV J3325, NMV J3792 and J3795 to J3797, unknown localities in Western Port. 64 specimens from various localities in Port Phillip Bay, under the following registration numbers: NMV J3236 (1), J3237 (4), J3240 (2), J3242 (1), J3243 (4), J3246 (4), J3249 (1), J3250 (1), J3251 (4), J3252 (2), J3253 (1), J3255 (1), J3257 (1), J3258 (1), J3260 (6), J3264 (1), J3265 (1), J3266 (5), J3267 (9), J3268 (1), J3273 (4), J3332 (8), J3333 (1). BASS STRAIT: 48 specimens, AM E5674; 28 specimens, AM P2326; E of Flinders Island, eastern Bass Strait, [approx. 40°01'S 148°02'E], FIS *Endeavour* collection. 5 specimens, AM E6524 and 5 specimens, AM P5914, eastern slope, Bass Strait, FIS *Endeavour* collection. 1 specimen, NMV J7655, 42 km SSW of Lakes Entrance, Victoria, eastern Bass Strait, 38°18.5'S 147°37.5'E, 46 m, muddy fine shell, otter trawl, M. Gomon & R. Wilson, 31 July 1983, FV *Silver Gull*,

stn BSS-210. 10 specimens, NMV J13995, 8 km S of South East Point, Wilsons Promontory, Victoria, central Bass Strait, 39°12.9'S 146°27.3'E, 65 m, medium sand, epibenthic sled, R. Wilson, 18 November 1981, RV *Tangaroa*, stn BSS-180. 1 specimen, NMV J13994, 43 km SE of Port Albert, Victoria, eastern Bass Strait, 38°53.7'S 147°06.5'E, 58 m, coarse shell, R. Wilson, 18 November 1981, RV *Tangaroa*, stn BSS-177. 1 specimen, NMV J13993, 33 km S of Deal Island, Tasmania, Central Bass Strait, 39°47.3'S 147°19.3'E, 60 m, muddy sand, epibenthic sled, R. Wilson, 14 November 1981, RV *Tangaroa*, stn BSS-161. 4 specimens, NMV J13992, 57 km S of Rodondo Island, central Bass Strait, 39°46.0'S 146°18.0'E, 80 m, muddy shell, epibenthic sled, R. Wilson, 13 November 1981, RV *Tangaroa*, cruise 81-T-1, stn BSS-159. 4 specimens, NMV J7612, 39 km NNE of Devonport, central Bass Strait, 40°49.8'S 146°31.3'E

to 40°48.2'S 146°33.7'E, 68–70 m, mud, otter trawl, M.F. Gomon, G.C.B. Poore & C.C. Lu, 4 February 1981, FRV *Hai Kung*, stn BSS-135. 11 specimens, NMV J13991, 5 km N of North Point, central Bass Strait, 40°40.3'S 145°15'E, 33 m, medium shell, epibenthic sled, M. Gomon and G.C.B. Poore on FRV *Sarda*, 4 November 1980, stn BSS 115. 7 specimens, NMV J11263, 47 km E of Cape Rochon, Three Hummock Island, central Bass Strait, 40°23.8'S 145°32'E, 65 m, muddy sand, epibenthic sled, M. Gomon & G.C.B. Poore, 3 November 1980, stn BSS-113. 17 specimens, NMV J13990, 23 km E of Cape Rochon, Three Hummock Island, central Bass Strait, 40°22.2'S 145°17'E, 40 m, sand, epibenthic sled, M. Gomon & G.C.B. Poore, 3 November 1980, FRV *Sarda*, stn BSS 112. 4 specimens, NMV J2312, 5 km E of Cape Edie, Robbins Island, central Bass Strait, 40°41.8'S 145°07'E, 16 m, fine shelly sand, M. Gomon & G.C.B. Poore, 3 November 1980, FRV *Sarda*, stn BSS-110. 63 specimens, NMV J13989, 9 km SSW of Cape Adansan, Three Hummock Island, central Bass Strait, 40°30.9'S 144°56'E, 27 m, very coarse sand, epibenthic sled, M. Gomon & G.C.B. Poore, 2 November 1980, FRV *Sarda*, stn BSS 109. 23 specimens, NMV J2320 and 10 specimens, AM P37399, 28 km E of Cape Farewell, King Island, central Bass Strait, 39°32.8'S 144°16'E, 18 m, fine sand, epibenthic sled, M. Gomon & G.C.B. Poore, 1 November 1980, FRV *Sarda*, stn BSS-107. 2 specimens, NMV J11253, 59 km W of Stokes Point, King Island, western Bass Strait, 40°07'S 143°14'E, 185 m, sandy mud, grab, G.C.B. Poore, 11 October 1980, HMAS *Kimbla*, stn BSS-104. TASMANIA: 1 male, AM E5680; 6 specimens, AM P5921; and 7 specimens, AM P18323; 16 km N of Circular Head, [approx. 40°40'S 145°18'E], 146–219 m, FIS *Endeavour* collection. 1 specimen, NMV J13997, 500 m W of Darlington, Maria Island, 42°35'S 148°02'E, 30 m, algal and drift holdfast fauna, trawl, R.S. Wilson, 23 April 1985, RV *Challenger*, NMV stn TAS-27. 1 specimen, NMV J13998, same locality, 30 m, NMV stn TAS-33. 1 specimen, NMV J14000, E of Maria Island, 42°36'S 148°10'E, 75 m, fine bryozoans and shell, epibenthic sled, R.S. Wilson, 23 April 1985, RV *Challenger*, NMV stn TAS-30. 9 specimens, AM P37213, entrance to Oyster Bay, Maria Island, [approx. 42°41'S 148°02'E], 29 July 1909, K. Sheard Collection. 2 specimens, AM E6603, off Maria Island, 143 m, FIS *Endeavour* collection. 1 male, AM P37215 (illustrated specimen) and 5 females, AM P37216, type locality. 2 specimens, SAMA C5981, off Gordon, D'Entrecasteaux Channel, [approx. 43°16'S 147°14'E], CSIR, 20 October 1938. 5 specimens, NMV J13999, 2.5 km SE of Birches Bay, D'Entrecasteaux Channel, 43°11'S 147°16'E, 10 m, lip dredge, R.S. Wilson, 16 April 1985, RV *Penghana*, NMV stn TAS-1. 7 specimens, AM P37212, D'Entrecasteaux Channel, 9 m, dredged on scallop banks, K. Sheard Collection. SOUTH AUSTRALIA: 6 specimens, AM P59046, Nepean Bay, Kangaroo Island, [approx. 35°42'S 137°37'E], dredged, F. Moorhouse, May 1938. 1 specimen, SAMA C5982, 8 miles W of Hallett Cove, Gulf St Vincent, [approx. 35°05'S 138°30'E], tow net, H.M. Hale & K. Sheard, 14 April 1945. 3 specimens, SAMA C5983, Dangerous Reef, Spencer Gulf, [approx. 34°49'S 136°12'E], dredged, K. Sheard. 11 specimens, AM P59047, unknown locality in Spencer Gulf and/or Gulf St Vincent.

Type locality. Derwent Estuary, D'Entrecasteaux Channel, Tasmania, Australia, [approx. 42°54'S 147°23'E].

Description. Based on neotype, female, 21.5 mm, ovigerous (14 eggs), AM P37214. Head much deeper than long, anterior margin with notch extended into a slit; rostrum absent; eye present, elongate, reniform. *Antenna 1* peduncular article 1 not ball-shaped proximally, distal margin with well-developed medial spine; peduncular article 2 medium length; flagellum without callynophore, calceoli absent. Antenna 2 flagellum about as long as that of antenna 1, without calceoli. Mouthpart bundle subconical. *Epistome/upper lip with broad mid-anterior bulge (lateral view).* Mandible lacinia mobilis a stemmed, distally-cusped blade; accessory setal row with intermediate setae; palp article 2 with 5 posterodistal setae, article 3 without A3-seta. Maxilliped outer plate with distal margin smooth, medial margin without notch.

Gnathopod 1 carpus subequal in length to propodus (0.9×); propodus, posterior margin without robust setae. *Gnathopod 2* palm slightly acute, with 2–4 lateral robust setae, 2–3 medial robust setae. Pereopods 3 and 4 merus and carpus without setal fringe. Pereopod 4 coxa with

anterior and posterior margins subparallel, anteroventral corner rounded. Pereopods 5–7 with distal articles elongate, dactyls short and stocky. Pereopod 5 basis expanded posteriorly, rounded. *Pereopod 7 basis subrectangular, posteroventral corner subquadrate*, posteroventral margin straight.

Epimeron 3 posterior margin smooth, with notch well above rounded posteroventral corner. *Uropod 1* peduncle dorsolateral margin with 18 robust setae; outer ramus without large spines between robust setae. *Uropod 2* inner ramus slightly constricted. *Uropod 3* rami lanceolate; without plumose setae; outer ramus 1-articulate. *Telson* moderately cleft (about 50%).

Male (sexually dimorphic characters). Based on male, 17.8 mm, AM P37215. Antenna 1 flagellum with callynophore (reduced). Antenna 2 flagellum with calceoli. Mandible palp article 2 with 14 posterodistal setae. Gnathopod 2 palm with 1 lateral robust seta and 2 medial robust setae.

Remarks. *Amaryllis macrophthalmalma* belongs to a small group of species with a smooth posterior margin on epimeron 3 and a subrectangular basis on pereopod 7 (*A. macrophthalmalma*, *A. philatelica* and *A. spencerensis*). Within this group *A. macrophthalmalma* and *A. spencerensis* both have a well-developed medial spine on peduncular article 1 of antenna 1 and a notch well above the rounded posteroventral corner on epimeron 3. In *Amaryllis macrophthalmalma* the posteroventral corner of the basis of pereopod 7 is subquadrate but not notched (it is notched in *A. spencerensis*), and there are more robust setae defining the palm of gnathopod 2 in the female.

Habitat. *Amaryllis macrophthalmalma* occurs most frequently on sand, shell and mud bottoms of both fine and coarse sediment.

Distribution. Southeastern Australia, predominantly Bass Strait and Tasmania; 6–219 m depth.

Amaryllis migo n.sp.

Figs. 23–25

Type material. HOLOTYPE, female, 10.2 mm, ovigerous (with 1 embryo), AM P37173; 1 PARATYPE, male, 5.2 mm, AM P37174; 3 PARATYPES, AM P37175; rocks near Migo Island, Port Harding, Torbay Bay, Western Australia, 35°04'S 117°39'E, 6–7 m, algae and sponge, J.K. Lowry, 15 December 1983, stn WA-154. 11 PARATYPES, AM P37176, type locality, 6–7 m, small branched alga with compound ascidian on underside of branches, R.T. Springthorpe & J.K. Lowry, 15 December 1983, stn WA-152.

Additional material. SOUTH AUSTRALIA: 1 specimen, AM P37177, Vivonne Bay, Kangaroo Island, [approx. 36°00'S 137°05'E], H.M. Hale and Tindale, January 1926, AM stn SA-85. 7 specimens, NMV J13978, NE side of Topgallant Island, Investigator Group, 33°43.0'S 134°36.6'E, 20 m, a brown alga *Cystophora* and a red alga, *Plocamium*, G.C.B. Poore & K. Brandon, 21 April 1985, NMV stn SA-80. 1 specimen, NMV J13979, same locality, 7 m, *Acrocarpia anciculata* and red algae, S. Shepherd & G.C.B. Poore, 20 April 1985, NMV stn SA-83. 2 specimens, NMV J13985, The Hotspot Reef, W of Flinders Island, 33°40.8'S 134°22.5'E, 21 m, erect hard bryozoan on vertical rock face, G.C.B. Poore, 22 April 1985, NMV stn SA-83. WESTERN AUSTRALIA: 3 specimens, NMV J13986, N side of Cape Riche, 34°37'S 118°47'E, 5 m, coralline and red algae, G.C.B. Poore & H.M. Lew Ton, 14 April 1985, NMV stn SWA-51. 27

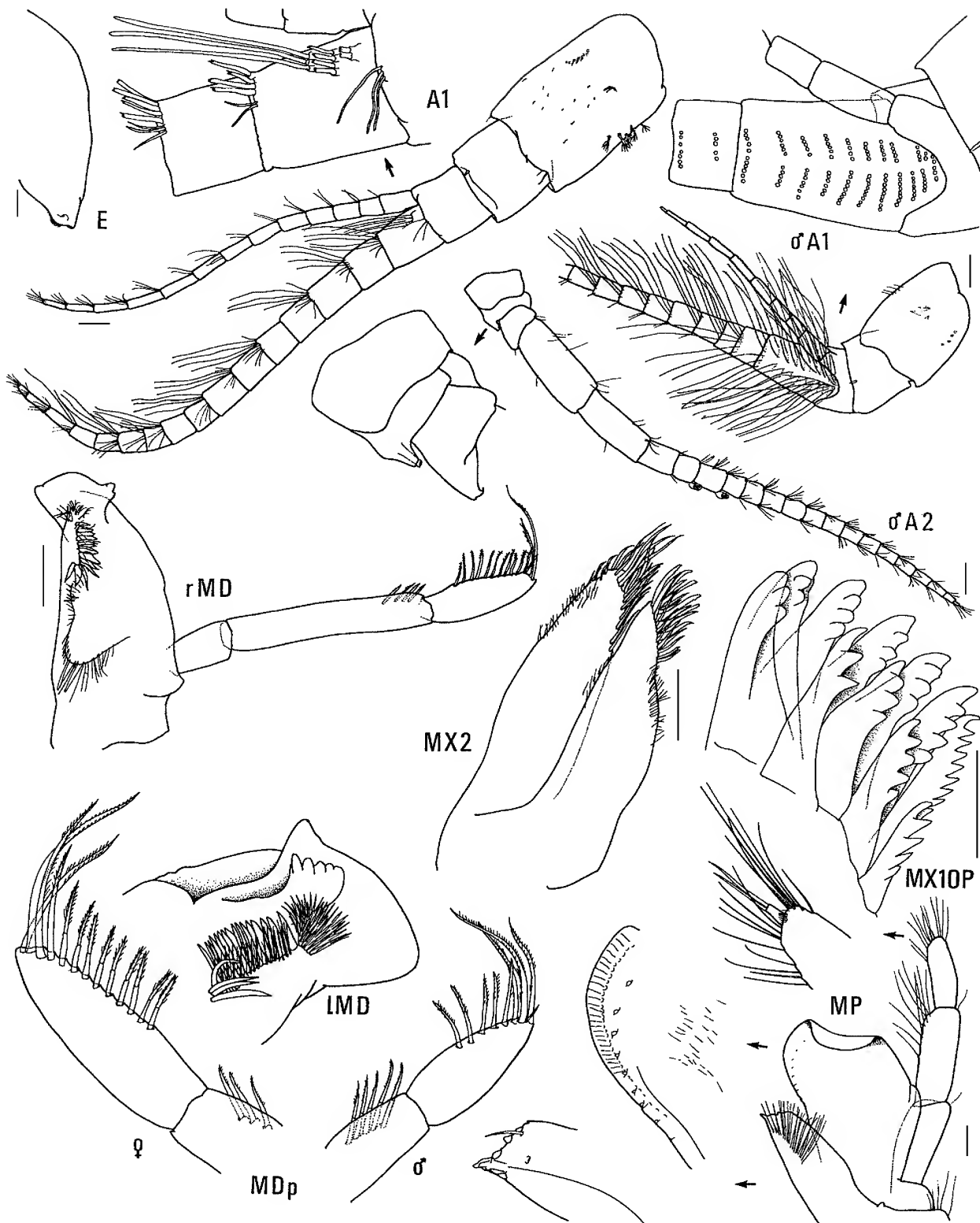


Figure 23. *Amaryllis migo* n.sp., holotype female, 10.2 mm, AM P37173; paratype male, 5.2 mm, AM P37174; Torbay Bay, Western Australia. Scale for MX1OP represents 0.05 mm; remainder represent 0.1 mm.

specimens, AM P37178, 2 km SE of South Point, Two Peoples Bay, 34°58'S 118°12'E, 6–10 m, alga with compound ascidian on back of fronds, J.K. Lowry, 16 December 1983, stn WA-177.

Type locality. Migo Island, Port Harding, Torbay Bay, Western Australia, 35°04'S 117°39'E, 6–7 m depth.

Description. Based on holotype female, 10.2 mm. Head much deeper than long, anterior margin with notch extended into a slit; rostrum absent; eye present, elongate, reniform. *Antenna 1* peduncular article 1 not ball-shaped proximally, distal margin without a medial spine; peduncular article 2 medium length; flagellum with weak callynophore, calceoli

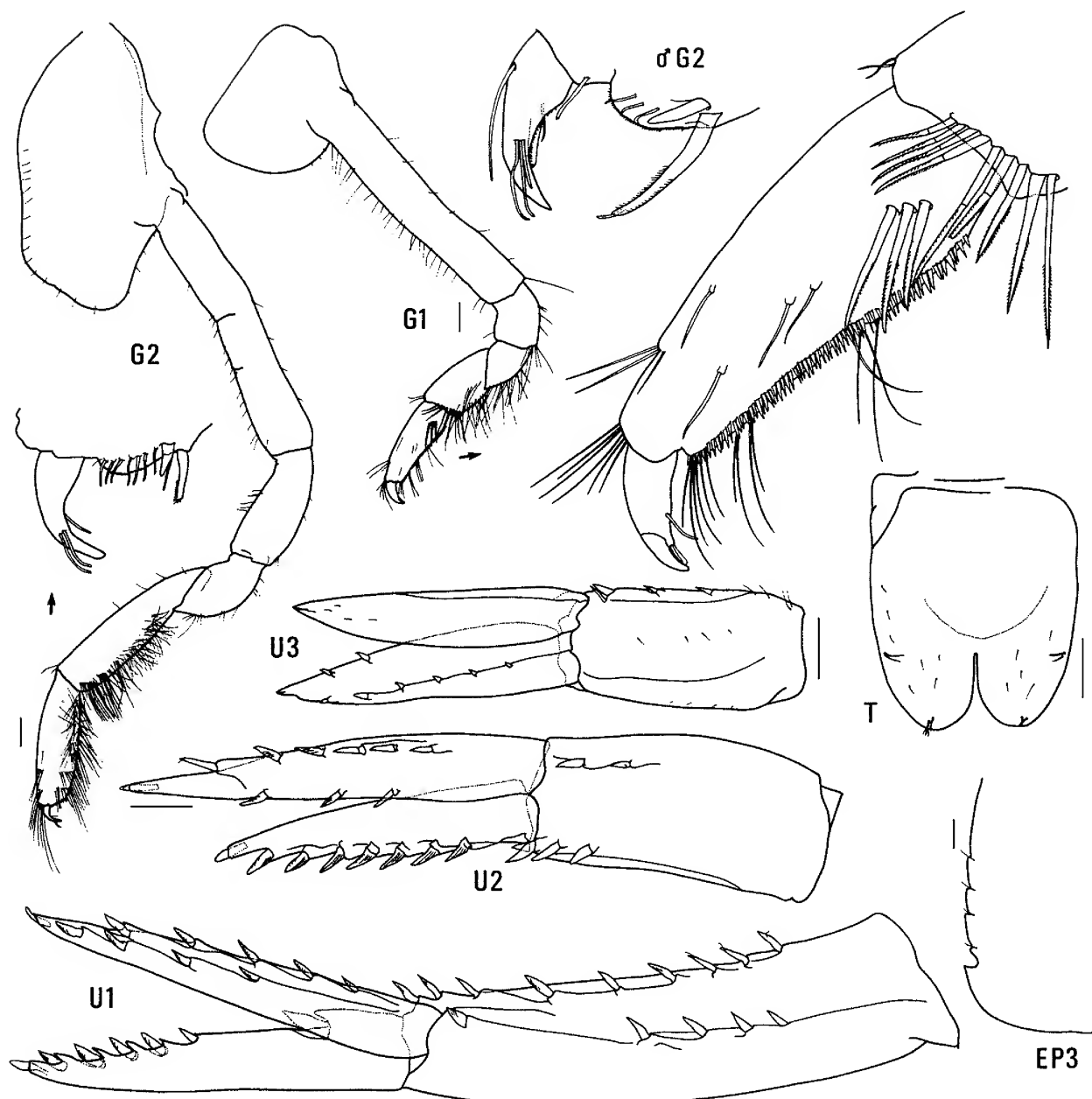


Figure 24. *Amaryllis migo* n.sp., holotype female, 10.2 mm, AM P37173; paratype male, 5.2 mm, AM P37174; Torbay Bay, Western Australia. Scales represent 0.1 mm.

absent. Antenna 2 flagellum about as long as that of antenna 1, without calceoli. Mouthpart bundle subconical. *Epistome/upper lip with broad mid-anterior bulge (lateral view)*. Mandible lacinia mobilis a stemmed, distally-cusped blade; accessory setal row with intermediate setae; palp article 2 with 3 posterodistal setae, article 3 without A3-seta. Maxilliped outer plate with distal margin smooth, medial margin without notch.

Gnathopod 1 carpus subequal in length to propodus; propodus, posterior margin without robust setae. Gnathopod 2 palm slightly acute, with no or 1 lateral robust seta, 1 medial robust seta. Pereopods 3 and 4 merus and carpus without setal fringe. Pereopod 4 coxa with anterior and posterior margins subparallel, anteroventral corner rounded. Pereopods 5–7 with distal articles elongate, dactyls short and stocky. Pereopod 5 basis expanded posteriorly, rounded. Pereopod 7 basis rounded posteriorly, posterodorsal corner

rounded, posterodorsal margin curved.

Epimeron 3 posterior margin serrate, with notch well above rounded posterodorsal corner. Uropod 1 peduncle dorsolateral margin with 9 robust setae; outer ramus with large spines between robust setae. Uropod 2 inner ramus slightly constricted. Uropod 3 rami lanceolate; without plumose setae; outer ramus 1-articulate. Telson moderately cleft (about 32%).

Male (sexually dimorphic characters). Based on paratype, male, 5.2 mm, AM P37174. Antenna 1 with strong callynophore. Antenna 2 flagellum with calceoli. Mandible palp article 2 with 5 posterodistal setae. Gnathopod 2 palm without lateral robust setae.

Etymology. The species is named after its type locality, Migo Bay.

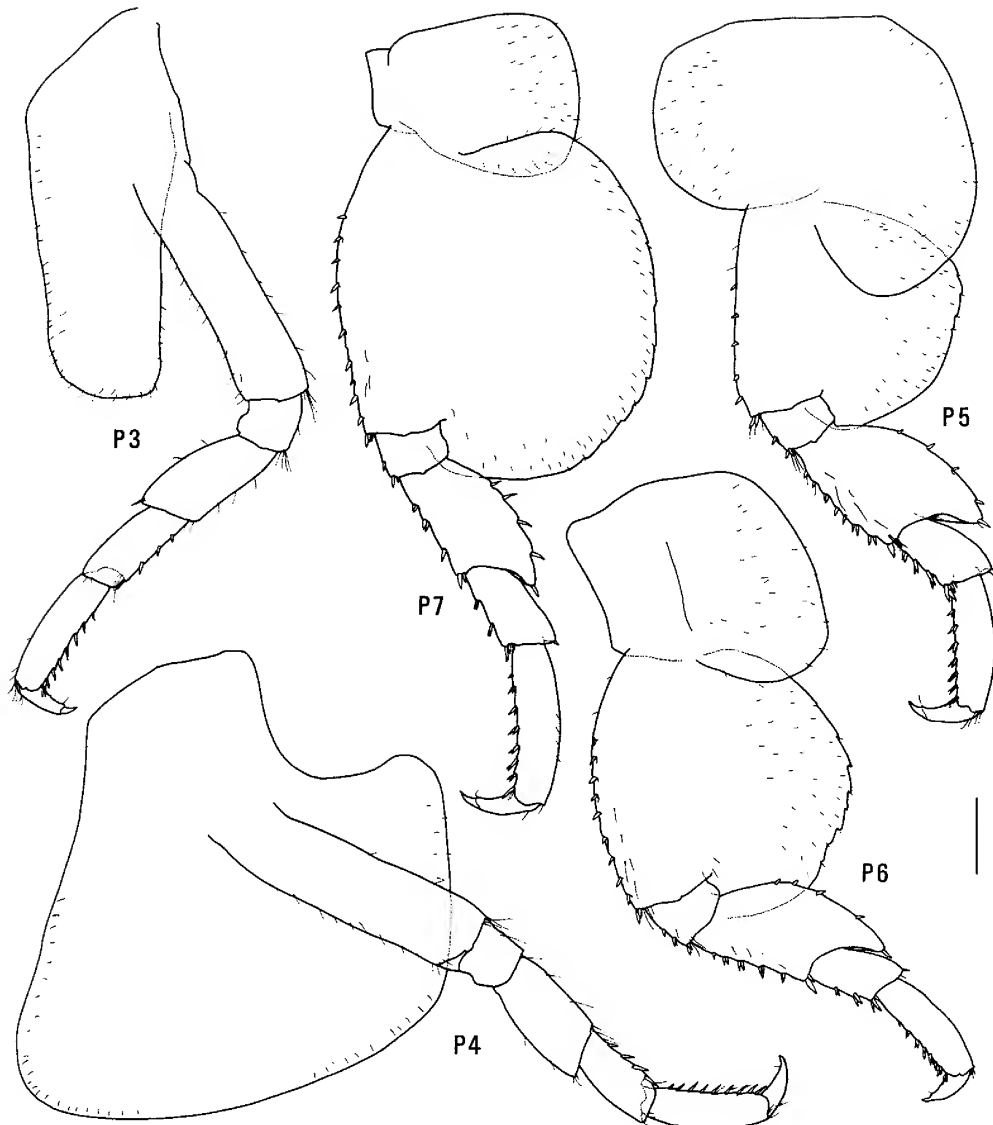


Figure 25. *Amaryllis migo* n.sp., holotype female, 10.2 mm, AM P37173, Torbay Bay, Western Australia. Scales represent 0.5 mm.

Remarks. *Amaryllis migo* is most similar to other *Amaryllis* species with a serrate posterior margin on epimeron 3, such as *A. carrascoi*, *A. croca*, *A. dianae* and *A. keablei*. *Amaryllis dianae*, *A. carrascoi* and *A. migo* all have a notch well above the posteroventral corner of epimeron 3, and only small serrations above the notch. *Amaryllis migo* is the only one of these three species with a rounded posteroventral corner on the basis of pereopod 7; it is the only species of *Amaryllis* with large spines between the robust setae of uropod 1 outer ramus.

Habitat. *Amaryllis migo* has been collected mostly from algae.

Distribution. Southern coast of Australia; 5–21 m depth.

***Amaryllis moona* n.sp.**

Figs. 26, 27

Type material. HOLOTYPE, female, 8.2 mm, AM P37243; 2 PARATYPES, male, AM P37371; Summercloud Bay, Wreck Bay, New South Wales, Australia, 35°10'S 150°42'E, 9–15 m, sponges, ascidians and algal holdfasts on underside of rocks, P. Hutchings, 29 November 1971, stn NSW-228. 1 PARATYPE, male, 4.8 mm, AM P37372, off Moona Moona Creek, Jervis Bay, NSW, Australia, Tasman Sea, 35°03.5'S 150°41'E, 8 m, algae and sponge on sandy rocks and mussels, J.K. Lowry, 19 June 1982, stn NSW-113.

Type locality. Summercloud Bay, Wreck Bay, NSW, Australia, 35°10'S 150°42'E, 9–15 m depth.

Description. Based on holotype female, 8.2 mm, AM P37243. Head much deeper than long, anterior margin with notch extended into a slit; rostrum absent; eye present, elongate, reniform. *Antenna 1* peduncular article 1 not ball-shaped proximally, *distal margin with small medial spine*; peduncular article 2 medium length; flagellum without

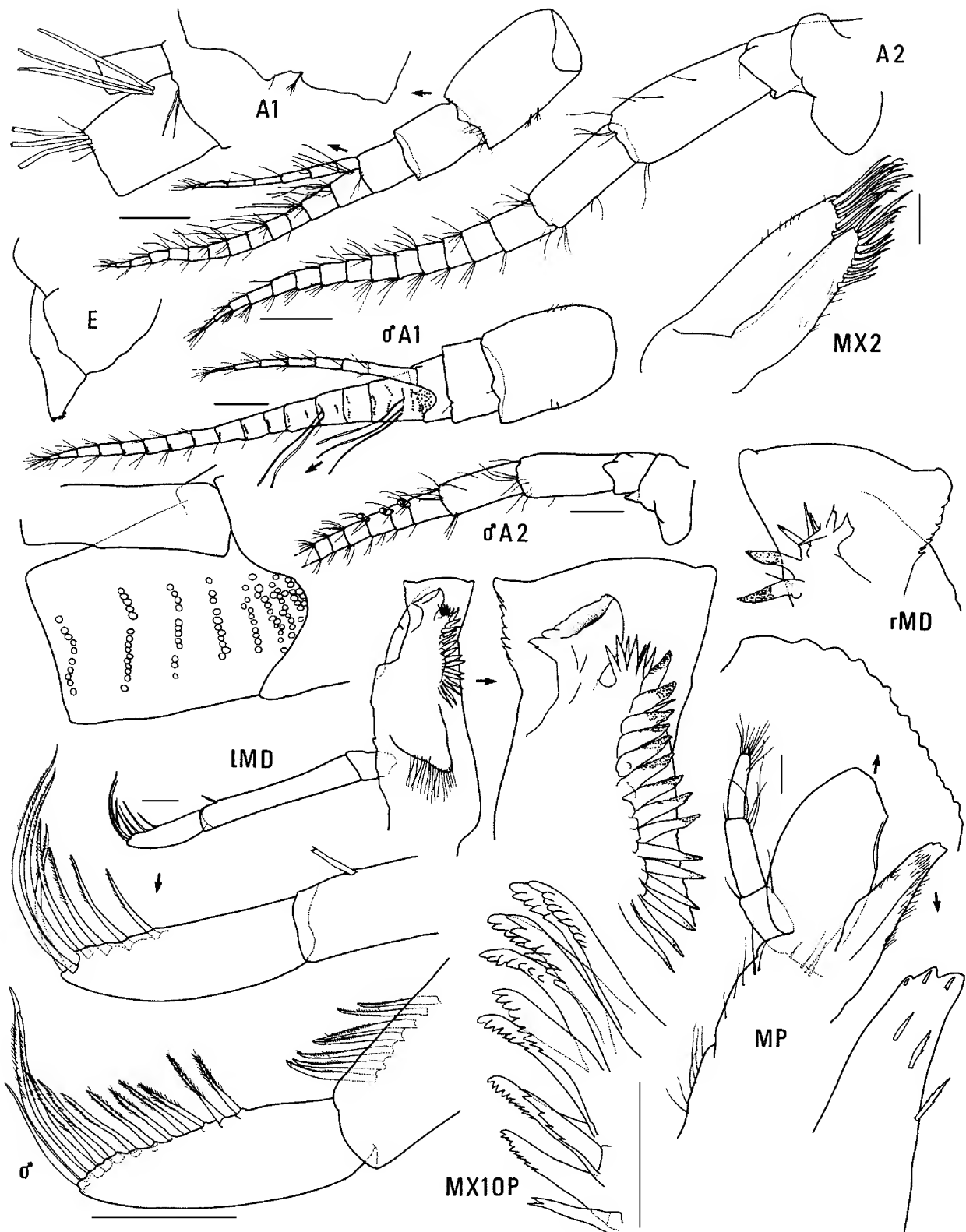


Figure 26. *Amaryllis moona* n.sp., holotype female, 8.2 mm, AM P37243; paratype male, 6.4 mm, AM P37371; Summercloud Bay, NSW. Scales for A1, 2 represent 0.2 mm; remainder represent 0.1 mm.

callynophore, calceoli absent. Antenna 2 flagellum about as long as that of antenna 1, without calceoli. Mouthpart bundle subconical. Epistome/upper lip almost straight (lateral view). Mandible lacinia mobilis a stemmed cup-like blade; accessory setal row without intermediate setae; palp article 2 with 1 posterodistal seta, article 3 without

A3-seta. Maxilliped outer plate with distal margin serrate, medial margin without notch.

Gnathopod 1 carpus longer than propodus (1.2×); propodus, posterior margin without robust setae. Gnathopod 2 palm slightly acute, without lateral robust setae, 1 medial robust seta. Pereopods 3 and 4 merus and carpus without

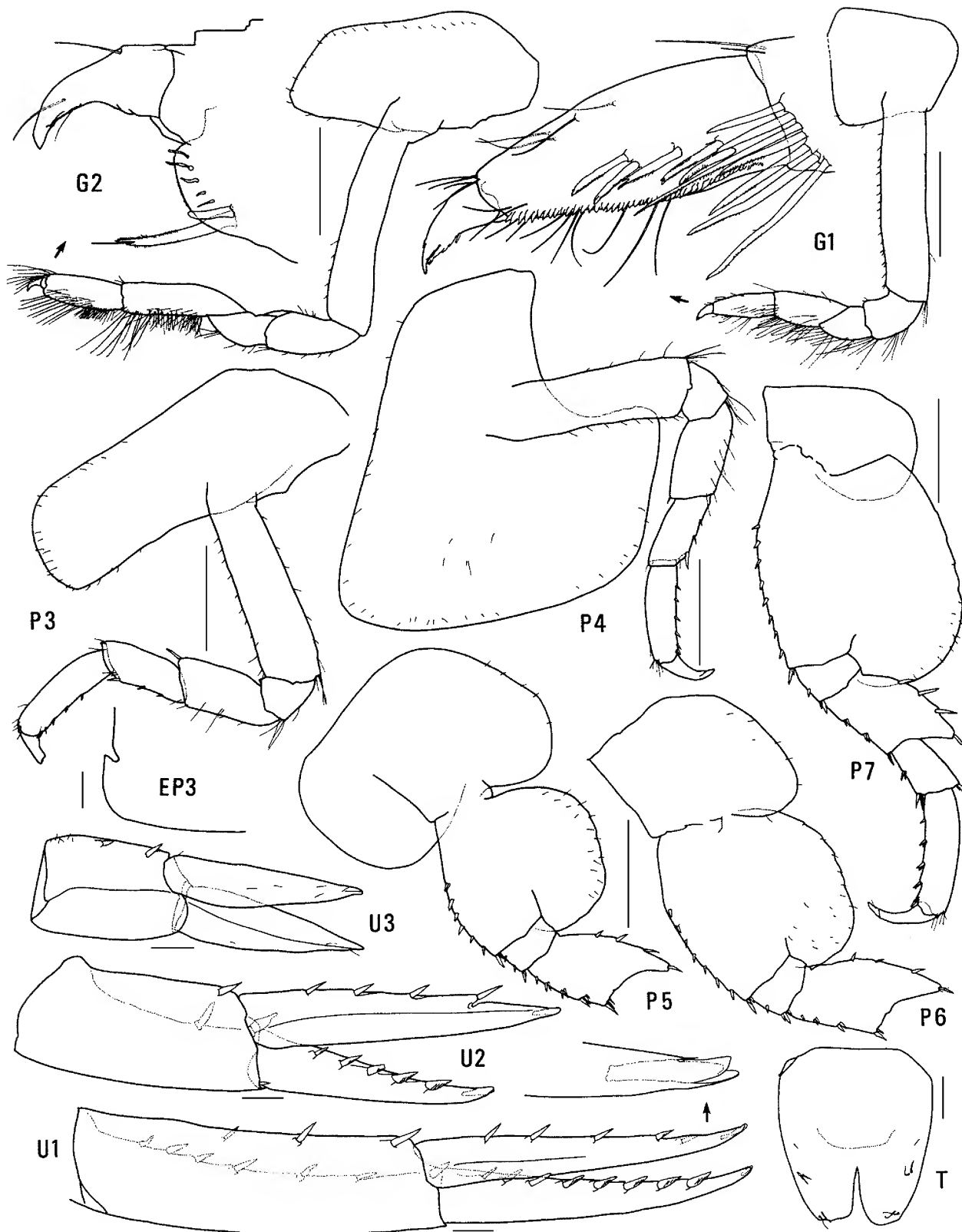


Figure 27. *Amaryllis moona* n.sp., holotype female, 8.2 mm, AM P37243; Summercloud Bay, NSW. Scales for G1, 2, P3–7 represent 0.5 mm; remainder represent 0.1 mm.

setal fringe. Pereopod 4 coxa with anterior and posterior margins subparallel, anteroventral corner rounded. Pereopods 5–7 with distal articles elongate, dactyls short and stocky. Pereopod 5 basis expanded posteriorly, rounded.

Pereopod 7 basis rounded posteriorly, posterodorsal corner rounded, posterodorsal margin curved.

Epimeron 3 posterior margin smooth, with notch well above rounded posterodorsal corner. Uropod 1 peduncle

dorsolateral margin with 7 robust setae; *outer ramus without large spines between robust setae*. *Uropod 2 inner ramus slightly constricted*. Uropod 3 rami lanceolate; without plumose setae; outer ramus 1-articulate. *Telson moderately cleft (about 34%)*.

Male (sexually dimorphic characters). Based on paratype male, 4.8 mm, AM P37372. Antenna 1 flagellum with callynophore. Antenna 2 flagellum with calceoli. Mandible palp article 2 with 7 posterodistal setae.

Etymology. Named for Moona Moona Creek.

Remarks. *Amaryllis moona* belongs to the group of species with a smooth posterior margin on epimeron 3 and a rounded posteroventral corner on the basis of pereopod 7. Within this group it is similar to *A. brevicornis* in having a nearly straight upper lip, but *A. moona* has significantly less robust setae at the corner of the palm of gnathopod 2 than does *A. brevicornis*. *Amaryllis moona* and *A. quokka* are the only two *Amaryllis* species with a cup-shaped lacinia mobilis; *A. moona* can be distinguished from *A. quokka* by the serrate distomedial margin of the maxilliped outer plate and the slightly acute palm on gnathopod 2.

Habitat. *Amaryllis moona* has been found only rarely, among mixed algae and sedentary invertebrates.

Distribution. Known only from the Jervis Bay area on the southeast coast of Australia; 8–15 m depth.

***Amaryllis olinda* n.sp.**

Figs. 28–30

Type material. HOLOTYPE, female, 8.9 mm, ovigerous, AM P37169; 1 PARATYPE, male, 5.5 mm, AM P37170; 10 PARATYPES, AM P37171; Port Arthur, Tasmania, Australia, [approx. 43°09'S 147°51'E], collected 28 July 1909, ex Keith Sheard Collection.

Additional material. BASS STRAIT: 1 specimen, AM E6523, east coast of Flinders Island, eastern Bass Strait, [approx. 40°01'S 148°02'E], FIS Endeavour collection. TASMANIA: 3 specimens, AM P37172, entrance to Oyster Bay, Maria Island, [approx. 42°40'S 148°03'E], collected 29 July 1909. 148 specimens, NMV J7606, 60 km ENE of Bold Head, King Island, Central Bass Strait, Australia, 39°56.4'S 144°48.1'E, 49 m, coarse shell, M.F. Gomon, G.C.B. Poore & C.C. Lu, 3 February 1981, FRV *Hai Kung*, stn BSS-128. 4 specimens, NMV J13988, 5 km E of Cape Edie, Robbins Island, Bass Strait, 40°41.8'S 145°07'E, 16 m, fine shelly sand, epibenthic sled, M. Gomon & G.C.B. Poore, 3 November 1980, FRV *Sarda*, stn BSS-110S.

Type locality. Port Arthur, Tasmania, Australia, Southern Ocean, [approx. 43°09'S 147°51'E].

Description. Based on holotype female, 8.9 mm, AM P37169. Head much deeper than long, anterior margin with notch extended into a slit; rostrum absent; eye present, elongate, reniform. *Antenna 1 peduncular article 1* not ball-shaped proximally, *distal margin without a medial spine*; peduncular article 2 medium length; *flagellum with callynophore*, calceoli absent. Antenna 2 flagellum about as long as that of antenna 1, without calceoli. Mouthpart bundle subconical. *Epistome/upper lip with broad mid-anterior bulge (lateral view)*. Mandible lacinia mobilis a stemmed, distally-cusped blade; *accessory setal row with intermediate setae*; palp article 2 with 7 posterodistal setae, article 3 without A3-seta. *Maxilliped outer plate with distal margin smooth, medial margin without notch*.

Gnathopod 1 carpus shorter than propodus (0.75×); propodus, posterior margin without robust setae. Gnathopod 2 palm slightly acute, with 1 lateral robust seta, 1 medial robust seta. Pereopods 3 and 4 merus and carpus without setal fringe. Pereopod 4 coxa with anterior and posterior margins subparallel, anteroventral corner rounded. Pereopods 5–7 with distal articles elongate, dactyls short and stocky. Pereopod 5 basis expanded posteriorly, rounded. *Pereopod 7 basis rounded posteriorly, posteroventral corner rounded, posteroventral margin curved*.

Epimeron 3 posterior margin smooth, with notch well above rounded posteroventral corner. Uropod 1 peduncle

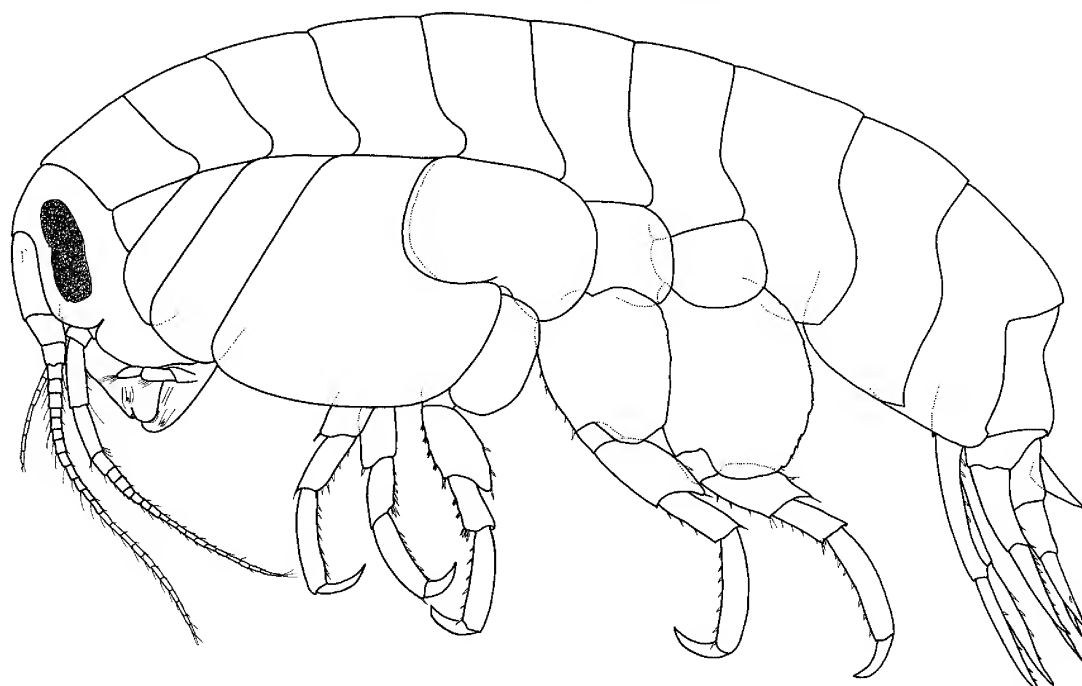


Figure 28. *Amaryllis olinda* n.sp., holotype female, 8.9 mm, AM P37169, Port Arthur, Tasmania.

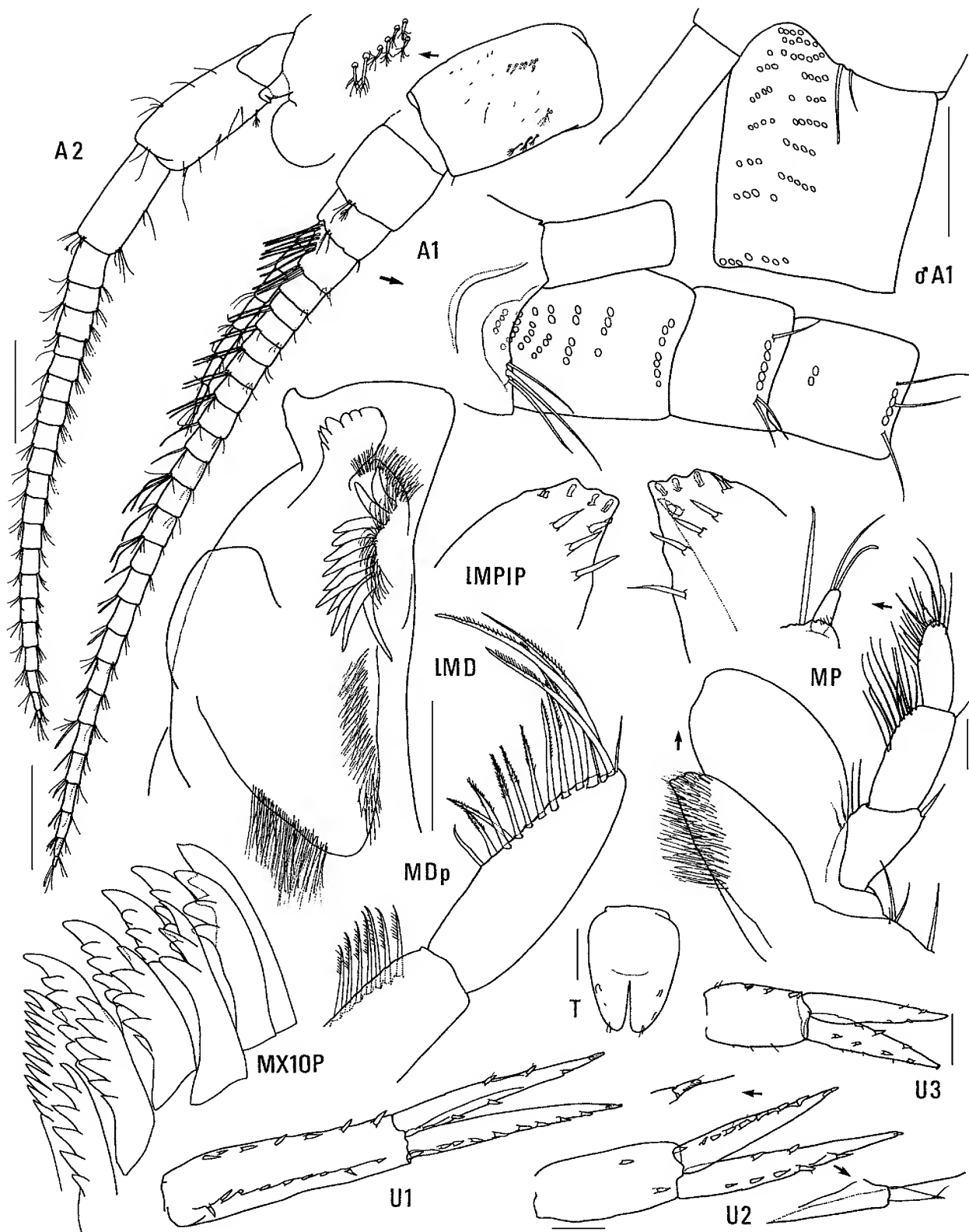


Figure 29. *Amaryllis olinda* n.sp., holotype female, 8.9 mm, AM P37169; paratype male, 5.5 mm, AM P37170; Port Arthur, Tasmania. Scales for MD, MP, δ A1 represent 0.1 mm; remainder represent 0.2 mm.

dorsolateral margin with 9 robust setae; outer ramus without large spines between robust setae. Uropod 2 inner ramus slightly constricted. Uropod 3 rami lanceolate; without plumose setae; outer ramus 1-articulate. Telson moderately cleft (about 40%).

Male (sexually dimorphic characters). Based on paratype male, 5.5 mm, AM P37170. Antenna 1 flagellum with calceoli. Antenna 2 flagellum with calceoli. Mandible palp article 2 with 5 posterodistal setae. Gnathopod 2 palm without lateral robust setae.

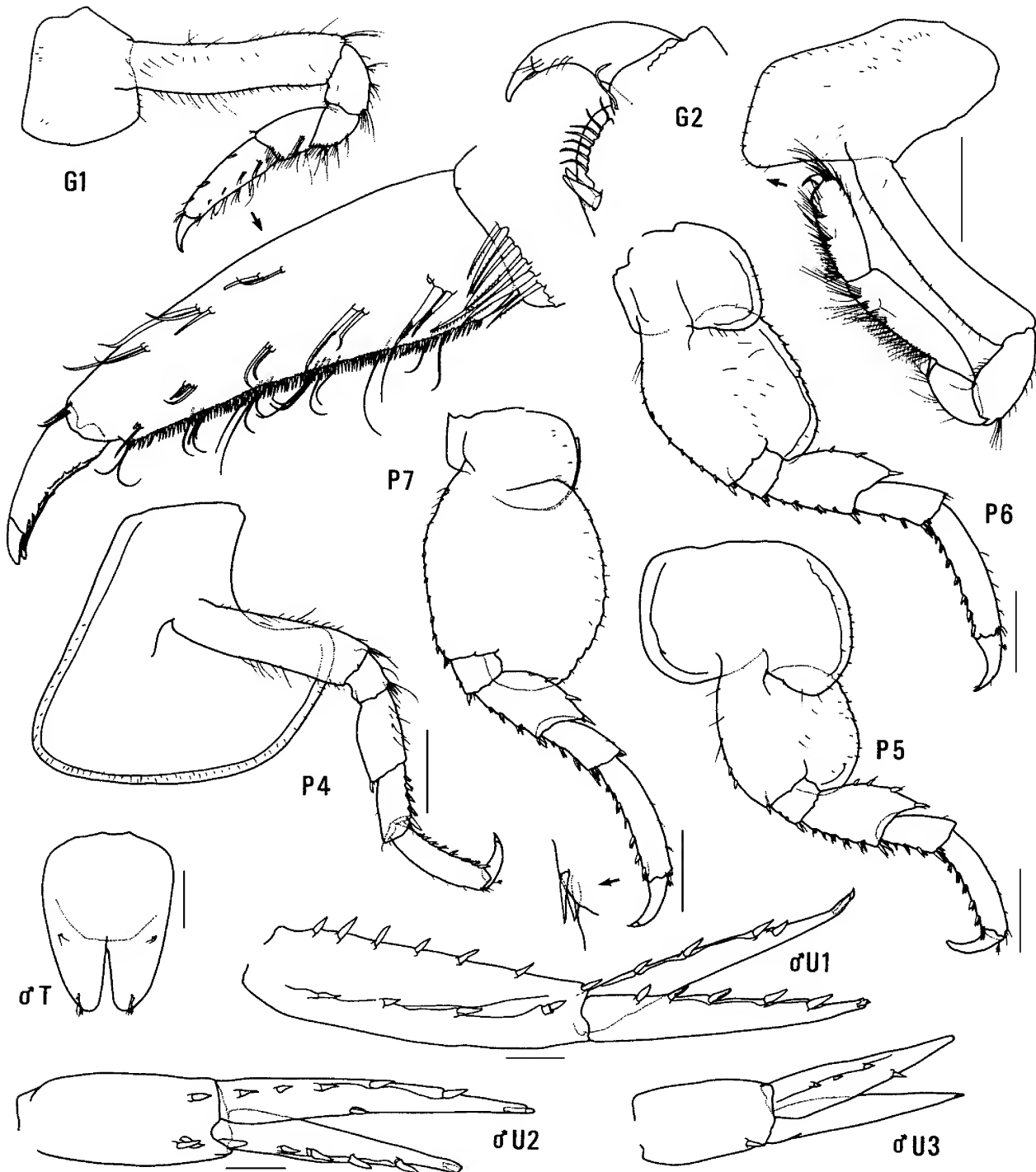


Figure 30. *Amaryllis olinda* n.sp., holotype female, 8.9 mm, AM P37169; paratype male, 5.5 mm, AM P37170; Port Arthur, Tasmania. Scales for U1–3, T represent 0.1 mm; remainder represent 0.5 mm.

Etymology. The species is named for the wooden barque *Olinda*, which sank in 1852 off Eddystone Point, Tasmania, while carrying a cargo of timber and potatoes from Hobart to Melbourne.

Remarks. *Amaryllis olinda* belongs to the group of species with a smooth posterior margin on epimeron 3 and a rounded posteroventral corner on the basis of pereopod 7 (*A. brevicornis*, *A. kamata*, *A. moona*, *A. quokka*). It has a curved

posteroventral margin on the basis of pereopod 7, similar to *A. moona* and *A. quokka*. It differs from these two species in having gnathopod 1 carpus shorter than the propodus.

Habitat. *Amaryllis olinda* has been collected from coarse sediments.

Distribution. Tasmania, Australia; 16–49 m depth.

Amaryllis philatelica n.sp.

Figs. 31–34, Plate 1b

Type material. HOLOTYPE, female, 20.5 mm, AM P37165; 1 PARATYPE, male, 18.2 mm, AM P37166; 2 PARATYPES, males, AM P37167; Montague Island, New South Wales, Australia, 36°15'S 150°14'E, 23 m, R. Kuiter, 28 December 1978. 1 PARATYPE, female, AM P26644, Montague Island, NSW, Australia, 36°15'S 150°14'E, 25 m, algae, R. Kuiter, 30 December 1977.

Additional material. NEW SOUTH WALES: 1 male, AM P30479, Point Perpendicular, Jervis Bay, 35°06'S 150°48'E, 20 m, on boulder surface, A. Jones & R. Hartnall, 25 May 1980. BASS STRAIT: 1 specimen, NMV J7653, 40 km SSW of Lakes Entrance, 38°18.0'S 147°37.0'E, 55 m, muddy fine shell, epibenthic sled, M. Gomon & R. Wilson, 31 July 1983, FV *Silver Gull*, stn BSS-209. TASMANIA: 5 specimens, AM P57882, Waterfall Bay, Tasman Peninsula, 43°04'S 147°56'E, 17–18 m, bryozoans and sponges on rock wall, K.L. Gowlett-Holmes, 7 December 1997. SOUTH AUSTRALIA: 3 specimens, SAMC C5984, 2 km S of SW tip of West Island, Franklin Island, Nuyts Archipelago, 32°27'S 133°40'E, 36.5 m, sand with low rock outcrops, P. Aerfeldt & N. Holmes, 23 February 1983. WESTERN AUSTRALIA: 1 specimen, AM P37168, SE of Foul Bay, 35°12'S 117°00'E, 75 m, CSIRO Fisheries, 8 August 1962, HMAS *Gascoyne*, stn G3/160/62.

Type locality. Montague Island, NSW, Australia, 36°15'S 150°14'E, 23 m depth.

Description. Based on holotype female, 20.5 mm, AM P37165. Head much deeper than long, anterior margin with notch extended into a slit; rostrum absent; eye present, elongate, reniform. *Antenna 1* peduncular article 1 not ball-shaped proximally, distal margin without a medial spine; peduncular article 2 medium length; flagellum with callynophore, calceoli absent. *Antenna 2* flagellum about as long as that of antenna 1, without calceoli. Mouthpart bundle subconical. *Epistome/upper lip* with broad mid-anterior bulge (lateral view). *Mandible lacinia mobilis* a stemmed, distally-cusped blade; accessory setal row with intermediate setae; palp article 2 with 13 posterodistal

setae, article 3 without A3-seta. *Maxilliped outer plate* with distal margin smooth, medial margin without notch.

Gnathopod 1 carpus subequal in length to propodus; propodus, posterior margin without robust setae. *Gnathopod 2* palm slightly acute, with 3 lateral robust setae, 2 medial robust setae. Pereopods 3 and 4 merus and carpus without setal fringe. Pereopod 4 coxa with anterior and posterior margins subparallel, anteroventral corner rounded. Pereopods 5–7 with distal articles elongate, dactyls short and stocky. Pereopod 5 basis expanded posteriorly, rounded. *Pereopod 7* basis subrectangular, posteroventral corner subquadrate, posteroventral margin straight.

Epimeron 3 posterior margin smooth, with notch slightly above rounded posteroventral corner. *Uropod 1* peduncle dorsolateral margin with 14 robust setae; outer ramus without large spines between robust setae. *Uropod 2* inner ramus not constricted. *Uropod 3* rami lanceolate; without plumose setae; outer ramus 1-articulate. *Telson* slightly cleft (about 25%).

Male (sexually dimorphic characters). Based on paratype male, 18.2 mm, AM P37166. Antenna 1 flagellum without callynophore. Antenna 2 flagellum with calceoli. Mandible palp article 2 with 26 posterodistal setae. Gnathopod 2 palm with 2 lateral robust setae.

Etymology. The specific name *philatelica* alludes to the species' public debut on an Australian two cent postage stamp issued in 1984. (The species was then incorrectly identified as *Waldeckia* sp.).

Remarks. *Amaryllis philatelica* appears to be most similar to a small group of species with a smooth posterior margin on epimeron 3 and a subrectangular basis on pereopod 7 (*A. macrophthalma*, *A. philatelica* and *A. spencerensis*). It differs from *A. macrophthalma* and *A. spencerensis* in that the notch on the posterior margin of epimeron 3 is only slightly above the posteroventral corner.

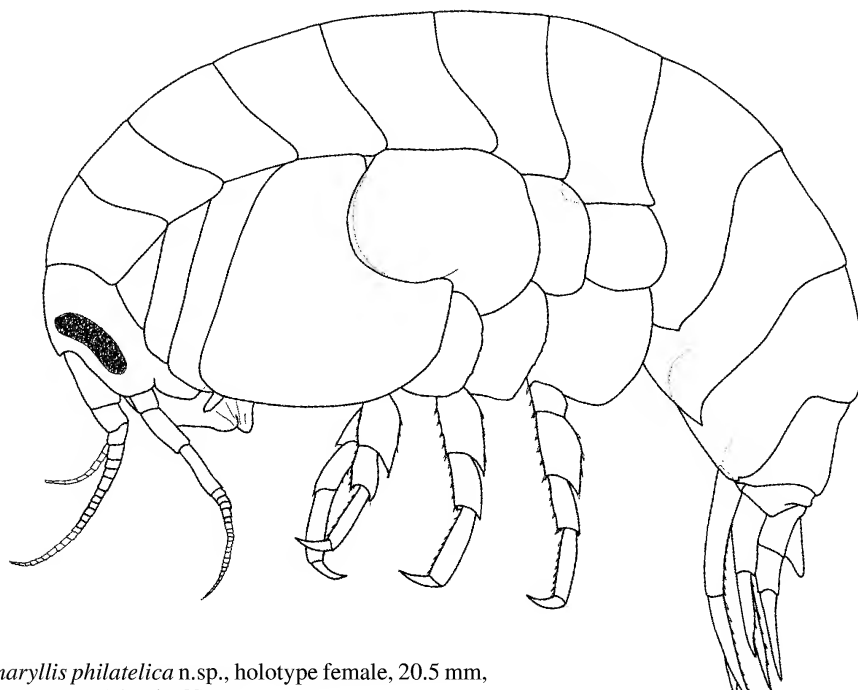


Figure 31. *Amaryllis philatelica* n.sp., holotype female, 20.5 mm, AM P37165, Montague Island, NSW.

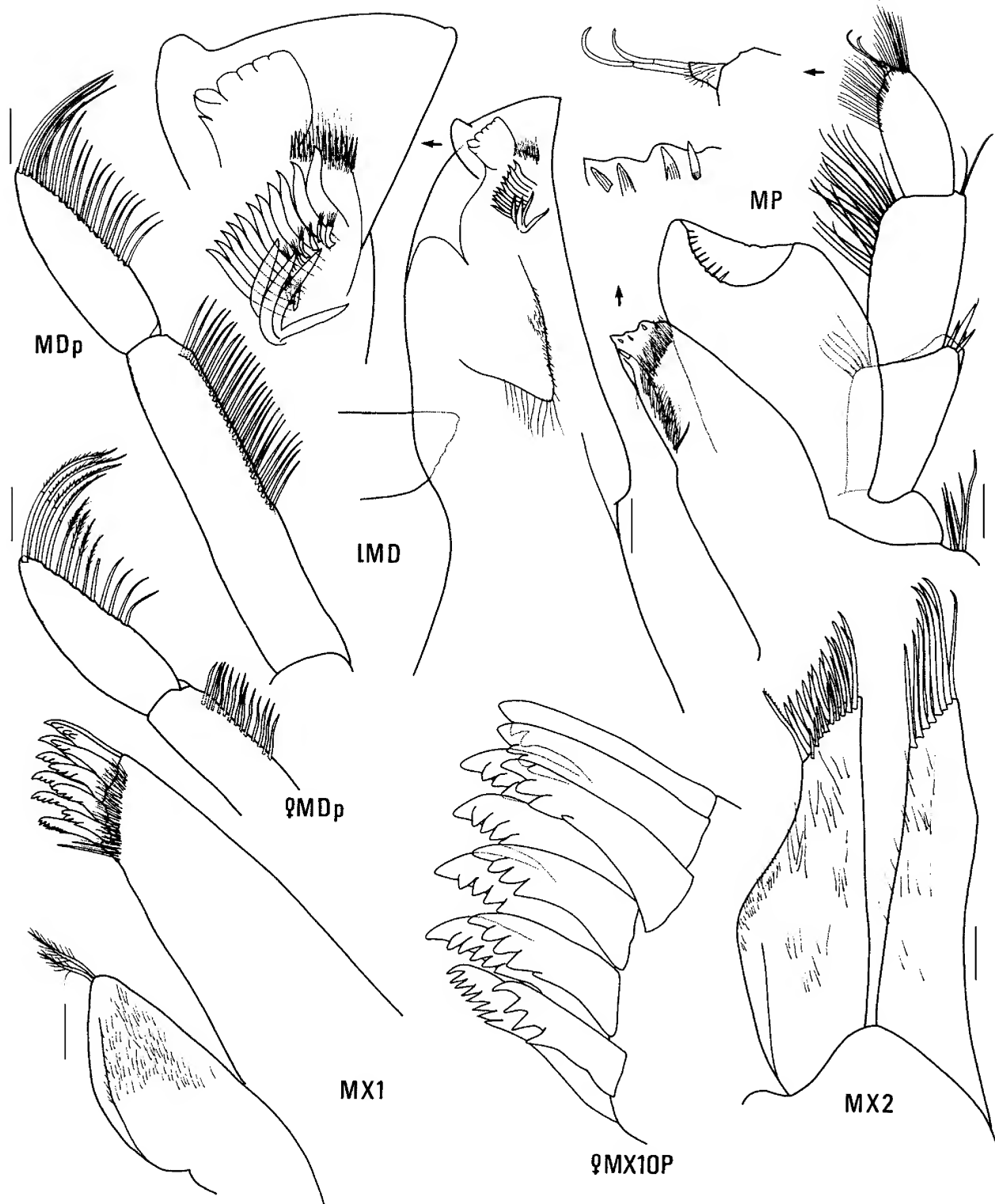


Figure 32. *Amaryllis philatelica* n.sp., holotype female, 20.5 mm, AM P37165; paratype male, 18.2 mm, AM P37166; Montague Island, NSW. Scales represent 0.1 mm.

Amaryllis philatelica is often found in association with the soft coral *Capnella gaboensis* and bryozoans of the genus *Triphyllozoon*. Judging from its subconical-shaped mouthpart bundle, *A. philatelica* might feed by nipping off the small polyps of its hosts.

This species has attracted the attention of scuba divers and underwater photographers, partly because of its (relatively) large size but mostly because of its striking

colour pattern. The body is a brilliant deep crimson with each segment of the pereon and pleon, the head, each of the coxae and the bases of pereopods 5 to 7 outlined in white; the antennae, protruding mouthparts and distal articles of the pereopods are orange/yellow and there is a single orange/yellow stripe along the dorsum. Lowry (in Karacsonyi, 1997) commented that the brilliant colour pattern might be a warning to potential predators that *A. philatelica* tastes

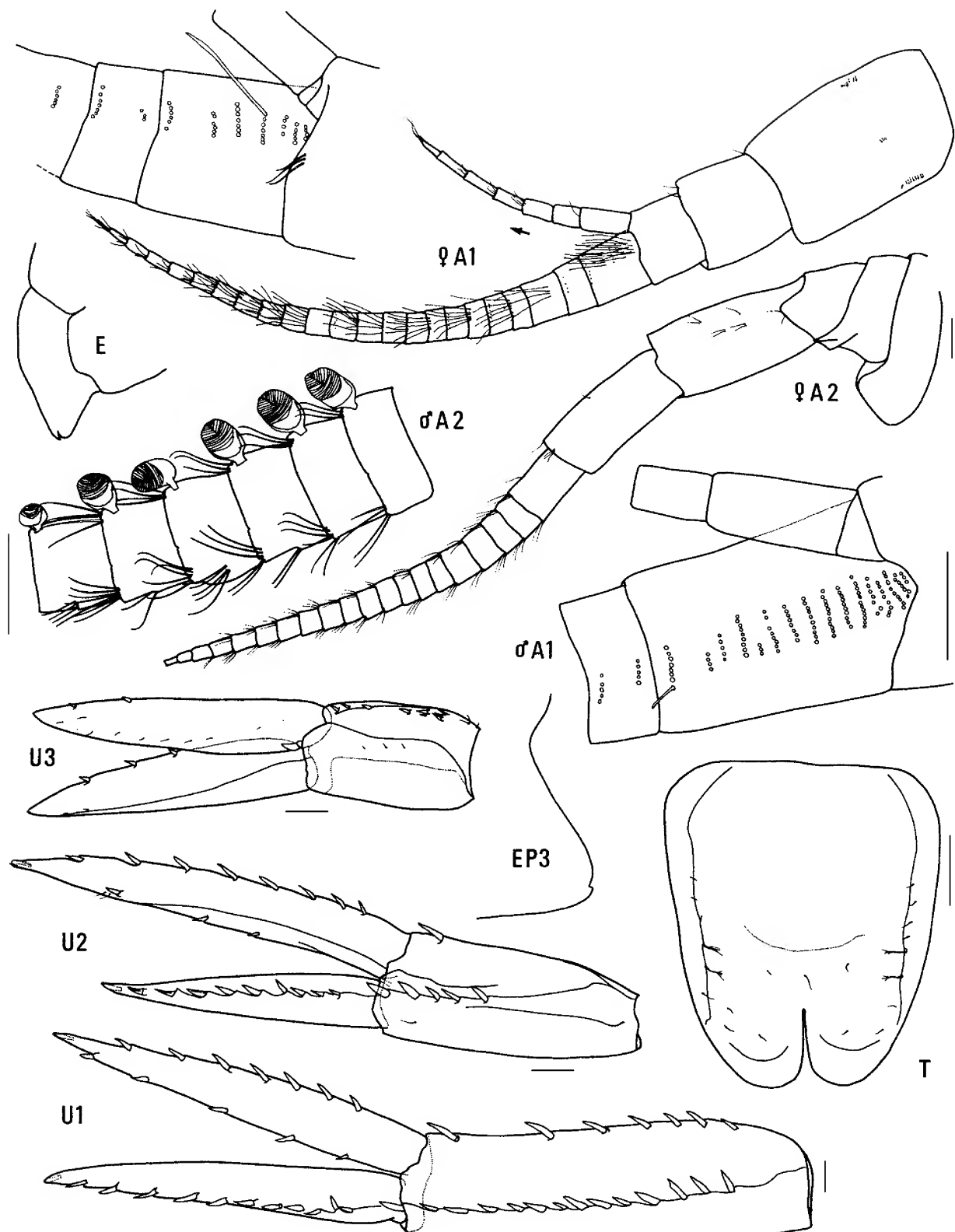


Figure 33. *Amaryllis philatelica* n.sp., holotype female, 20.5 mm, AM P37165; paratype male, 18.2 mm, AM P37166; Montague Island, NSW. Scales represent 0.2 mm.

unpleasant. The fact that individuals show non-cryptic behaviour—they do not avoid divers and have been known to leave their host and sit on the hand or head of a diver trying to photograph them (Karacsonyi, pers. comm.)—is circumstantial evidence for this theory.

The original colour photographs used to produce the 1984 postage stamp were taken by Rudi Kuitert, at Montague Island. They have been subsequently reproduced on postcards and as an illustration of *Amaryllis* sp. in Debelius (1999) and Edgar (1997). Some stunning photographs of

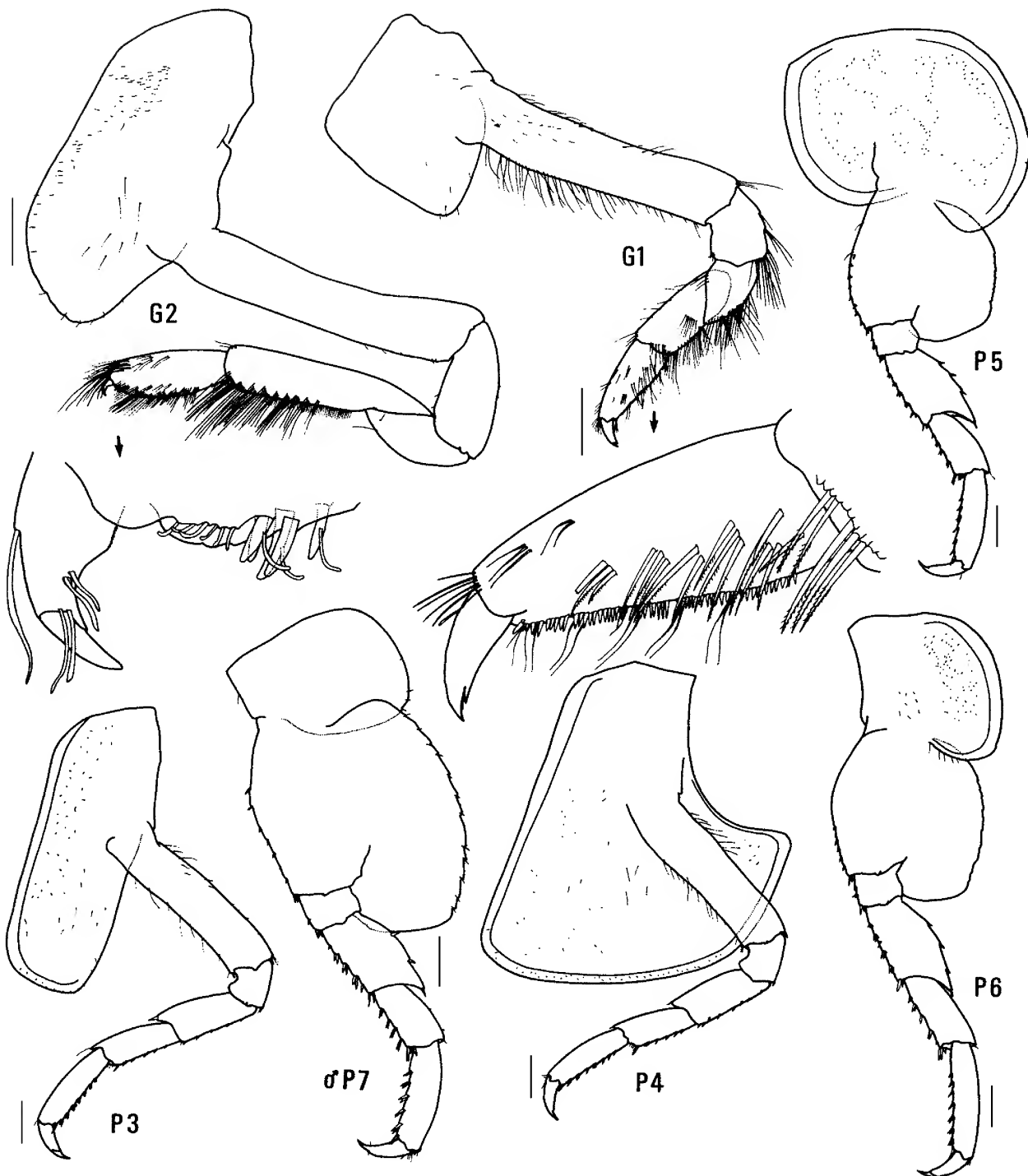


Figure 34. *Amaryllis philatelica* n.sp., holotype female, 20.5 mm, AM P37165; paratype male, 18.2 mm, AM P37166; Montague Island, NSW. Scales represent 0.5 mm.

“the red sea flea” were taken by Tony Karacsnyi, near Ulladulla, and published in *Australian Geographic* (Karacsnyi, 1997) and as a poster released by *Sportdiving Magazine*.

Habitat. *Amaryllis philatelica* has been recorded and collected on bryozoans, soft corals and sponges.

Distribution. Southeastern and southern Australia; from Solitary Islands on the east coast to Foul Bay in southwestern Australia; 20–75 m depth.

***Amaryllis quokka* n.sp.**

Figs. 35–37

Type material. HOLOTYPE, female, 13.4 mm, ovigerous, AM P37373; 1 PARATYPE, male, 8.0 mm, AM P37374; Cathedral Rock, Rottnest Island, Western Australia, eastern Indian Ocean, 32°01.5'S 115°27'E, 3 m, orange tunicates under limestone rock overhangs, J.K. Lowry, 21 December 1983, stn WA-247.

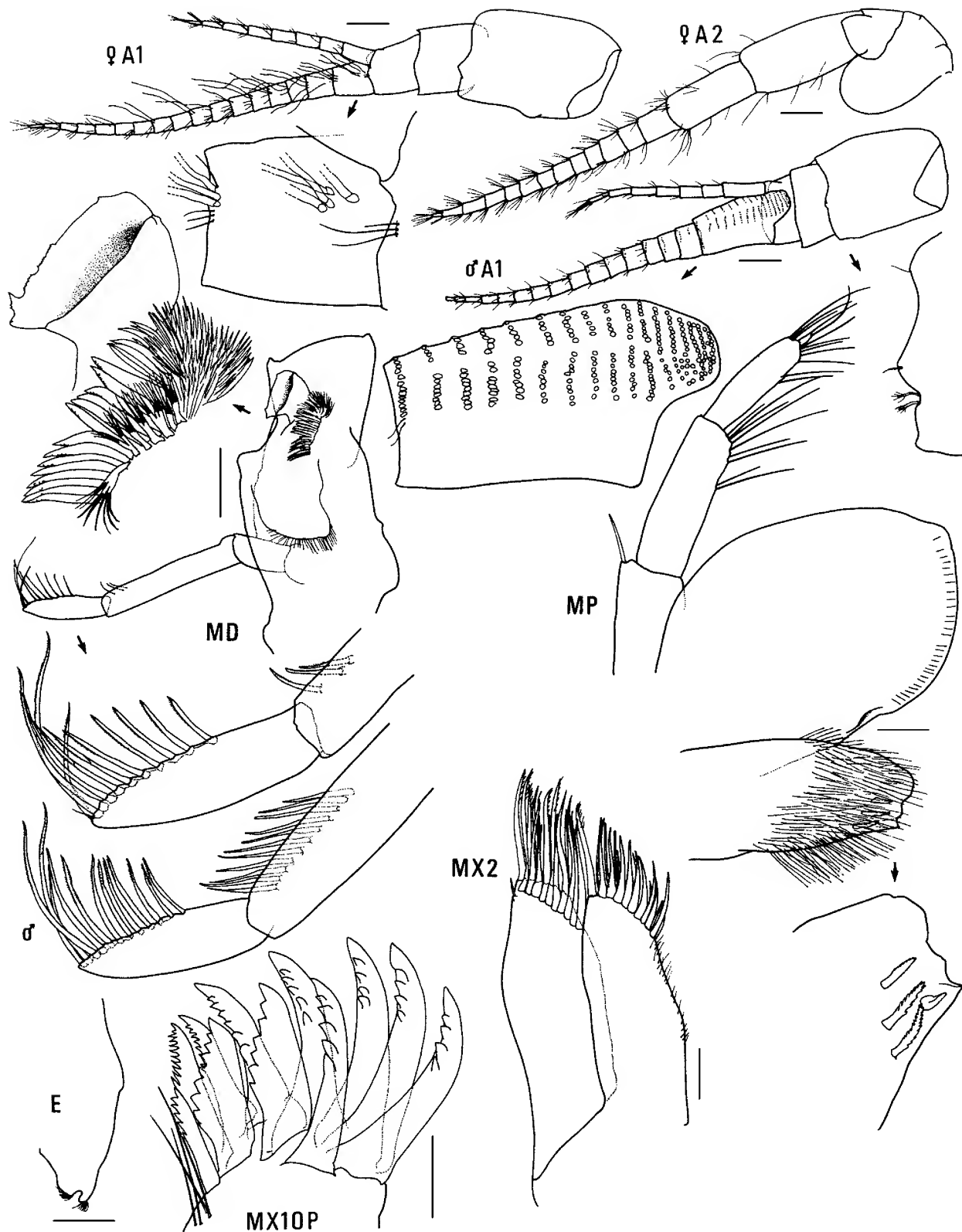


Figure 35. *Amaryllis quokka* n.sp., holotype female, 13.4 mm, AM P37373; paratype male, 8.0 mm, AM P37374; Rottnest Island, Western Australia. Scales for A1, 2, MD represent 0.2 mm; remainder represent 0.1 mm.

Additional material. SOUTH AUSTRALIA: 10 specimens, AM P57867, Blanche Harbour, Spencer Gulf, [approx. 32°42'S 137°46'E], 9 m, K. Sheard, 8 March 1938, FL Whyalla. 7 specimens, AM P57868, behind Lowly Point, Spencer Gulf, [approx. 33°S 137°46'E], 18 m, K. Sheard, 7 March 1938, FL Whyalla. 1 specimen, SAMA C5985, Dangerous Reef, Spencer Gulf, [approx. 34°49'S 136°12'E], dredged, K. Sheard. 1

specimen, AM P57869, Nepean Bay, Kangaroo Island, 35°42'S 137°37'E, dredged, F. Moorhouse, May 1938. 1 specimen, SAMA C5986, Nepean Bay, Kangaroo Island, [approx. 35°42'S 137°37'E], dredged, F. Moorhouse, 7-9 May 1938. 3 specimens, AM P57870, Gulf St Vincent, Fulton, 1902. WESTERN AUSTRALIA: 2 specimens, NMV J13980, N side of Cape Riche, 34°37'S 118°47'E, 6 m, sponges on vertical rock face,

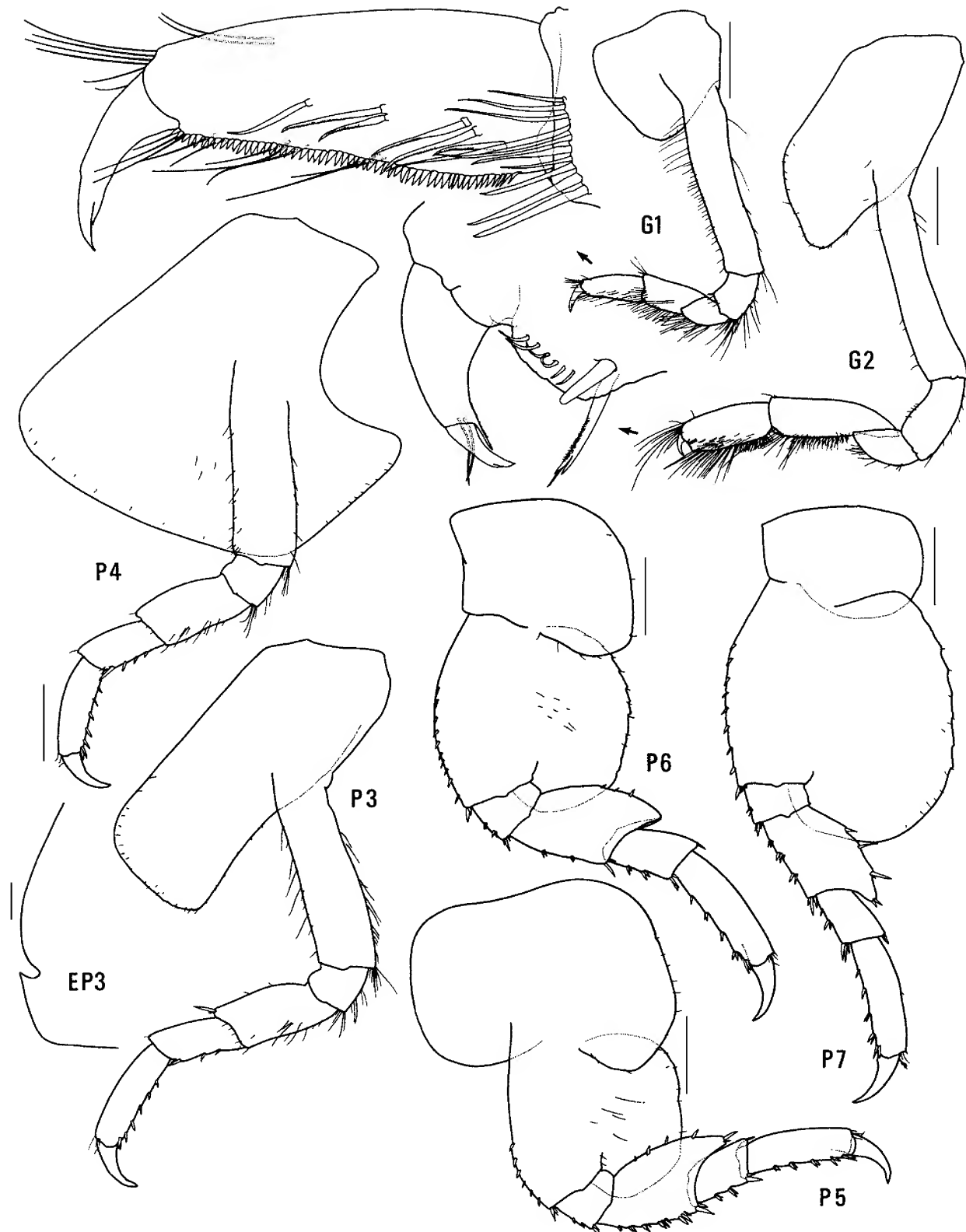


Figure 36. *Amaryllis quokka* n.sp., holotype female, 13.4 mm, AM P37373, Rottnest Island, Western Australia. Scale for EP3 represents 0.1 mm; remainder represent 0.5 mm.

G.C.B. Poore & H.M. Lew Ton, 14 April 1985, stn SWA-47. 1 specimen, NMV J13981, N end of Little Beach, Two Peoples Bay, $34^{\circ}58.4'S$ $118^{\circ}11.7'E$, 6 m, tufted algae on boulders, G.C.B. Poore & H.M. Lew Ton, 5 April 1985, stn SWA-11. 1 specimen, AM P37375, Vancouver Peninsula, near Mistaken Island, King George Sound, $35^{\circ}04'S$ $117^{\circ}56'E$, 2 m, sponges, J.K. Lowry, 13 December 1983, stn WA-103. 10 specimens,

AM P37376, off Possession Point, King George Sound, $35^{\circ}02'S$ $117^{\circ}55'E$, 7 m, brown algae, bryozoans and sponge, R. Springthorpe & J.K. Lowry, 14 December 1983, stn WA-133. 9 specimens, AM P37377, same locality, 7 m, mixed sponges and algae, J.K. Lowry, 14 December 1983, stn WA-135.

Type locality. Cathedral Rock, Rottnest Island, Western

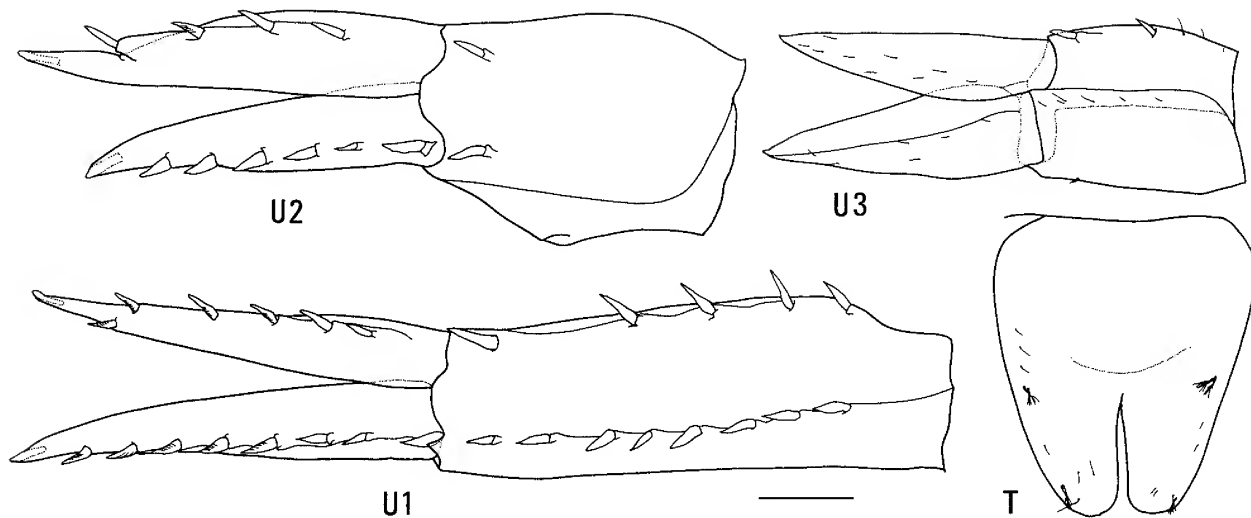


Figure 37. *Amaryllis quokka* n.sp., holotype female, 13.4 mm, AM P37373, Rottnest Island, Western Australia. Scale represents 0.2 mm.

Australia, eastern Indian Ocean, 32°01.5'S 115°27'E, 3 m depth.

Description. Based on holotype female, 13.4 mm, AM P37373. Head much deeper than long, anterior margin with notch extended into a slit; rostrum absent; eye present, elongate, reniform. Antenna 1 peduncular article 1 not ball-shaped proximally, distal margin with small medial spine; peduncular article 2 medium length; flagellum with callynophore (vestigial), calceoli absent. Antenna 2 flagellum about as long as that of antenna 1, without calceoli. Mouthpart bundle subconical. Epistome/upper lip with broad mid-anterior bulge (lateral view). Mandible lacinia mobilis a stemmed, cup-like blade; accessory setal row with intermediate setae; palp article 2 with 3 posterodistal setae, article 3 without A3-seta. Maxilliped outer plate with distal margin smooth, medial margin without notch.

Gnathopod 1 carpus subequal in length to propodus; propodus, posterior margin without robust setae. Gnathopod 2 palm transverse, without lateral robust setae, with 1 medial robust seta. Pereopods 3 and 4 merus and carpus without setal fringe. Pereopod 4 coxa with anterior and posterior margins subparallel, anteroventral corner rounded. Pereopods 5–7 with distal articles elongate, dactyls short and stocky. Pereopod 5 basis expanded posteriorly, rounded. Pereopod 7 basis rounded posteriorly, posteroventral corner rounded, posteroventral margin curved.

Epimeron 3 posterior margin smooth, with notch well above rounded posteroventral corner. Uropod 1 peduncle dorsolateral margin with 9 robust setae; outer ramus without large spines between robust setae. Uropod 2 inner ramus slightly constricted. Uropod 3 rami lanceolate; without plumose setae; outer ramus 1-articulate. Telson moderately cleft (about 46%).

Male (sexually dimorphic characters). Based on paratype male, 8.0 mm, AM P37374. Antenna 1 flagellum with callynophore. Mandible palp article 2 with 11 posterodistal setae.

Etymology. The species name *quokka* is a reference to the small marsupials that inhabit Rottnest Island.

Remarks. *Amaryllis quokka* belongs to the group of species with a smooth posterior margin on epimeron 3 and a rounded posteroventral corner on the basis of pereopod 7 (*A. brevicornis*, *A. kamata*, *A. moona*, *A. olinda*). Within this group it differs from all other species in the transverse palm of gnathopod 2.

Habitat. *Amaryllis quokka* has been collected on sedentary invertebrates, most often sponges.

Distribution. Southern and southwestern Australia, from the South Australian Gulfs to Rottnest Island; 3–18 m depth.

Amaryllis spencerensis n.sp.

Figs. 38–40

Type material. HOLOTYPE, female, 16.0 mm, ovigerous (15 eggs), AM P37096; 3 PARATYPES, female, AM P37097; 19 km from Mount Young, toward Wallaroo, Spencer Gulf, South Australia, [approx. 33°18'S 137°31'E], 18 m, K. Sheard on FL Whyalla, 8 March 1938. 1 PARATYPE, male, 11.0 mm, AM P37098, Western Shoal, Spencer Gulf, South Australia, [approx. 33°09'S 137°31'E], 9 m, K. Sheard on FL Whyalla, 10 March 1938. 2 PARATYPES, female, SAMA C5987, Dangerous Reef, Spencer Gulf, South Australia, [approx. 34°49'S 136°12'E], dredged, K. Sheard.

Additional material. Three females, AM P37099, unknown locality in Spencer Gulf and/or Gulf St Vincent, South Australia.

Type locality. 19 km from Mount Young, toward Wallaroo, Spencer Gulf, South Australia, [approx. 33°18'S 137°31'E], 18 m depth.

Description. Based on holotype female, 16.0 mm, AM P37096. Head much deeper than long, anterior margin with notch extended into a slit; rostrum absent; eye present, elongate, reniform. *Antenna 1* peduncular article 1 not ball-shaped proximally, *distal margin with well-developed medial spine*; peduncular article 2 medium length; flagellum without *callynophore*, calceoli absent. *Antenna 2* flagellum about as long as that of antenna 1, without calceoli. Mouthpart bundle subconical. *Epistome/upper lip with strong mid-anterior angle (lateral view)*. *Mandible lacinia mobilis* a stemmed, distally-cusped blade; *accessory setal row with intermediate setae*; *palp article 2* with 2

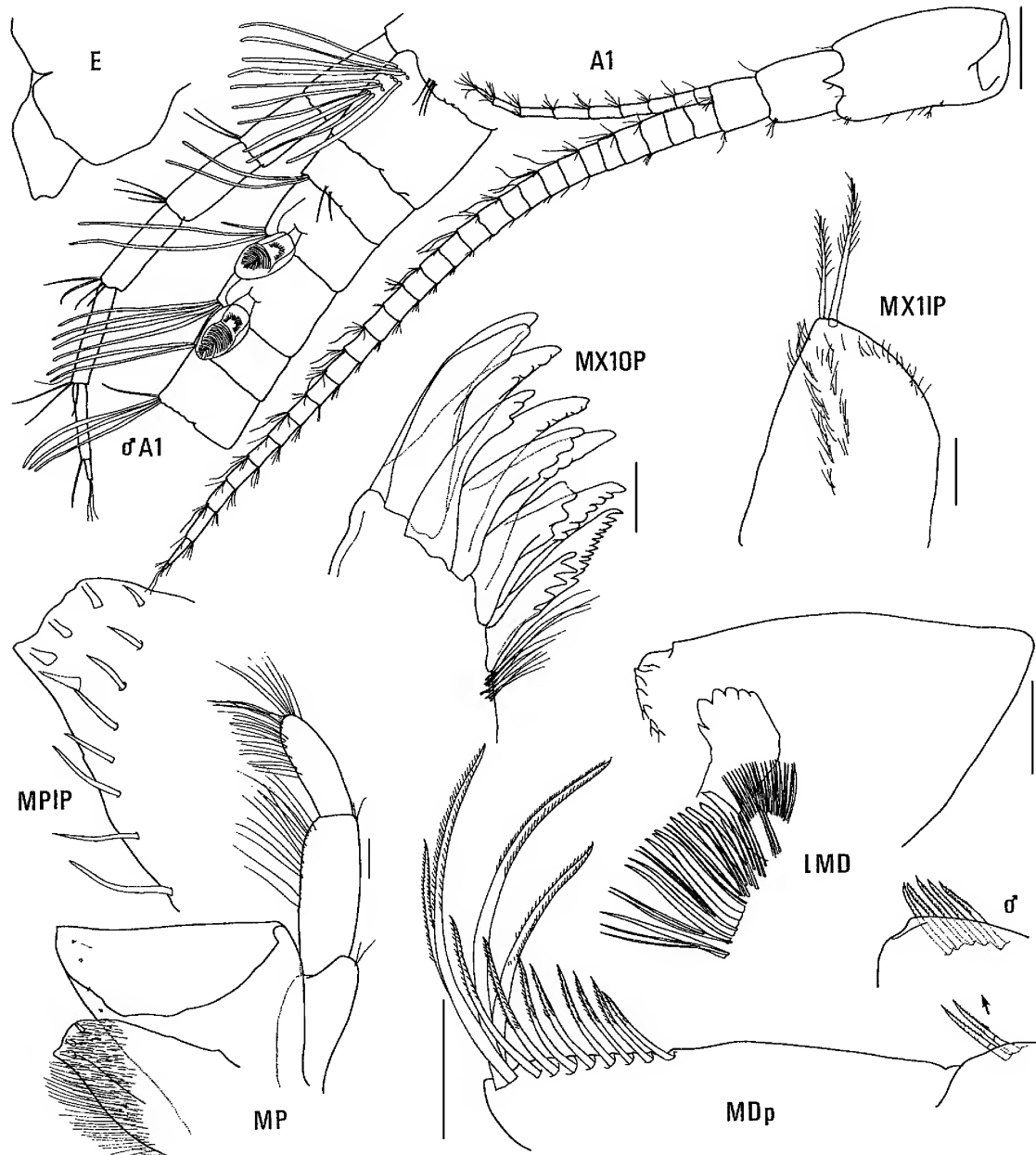


Figure 38. *Amaryllis spencerensis* n.sp., holotype female, 16.0 mm, AM P37096; paratype male, 11.0 mm, AM P37098; Spencer Gulf, South Australia. Scale for A1 represents 0.5 mm; remainder represent 0.1 mm.

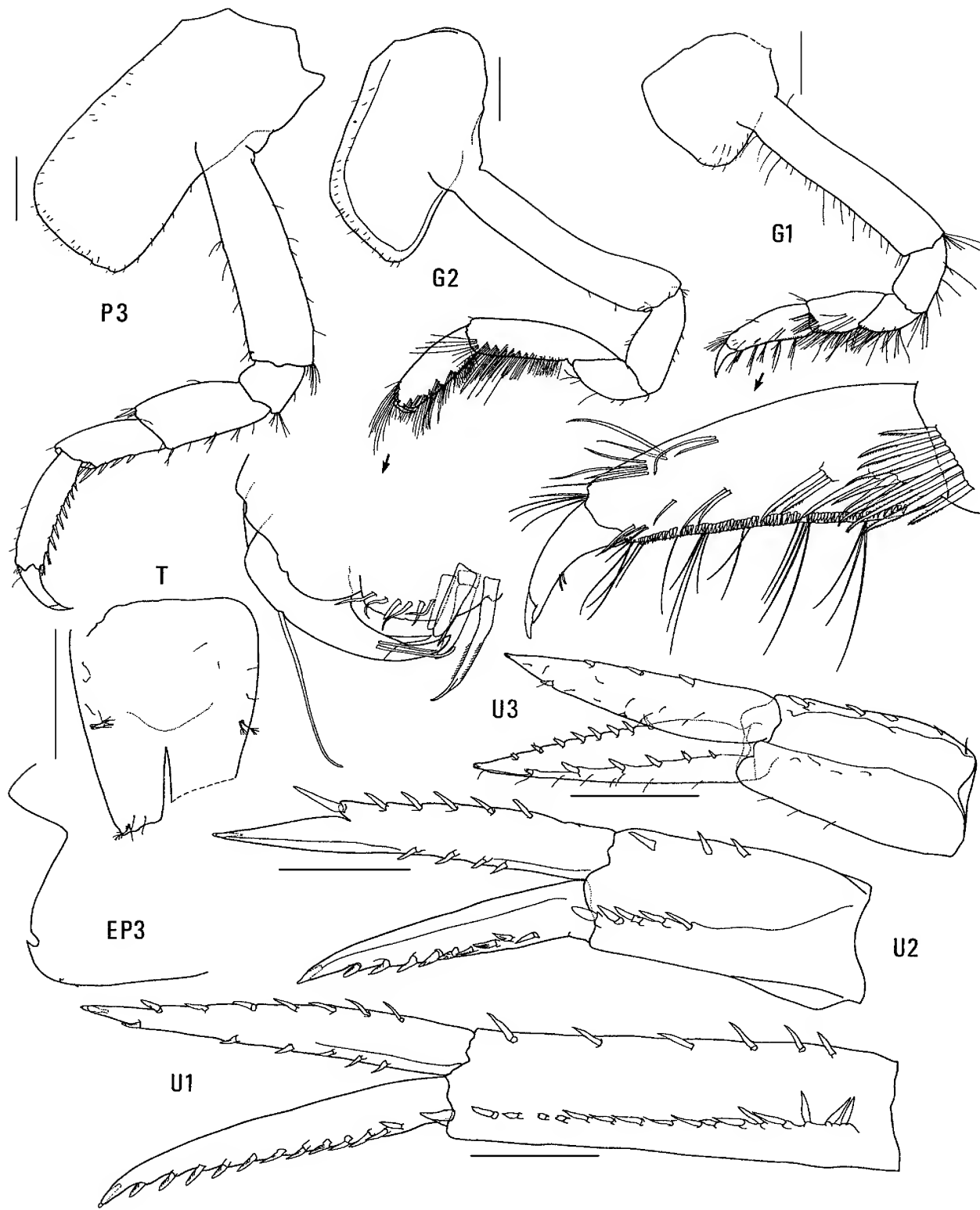


Figure 39. *Amaryllis spencerensis* n.sp., holotype female, 16.0 mm, AM P37096, Spencer Gulf, South Australia. Scales represent 0.5 mm.

posterodistal setae, article 3 without A3-seta. *Maxilliped outer plate with distal margin smooth*, medial margin without notch.

Gnathopod 1 carpus subequal in length to propodus (0.9×); propodus, posterior margin without robust setae. Gnathopod 2 palm slightly acute, with 2 lateral robust setae, 1 medial robust seta. Pereopods 3 and 4 merus and carpus without setal fringe. Pereopod 4 coxa with anterior and

posterior margins subparallel, anteroventral corner rounded. Pereopods 5–7 with distal articles elongate, dactyls short and stocky. Pereopod 5 basis expanded posteriorly, rounded. *Pereopod 7 basis subrectangular, posteroventral corner notched, posteroventral margin straight.*

Epimeron 3 posterior margin smooth, with notch well above rounded posteroventral corner. Uropod 1 peduncle

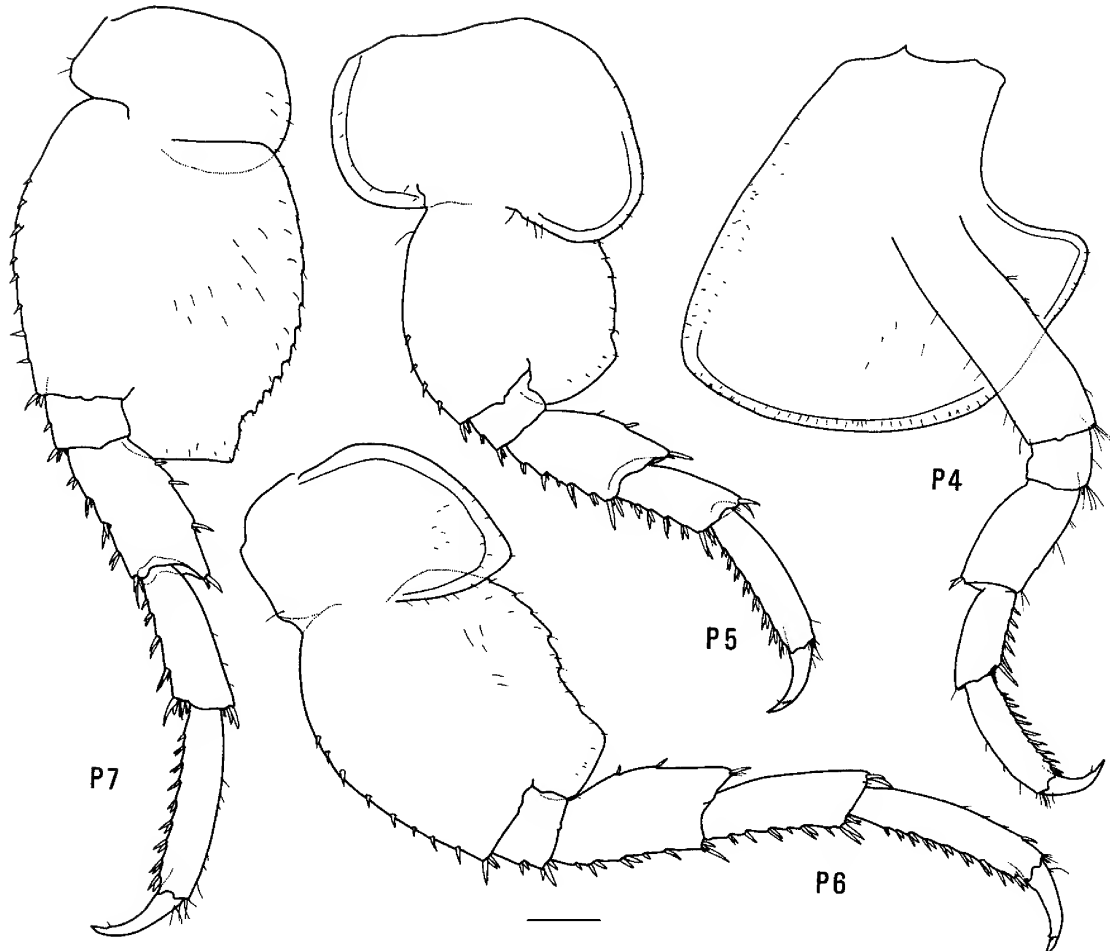


Figure 40. *Amaryllis spencerensis* n.sp., holotype female, 16.0 mm, AM P37096, Spencer Gulf, South Australia. Scale represents 0.5 mm.

dorsolateral margin with 17 robust setae; *outer ramus without large spines between robust setae*. Uropod 2 inner ramus slightly constricted. Uropod 3 rami lanceolate; without plumose setae; outer ramus 1-articulate. Telson moderately cleft (about 37%).

Male (sexually dimorphic characters). Based on paratype male, 11 mm, AM P37098. Antenna 1 flagellum with callynophore, with calceoli. Antenna 2 flagellum with calceoli. Mandible palp article 2 with 5 posterodistal setae. Gnathopod 2 palm with 1 lateral robust seta.

Etymology. Named for the type locality, Spencer Gulf.

Remarks. *Amaryllis spencerensis* belongs to a small group of species with a smooth posterior margin on epimeron 3 and a subrectangular basis on pereopod 7 (*A. macrophthalmus*, *A. philatelica* and *A. spencerensis*). Within this group *A. macrophthalmus* and *A. spencerensis* both have a well-developed medial spine on peduncular article 1 of antenna 1 and a notch above the rounded posteroventral corner on epimeron 3. In *A. spencerensis* the posteroventral corner of the basis of pereopod 7 is notched, in contrast to subquadrate in *A. macrophthalmus*, and there are significantly less robust setae defining the palm of gnathopod 2 in the female.

Habitat. Not known.

Distribution. Known only from Spencer Gulf, South Australia; 9–18 m depth.

Bamarooka n.gen.

Diagnosis. Mouthpart bundle subconical. Mandible palp article 3 without A3-seta. Pereopod 4 coxa with anterior margin slightly obtuse, posterior margin rounded. Pereopods 5–7 with distal articles elongate. Uropod 3 rami lanceolate; without plumose setae in male and female; outer ramus 1-articulate.

Type species. *Amaryllis bathycephala* Stebbing, 1888.

Species composition. *Bamarooka* contains six species: *B. anomala* n.sp.; *B. bathycephala* (Stebbing, 1888); *B. dinjerra* n.sp.; *B. endota* n.sp.; *B. kimbla* n.sp. and *B. tropicalis* n.sp.

Etymology. *Bamarooka* is an Australian Aboriginal word meaning “oval shield”, an allusion to coxa 4.

Remarks. Species of *Bamarooka* are mainly tropical amphipods distinguished from other amaryllidines by their strangely shaped coxa 4. Species level variation in *Bamarooka* is high, particularly in the eyes and the basis of pereopods 5 to 7. *Bamarooka* also occurs outside Australia, in New Caledonia (unpublished records) (see Fig. 41).

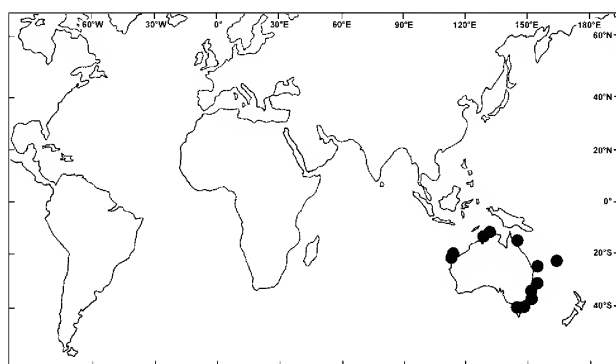
Distribution. Northwestern, northern and eastern coasts of Australia; New Caledonia; 2–175 m depth.

Key to species of *Bamarooka*

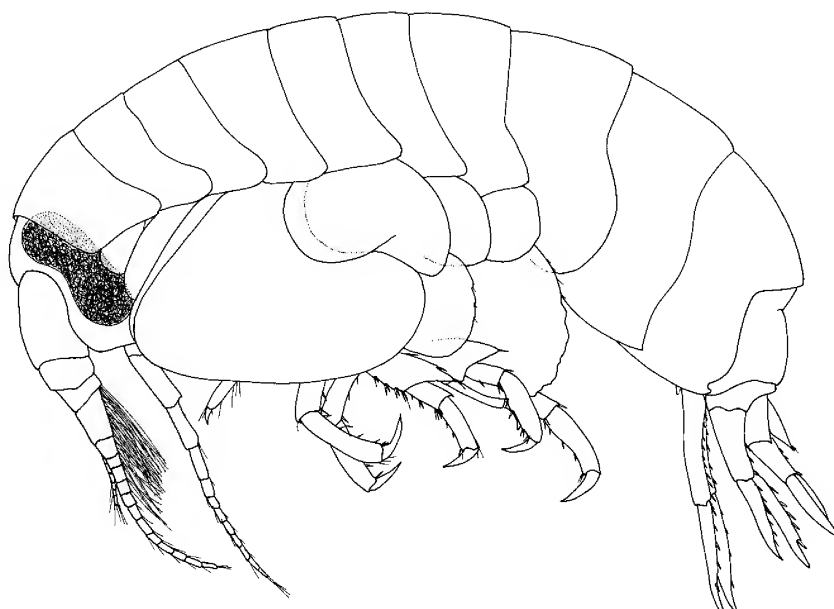
- 1 Head without rostrum; eye reniform 2
- Head with rostrum; eye ventrally tapered 3
- 2 Antenna 1 peduncular article 1 distal margin with small medial spine. Pereopod 5 basis expanded posteriorly, not linear *B. tropicalis*
- Antenna 1 peduncular article 1 distal margin without medial spine. Pereopod 5 basis not expanded, linear *B. anomala*
- 3 Pereopod 5 basis not pear-shaped. Female gnathopod 2 palm without lateral robust setae 4
- Pereopod 5 basis pear-shaped (expanded posterodistally). Female gnathopod 2 palm with 1–4 lateral robust setae *B. bathycephala*
- 4 Pereopod 5 basis with proximal posterior shoulder sloped 5
- Pereopod 5 basis almost round *B. endota*
- 5 Head with rostrum rounded. Female gnathopod 2 palm with 1 medial robust seta *B. dinjerra*
- Head with rostrum blunt cone-shaped. Female gnathopod 2 palm with 3 or 4 medial robust setae *B. kimbla*

Bamarooka anomala n.sp.

Figs. 42–44

Figure 41. Distribution of the genus *Bamarooka*.

Type material. HOLOTYPE, female, 10.2 mm, with 15 embryos, AM P36878; 1 PARATYPE, male, 6.5 mm, AM P36879; North West Shelf, NW of Port Hedland, Western Australia, eastern Indian Ocean, 19°28.3'S 118°55.2'E to 19°28.4'S 118°55.6'E, 38–39 m, epibenthic sled, 31 August 1983, FRV *Soela*, CSIRO NWS stn 04.B9.S. 1 PARATYPE, female, AM P36880, same locality, 19°54.6'S 117°56.0'E to 19°55.1'S 117°55.6'E, 44 m, epibenthic sled, 18 February 1983, FRV *Soela*, CSIRO NWS stn 01.B3.S. 1 PARATYPE, AM P36881, same locality, 19°28.6'S 118°55.0'E to 19°28.2'S 118°55.3'E, 39 m, epibenthic sled, 28 June 1983, FRV *Soela*, CSIRO NWS stn 03.B9.S. 1 PARATYPE, AM P36882, same locality, 19°29.6'S 118°52.2'E to 19°29.4'S

Figure 42. *Bamarooka anomala* n.sp., paratype male, 6.5 mm, AM P36879, North West Shelf, Western Australia.

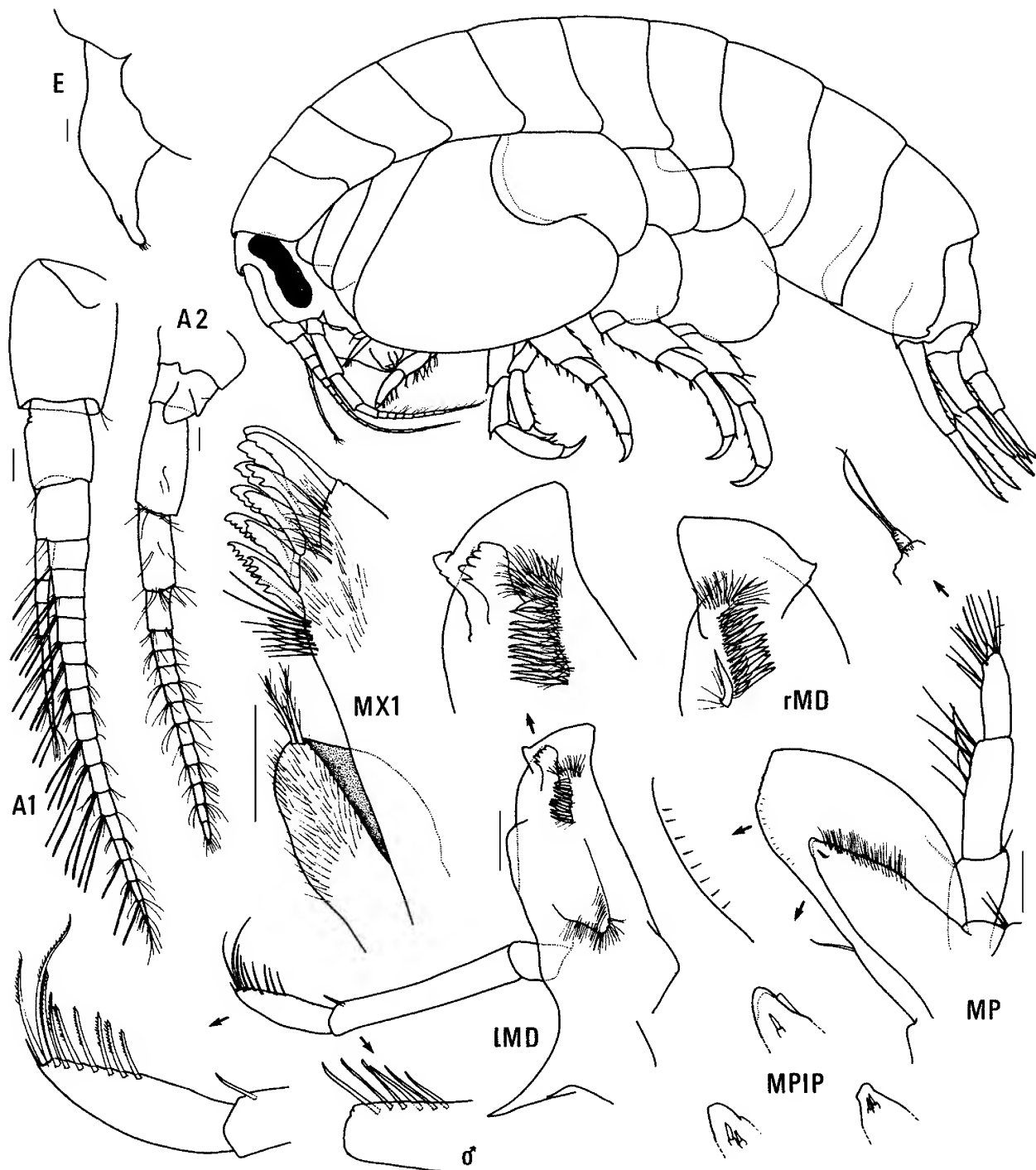


Figure 43. *Bamarooka anomala* n.sp., holotype female, 10.2 mm, AM P36878; paratype male, 6.5 mm, AM P36879; North West Shelf, Western Australia. Scales represent 0.1 mm.

118°52.8'E, 38 m, epibenthic sled, 30 August 1983, FRV *Soela*, CSIRO NWS stn 04.B8.S. 1 PARATYPE, female, AM P36883, same locality, 19°29.6'S 118°52.2'E to 19°29.6'S 118°51.4'E, 36–38 m, epibenthic sled, 25 October 1983, FRV *Soela*, CSIRO NWS stn 05.D4.S. 1 PARATYPE, female, AM P36884, same locality, 19°29.6'S 118°51.7'E to 19°29.9'S 118°51.0'E, 40–41 m, epibenthic sled, 25 October 1983, FRV *Soela*, CSIRO NWS stn 05.D7.S. 2 PARATYPES, male and juvenile, AM P36885, same locality, 19°29.4'S 118°52.5'E to 19°30.0'S 118°51.6'E, 38 m, epibenthic sled, 25 October 1983, FRV *Soela*, CSIRO NWS stn 05.D8.S. 1 PARATYPE, female,

AM P36886, same locality, 19°27.2'S 118°58.6'E to 19°26.7'S 118°58.3'E, 36–46 m, epibenthic sled, 8 December 1982, FRV *Soela*, CSIRO NWS stn 06.B9.S. 1 PARATYPE, female, NMV J7665, North West Shelf, between Port Hedland and Dampier, Western Australia, 19°37.00'S 118°53.00'E, 30–31 m, coarse shell, dredge, 3 June 1983, G.C.B. Poore & H.M. Lew Ton, FRV *Soela*, NMV stn NWA-14. 1 PARATYPE, NMV J13935, North West Shelf, between Port Hedland and Dampier, Western Australia, 19°39.00'S 116°31.00'E to 19°39.00'S 116°43.00'E, 46 m, bryozoans, dredge, 7 June 1983, G.C.B. Poore & H.M. Lew Ton, FRV *Soela*, NMV stn NWA-33.

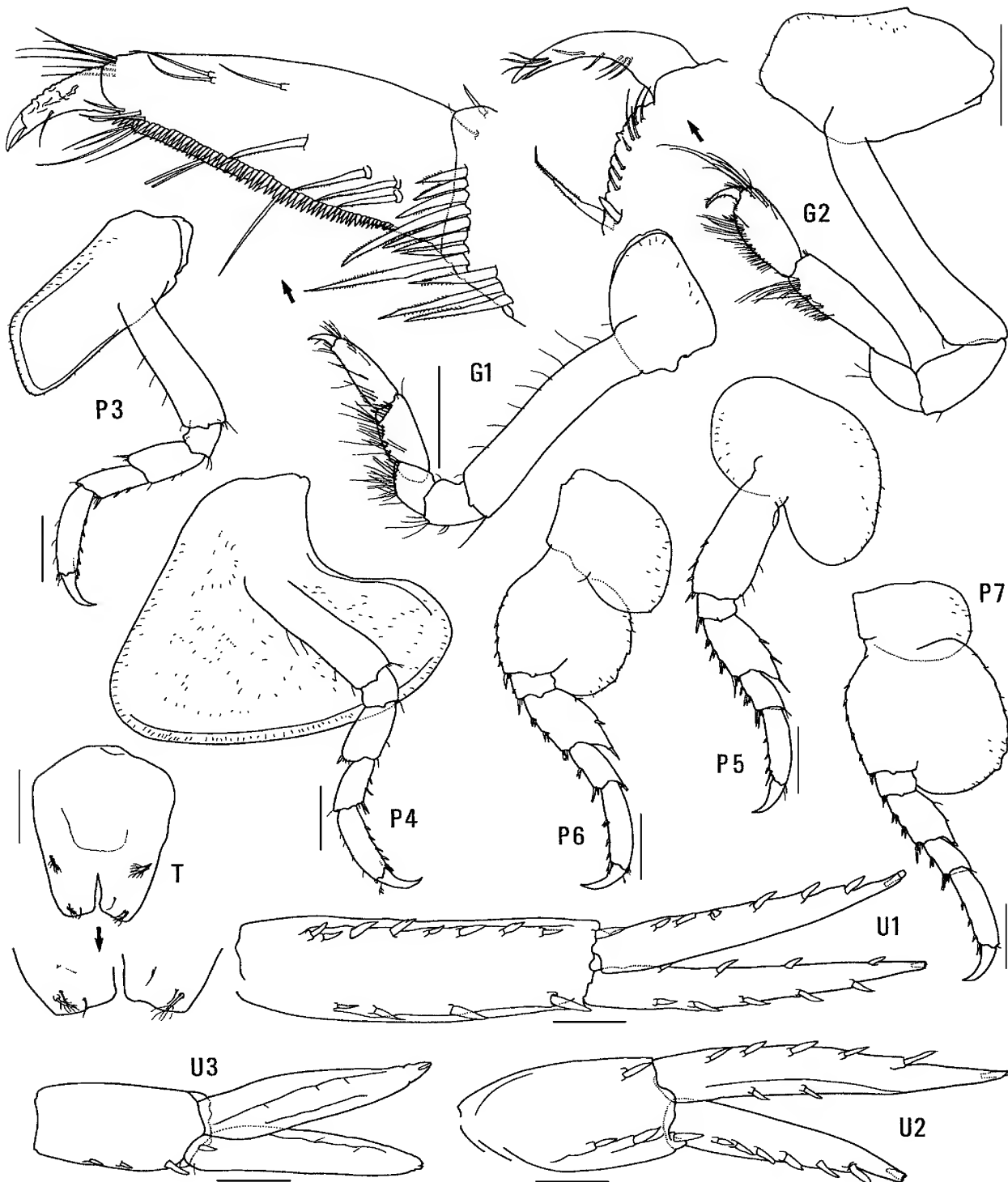


Figure 44. *Bamarooka anomala* n.sp., holotype female, 10.2 mm, AM P36878; North West Shelf, Western Australia. Scales for U1–3, T represent 0.2 mm; remainder represent 0.5 mm.

Additional material. WESTERN AUSTRALIA: 4 specimens, AM P36887, inshore limestone reef, North West Cape, 22°00'S 113°55'E, 2 m, coralline alga *Halimeda*, R. Springthorpe, 31 December 1983, stn WA-329. NORTHERN TERRITORY: 1 specimen, AM P58074, patch reef, north side of New Year Island, Arafura Sea, 10°54'S 133°02'E, 10 m, hydroids on coral, G.C.B. Poore, 14 October 1982, stn NT-17. 1 specimen, AM P36888, coral patch reefs at NW end of McCluer Island, 11°02'S 132°58'E, 8 m, sponges, J.K. Lowry, 16 October 1982, stn NT-42.

Type locality. North West Shelf, northwest of Port Hedland, Western Australia, eastern Indian Ocean, 19°28.3'S

118°55.2'E to 19°28.4'S 118°55.6'E, 38–39 m depth.

Description. Based on holotype female, 10.2 mm, AM P36878. Head much deeper than long, anterior margin with notch extended into a slit; *rostrum absent*; eye present, *elongate, reniform*. Antenna 1 peduncular article 1 not ball-shaped proximally, *distal margin without a medial spine*; peduncular article 2 medium length; flagellum without callynophore, calceoli absent. Antenna 2 flagellum about as long as that of antenna 1, without calceoli. Mouthpart

bundle subconical. *Epistome/upper lip with strong mid-anterior angle (lateral view)*. *Mandible lacinia mobilis a stemmed, distally-cusped blade; accessory setal row with intermediate setae; palp article 2 with 1 posterodistal seta, article 3 without A3-seta*. Maxilliped outer plate with distal margin smooth, medial margin without notch.

Gnathopod 1 carpus subequal in length to propodus; propodus, posterior margin without robust setae. *Gnathopod 2 palm slightly acute, with no lateral robust setae, 1 medial robust seta*. Pereopods 3 and 4 merus and carpus without setal fringe. Pereopod 4 coxa with anterior margin slightly obtuse, posterior margin rounded, anteroventral corner rounded. Pereopods 5–7 with distal articles elongate, dactyli short and stocky. *Pereopod 5 basis not expanded posteriorly (linear)*. Pereopod 7 basis rounded posteriorly, posteroventral corner rounded, posteroventral margin curved.

Epimeron 3 posterior margin smooth, with notch slightly above rounded posteroventral corner. Uropod 1 peduncle dorsolateral margin with 9 robust setae; outer ramus without large spines between robust setae. *Uropod 2 inner ramus slightly constricted*. Uropod 3 rami lanceolate, without plumose setae; outer ramus 1-articulate. Telson slightly cleft (about 22%).

Male (sexually dimorphic characters). Based on paratype male, 6.5 mm, AM P36879 (possibly not fully mature). Antenna 1 flagellum with callynophore. Antenna 2 flagellum without calceoli. Mandible palp article 2 with 6 posterodistal setae.

Etymology. The name reflects the unusual set of characters which defines this species within the genus *Bamarooka*.

Remarks. Two species of *Bamarooka* (*B. anomala* and *B. tropicalis*) have elongate, reniform eyes. They are easily distinguished from each other by their fifth pereopods, which have a linear basis in *B. anomala* and an expanded basis in *B. tropicalis*.

Habitat. *Bamarooka anomala* has been collected from coralline algae, bryozoans, sponges, hydroids and coarse shell sediment but its habitat is not specifically known.

Distribution. Northwestern and northern Australia; 30–46 m depth on North West Shelf and 2–10 m depth at inshore sites.

Bamarooka bathycephala (Stebbing)

Figs. 45–47

Amaryllis bathycephalus Stebbing, 1888: 699, pl. 27.

Amaryllis bathycephala.—Stebbing, 1906: 24.—Stebbing, 1910a: 633 (list).—Sheard, 1937: 18 (list).—Thurston & Allen, 1969: 354.

Amaryllis macropthalmus.—Della Valle, 1893: 781 (in part).

Material examined. NEW SOUTH WALES: 1 specimen, AM P58124, between Lion Island and Barrenjoey Head, Broken Bay, [approx. 33°33'S 151°22'E], 25 m, SPCC/UTS, 8 October 1991. 1 specimen, AM P24058, E of Burwood Beach, 32°58'S 151°45'E, 28 m, mud and gravel, shipwreck, 18 December 1975, HDWBS stn 06010304. 1 specimen, AM P58754, Cape Banks, 34°00'S 151°16'E, 45–50 m, The Ecology Lab, January 1991. 1 specimen, P58755, SE of Bate Bay, 34°5.9'S 151°12'E, 35–40 m, The Ecology Lab, January 1991, stn S2T4. 1 specimen, AM P58756, same locality, 35–40 m, The Ecology Lab, July 1990, stn S3T2. 3 specimens, AM P58757, same locality, 35–40 m, The Ecology Lab, January 1991, stn S3T4. 1 specimen, AM P46444, Bass Point, 34°36'S 150°54'E, 35–40 m, The Ecology Lab, 1 February 1990, stn S1R3. 1 specimen, AM P58758, same locality, The Ecology Lab, November 1990, stn S1T3. 1 specimen, AM P52920, Wattamolla, 34°08'S 151°08.5'E,

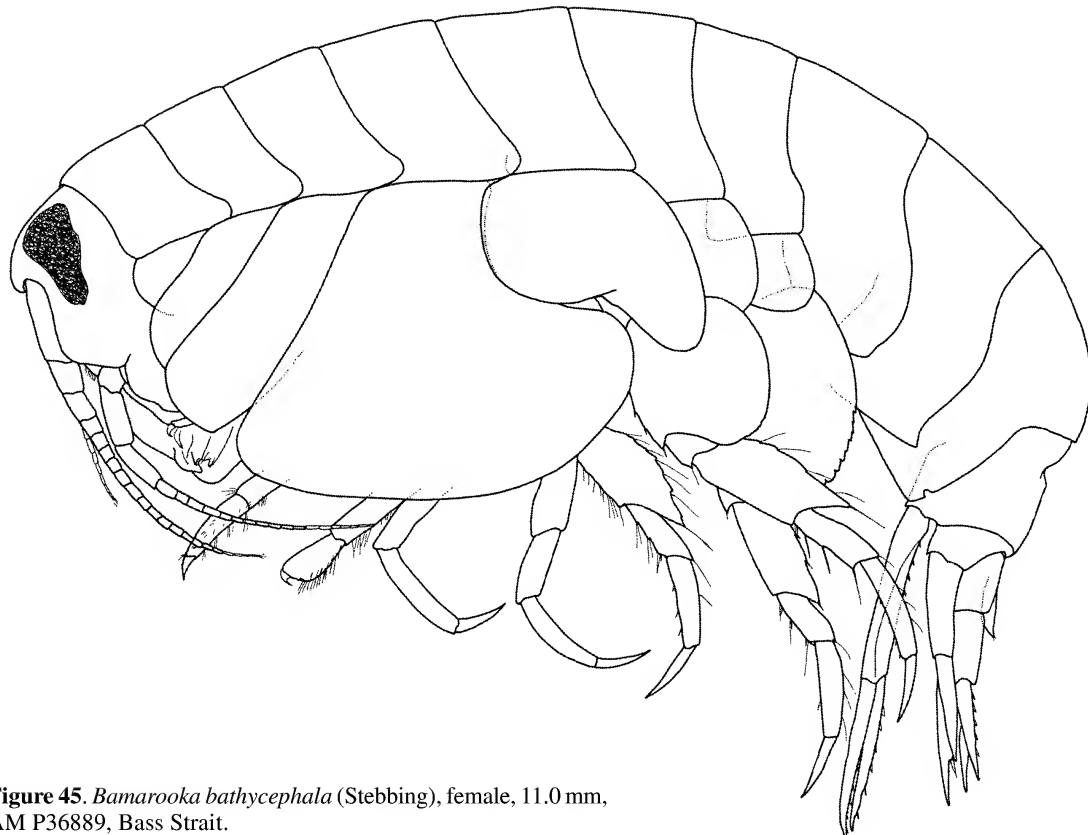


Figure 45. *Bamarooka bathycephala* (Stebbing), female, 11.0 mm, AM P36889, Bass Strait.

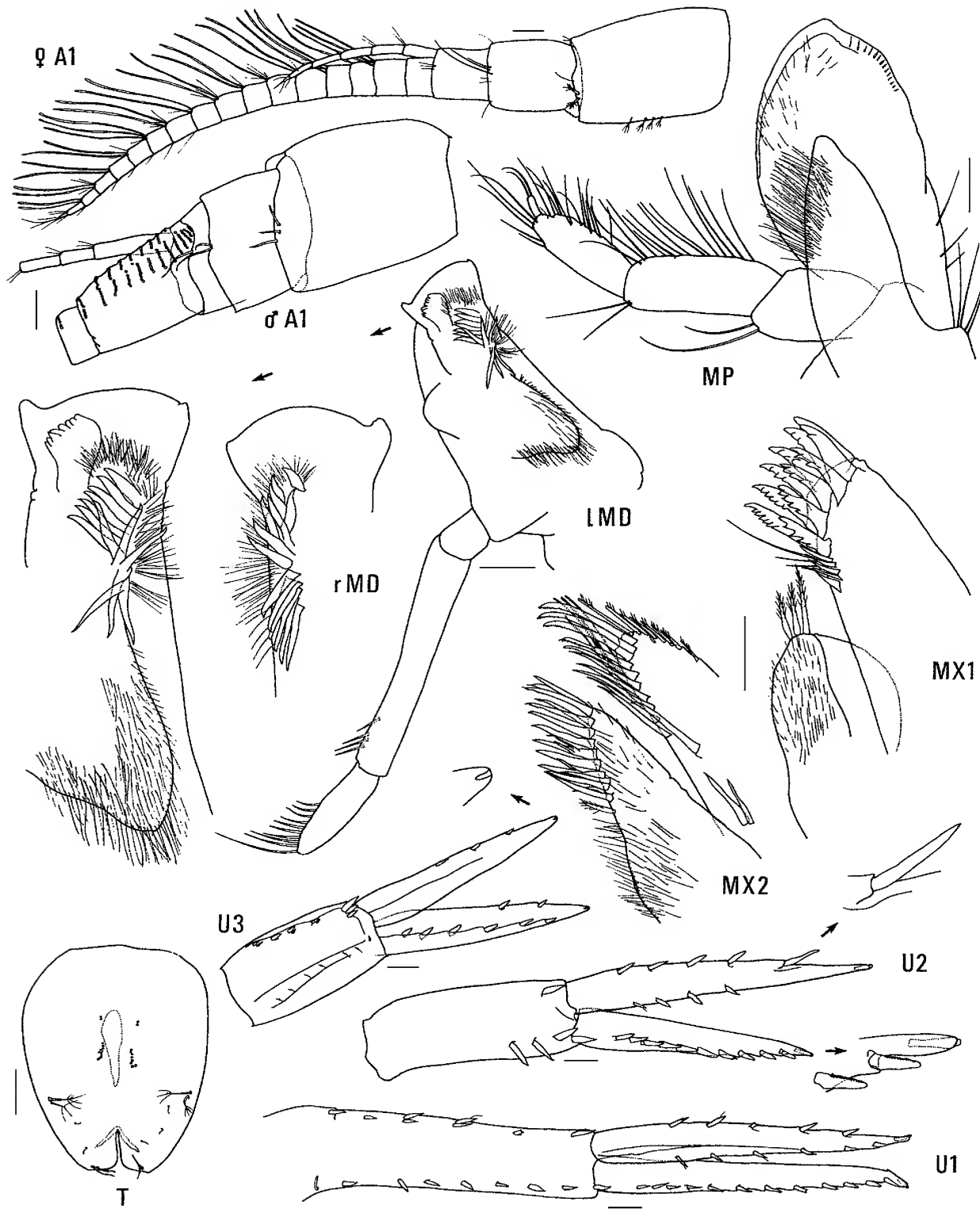


Figure 46. *Bamarooka bathycephala* (Stebbing), female, 11.0 mm, AM P36889; male, 7.2 mm, AM P36889; Bass Strait. Scales represent 0.1 mm.

45–50 m, The Ecology Lab, June 1990, stn S2R4. BASS STRAIT: 9 specimens, NMV J2310, 42 km SW of Babel Island, Tasmania, eastern Bass Strait, 40°13.8'S 148°39.6'E, 60 m, muddy sand, epibenthic sled, R. Wilson, 14 November 1981, RV *Tangaroa*, stn BSS-165. 1 specimen, NMV J13928, 32 km SSW of Cape Otway, western Bass Strait, 39°09'S 143°26'E, 85 m, coarse carbonate sand, G.C.B. Poore, 8 October 1980, HMAS *Kimbla*, cruise 80-K-1, stn BSS-55. 2 specimens, NMV J7450, 31 km SSW of Cape Otway, western Bass Strait, 39°08'S 143°24'E, 77 m, medium sand, grab, G.C.B. Poore, 8 October 1980, HMAS *Kimbla*,

stn BSS-56G. 1 specimen, NMV J7452, 35 km SSW of Cape Otway, Victoria, western Bass Strait, 39°06'S 143°21'E, 59 m, coarse sand, dredge, G.C.B. Poore, 8 October 1980, HMAS *Kimbla*, stn BSS-57D. 1 specimen, NMV J13929, 42 km NW of Cape Farewell, King Island, western Bass Strait, 39°19'S 143°38'E, 95 m, coarse sand, carbonate, G.C.B. Poore, 10 October 1980, HMAS *Kimbla*, cruise 80-K-1, stn BSS 76. 10 specimens, NMV J13930, 6 km NE of Stanley, Tasmania, central Bass Strait, 40°48.8'S 145°22'E, 22 m, fine sand, M. Gomon & G.C.B. Poore, 4 November 1980, FRV *Sarda*, stn BSS 114. 9 specimens, NMV J2309, 25

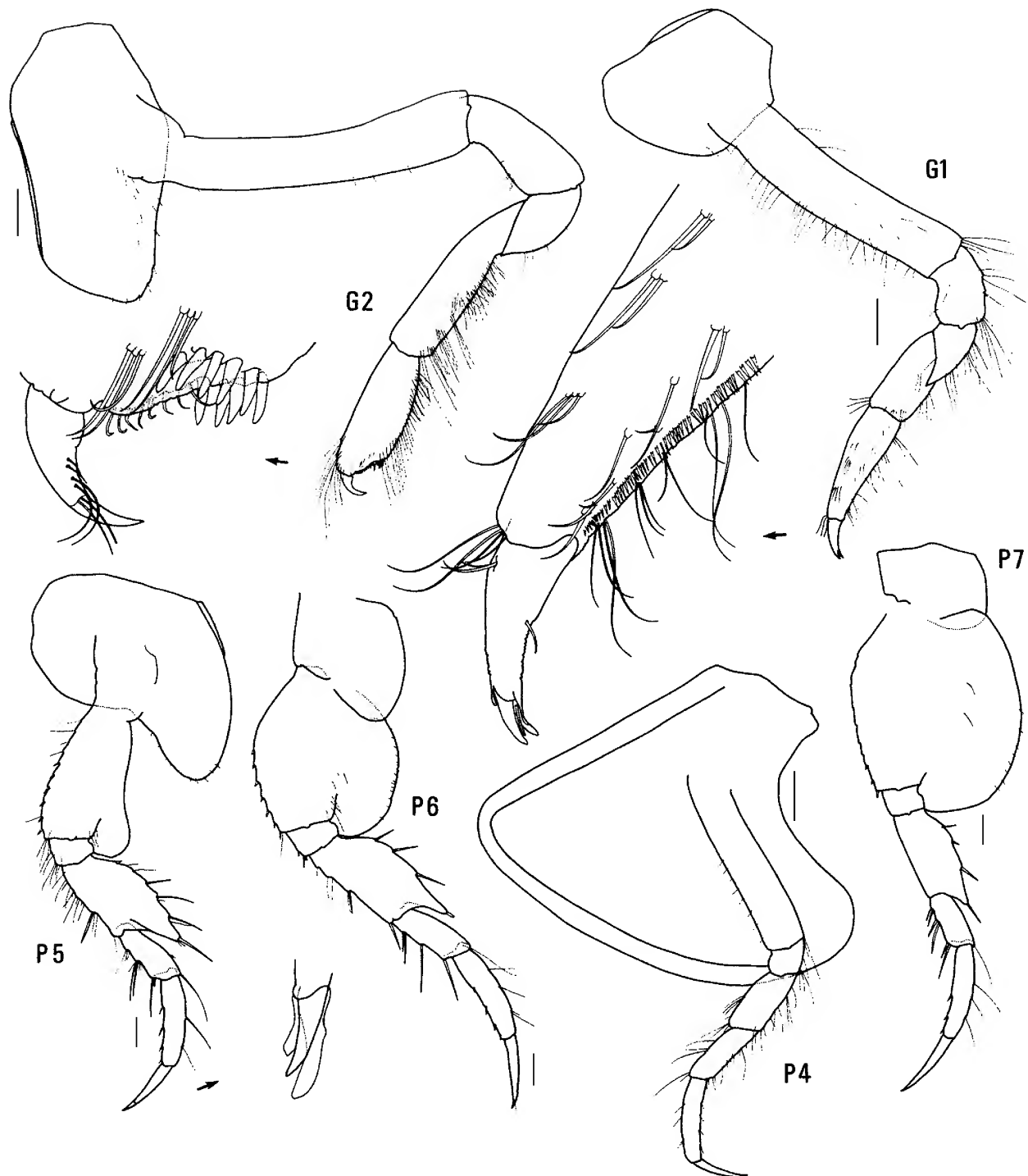


Figure 47. *Bamarooka bathycephala* (Stebbing), female, 11.0 mm, AM P36889, Bass Strait. Scales represent 0.2 mm.

km S of Cape Otway, Victoria, western Bass Strait, 39°06'S 143°35.8'E, 95 m, fine sand, dredge, M. Gomon *et al.*, 31 January 1981, FRV *Hai Kung*, stn BSS-118D. 53 specimens, NMV J13931; 30 specimens, AM P36889; 26 km SW of Cape Otway, Victoria, western Bass Strait, 39°01.0'S 143°22'E, 84 m, medium sand, epibenthic sled, M. Gomon *et al.*, 31 January 1981, FRV *Hai Kung*, stn BSS-120. 5 specimens, NMV J13932; 31 km S of Cape Otway, Victoria, western Bass Strait, 39°01.0'S 143°15.2'E, 84 m, medium sand, epibenthic sled, M. Gomon *et al.*, 31 January 1981, FRV *Hai Kung*, stn BSS-121. 2 specimens, NMV J48798, 94 km N of North Point, Flinders Island, eastern Bass Strait, 38°53.7'S 147°55.2'E, 71 m, medium sand, epibenthic sled, R. Wilson, 17 November 1981, RV *Tangaroa*, stn BSS 171S. 8 specimens, NMV J3769, 25 km S of Aireys Inlet, Victoria, central Bass Strait, 38°44.6'S 144°09.0'E, 77 m, fine sand, epibenthic sled, R. Wilson, 19 November 1981, RV *Tangaroa*,

stn BSS-182. 1 specimen, NMV J3772, 15 km SW of Point Reginald, Victoria, western Bass Strait, 38°50.0'S 143°07.5'E, 69 m, fine sand, grab, R. Wilson, 20 November 1981, RV *Tangaroa*, stn BSS-186. 2 specimens, NMV J13933, 70 km SW of Cape Otway, Victoria, western Bass Strait, 39°26.3'S 143°06.8'E, 115 m, sand, epibenthic sled, R. Wilson, 21 November 1981, RV *Tangaroa*, stn BSS-194. 6 specimens, NMV J13934, 65 km S of Cape Schanck, Victoria, central Bass Strait, 39°08.3'S 144°43.9'E, 66 m, coarse sand, R. Wilson, 23 November 1981, RV *Tangaroa*, stn BSS-201.

Type locality. Off mouth of Port Phillip Bay, Bass Strait, Australia, 38°22.5'S 144°36.5'E, 60 m depth.

Description. Based on female, 11 mm, AM P36889. Head much deeper than long, anterior margin with notch extended into a slit; *rostrum present*, anteriorly rounded; *eye present, ventrally tapered*. *Antenna 1 peduncular article 1* not ball-shaped proximally, *distal margin with small medial spine*; peduncular article 2 medium length; flagellum without callynophore, calceoli absent. Antenna 2 flagellum about as long as that of antenna 1, without calceoli. Mouthpart bundle subconical. *Epistome/upper lip with broad mid-anterior bulge (lateral view)*. Mandible lacinia mobilis a stemmed, distally-cusped blade; accessory setal row with intermediate setae; *palp article 2 with 4 posterodistal setae*, article 3 without A3-seta. Maxilliped outer plate with distal margin smooth, medial margin without notch.

Gnathopod 1 carpus shorter than propodus (0.8x); propodus, posterior margin without robust setae. *Gnathopod 2 palm acute, with 3 lateral robust setae, 6 medial robust setae*. Pereopods 3 and 4 merus and carpus without setal fringe. Pereopod 4 coxa with anterior margin slightly obtuse, posterior margin rounded, anteroventral corner rounded. Pereopods 5–7 with distal articles elongate, dactyli long and slender. *Pereopod 5 basis expanded posterodistally (pear-shaped)*. Pereopod 7 basis subrectangular, posteroventral corner rounded, posteroventral margin straight.

Epimeron 3 posterior margin smooth, with notch well above rounded posteroventral corner. Uropod 1 peduncle dorsolateral margin with 11 robust setae; outer ramus without large spines between robust setae. *Uropod 2 inner ramus slightly constricted*. Uropod 3 rami lanceolate; without plumose setae; outer ramus 1-articulate. Telson slightly cleft (about 20%).

Male (sexually dimorphic characters). Based on male, 7.2 mm, AM P36889. Antenna 1 flagellum with callynophore. Antenna 2 flagellum with calceoli. Gnathopod 2 palm without lateral robust setae, with 2 medial robust setae.

Variation. This species shows considerable variation in the robust-setae formula of gnathopod 2 palm. This variation

is correlated with the size and/or sex of specimens. For males the range is from 0/1 through 0/2 to 1/2; for females the known range is from 1/4 through 2/4, 4/4 to 4/5. Stebbing (1888: 701) recorded “a row of three short stout spines [= robust setae]... on one side and one or two more on the other”.

An 8.3 mm ovigerous female from east of Burwood Beach, NSW, differs slightly from the Bass Strait population in that the rostrum is slightly less produced, the eye is not quite so tapered and the basis of pereopod 5 is slightly broader distally.

Remarks. Most species of *Bamarooka* (*B. bathycephala*, *B. dinjerra*, *B. endota* and *B. kimbla*) have ventrally tapered eyes. *Bamarooka bathycephala* differs from all of these species in the basis of pereopod 5, which is pear-shaped.

Habitat. *Bamarooka bathycephala* has been collected frequently on sandy sediments and occasionally on mud.

Distribution. Southeastern Australia, from Sydney to Bass Strait; 22–115 m depth.

Bamarooka dinjerra n.sp.

Figs. 48–50

Type material. HOLOTYPE, female, 4.8 mm, with 4 embryos, AM P36890; 1 PARATYPE, male, 3.2 mm, AM P36891; northwest of Port Hedland, North West Shelf, Western Australia, eastern Indian Ocean, 20°00.3'S 117°00.4'E to 20°00.5'S 117°00.0'E, 53 m, epibenthic sled, 22 February 1983, FRV *Soela*, CSIRO NWS stn 01.B17.S. 1 PARATYPE, AM P58123, same locality, 19°05.2'S 118°57.6'E to 19°05.3'S 118°56.7'E, 82 m, epibenthic sled, 14 February 1983, FRV *Soela*, CSIRO NWS stn 01.B10.S. 5 PARATYPES, AM P36892, same locality, 19°59.3'S 117°03.6'E to 19°59.6'S 117°03.0'E, 52 m, epibenthic sled, 22 February 1983, FRV *Soela*, CSIRO NWS stn 01.B16.S.

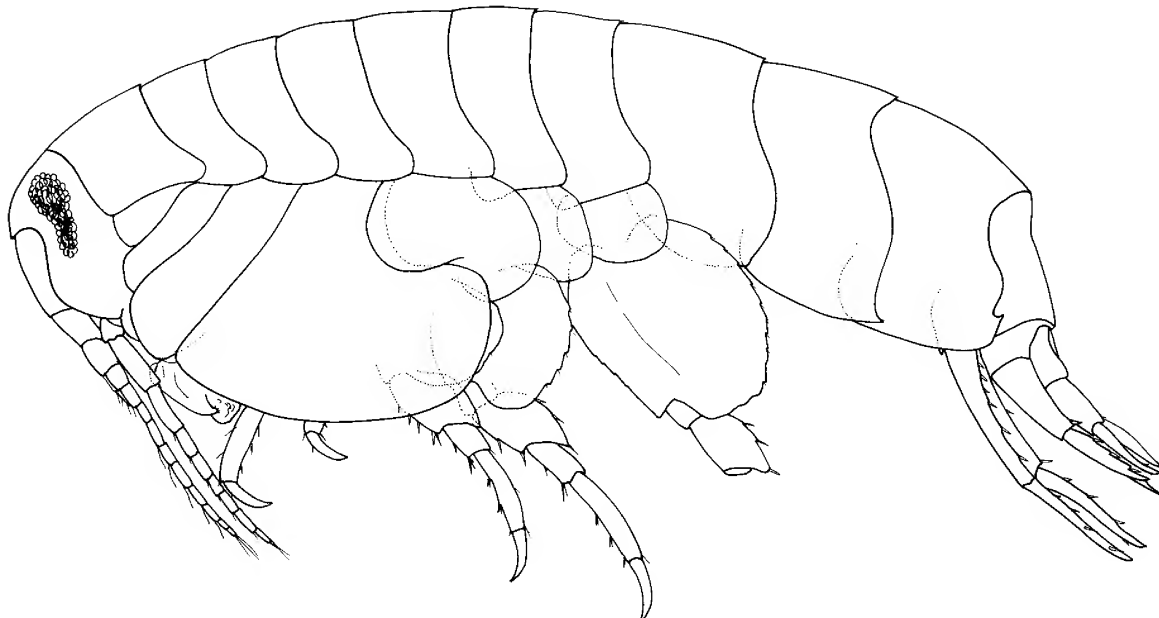


Figure 48. *Bamarooka dinjerra* n.sp., paratype female, 3.5 mm, AM P36892; North West Shelf, Western Australia.

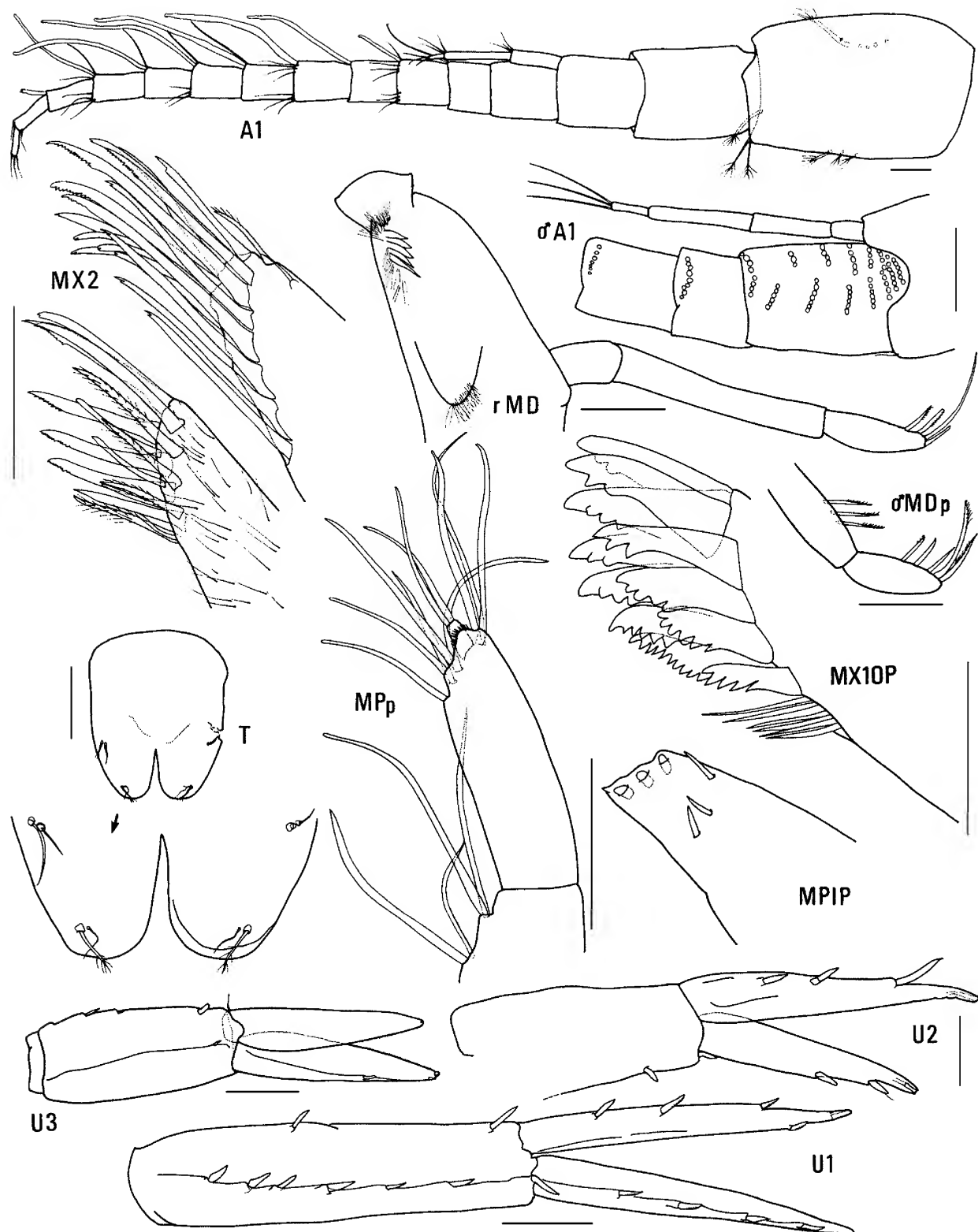


Figure 49. *Bamarooka dinjerra* n.sp., holotype female, 4.8 mm, AM P36890; paratype male, 3.2 mm, AM P36891, North West Shelf, Western Australia. Scales for U1–3, T represent 0.1 mm; remainder represent 0.05 mm.

1 PARATYPE, AM P36893, same locality, 19°56.9'S 117°53.7'E to 19°56.4'S 117°53.8'E, 42–43 m, epibenthic sled, 22 April 1983, FRV *Soela*, CSIRO NWS stn 02.B2.S. 1 PARATYPE, AM P36894, same locality, 19°28.6'S 118°55.0'E to 19°28.2'S 118°55.5'E, 40–38 m, epibenthic

sled, 26 April 1983, FRV *Soela*, CSIRO NWS stn 02.B9.S. 1 PARATYPE, AM P36895, same locality, 20°00.2'S 117°00.5'E to 20°00.4'S 116°59.9'E, 52 m, epibenthic sled, 4 September 1983, FRV *Soela*, CSIRO NWS stn 04.B17.S. 1 PARATYPE, AM P36896, same locality, 19°55.5'S 117°55.8'E to 19°55.1'S

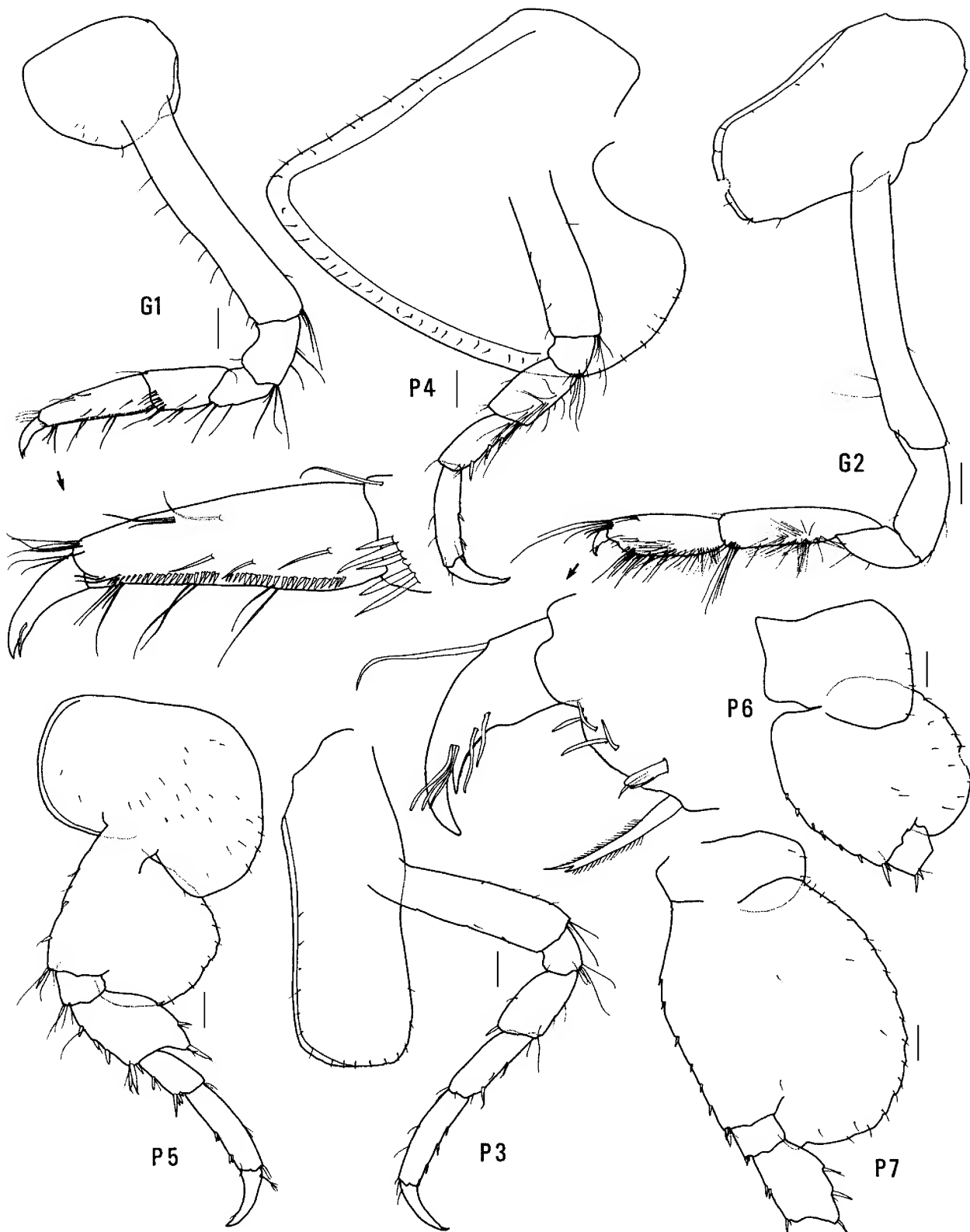


Figure 50. *Bamarooka dinjerra* n.sp., holotype female, 4.8 mm, AM P36890; North West Shelf, Western Australia. Scales represent 0.1 mm.

117°56.2'E, 40–41 m, epibenthic sled, 26 October 1983, FRV *Soela*, CSIRO NWS stn 05.B3.S. 1 PARATYPE, NMV J13936, same locality, 20°01'S 117°17'E to 20°00'S 117°18'E, 46 m, coarse shell, dredge, G.C.B. Poore & H.M. Lew Ton, FRV *Soela*, 2 June 1983, FRV *Soela*, NMV stn NWA-5.

Type locality. Northwest of Port Hedland, North West Shelf, Western Australia, eastern Indian Ocean, 20°00.3'S 117°00.4'E to 20°00.5'S 117°00.0'E, 53 m depth.

Description. Based on holotype female, 4.8 mm, (AM P36890). Head much deeper than long, anterior margin with notch extended into a slit; *rostrum present*, anteriorly rounded; *eye* present, ventrally tapered. *Antenna 1* peduncular article 1 not ball-shaped proximally, *distal margin with small medial spine*; peduncular article 2 medium length; flagellum without callynophore, calceoli absent. *Antenna 2* flagellum about as long as that of antenna 1, without calceoli. Mouthpart bundle subconical. *Epistome/upper lip almost straight (lateral view)*. *Mandible lacinia mobilis* a stemmed, distally-cusped blade; accessory setal row with intermediate setae; *palm article 2 without posterodistal setae*, article 3 without A3-seta. Maxilliped outer plate with distal margin smooth, medial margin without notch.

Gnathopod 1 carpus subequal in length to propodus (0.9x); propodus, posterior margin without robust setae. *Gnathopod 2* palm acute, with no lateral robust setae, 1 medial robust seta. Pereopods 3 and 4 merus and carpus without setal fringe. Pereopod 4 coxa with anterior margin slightly obtuse, posterior margin rounded, anteroventral corner rounded. Pereopods 5–7 with distal articles elongate, dactyli long and slender. *Pereopod 5 basis expanded posteriorly*, rounded with sloping posteroproximal shoulder. Pereopod 7 basis rounded posteriorly, posteroventral corner rounded, posteroventral margin curved.

Epimeron 3 posterior margin smooth, with notch well above rounded posteroventral corner. Uropod 1 peduncle dorsolateral margin with 7 robust setae; outer ramus without large spines between robust setae. *Uropod 2 inner ramus slightly constricted*. Uropod 3 rami lanceolate; without plumose setae; outer ramus 1-articulate. Telson moderately cleft (about 33%).

Male (sexually dimorphic characters). Based on paratype male, 3.2 mm, AM P36891. Antenna 1 flagellum with callynophore. Antenna 2 flagellum with calceoli. Mandible palp article 2 with 3 posterodistal setae.

Etymology. The specific name is an Australian Aboriginal word meaning “west”.

Remarks. Most species of *Bamarooka* (*B. bathycephala*, *B. dinjerra*, *B. endota* and *B. kimbla*) have ventrally tapered eyes. *Bamarooka dinjerra* and *B. endota* are very similar. They differ in the basis of pereopod 5, which has a sloped proximal posterior shoulder in *B. dinjerra* and is almost round in *B. endota*.

Habitat. Generally not known; taken on one occasion on a coarse shell bottom.

Distribution. North West Shelf, off Western Australia, Indian Ocean; 40–82 m depth.

Bamarooka endota n.sp.

Figs. 51–54

Amaryllis macrophthalmus.—Stebbing, 1910a: 569 (in part, part = *A. kamata*).

Type material. HOLOTYPE, female, 7.5 mm, ovigerous (5 eggs), NMV J13937; 1 PARATYPE, male, 5.9 mm, NMV J13938; 10 PARATYPES, 4.0–8.8 mm, AM P36897; 66 km south of Rodondo Island, central Bass Strait, Australia, 39°48.6'S 146°18.8'E, 82 m, sand, silt and mud, epibenthic sled, R. Wilson, 23 November 1981, RV *Tangaroa*, cruise 81-T-1, stn BSS-158S. 10 PARATYPES, AM P59022; 23 PARATYPES, NMV J13939; 57 km S of Rodondo Island, central Bass Strait, Australia, 39°46.0'S 146°18.0'E, 80 m, muddy shell, epibenthic sled, R. Wilson, 13 November 1981, RV *Tangaroa*, stn BSS-159S. 4 PARATYPES, NMV J13945, 57 km S of Rodondo Island, central Bass Strait, Australia, 39°43.5'S 146°18.8'E, 80 m, muddy shell, grab, G.C.B. Poore, 13 November 1981, RV *Tangaroa*, stn BSS-159G.

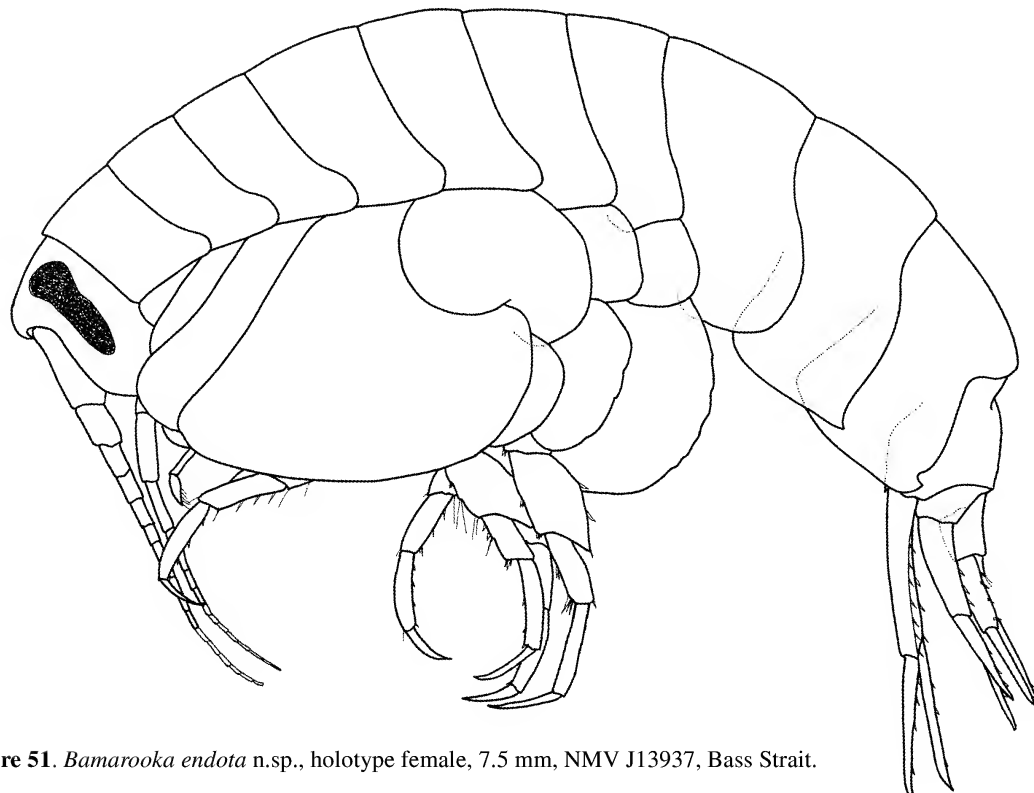


Figure 51. *Bamarooka endota* n.sp., holotype female, 7.5 mm, NMV J13937, Bass Strait.

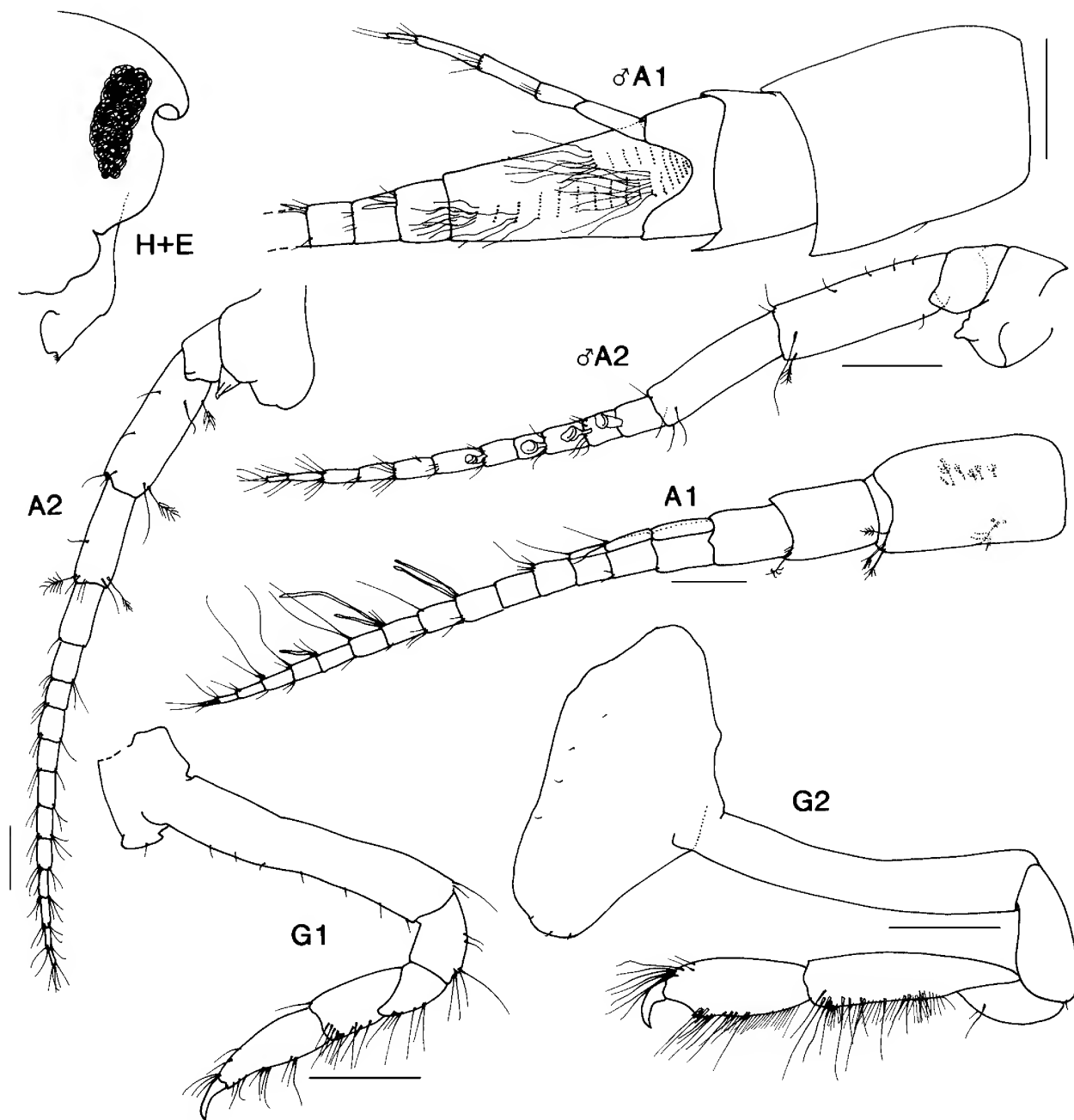


Figure 52. *Bamarooka endota* n.sp., holotype female, 7.5 mm, NMV J13937; paratype male, 5.9 mm, NMV J13938; Bass Strait. Scales for A1, 2 represent 0.2 mm; remainder represent 0.5 mm.

Additional material. NEW SOUTH WALES: 1 specimen, AM P36904, E of Newcastle, 32°53'S 152°35'E, 146–165 m, 15 August 1985, FRV *Kapala*, stn K85-12-23. 12 specimens, AM P37397, SE of Broken Bay, 33°36'S 151°30'E to 33°37'S 151°29'E, 71–75 m, benthic trawl, 10 February 1986, *Kapala*, stn K86-01-02. 2 females, 2 males, AM P36905, E of Long Reef Point, 33°43'S 151°46'E to 33°44'S 151°46'E, 174 m, trawl, 19 December 1985, FRV *Kapala*, stn K85-21-08. 5 specimens, AM P36902, E of Long Reef Point, 33°46'S 151°43'E, 175 m, dredged, 5 December 1977, FRV *Kapala*, stn K77-23-01. 5 females, AM P36903, E of Bondi, 33°52'S 151°23'E, 80 m, dredged, 11 December 1980, FRV *Kapala*, stn K80-20-11. 1 male, AM P22060, E of Malabar, 33°58.0'S 151°20.6'E, 75 m, sandy gravel, shipek grab, 25 May 1972, AMSBS stn C6. 2 females, AM P36899, 8–9.5 km E of Coogee, [approx. 33°57'S 151°21.5'E], 90–91 m, fine sand, E.R. Waite, 15 March 1898, HMCS *Thetis*, stn 44. 1 specimen, AM P36901, 4–6 km E of Botany Bay, [approx. 34°01'S 151°19'E], 60–102 m, trawl, F.A. McNeill & A. Livingstone, August 1921, ST *Goonambee*. 1 specimen, AM P37398, E of Port Hacking, [approx. 34°03'S 151°12'E], 40–69 m, sand, E.R. Waite, 10 March 1898, HMCS *Thetis*, stn 35. 1 female, AM P36898, 3–4 km off

Botany Bay, [approx. 34°05'S 151°15'E], 91–95 m, mud, E.R. Waite, 11 March 1898, HMCS *Thetis*, stn 37. 3 females, AM P36900, 5.5–6.5 km E of Wattamolla, [approx. 34°10'S 151°11'E], 108–99 m, mud, E.R. Waite, 22 March 1898, HMCS *Thetis*, stn 57. 2 specimens, AM P36908, off Montague Island, [approx. 36°15'S 150°14'E], from stomach of jackass fish *Nemadactylus macropterus*, April 1939, K. Sheard Collection. BASS STRAIT: 2 specimens, AM P58119, eastern Bass Strait, 38°59.1'S 148°31.6'E, 125 m, benthic sled, P.B. Berents, 27 August 1994, FRV *Southern Surveyor*, stn SS 05/94/60. 1 male, 3 females, NMV J13940, 85 km NE of North Point, Flinders Island, eastern Bass Strait, 39°02.4'S 148°30.6'E, 120 m, muddy sand, R. Wilson, 15 November 1981, RV *Tangaroa*, stn BSS-169. 5 specimens, NMV J13941, 100 km NE of North Point, Flinders Island, eastern Bass Strait, 31°51.8'S 148°26.5'E, 130 m, fine sand, epibenthic sled, R. Wilson, 15 November 1981, RV *Tangaroa*, stn BSS-170S. 1 female, NMV J7628, 100 km NE of North Point, Flinders Island, eastern Bass Strait, 31°51.8'S 148°26.5'E, 130 m, fine sand, grab, R. Wilson, 15 November 1981, RV *Tangaroa*, stn BSS-170G. 18 specimens, NMV J13942, 38 km SW of Cape Paterson, central Bass Strait, 38°56.4'S 145°16.6'E, 70 m, fine sand, epibenthic sled, R. Wilson, 12

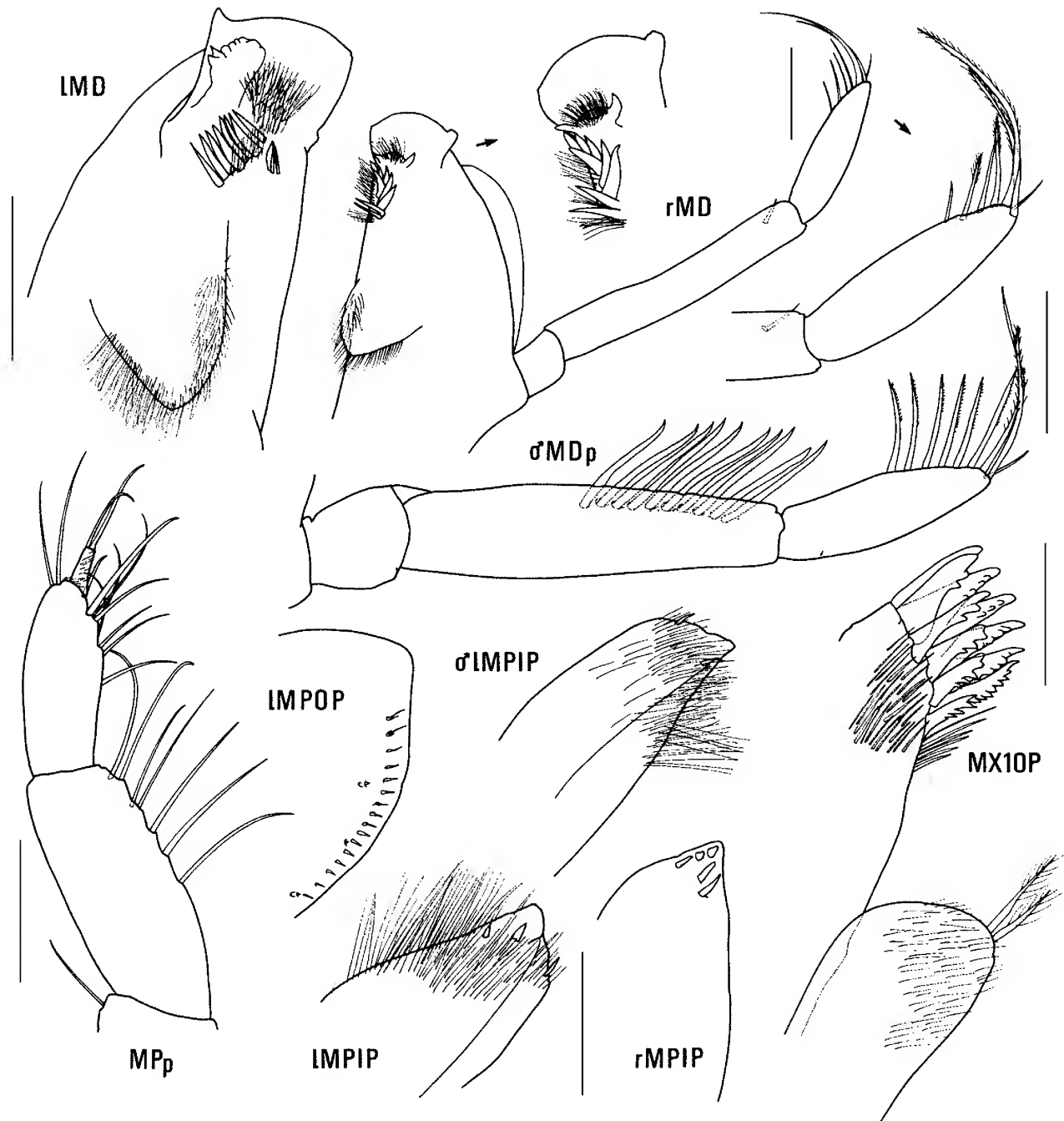


Figure 53. *Bamarooka endota* n.sp., holotype female, 7.5 mm, NMV J13937; paratype male, 5.9 mm, NMV J13938; Bass Strait. Scales represent 0.1 mm

November 1981, RV *Tangaroa*, stn BSS-155S. 8 specimens, NMV J13943, 100 km SSE of Cape Liptrap, central Bass Strait, Australia, 39°45.9'S 145°33.5'E, 74 m, muddy fine sand, epibenthic sled, R. Wilson, 13 November 1981, RV *Tangaroa*, stn BSS-156S. 1 specimen NMV J13944, 65 km ENE of Cape Rochon, Three Hummock Island, 40°10.9'S 145°44.3'E, 75 m, shell, bryozoans and mud, epibenthic sled, R. Wilson, 13 November 1981, RV *Tangaroa*, stn BSS-157S.

Type locality. 66 km south of Rodondo Island, central Bass Strait, Australia, 39°48.6'S 146°18.8'E, 82 m depth.

Description. Based on holotype female, 7.5 mm, NMV J13937. Head much deeper than long, anterior margin with notch extended into a slit; rostrum present, anteriorly truncated; eye present, ventrally tapered. Antenna 1 peduncular article 1 not ball-shaped proximally, distal

margin without a medial spine; peduncular article 2 medium length; flagellum without callynophore, calceoli absent. Antenna 2 flagellum about as long as that of antenna 1, without calceoli. Mouthpart bundle subconical. Epistome/upper lip with broad mid-anterior bulge (lateral view). Mandible lacinia mobilis a stemmed, distally-cusped blade; accessory setal row with intermediate setae; palp article 2 with 1 posterodistal seta, article 3 without A3-seta. Maxilliped outer plate with distal margin smooth, medial margin without notch.

Gnathopod 1 carpus subequal in length to propodus (0.9x); propodus, posterior margin without robust setae. Gnathopod 2 palm slightly acute, with no lateral robust setae, 3 medial robust setae. Pereopods 3 and 4 merus and

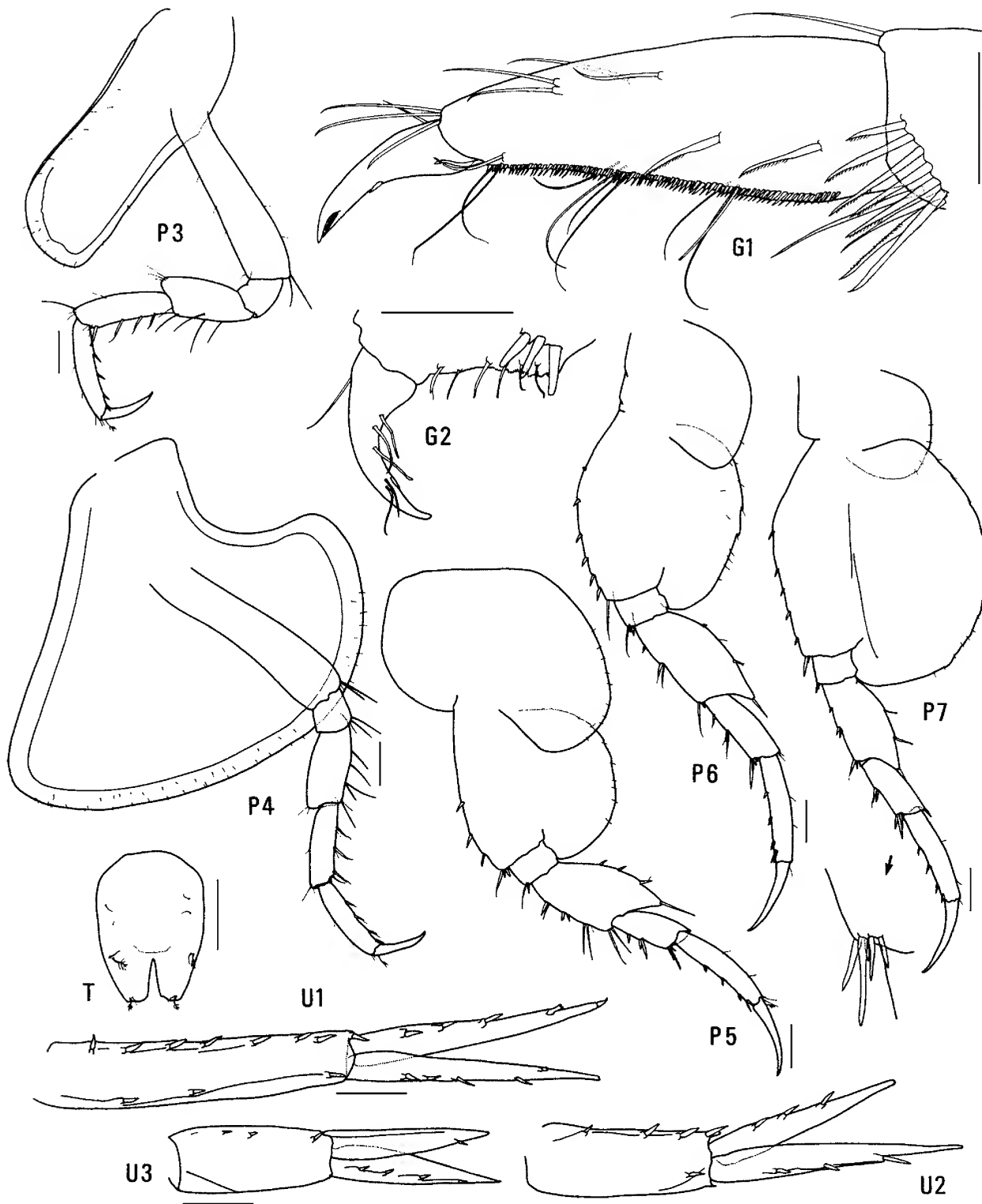


Figure 54. *Bamarooka endota* n.sp., holotype female, 7.5 mm, NMV J13937, Bass Strait. Scales for G1, 2 represent 0.1 mm; remainder represent 0.2 mm.

carpus without setal fringe. Pereopod 4 coxa with anterior margin slightly obtuse, posterior margin rounded, anteroventral corner rounded. Pereopods 5–7 with distal articles elongate, dactyli long and slender. Pereopod 5 basis expanded posteriorly, rounded. Pereopod 7 basis rounded posteriorly, posteroventral corner rounded, posteroventral margin curved.

Epimeron 3 posterior margin smooth, with notch well above rounded posteroventral corner. Uropod 1 peduncle dorsolateral margin with 8 robust setae; outer ramus without large spines between robust setae. Uropod 2 inner ramus slightly constricted. Uropod 3 rami lanceolate; without plumose setae; outer ramus 1-articulate. Telson slightly cleft (about 28%).

Male (sexually dimorphic characters). Based on paratype male, 5.9 mm, NMV J13938. Antenna 1 flagellum with callynophore. Antenna 2 flagellum with calceoli. Mandible palp article 2 with 10 posterodistal setae. Gnathopod 2 palm with 1 medial robust seta.

Etymology. The specific name is an Australian Aboriginal word meaning “beautiful”.

Remarks. Most species of *Bamarooka* (*B. bathycephala*, *B. dinjerra*, *B. endota* and *B. kimbla*) have ventrally tapered eyes. *Bamarooka endota* and *B. dinjerra* are very similar. They differ in the basis of pereopod 5, which is almost round in *B. endota* and has a sloped proximal posterior shoulder in *B. dinjerra*.

Although *B. endota* and *B. bathycephala* both occur in Bass Strait in similar depth range, the two species have not been taken in the same samples. *Bamarooka bathycephala* is found most often on clean sand bottoms whereas *B. endota* is most often found on muddy sand.

Habitat. *Bamarooka endota* occurs on fine and coarse sediments.

Distribution. Southeastern Australia, from central NSW to Bass Strait; 40–175 m depth.

***Bamarooka kimbla* n.sp.**

Figs. 55–57

Type material. HOLOTYPE, female, 9.3 mm, AM P36906; 1 PARATYPE, female, 7.8 mm, AM P36907; northeast of Lady Elliott Island, Capricorn Channel, Queensland, Australia, 24°03.7'S 152°49.4'E, 150 m, rubble, large sled dredge, P. Colman, G. Hangay & S. Keable, 4 July 1984, RV *Kimbla*, stn 3.

Type locality. Northeast of Lady Elliott Island, Capricorn Channel, Queensland, Australia, 24°03.7'S 152°49.4'E, 150 m depth.

Description. Based on holotype female, 9.3 mm, AM P36906. Head much deeper than long, anterior margin with notch extended into a slit; *rostrum present*, cone-shaped; *eye present, ventrally tapered*. Antenna 1 peduncular article 1 not ball-shaped proximally, *distal margin with small medial spine*; peduncular article 2 medium length; flagellum without callynophore, calceoli absent. Antenna 2 flagellum about as long as that of antenna 1, without calceoli. Mouthpart bundle subconical. *Epistome/upper lip with broad mid-anterior bulge (lateral view)*. Mandible lacinia mobilis a stemmed, distally-cusped blade; accessory setal row with intermediate setae; *palm article 2 with 2 posterodistal setae*, article 3 without A3-seta. Maxilliped outer plate with distal margin smooth, medial margin without notch.

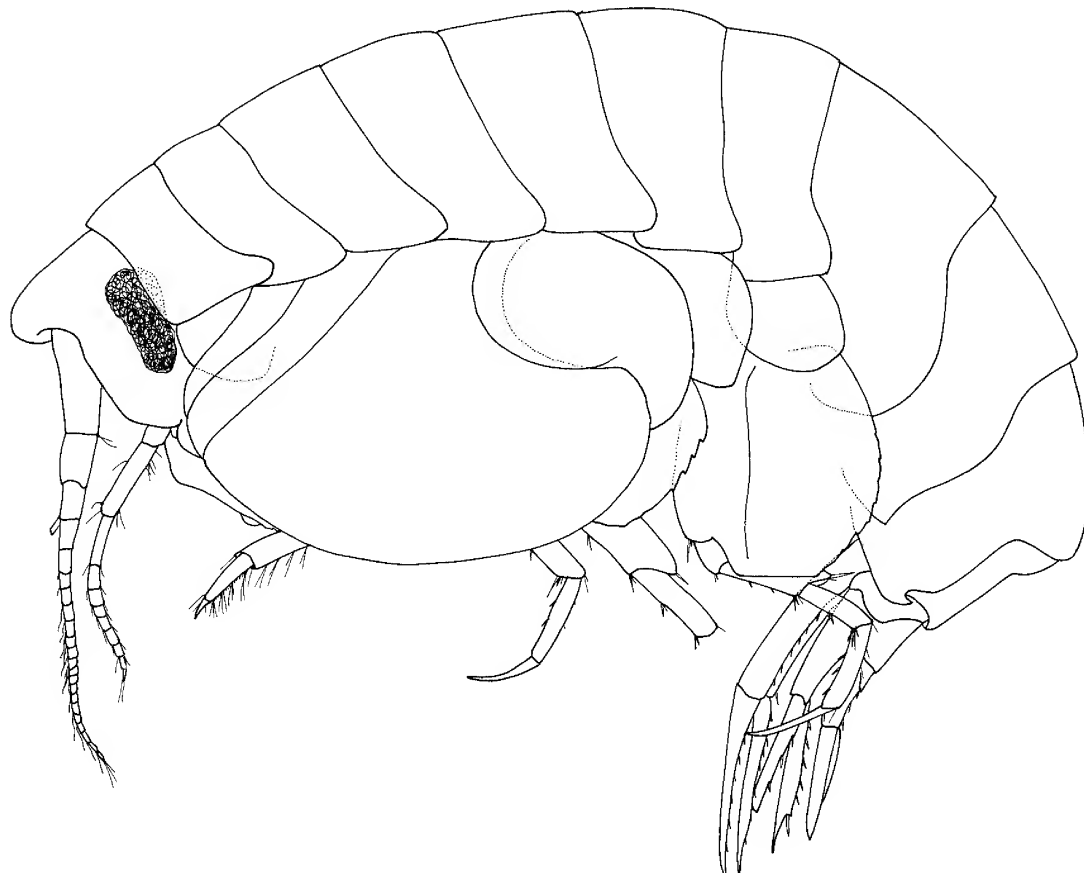


Figure 55. *Bamarooka kimbla* n.sp., paratype female, 7.8 mm, AM P36907, Capricorn Channel, Queensland.

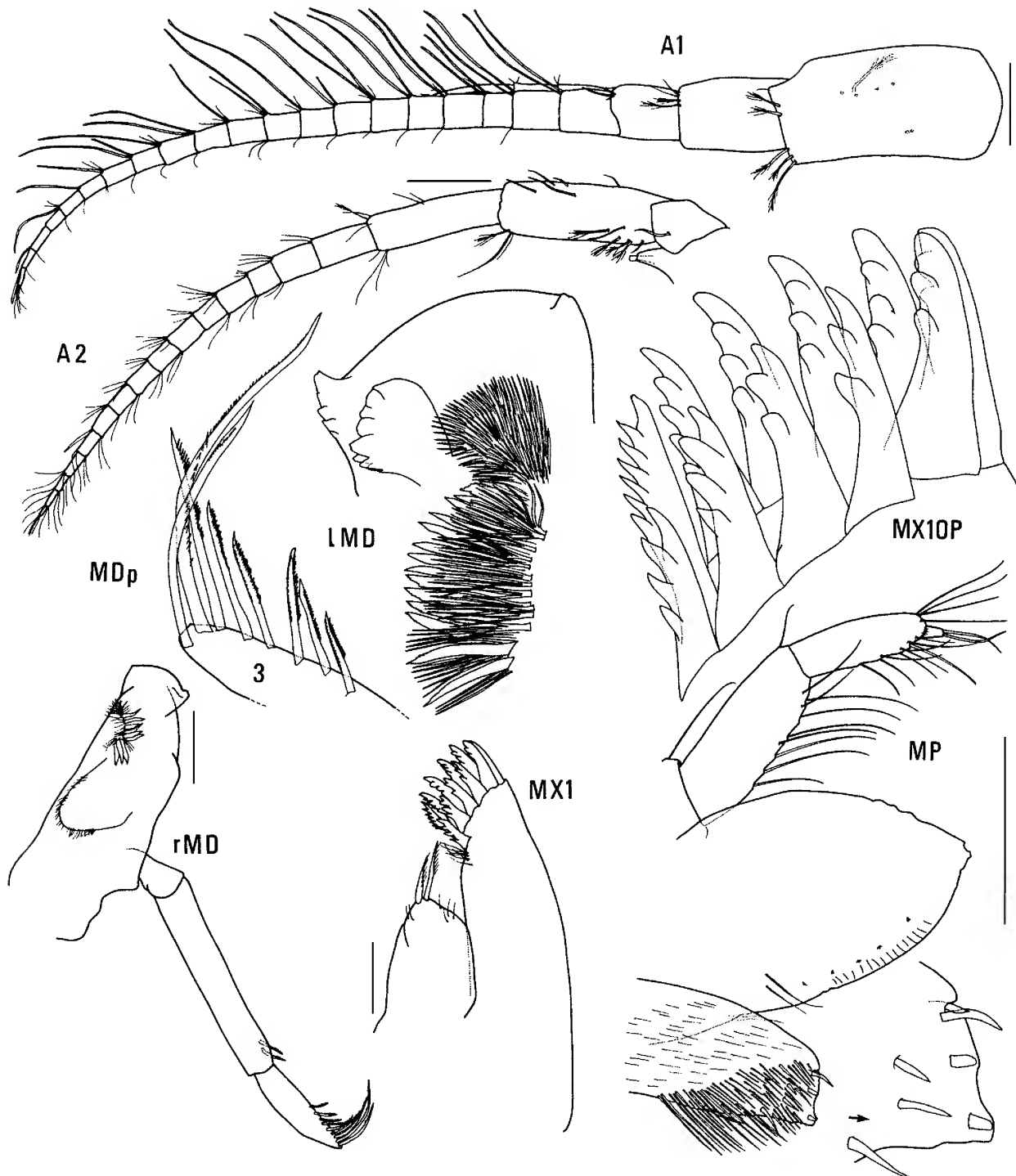
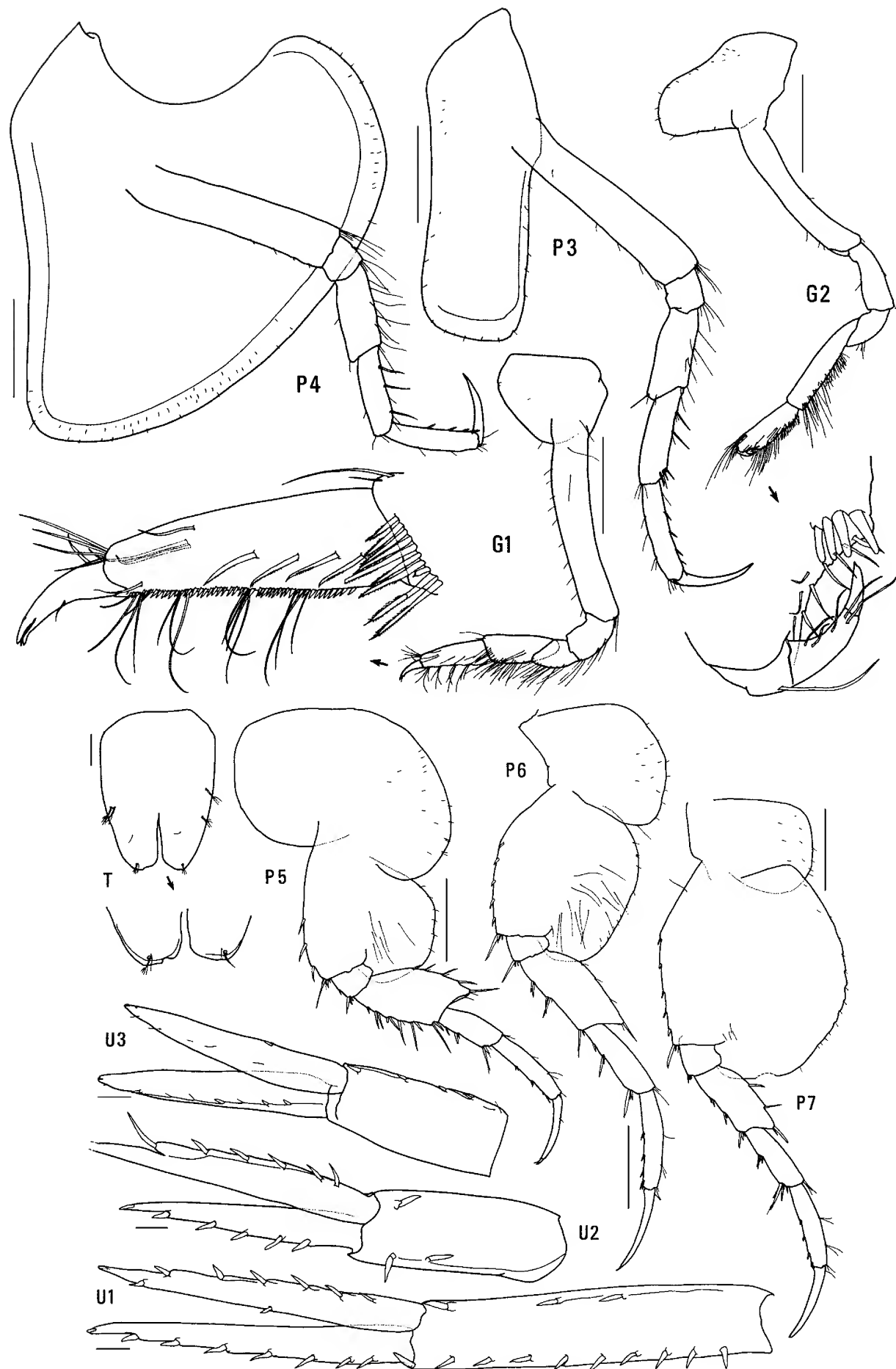


Figure 56. *Bamarooka kimbla* n.sp., holotype female, 9.3 mm, AM P36906, Capricorn Channel, Queensland. Scales represent 0.1 mm.

Gnathopod 1 carpus subequal in length to propodus; propodus, posterior margin without robust setae. Gnathopod 2 palm acute, with no lateral robust setae, 4 medial robust setae. Pereopods 3 and 4 merus and carpus without setal fringe. Pereopod 4 coxa with anterior margin slightly obtuse, posterior margin rounded, anteroventral corner rounded.

Pereopods 5–7 with distal articles elongate, dactyli long and slender. Pereopod 5 basis expanded posteriorly, rounded with sloping posteroproximal shoulder. Pereopod 7 basis rounded posteriorly, posteroventral corner rounded, posteroventral margin straight.

Figure 57. *Bamarooka kimbla* n.sp., holotype female, 9.3 mm, AM P36906, Capricorn Channel, Queensland. Scales for G1,2, P5–7 represent 0.5 mm; remainder represent 0.1 mm.



Epimeron 3 posterior margin smooth, with notch well above rounded posteroventral corner. Uropod 1 peduncle dorsolateral margin with 10 robust setae; outer ramus without large spines between robust setae. *Uropod 2 inner ramus moderately constricted*. Uropod 3 rami lanceolate; without plumose setae; outer ramus 1-articulate. Telson moderately cleft (about 32%).

Etymology. The specific name is taken from the research vessel *Kimbla*, which collected the type material.

Remarks. Most species of *Bamarooka* (*B. bathycephala*, *B. dinjerra*, *B. endota* and *B. kimbla*) have ventrally tapered eyes. *Bamarooka kimbla* differs from all of these species in the cone-shaped rostrum.

Distribution. Northeastern Australia; 150 m depth.

Bamarooka tropicalis n.sp.

Figs. 58–60

Type material. HOLOTYPE, female, 6.0 mm, ovigerous (5 eggs), AM P37074; 1 PARATYPE, male, 3.9 mm, AM P37075; 5 PARATYPES, AM P37076; northwest of Port Hedland, North West Shelf, Western Australia, eastern Indian Ocean, 19°29.2'S 118°52.5'E to 19°29.5'S 118°52.3'E, 40–41 m, epibenthic sled, 28 June 1983, FRV *Soela*, CSIRO stn NWS 03.B8.S. 5 PARATYPES, AM P37077, same locality, 19°29.6'S 118°52.2'E to 19°29.4'S 118°52.8'E, 38 m, epibenthic sled, 30 August 1983, CSIRO stn NWS 04.B8.S. 6 PARATYPES, AM P37078, same locality, 19°29.4'S 118°52.5'E to 19°30.0'S 118°51.6'E, 38 m, epibenthic sled, 25 October 1983, FRV *Soela*, CSIRO NWS stn 05.D8.S. 10 PARATYPES, NMV J7667, North West Shelf, Western Australia, eastern Indian Ocean, 19°39'S 116°22'E to 19°39'S 116°43'E, 46 m, bryozoans, G.C.B. Poore & H.M. Lew Ton, 7 June 1983, FRV *Soela*, stn NWA-33.

Additional material. WESTERN AUSTRALIA: 19 specimens, AM P37079, to P37087, from 9 CSIRO North West Shelf stations close to type locality, 36–40 m, dredged, June–October 1983. NORTHERN TERRITORY: 1 specimen, AM P58075, S side of New Year Island, Arafura Sea, 10°54'S 133°02'E, 14 m, hydroids, G.C.B. Poore, 14 October 1982, stn NT-20. 2 specimens, AM P58076, same locality, 14 m, alga *Padina*, J.K. Lowry, 14 October 1982, stn NT-25. 1 specimen, AM P58077, same locality, 14 m, rubble, J.K. Lowry, 14 October 1982, stn NT-26. 1 specimen, AM P37088, patch reefs at NW end of McCluer Island, 11°02'S 132°58'E, 8 m, red algae and sediment, J.K. Lowry, 16 October 1982, stn NT-38. 2 specimens, AM P58078, S end of McCluer Island, Arafura Sea, 11°06'S 133°00'E, 8 m, coral rubble, G.C.B. Poore, 17 October 1982, stn NT-55. 1 specimen, AM P58079, same locality, 8 m, red algae *?Champsia*, J.K. Lowry, 17 October 1982, stn NT-58. 14 specimens, AM P37089, same locality, 8 m, *Acropora* base, P. Horner, 17 October 1982, stn NT-59. 3 specimens, AM P58080, same locality, 8 m, coral rubble with encrusting invertebrates, J.K. Lowry, 17 October 1982, stn NT-60. 2 specimens, AM P37090, same locality, 8 m, *Seriatopora hystrrix*, J.K. Lowry, 17 October 1982, stn NT-61. 6 specimens, AM P37091, W of East Point, north end of Fannie Bay, Darwin, 11°24.5'S 130°48.5'E, 8–10 m, encrusting ascidian *Didemnum psammodes*, J.K. Lowry, 26 October 1982, stn NT-97. 3 specimens, AM P58081, same locality, 8–10 m, red alga, J.K. Lowry, 26 October 1982, stn NT-103. 1 specimen, AM P18172, Port Darwin, [approx. 12°27'S 130°50'E], W.E.J. Paradice on HMAS *Geranium*. QUEENSLAND: 1 specimen, AM P37092, fringing reef between Bird Islet and South Island, Lizard Island, 14°40'S 145°28'E, 24.4–27.4

m, *Halophila*, mixed algae and coral rubble, J.K. Lowry, 7 October 1978, stn QLD-21. 4 specimens, AM P37093, same locality, 27.6 m, *Halophila*, mixed algae and sediment from seagrass beds on reef base, J.K. Lowry & P.C. Terrill, 9 October 1978, stn QLD-27&28. 1 specimen, AM P37094, Lizard Island, 3 m, plankton tow in lagoon, J.M. Leis, 17 October 1979, stn JML 17.10.2. 1 specimen, AM P37095, between Lizard Island and Carter Reef, 32–38 m, algae and sediment, epibenthic sled, J.M. Leis, 26 November 1981, stn JML 81/26-1-4.

Type locality. Northwest of Port Hedland, North West Shelf, Western Australia, eastern Indian Ocean, 19°29'S 118°52'E, 40–41 m depth.

Description. Based on holotype female, 6.0 mm, AM P37074. Head much deeper than long, anterior margin with notch extended into a slit; *rostrum absent; eye elongate, reniform*. *Antenna 1 peduncular article 1* not ball-shaped proximally, *distal margin with small medial spine*; peduncular article 2 medium length; flagellum without callynophore, calceoli absent. *Antenna 2 flagellum* about as long as that of antenna 1, without calceoli. Mouthpart bundle subconical. *Epistome/upper lip almost straight (lateral view)*. *Mandible lacinia mobilis* a stemmed, distally-cusped blade; accessory setal row with intermediate setae; *palp article 2 without posterodistal setae*, article 3 without A3-seta. Maxilliped outer plate with distal margin smooth, medial margin without notch.

Gnathopod 1 carpus shorter than propodus (0.8x); propodus, posterior margin without robust setae. *Gnathopod 2* palm slightly acute, *with no lateral robust setae, 1 medial robust seta*. Pereopods 3 and 4 merus and carpus without setal fringe. Pereopod 4 coxa with anterior margin slightly obtuse, posterior margin rounded, anteroventral corner rounded. Pereopods 5–7 with distal articles elongate, dactyli short and stocky. *Pereopod 5 basis expanded posteriorly*, rounded with sloping posteroproximal shoulder. Pereopod 7 basis rounded posteriorly, posteroventral corner rounded, posteroventral margin curved.

Epimeron 3 posterior margin smooth, with notch well above rounded posteroventral corner. Uropod 1 peduncle dorsolateral margin with 7 robust setae; outer ramus without large spines between robust setae. *Uropod 2 inner ramus slightly constricted*. Uropod 3 rami lanceolate; without plumose setae; outer ramus 1-articulate. Telson moderately cleft (about 36%).

Male (sexually dimorphic characters). Based on paratype male, 3.9 mm, AM P37075. Antenna 1 flagellum with callynophore. Mandible palp article 2 with 1 posterodistal seta.

Etymology. The specific name is a reference to the species' distribution in Australia.

Remarks. *Bamarooka anomala* and *B. tropicalis* both have elongate, reniform eyes. They are easily distinguished from each other by their fifth pereopods, which have a linear basis in *B. anomala* and an expanded basis in *B. tropicalis*.

Habitat. *Bamarooka tropicalis* has been found with algae, seagrasses, sediments, ascidians, bryozoa and hydroids, but most commonly among corals and coral rubble.

Distribution. Northern Australia, from North West Shelf off Western Australia to northern Great Barrier Reef, Queensland; 3–40 m depth.

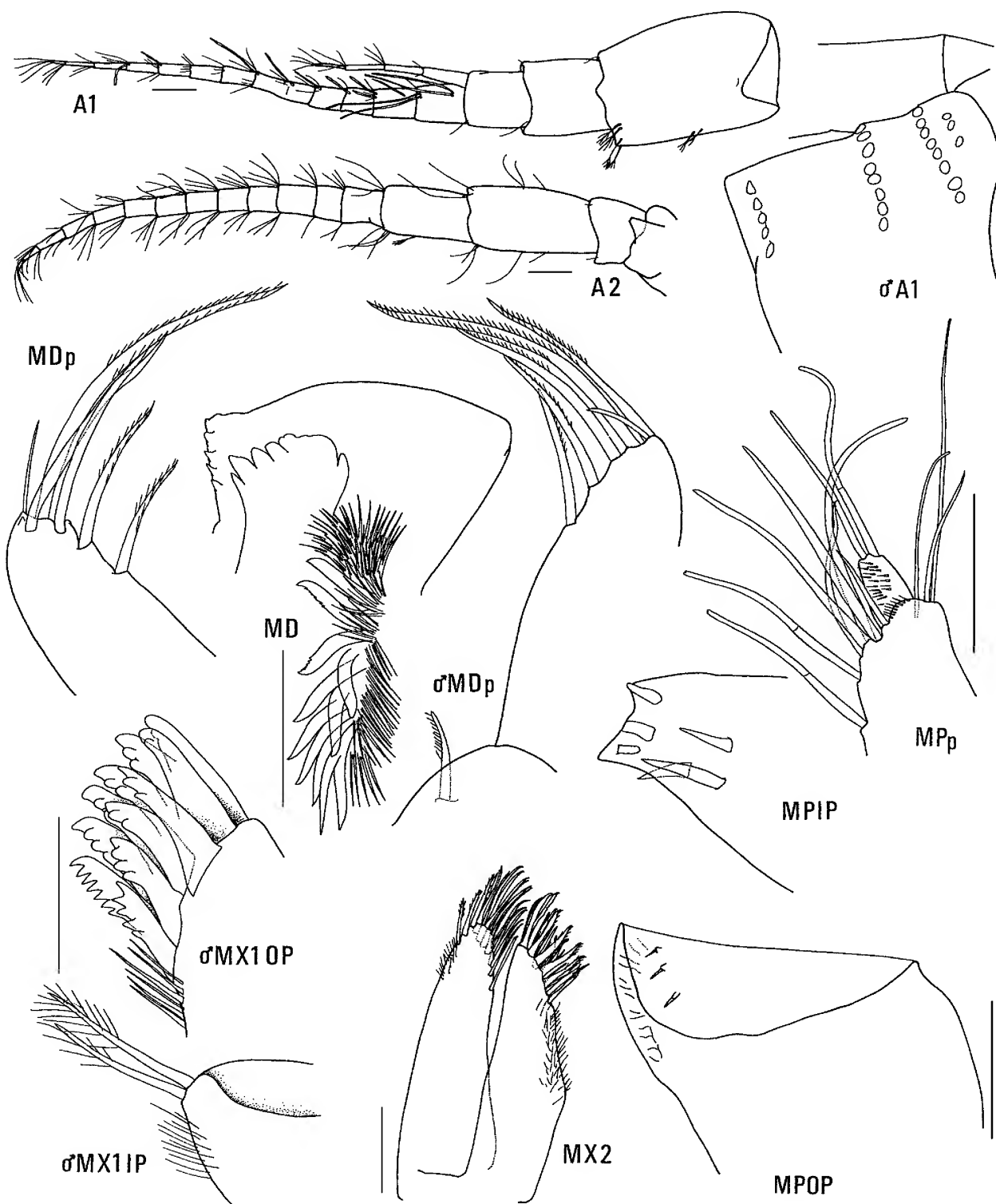


Figure 58. *Bamarooka tropicalis* n.sp., holotype female, 6.0 mm, AM P37074; paratype male, 3.9 mm, AM P37075; North West Shelf, Western Australia. Scales for A1, 2, MX2, MPOP represent 0.1 mm; remainder represent 0.05 mm.

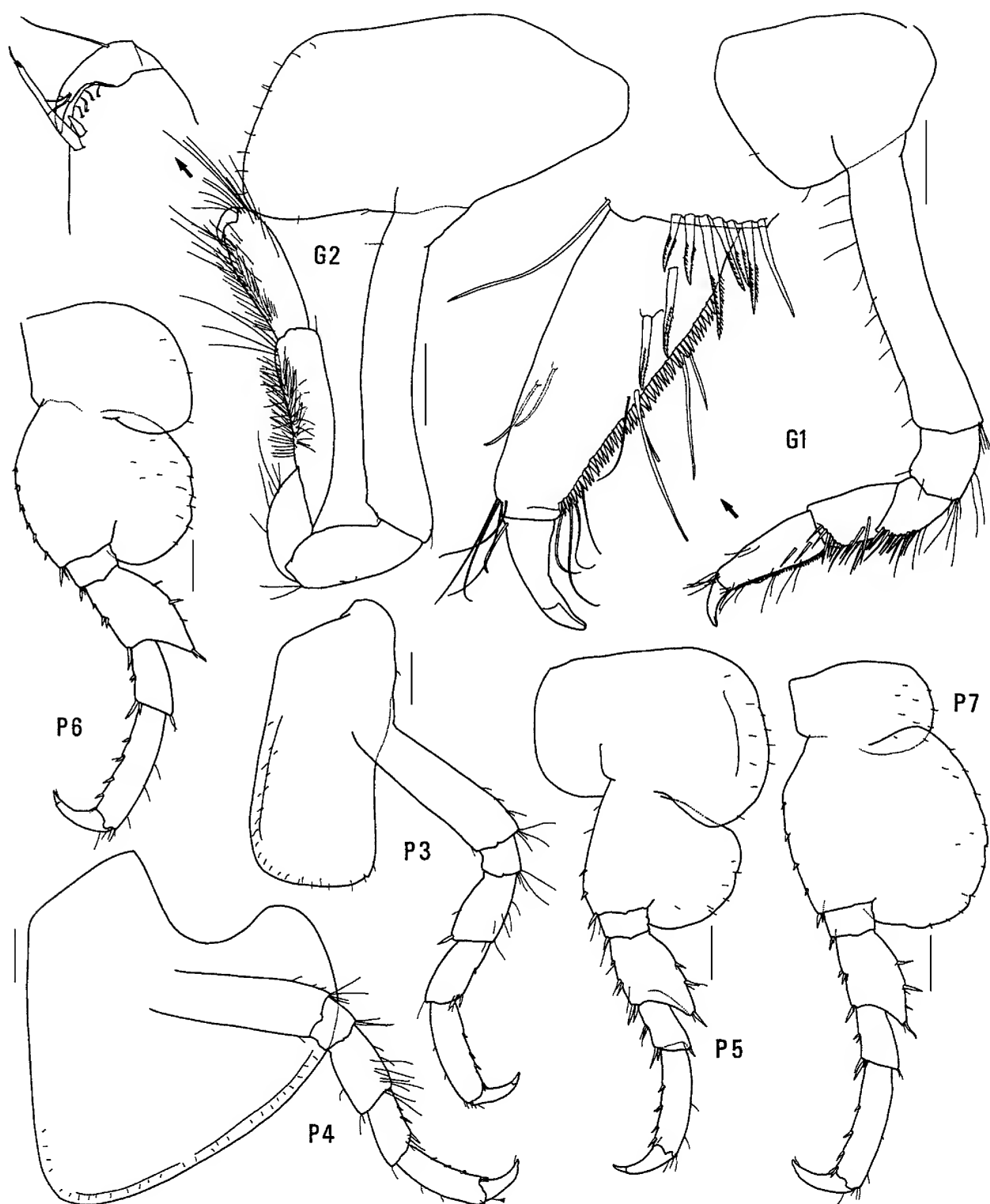


Figure 59. *Bamarooka tropicalis* n.sp., holotype female, 6.0 mm, AM P37074, North West Shelf, Western Australia. Scales represent 0.2 mm.

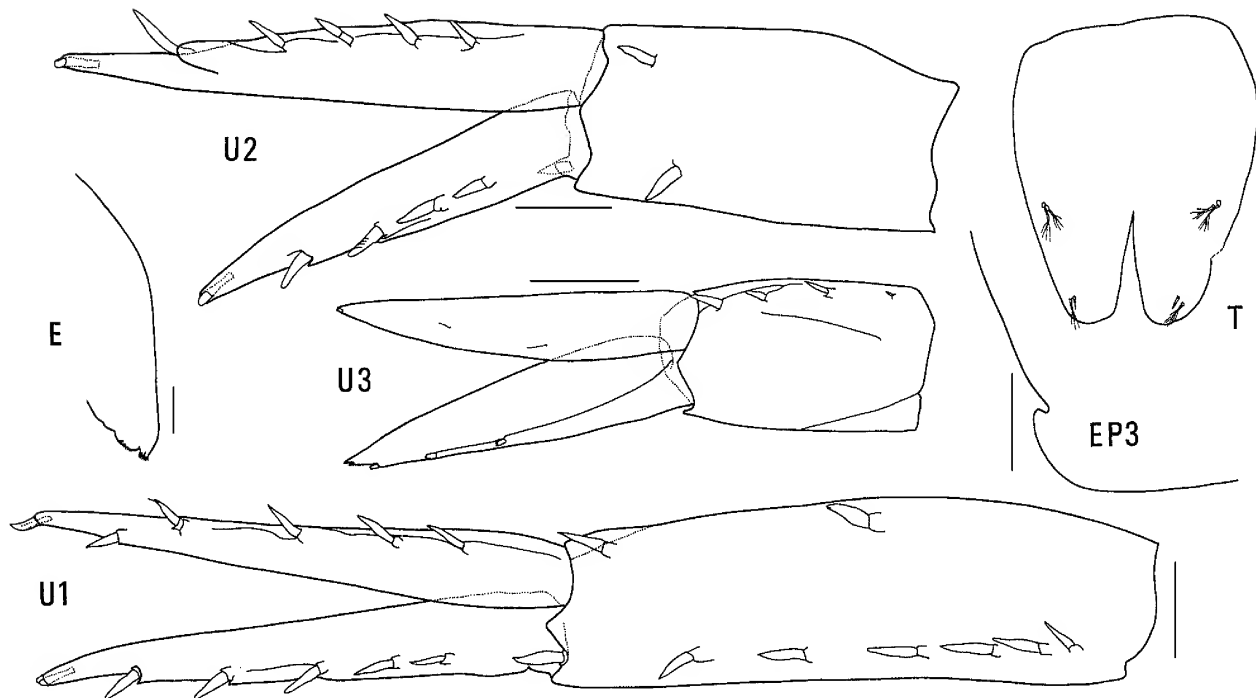


Figure 60. *Bamarooka tropicalis* n.sp., holotype female, 6.0 mm, AM P37074, North West Shelf, Western Australia. Scales represent 0.1 mm.

Erikus Lowry & Stoddart

Erikus Lowry & Stoddart, 1987: 1303.

Diagnosis. Mouthpart bundle subconical. Mandible palp article 3 with proximal A3-seta. Pereopod 4 coxa with anterior and posterior margins subparallel. Pereopods 5–7 with distal articles elongate. Uropod 3 rami lanceolate; with plumose setae in male and female; outer ramus 2-articulate.

Type species. *Erikus dahli* Lowry & Stoddart, 1987, by original designation.

Species composition. *Erikus* contains one species: *E. dahli* Lowry & Stoddart, 1987.

Remarks. When Lowry & Stoddart (1987) described *Erikus dahli* they recorded the uropod 3 outer ramus as 1-articulate. Closer examination has shown that a small, spine-like second article is present. None of the Australian species of *Amaryllis* have a 2-articulate outer ramus on uropod 3 but specimens in several non-Australian literature records of “*Amaryllis macrophthalma*” clearly do. Material from Patagonia (Stebbing, 1888), Argentina (Alonso, 1987), Mauritius (Ledoyer, 1978), Madagascar (Ledoyer, 1979; 1986) and the Red Sea (Lyons & Myers, 1991) all have the spine-like article 2 either illustrated or described. Stebbing (1908: South African material) and Schellenberg (1931: South American material) have recorded “*Amaryllis macrophthalma*” with plumose setae on male pereopods 3 and 4; Stebbing (1908: South African material), K.H. Barnard (1916: South African material), Ledoyer (1979; 1986: material from Madagascar) have recorded “*Amaryllis macrophthalma*” with pappose setae on uropod 3; and Ledoyer (1986: material from Madagascar) has recorded “*Amaryllis macrophthalma*” with A3-setae on the mandibular palp. None of these characters occur in any Australian species of

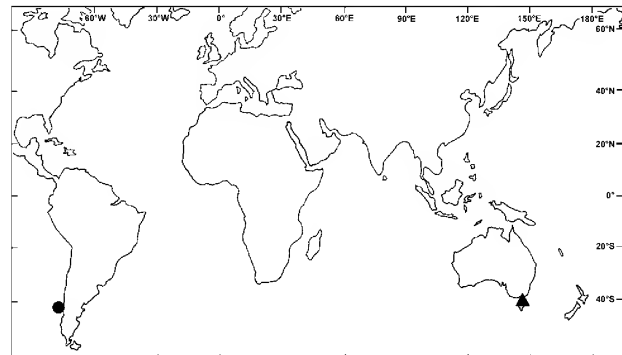


Figure 61. ● Distribution of genus *Erikus*; ▲ Distribution of genus *Wonga*.

Amaryllis, but all three characters occur in *Erikus dahli*. In our opinion none of these records belong in the genus *Amaryllis*; they most likely belong in the genus *Erikus*.

Distribution. *Erikus* is a shallow-water genus currently known from southern South America, but there is evidence that it also occurs in Africa (see Fig. 61).

Wonga n.gen.

Diagnosis. Mouthpart bundle conical. Mandible palp article 3 without A3-seta. Pereopod 4 coxa with anterior and posterior margins subparallel. Pereopods 5–7 with distal articles short. Uropod 3 rami clasper-like; without plumose setae in female [male not known]; outer ramus 1-articulate.

Type species. *Wonga wonga* n.sp.

Species composition. *Wonga* contains one species: *Wonga wonga* n.sp.

Etymology. The genus takes its name from the Australasian Steam Navigation Company's screw steamer *Wonga Wonga*, introduced as a Bass Strait ferry in 1855.

Distribution. Southeastern Australia; 140 m depth (see Fig. 61).

***Wonga wonga* n.sp.**

Figs. 62–65

Type material. HOLOTYPE, female, 6.2 mm, ovigerous (2 eggs), AM P36871; 100 km northeast of North Point, Flinders Island, eastern Bass Strait, Australia, 38°52.6'S 148°26.5'E, 140 m, fine sand, epibenthic sled, R. Wilson, 15 November 1981, RV *Tangaroa*, stn BSS 170S.

Type locality. 100 km northeast of North Point, Flinders Island, eastern Bass Strait, Australia, 38°52.6'S 148°26.5'E, 140 m, depth.

Description. Based on holotype female, 6.2 mm, AM P36871. Head much deeper than long, anterior margin with notch extended into a slit; rostrum absent; eye present, elongate, reniform. Antenna 1 peduncular article 1 not ball-shaped proximally, distal margin with small medial spine; peduncular article 2 medium length; flagellum with callynophore, calceoli absent. Antenna 2 flagellum about as long as that of antenna 1, without calceoli. Mouthpart bundle conical. Epistome/upper lip almost straight (lateral view). Mandible lacinia mobilis a stemmed, distally-cusped blade; accessory setal row with intermediate setae; palp article 2 with 2 posterodistal setae, article 3 without A3-seta. Maxilliped outer plate with distal margin smooth, medial margin without notch.

Gnathopod 1 carpus subequal in length to propodus (0.9×); propodus, posterior margin without robust setae. Gnathopod 2 palm transverse, without lateral robust setae, with 1 medial robust seta. Pereopods 3 and 4 merus and carpus without setal fringe. Pereopod 4 coxa with anterior and posterior margins subparallel, anteroventral corner rounded. Pereopods 5–7 with distal articles short, dactyls short and stocky. Pereopod 5 basis expanded posteriorly, rounded. Pereopod 7 basis subquadrate, posteroventral corner subquadrate, posteroventral margin straight.

Epimeron 3 posterior margin smooth, with notch well above rounded posteroventral corner. Uropod 1 peduncle dorsolateral margin with 5 robust setae; outer ramus without large spines between robust setae. Uropod 2 inner ramus not constricted. Uropod 3 rami clasper-like; without plumose setae; outer ramus 1-articulate. Telson moderately cleft (about 32%).

Etymology. The species takes its name from the Port Jackson tugboat *Wonga*.

Remarks. The telson is shortened and only slightly cleft in *Wonga wonga*, and the rami of the third uropods are modified into a clamp-like structure, conditions which might be associated with a sedentary life-style. These modifications make *W. wonga* a distinctive species, but unfortunately nothing is known of its behaviour and little more of its habitat.

Habitat. *Wonga wonga* is known from only one collection, on a fine sand bottom.

Distribution. Bass Strait, southeastern Australia; 140 m depth.

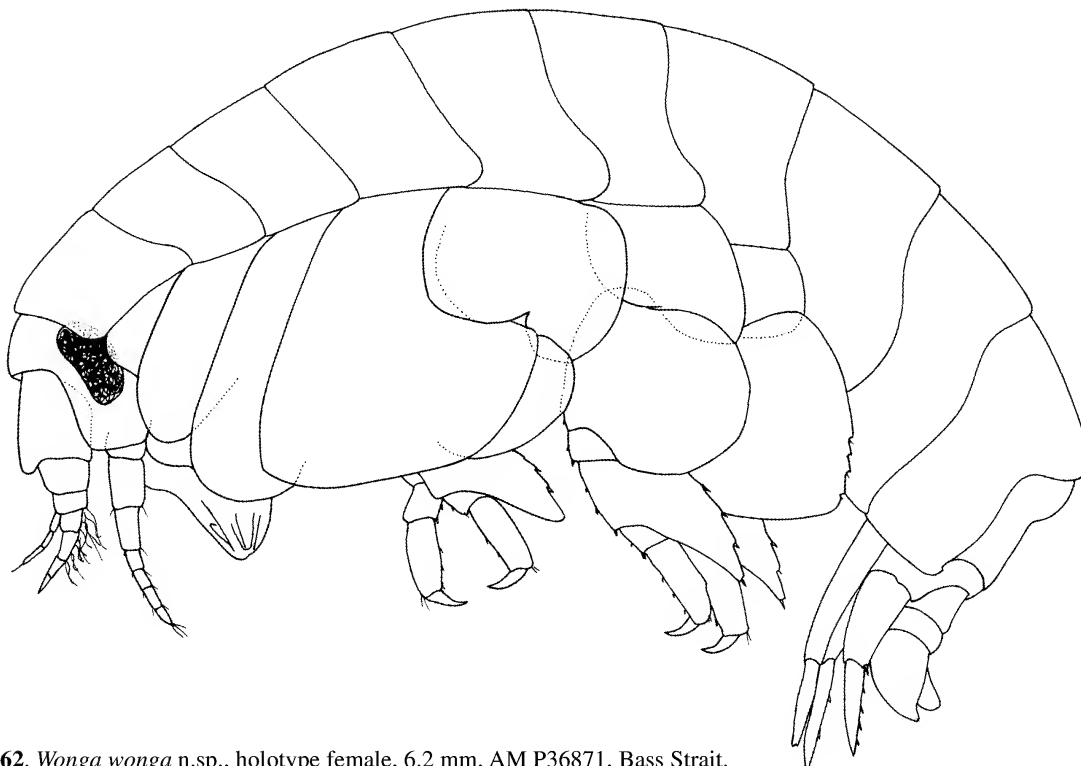


Figure 62. *Wonga wonga* n.sp., holotype female, 6.2 mm, AM P36871, Bass Strait.

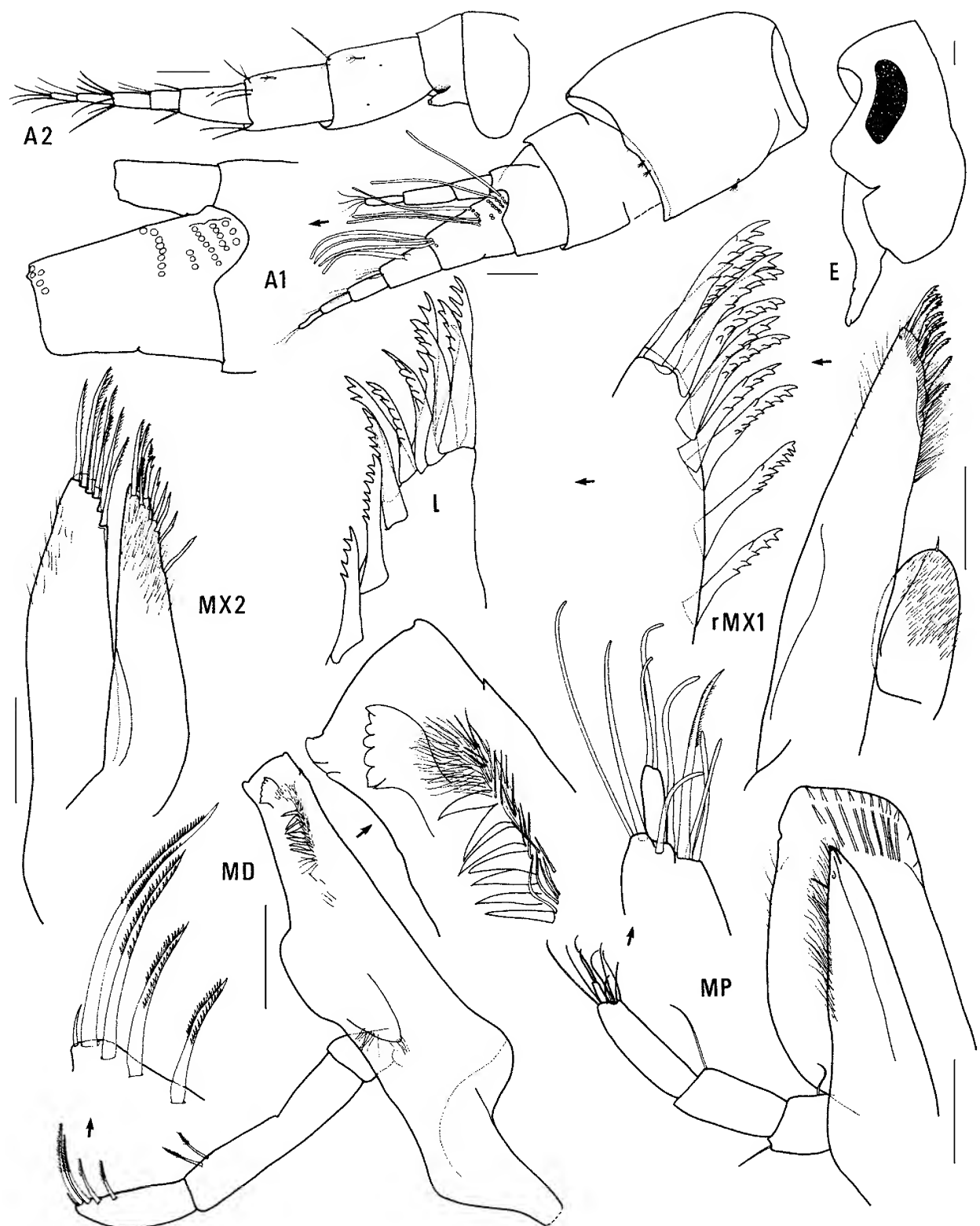


Figure 63. *Wonga wonga* n.sp., holotype female, 6.2 mm, AM P36871, Bass Strait. Scales represent 0.1 mm.

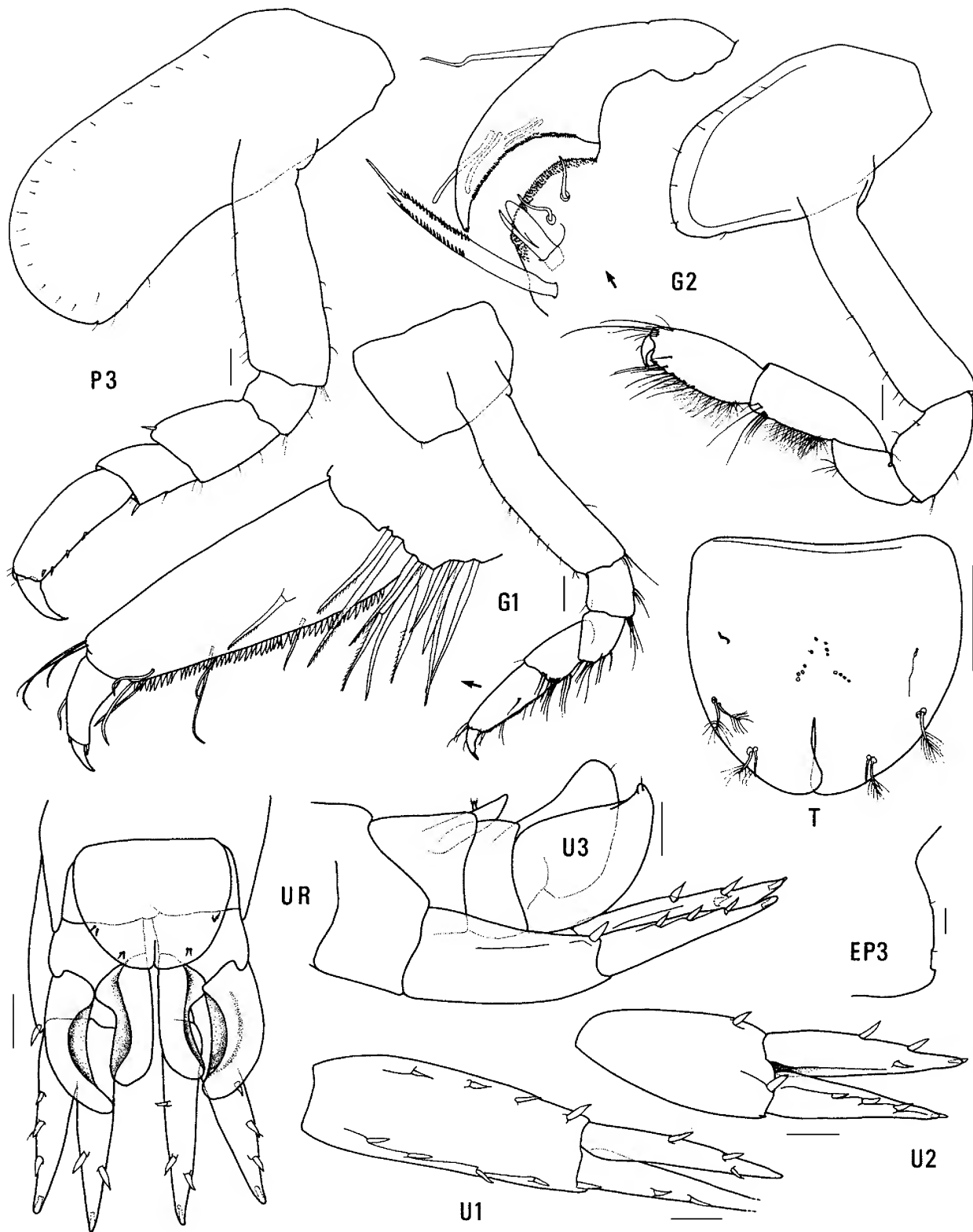


Figure 64. *Wonga wonga* n.sp., holotype female, 6.2 mm, AM P36871, Bass Strait. Scales represent 0.1 mm.

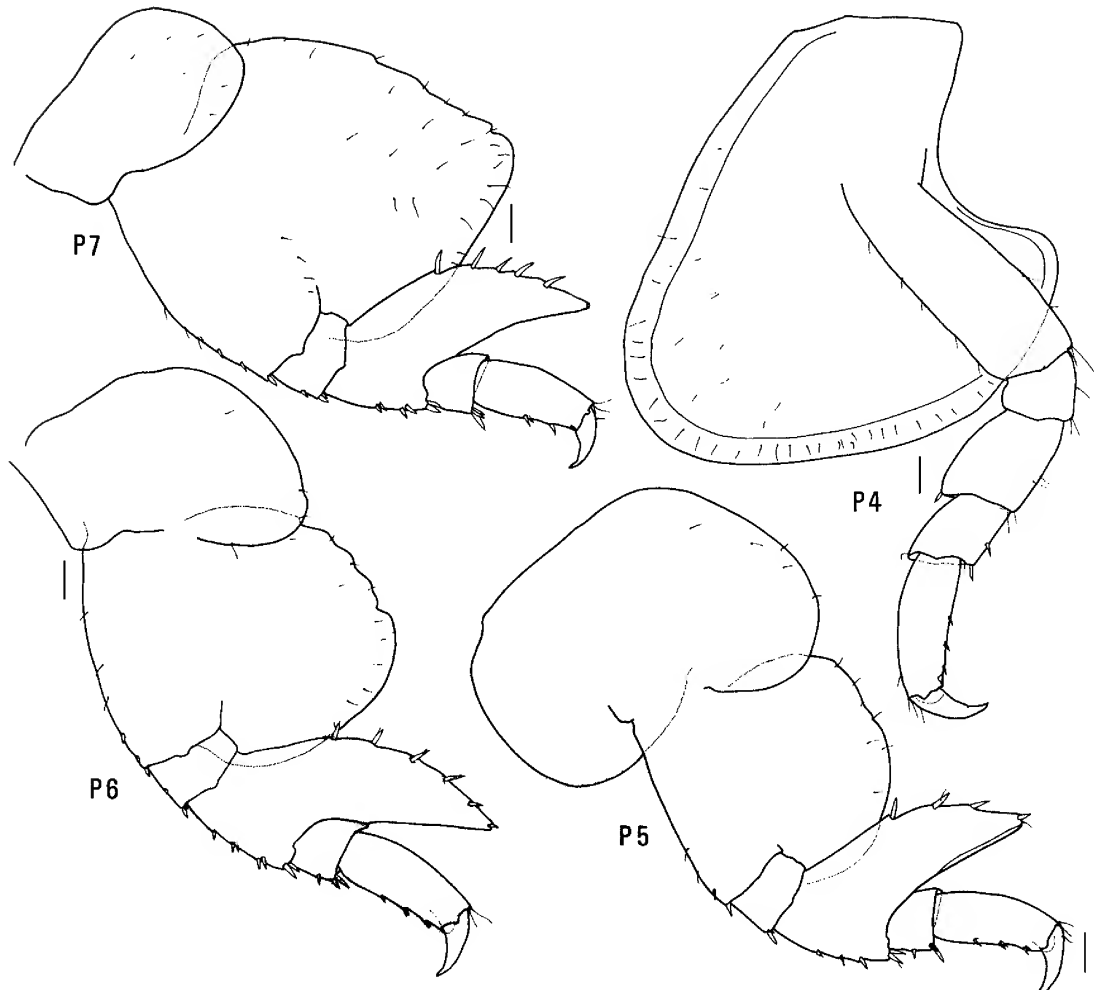


Figure 65. *Wonga wonga* n.sp., holotype female, 6.2 mm, AM P36871, Bass Strait. Scales represent 0.1 mm.

Vijayiinae n.subfam.

Diagnosis. Mouthpart bundle subquadrate. Gnathopod 1 propodus with robust setae along posterior margin. Epimeron 3 with notch immediately above posteroventral corner.

Type genus. *Vijaya* Walker, 1904.

Generic composition. The subfamily contains four genera: *Bathyamaryllis* Pirlot, 1933; *Devo* n.gen.; *Pseudamaryllis* Andres, 1981 and *Vijaya* Walker, 1904.

Remarks. Vijayiines are mostly a free-living deep-water group. Except for *Vijaya tenuipes* and one species of *Pseudamaryllis*, the vijayiines have been found in the deep seas of the North and South Atlantic Oceans, the Red Sea and western South Pacific Ocean.

Bathyamaryllis Pirlot

Bathyamaryllis Pirlot, 1933: 123.—K.H. Barnard, 1940: 441.—J.L. Barnard, 1969: 328.—Barnard & Karaman, 1991: 470.

Diagnosis. Head with rostrum anteriorly rounded or truncated; eye reniform or oval. Antenna 1 peduncular article 1 ball-shaped proximally; peduncular article 2 medium length or long; callynophore absent in female,

present in male. Antenna 2 flagellum about as long as that of antenna 1 in female, longer than body in male [where known]. Mandible palp article 3 with proximal A3-seta in male [where known], without proximal A3-seta in female. Pereopod 4 coxa with anterior and posterior margins subparallel or with anterior margin slightly obtuse, posterior margin straight. Uropod 3 rami with plumose setae in male [where known], without plumose setae in female; outer ramus 1-articulate or 2-articulate.

Type species. *Bathyamaryllis perezii* Pirlot, 1933, by original designation.

Species composition. *Bathyamaryllis* contains 5 species: *B. haswelli* (Stebbing, 1888), *B. kapala* n.sp., *B. ouvea* Lowry & Stoddart, 1994, *B. perezii* Pirlot, 1933 and *B. pulchellus* (Bonnier, 1896).

Remarks. Within the vijayiine group *Devo* and *Bathyamaryllis* are probably sister taxa. Both have the unusual proximal ball-shaped peduncular article 1 on antenna 1.

The deepwater genera *Bathyamaryllis* and *Devo* are the most widespread amaryllid genera with species in the Atlantic and the Indo-West Pacific. The Indo-West Pacific species of *Bathyamaryllis* (*B. kapala*, *B. ouvea* and *B. perezii*) all have a moderately constricted inner ramus on uropod 2 and a 2-articulate outer ramus on uropod 3; the two North Atlantic species (*B. haswelli* and *B. pulchellus*)

have only a slightly constricted inner ramus on uropod 2 and a 1-articulate uropod 3. These differences suggest two distinct species groups within the genus.

Mature males of *Bathyamaryllis* species are not well known. Males have never been recorded for *B. haswelli* or *B. perezii*. The only male known of our new species *B. kapala* is immature. Stephensen (1923: 44) reported a male of *B. pulchellus* in which antenna 2 was "twice as long as antenna 1", but had no calceoli, and setae were present on article 2 of the mandibular palp. The 7.7 mm male of *B. ouvea* illustrated in Lowry & Stoddart (1994, fig. 7), is immature. The 8 mm male of their fig. 10 had both antennae 2 broken; antenna 1 and the remaining articles of antenna 2 had no calceoli; it did have a well-developed callynophore on antenna 1, brush setae on the peduncle of antenna 2, numerous setae on articles 2 and 3 of the mandibular palp, a brush of setae on merus and carpus of pereopods 3 and 4, and plumose setae on the rami of uropod 3.

Distribution. Western and eastern North Atlantic Ocean, Indonesia, eastern Australia and western South Pacific Ocean; 120–1919 m depth (see Fig. 66).

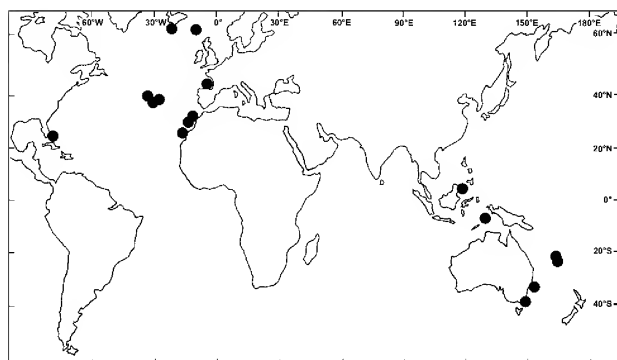


Figure 66. Distribution of genus *Bathyamaryllis*.

Key to species of *Bathyamaryllis*

- 1 Pereopod 4 coxa with anterior margin slightly obtuse, posterior margin straight 2
- Pereopod 4 coxa anterior and posterior margins subparallel 3
- 2 Head with rostrum anteriorly rounded. Gnathopod 1 carpus longer than propodus *B. kapala*
- Head with rostrum anteriorly truncated. Gnathopod 1 carpus subequal to propodus *B. ouvea*
- 3 Head anterior margin with a notch only. Gnathopod 1 carpus longer than propodus *B. haswelli*
- Head anterior margin with a notch extended into a slit. Gnathopod 1 carpus subequal to propodus 4
- 4 Gnathopod 2 palm acute. Pereopod 4 coxa with anteroventral corner subquadrate *B. pulchellus*
- Gnathopod 2 palm transverse. Pereopod 4 coxa with anteroventral corner rounded *B. perezii*

Bathyamaryllis kapala n.sp.

Figs. 67–69

Type material. HOLOTYPE, female, 11.5 mm, ovigerous (16 eggs), AM P36868, southeast of Broken Bay, New South Wales, Australia, 33°37'S 152°04'E to 33°39'S 152°02'E, 897–924 m, dredge, R.T. Springthorpe, 10 December 1980, FRV *Kapala*, stn K80-20-09. 1 PARATYPE, immature, AM P36869, E of Broken Bay, NSW, Australia, 33°31'S 152°08'E to 33°33'S 152°07'E, 914 m, dredge, R.T. Springthorpe, 10 December 1980, FRV *Kapala*, stn K80-20-08. 3 PARATYPES (2 females and 1 immature male), AM P36870, E of Broken Bay, NSW, Australia, 33°30'S 152°09'E to 33°33'S 152°11'E, 922–1015 m, beam trawl, R.T. Springthorpe, 12 February 1986, FRV *Kapala*, stn K86-01-08. 1 PARATYPE, female, AM P58308, E of Broken Bay, NSW, Australia, 33°30'S 152°12'E to 33°33'S 152°09'E, 1036–1049 m, dredge, R.T. Springthorpe, 12 February 1986, FRV *Kapala*, stn K86-01-10. 5 PARATYPES (1 ovigerous female, 4 juveniles), NMV J48797, 54 km ESE of Nowra, NSW, Australia, 34°52.72'S 151°15.04'E, 996 m, mud, fine sand, fine shell, epibenthic sled, G.C.B. Poore *et al.*, 22 October 1988, RV *Franklin*, stn SLOPE 53. 1 PARATYPE,

NMV J48796, 76 km S of Point Hicks, Victoria, Australia, 38°29.33'S 149°19.98'E, 1840 m, sandy mud, fine shell, epibenthic sled, G.C.B. Poore *et al.*, 26 October 1988, RV *Franklin*, stn SLOPE 69.

Type locality. Southeast of Broken Bay, NSW, Australia, Tasman Sea, 33°37'S 152°04'E to 33°39'S 152°02'E, 896–924 m depth.

Description. Based on holotype female, 11.5 mm, AM P36868. Head much deeper than long, *anterior margin with notch extended into a slit*; rostrum present, *anteriorly rounded*; eye present or apparently absent, elongate, reniform. *Antenna 1* peduncular article 1 ball-shaped proximally (slightly), distal margin with large medial spine; *peduncular article 2* long, *length 2× breadth*; flagellum without callynophore, calceoli absent. *Antenna 2* flagellum about as long as that of antenna 1. Mouthpart bundle subquadrate. Mandible lacinia mobilis a stemmed distolaterally cusped blade; accessory setal row with intermediate setae; palp article 2 without posterodistal setae, article 3 without A3-seta. Maxilliped outer plate with distal margin serrate (minutely), medial margin without notch.

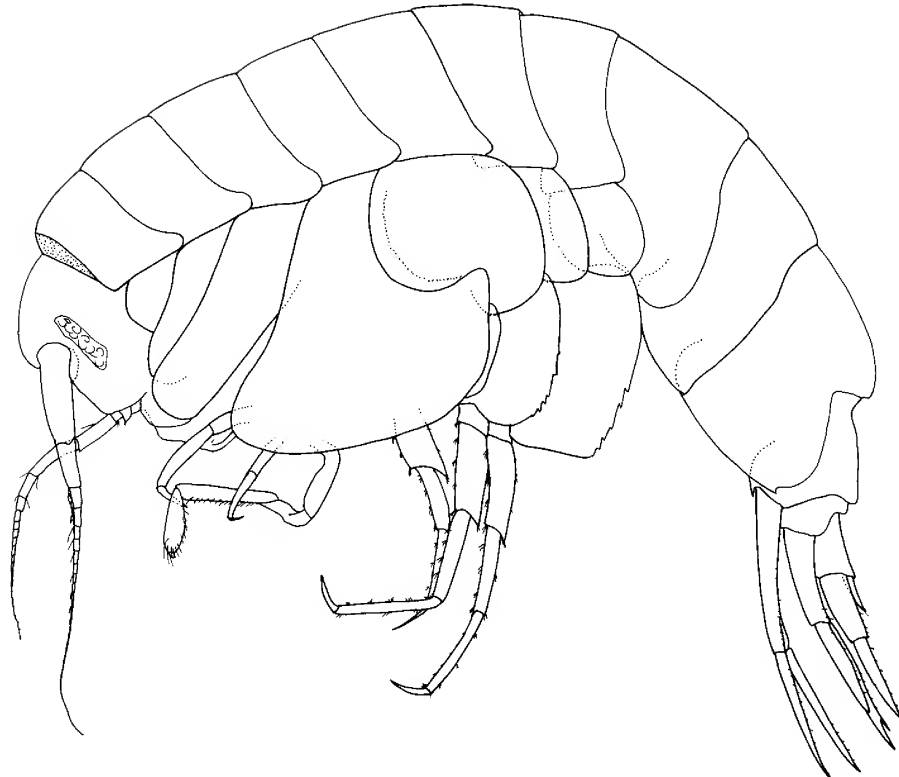


Figure 67. *Bathymaryllis kapala* n.sp., holotype female, 11.5 mm, AM P36868, southeast of Broken Bay, NSW.

Gnathopod 1 carpus longer than propodus (1.3×); propodus, posterior margin with robust setae. Gnathopod 2 palm acute, with 1 lateral robust seta, 1 medial robust seta. Pereopods 3 and 4 merus and carpus without setal fringe. Pereopod 4 coxa with anterior margin slightly obtuse, posterior margin straight, anteroventral corner rounded. Pereopods 5–7 with distal articles elongate, dactyls short and slender. Pereopod 5 basis expanded posteriorly, rounded. Pereopod 7 basis subrectangular, posteroventral corner subquadrate, posteroventral margin straight.

Epimeron 3 posterior margin smooth, with notch immediately above acute posteroventral corner. Uropod 1 peduncle dorsolateral margin with 12 robust setae; outer ramus without large spines between robust setae. Uropod 2 inner ramus moderately constricted. Uropod 3 rami lanceolate; without plumose setae; outer ramus 2-articulate. Telson moderately cleft (about 35%).

Etymology. Named for the former New South Wales Fisheries Research Vessel, the FRV *Kapala*, which made many valuable collections of marine invertebrates off the coast of New South Wales.

Remarks. All three Indo-West Pacific species of *Bathymaryllis* are very similar. *Bathymaryllis kapala* can be distinguished from *B. perezii* by the shape of coxa 4, which has a slightly obtuse anterior margin and a straight posterior margin in *B. kapala*, but subparallel anterior and posterior margins in *B. perezii*. It can be distinguished from *B. ouvea* by the shape of the rostrum, which is rounded in *B. kapala* and truncated in *B. ouvea*.

Habitat. *Bathymaryllis kapala* has been collected from sand and mud bottoms but its habitat is generally not known.

Distribution. Southeastern Australia, Tasman Sea; 896–1840 m depth.

***Devo* n.gen.**

Diagnosis. Head with rostrum cone-shaped; eye, when present, oval. Antenna 1 peduncular article 1 ball-shaped proximally; peduncular article 2 long; callynophore absent in female, present in male. Antenna 2 flagellum about as long as that of antenna 1 in female, longer than body in male. Mandible palp article 3 without proximal A3-seta. Pereopod 4 coxa with anterior margin slightly obtuse, posterior margin rounded or with anterior margin slightly obtuse, posterior margin straight. Uropod 3 rami with plumose setae in male, with or without plumose setae in female; outer ramus 1-articulate or 2-articulate.

Type species. *Devo grahami* n.sp.

Species composition. *Devo* contains four species: *D. conocephala* (K.H. Barnard, 1925), *D. dubuc* n.sp., *D. grahami* n.sp. and *D. rostrata* (Chevreux, 1911).

Etymology. The name *Devo* is an allusion to a recent American music group of the same name, whose members wore peculiar cone-shaped head coverings.

Remarks. *Devo* forms a distinctive group of species, distinguished from other vijayiines by their strongly flared fourth coxae and well-developed rostrums. Species in the genus *Devo* appear to be more adapted for a pelagic lifestyle than are other amaryllidids.

Distribution. Eastern North and South Atlantic Oceans, southwestern Indian Ocean and western South Pacific Ocean; 500–1840 m depth (see Fig. 70).

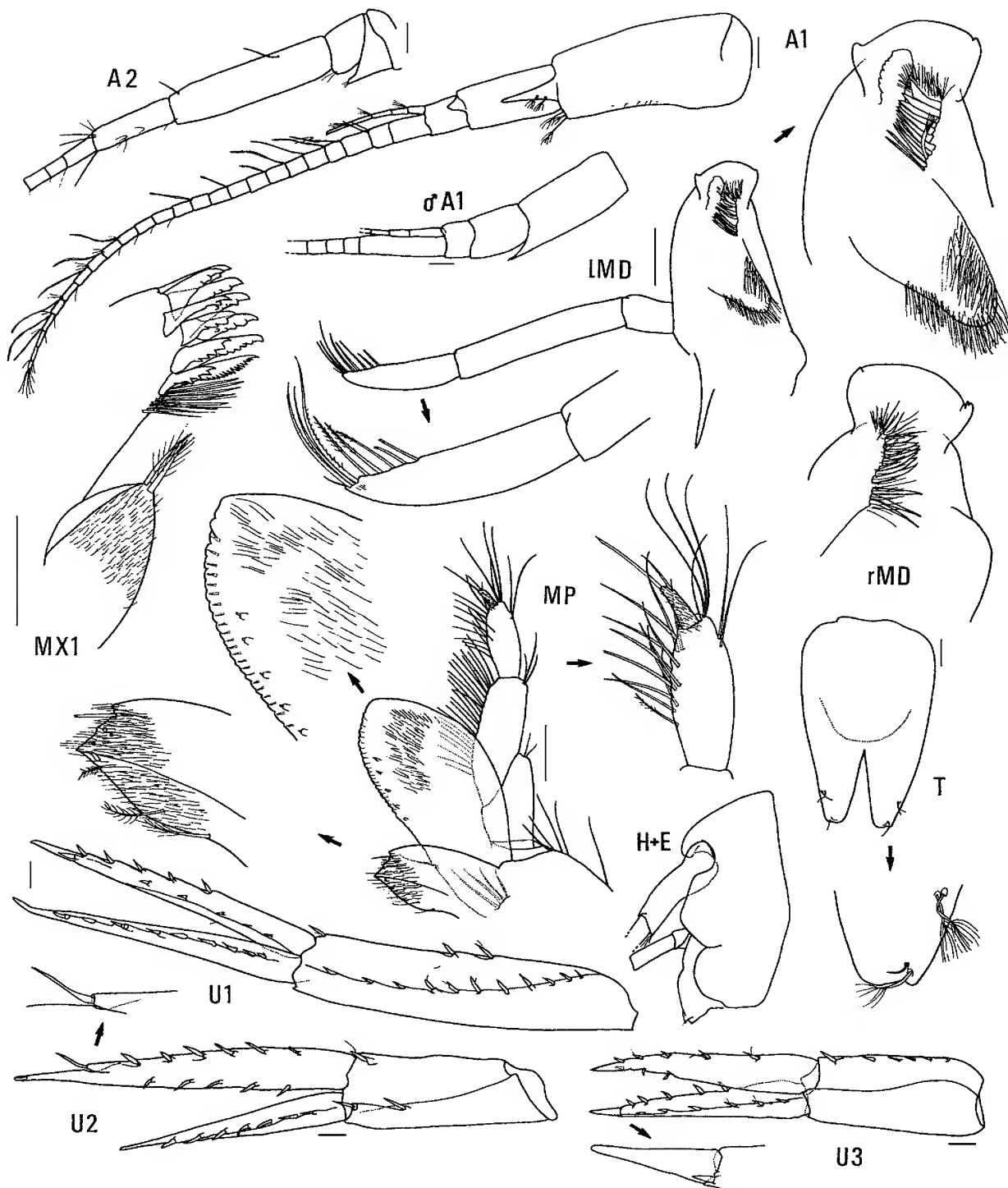


Figure 68. *Bathyamaryllis kapala* n.sp., holotype female, 11.5 mm, AM P36868, southeast of Broken Bay, NSW; paratype immature male, 7.5 mm, AM P36870, east of Broken Bay, NSW. Scales represent 0.1 mm.

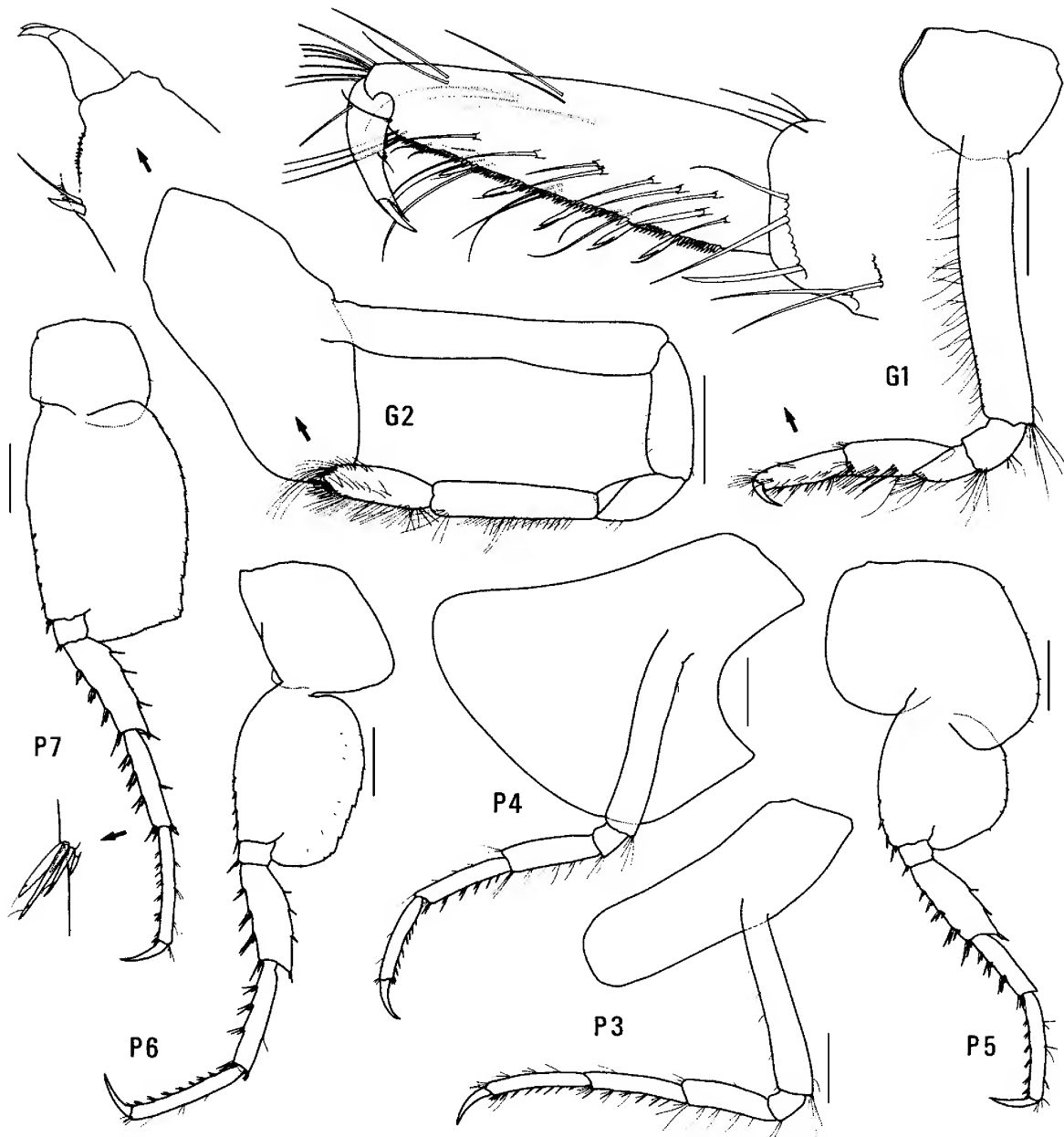


Figure 69. *Bathyamaryllis kapala* n.sp., holotype female, 11.5 mm, AM P36868, southeast of Broken Bay, NSW. Scales represent 0.5 mm.

Key to species of *Devo*

- 1 Head much deeper than long 2
- Head about as deep as long *D. rostrata*
- 2 Head anterior margin with notch or with notch extended into a slit. Pereopod 4 coxa with anteroventral corner rounded 3
- Head anterior margin without notch or slit. Pereopod 4 coxa with anteroventral corner subquadrate *D. conocephalus*
- 3 Head anterior margin with notch extended into a slit. Female uropod 3 without plumose setae *D. dubuc*
- Head anterior margin with notch only. Female uropod 3 with plumose setae *D. grahami*

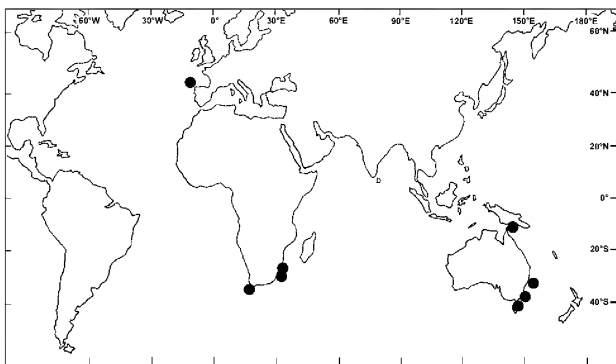


Figure 70. Distribution of genus *Devo*.

Devo dubuc n.sp.

Figs. 71, 72

Type material. HOLOTYPE, female, 7.2 mm, with non-setose oostegites, NMV J48795; 1 PARATYPE, male, 7.5 mm, NMV J48794; 1 PARATYPE, male, 7.4 mm, NMV J48793; 10 PARATYPES, NMV J15795; 10 PARATYPES, AM P58963; 48 km east-north-east of Cape Tourville, Tasmania, Australia, 42°00.25'S 148°43.55'E, 1264 m, gravel with lumps of sandy mud aggregate, epibenthic sled, G.C.B. Poore *et al.*, 30 October 1988, RV *Franklin*, stn SLOPE 81.

Type locality. 48 km east-north-east of Cape Tourville, Tasmania, Australia, 42°00.25'S 148°43.55'E, 1264 m depth.

Description. Based on holotype female, 7.2 mm, NMV J48795. Head much deeper than long, anterior margin with notch extended into a slit; rostrum present, cone-shaped; eye apparently absent. Antenna 1 peduncular article 1 ball-shaped proximally, distal margin with well-developed medial spine; peduncular article 2 long, length 4.5× breadth; flagellum without callynophore, calceoli absent. Antenna 2 flagellum about as long as that of antenna 1, without calceoli. Mouthpart bundle subquadrate. Mandible lacinia mobilis a stemmed distolaterally cusped blade; accessory setal row with intermediate setae; palp article 2 without posterodistal setae, article 3 without A3-seta. Maxilliped outer plate with distal margin smooth, medial margin without notch.

Gnathopod 1 carpus longer than propodus (1.2×); propodus, posterior margin with robust setae. Gnathopod 2 palm acute, without lateral robust setae, with 1 medial robust seta. Pereopods 3 and 4 merus and carpus without setal fringe. Pereopod 4 coxa with anterior margin slightly obtuse, posterior margin straight, anteroventral corner subquadrate. Pereopods 5–7 with distal articles elongate, dactyls long and slender. Pereopod 5 basis expanded posteriorly, rounded. Pereopod 7 basis subrectangular, posteroventral corner rounded, posteroventral margin straight.

Epimeron 3 posterior margin smooth, with notch immediately above acute posteroventral corner. Uropod 1 peduncle dorsolateral margin with 11 robust setae; outer ramus without large spines between robust setae. Uropod 2 inner ramus moderately constricted. Uropod 3 rami lanceolate; without plumose setae; outer ramus 2-articulate. Telson moderately cleft (about 40%).

Male (sexually dimorphic characters). Based on paratype male, 7.5 mm. Antenna 1 flagellum with callynophore, with

calceoli. Mandible palp article 2 with 8 posterodistal setae. Pereopods 3 and 4 merus and carpus with setal fringe. Uropod 3 rami with plumose setae.

Etymology. Named for the whaling ship *Dubuc*, scuttled off Kangaroo Bluff, Bellrieve, in the Derwent River, Tasmania, in November 1808.

Remarks. The main difference between *D. dubuc* and *D. grahami* is the anterior margin of the head, which has a notch extended into a slit in *D. dubuc* but only a simple notch in *D. grahami*. In addition, *D. dubuc* does not have plumose setae on uropod 3 of the female.

Habitat. *Devo dubuc* is known from only one collection, on a coarse sediment bottom.

Distribution. Southeastern Australia, Tasman Sea; 1264 m depth.

Devo grahami n.sp.

Figs. 73–75, Plate 1c

Type material. HOLOTYPE, female, 7.7 mm, ovigerous (8 eggs), AM P36872; 1 PARATYPE, male, 9.3 mm, AM P36873; 5 PARATYPES, AM P36874; E of Broken Bay, New South Wales, Australia, 33°31'S 152°08'E to 33°33'S 152°07'E, 914 m, dredge, R.T. Springthorpe, 10 December 1980, FRV *Kapala*, stn K80-20-8. 5 PARATYPES, AM P56969, E of Broken Bay, NSW, Australia, 33°29'S 152°12'E to 33°27'S 152°14'E, 1143–1200 m, beam trawl, R.T. Springthorpe, 12 February 1986, FRV *Kapala*, stn K86-01-09. 5 PARATYPES (4 males, 1 female), AM P36875, E of Broken Bay, NSW, Australia, 33°30'S 152°12'E to 33°33'S 152°09'E, 1036–1049 m, R.T. Springthorpe, 12 February 1986, *Kapala*, stn K86-01-10. 1 PARATYPE, female, AM P36876, SE of Broken Bay, NSW, Australia, 33°41'S 152°01'E, 1125 m, epibenthic sled, 11 December 1978, FRV *Kapala*, stn K78-27-03. 1 PARATYPE, immature male, 7.0 mm, AM P36877, E of Port Jackson, NSW, Australia, 33°48'S 151°52'E, 549 m, sled/dredge, 3 December 1979, FRV *Kapala*, stn K79-20-02. 2 PARATYPES (1 mature male, 1 immature male), NMV J48792; 54 km ESE of Nowra, NSW, Australia, 34°52.72'S 151°15.04'E, 996 m, mud, fine sand, fine shell, epibenthic sled, G.C.B. Poore *et al.*, 22 October 1988, RV *Franklin*, stn SLOPE 53.

Additional material. Two specimens, AM P56970, E of Cape York, Australia, Coral Sea, 10°32.72'S 144°12.8'E, epibenthic sled, 780–795 m, P. Hutchings *et al.*, 20 August 1988, RV *Franklin*, stn 06/88-03. 1 specimen + fragment, NMV J48791, S of Point Hicks, Victoria, 38°21.90'S 149°20.00'E, 1000 m, epibenthic sled, G.C.B. Poore *et al.*, 23 July 1986, RV *Franklin*, stn SLOPE 32. 1 specimen, NMV J48790, S of Point Hicks, Victoria, 38°19.10'S 149°14.30'E, 600 m, coarse sand, epibenthic sled, M.F. Gomon *et al.*, 24 July 1986, RV *Franklin*, stn SLOPE 39. 19 specimens, NMV J48789, 76 km S of Point Hicks, Victoria, 38°29.33'S 149°19.98'E, 1840 m, sandy mud, fine shell, epibenthic sled, G.C.B. Poore *et al.*, 26 October 1988, RV *Franklin*, stn SLOPE 69. 4 specimens, NMV J48788, off Freycinet Peninsula, Tasmania, 42°2.20'S 148°38.70'E, 800 m, coarse shelly sand, epibenthic sled, M.F. Gomon *et al.*, 27 July 1986, RV *Franklin*, stn SLOPE 45. 5 specimens, NMV J48787, off Freycinet Peninsula, Tasmania, 42°0.20'S 148°37.70'E, 720 m, coarse shelly sand, epibenthic sled, M.F. Gomon *et al.*, 27 July 1986, RV *Franklin*, stn SLOPE 46.

Type locality. East of Broken Bay, NSW, Australia, Tasman Sea, 33°31'S 152°08'E to 33°33'S 152°07'E, 914 m depth.

Description. Based on holotype female, 7.7 mm, AM P36872. Head much deeper than long, anterior margin with notch; rostrum present, cone-shaped; eye present, elongate,

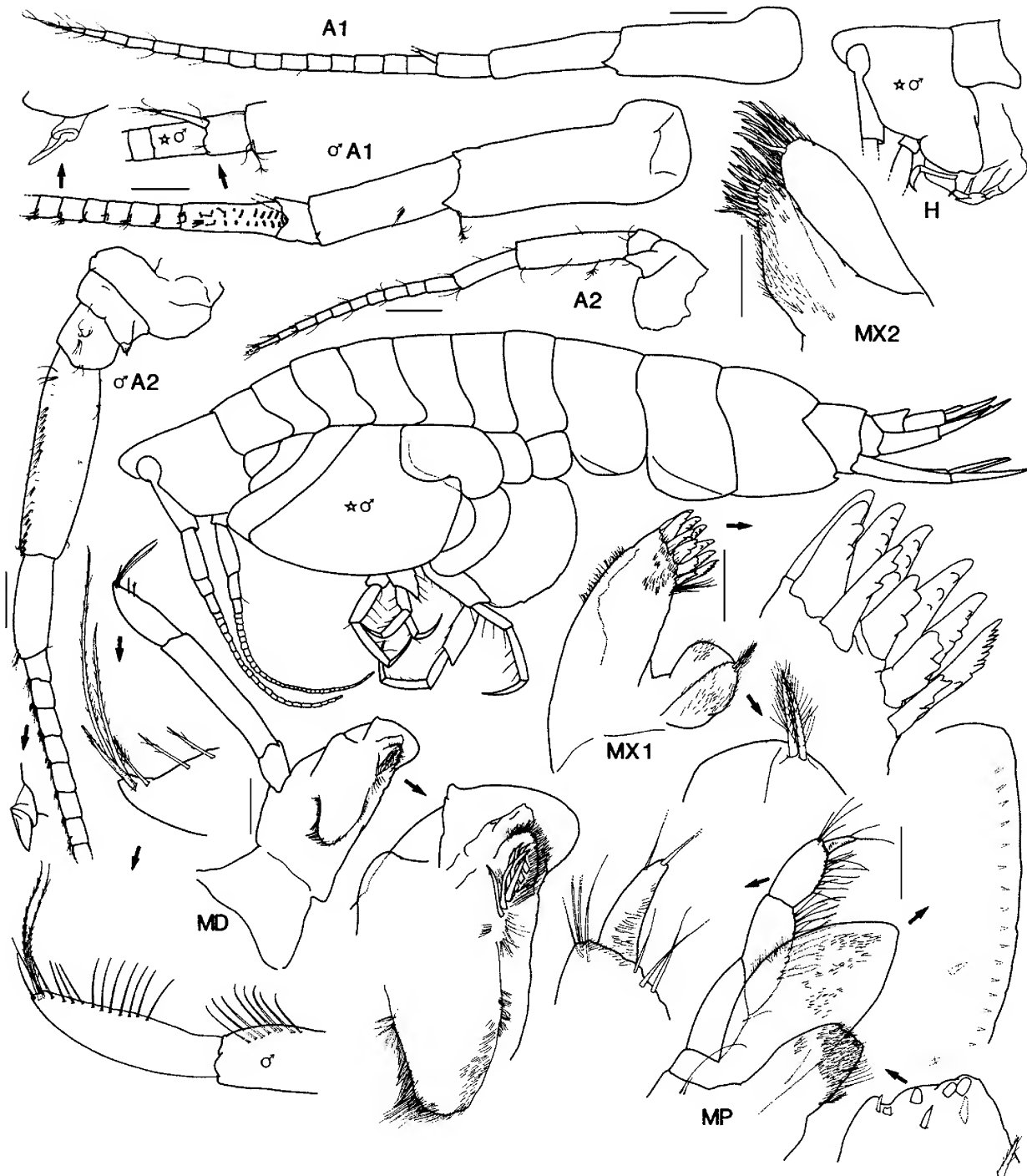


Figure 71. *Devo dubuc* n.sp., holotype female, 7.2 mm, NMV J48795; paratype male, 7.5 mm, NMV J48794; \star paratype immature male, 7.4 mm, NMV J48793; off Cape Tourville, Tasmania. Scales for A1, A2 represent 0.2 mm; remainder represent 0.1 mm.

oval. Antenna 1 peduncular article 1 ball-shaped proximally, distal margin with well-developed medial spine; peduncular article 2 long, length $5\times$ breadth; flagellum without callynophore, calceoli absent. Antenna 2 flagellum about as long as that of antenna 1, without calceoli. Mouthpart bundle subquadrate. Epistome/upper lip almost straight (lateral view). Mandible lacinia mobilis a stemmed distolaterally cusped blade; accessory setal row with

intermediate setae; palp article 2 without posterodistal setae, article 3 without A3-seta. Maxilliped outer plate with distal margin smooth, medial margin without notch.

Gnathopod 1 carpus longer than propodus (1.3 \times); propodus, posterior margin with robust setae. Gnathopod 2 palm acute, without lateral robust setae, 1 medial robust seta. Pereopods 3 and 4 merus and carpus without setal fringe. *Pereopod 4 coxa with anterior margin slightly*

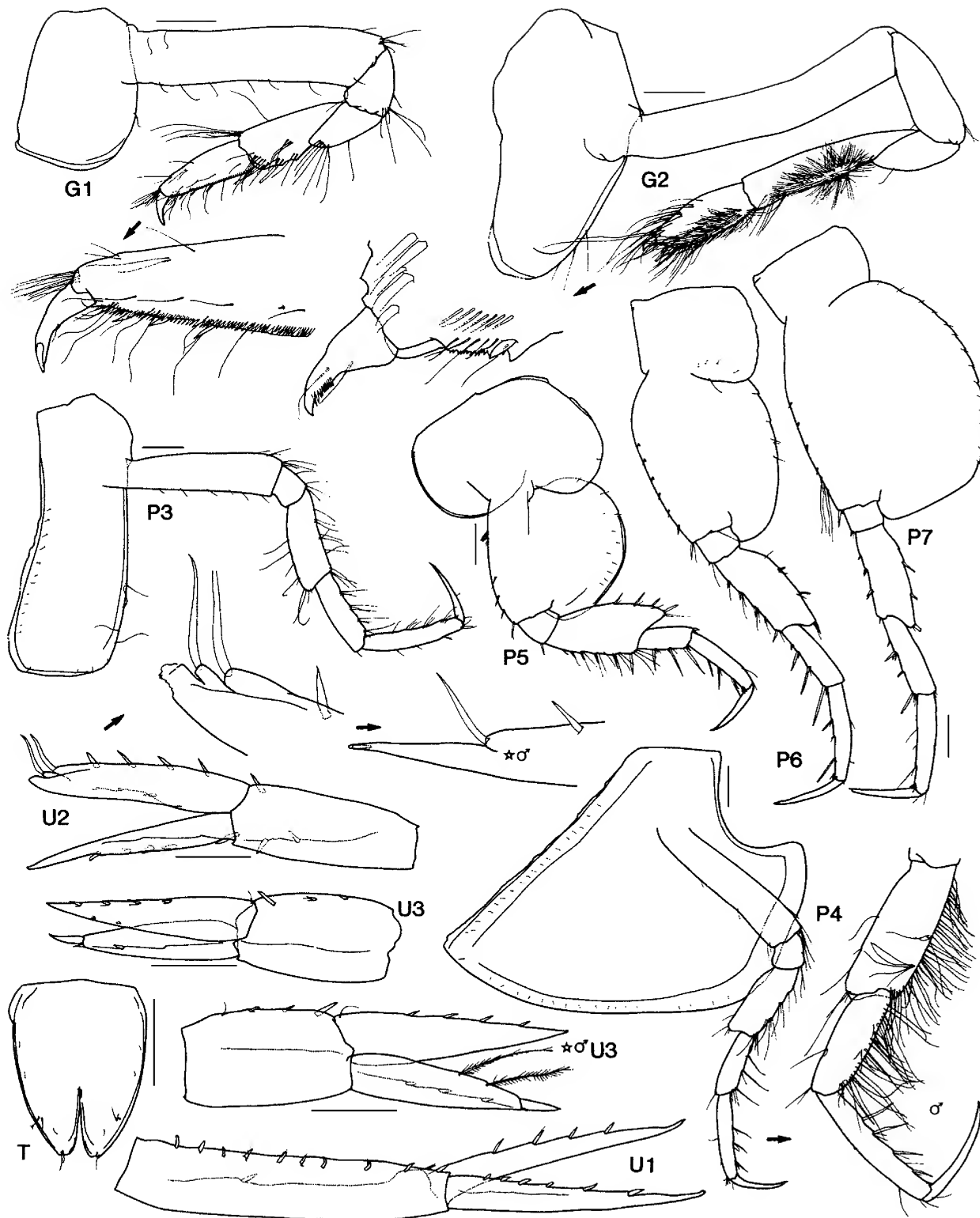
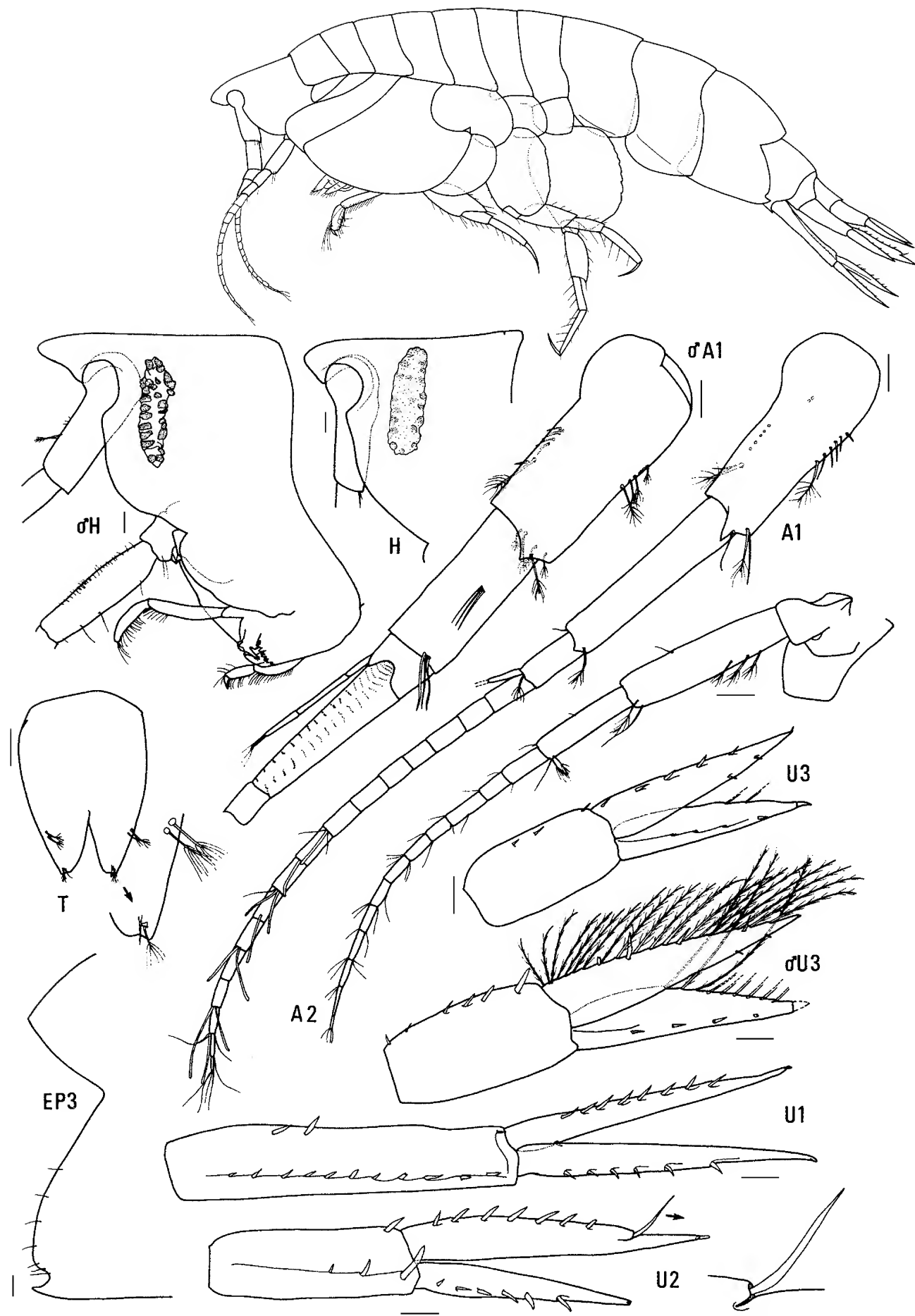


Figure 72. *Devo dubuc* n.sp., holotype female, 7.2 mm, NMV J48795; paratype male, 7.5 mm, NMV J48794; \star paratype immature male, 7.4 mm, NMV J48793; off Cape Tourville, Tasmania. Scales represent 0.2 mm.

Figure 73. *Devo grahami* n.sp., whole animal: paratype immature male, 7.0 mm, AM P36877; δ : paratype mature male, 9.3 mm, AM P36873; remainder: holotype female, 7.7 mm, AM P36872; east of Broken Bay, NSW. Scales represent 0.1 mm.



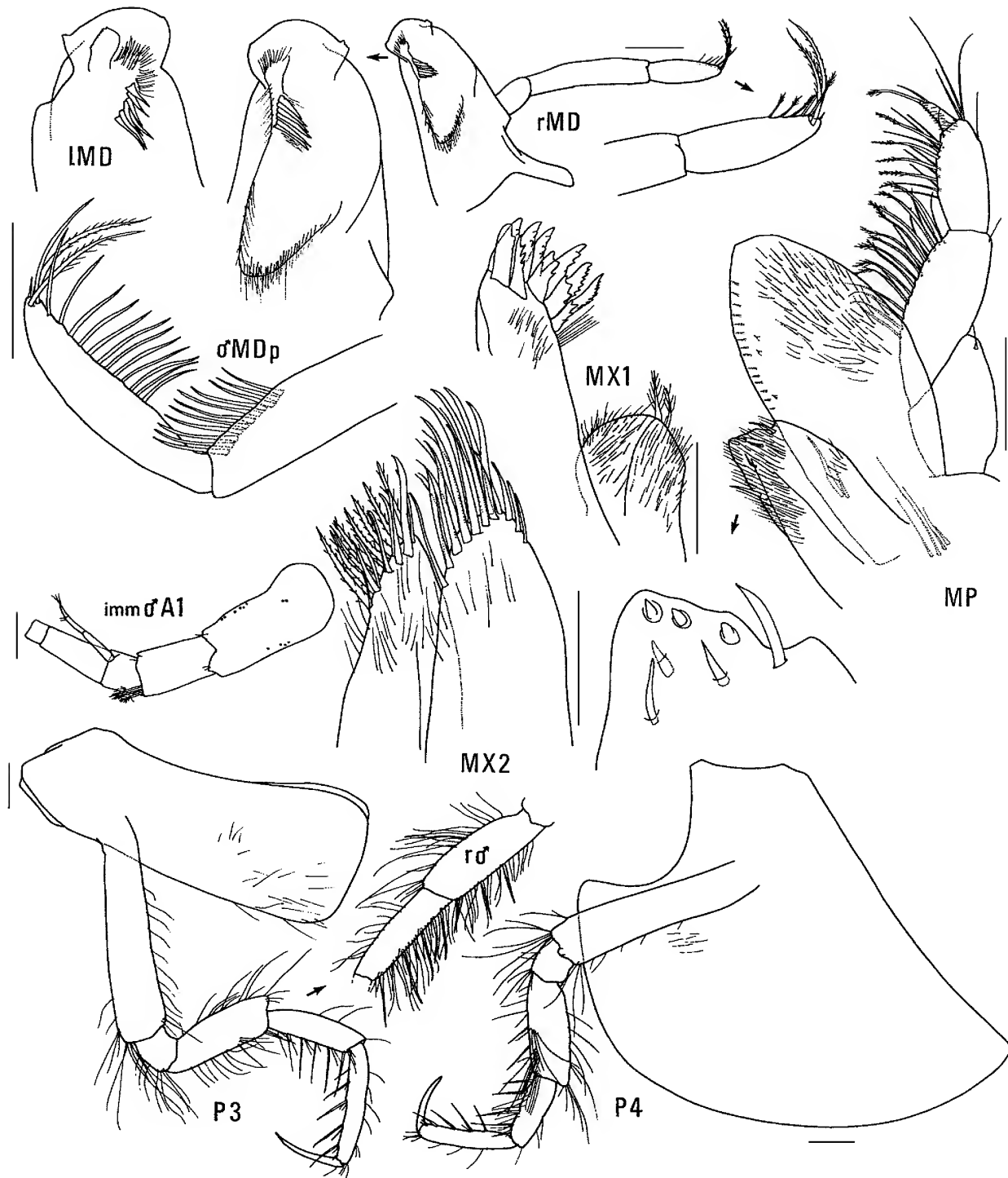


Figure 74. *Devo grahami* n.sp., holotype female, 7.7 mm, AM P36872; paratype mature male, 9.3 mm, AM P36873; paratype immature male, 7.0 mm, AM P36877; east of Broken Bay, NSW. Scales for P3, 4 represent 0.2 mm; remainder represent 0.1 mm.

obtuse, posterior margin straight, anteroventral corner subquadrate. Pereopods 5–7 with distal articles elongate, dactyls long and slender. Pereopod 5 basis expanded posteriorly, rounded. Pereopod 7 basis subrectangular, posteroventral corner rounded, posteroventral margin curved.

Epimeron 3 posterior margin smooth, with notch immediately above acute posteroventral corner. Uropod 1 peduncle dorsolateral margin with 12 robust setae; outer

ramus without large spines between robust setae. Uropod 2 inner ramus moderately constricted. Uropod 3 rami lanceolate; with a few plumose setae; outer ramus 2-articulate. Telson slightly cleft (about 30%).

Male (sexually dimorphic characters). Based on paratype male, 9.3 mm, AM P36873. Antenna 1 flagellum with callynophore, with calceoli. Mandible palp article 2 with 11 posterodistal setae. Pereopods 3 and 4 merus and carpus



Figure 75. *Devo grahami* n.sp., holotype female, 7.7 mm, AM P36872, east of Broken Bay, NSW. Scales represent 0.2 mm.

with setal fringe. Uropod 3 rami with plumose setae.

Etymology. Named for Ken Graham, fisheries biologist on the FRV *Kapala*, who helped immensely over the years in collecting amphipods and other invertebrates during the cruises of the *Kapala*.

Remarks. *Devo grahami* is very similar to *D. dubuc* but is distinguished by the notch on the anterior margin of the

head not extended into a slit, and by plumose setae present on uropod 3 of the female.

Habitat. *Devo grahami* has been collected on fine and coarse sediment bottoms.

Distribution. Southeastern Australia, Tasman Sea; 549–1840 m depth.

Pseudamaryllis Andres

Pseudamaryllis Andres, 1981: 464.—Barnard & Karaman, 1991: 521.—Lowry & Stoddart, 1993: 98.
Amaryllis.—Ledoyer, 1986: 717 (in part).
Paravijaya Ren, 1998: 156, 162.

Diagnosis. Head with rostrum anteriorly rounded or absent; eye reniform. Antenna 1 peduncular article 1 not ball-shaped proximally; peduncular article 2 medium length; callynophore present in female and male. Antenna 2 flagellum about as long as that of antenna 1 in female and male. Mandible palp article 3 with or without proximal A3-seta. Pereopod 4 coxa with anterior and posterior margins subparallel. Uropod 3 rami without plumose setae in male and female; outer ramus 1-articulate.

Type species. *Pseudamaryllis nonconstricta* Andres, 1981, by original designation.

Species composition. *Pseudamaryllis* contains two species: *P. andresi* Lowry & Stoddart, 1993 and *P. nonconstricta* Andres, 1981.

Remarks. Ren (1998) established the genus *Paravijaya*, which he compared to and distinguished from the genera *Amaryllis*, *Pseudamaryllis* and *Vijaya*. *Paravijaya* was distinguished from *Pseudamaryllis* by: the labrum and epistome being coalesced, peduncular article 1 of antenna 1 being longer than other articles, and inner ramus of uropod 2 with a small notch. Ren was apparently unaware of the publication by Lowry & Stoddart (1993), which established a new species of *Pseudamaryllis* and slightly expanded the generic diagnosis. *Paravijaya* is a synonym of *Pseudamaryllis* and *Pa. apiculata* Ren, 1998, is the same species described by Lowry & Stoddart (1993) as *Ps. andresi*.

Pseudamaryllis is the only amaryllid genus with the combination of a callynophore in the female and robust setae on the propodus of gnathopod 1.

Distribution. Western Indian Ocean, Red Sea and South China Sea; 90–1544 m depth (see Fig. 76).

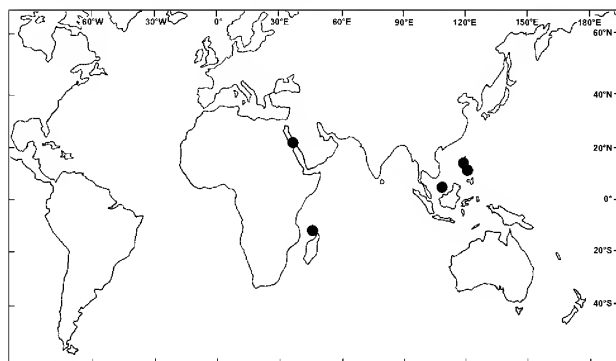


Figure 76. Distribution of genus *Pseudamaryllis*.

Pseudamaryllis andresi Lowry & Stoddart

Pseudamaryllis andresi Lowry & Stoddart, 1993: 99, figs. 28–30.—Springthorpe & Lowry, 1994: 8.
Paravijaya apiculata Ren, 1998: 157, 162, figs. 1, 2.

Distribution. Spratly Islands and Philippines, South China Sea; 90–127 m depth.

Vijaya Walker

Vijaya Walker, 1904: 241.—Stebbing, 1906: 717.—Gurjanova, 1962: 45.—J.L. Barnard, 1964: 63.—J.L. Barnard, 1969: 368.—Barnard & Karaman, 1991: 541.—Lowry & Stoddart, 2002.

Diagnosis. Head with rostrum anteriorly rounded; eye ventrally tapered. Antenna 1 peduncular article 1 not ball-shaped proximally; peduncular article 2 medium length; callynophore absent in female, present in male. Antenna 2 flagellum about as long as that of antenna 1 in female, longer than body in male. Mandible palp article 3 with proximal A3-seta in male, without proximal A3-seta in female. Pereopod 4 coxa with anterior and posterior margins subparallel. Uropod 3 rami with plumose setae in male and female; outer ramus 1-articulate.

Type species. *Vijaya tenuipes* Walker, 1904, by monotypy.

Species composition. *Vijaya* contains one species: *V. tenuipes* Walker, 1904.

Remarks. When Pirlot (1933) described *Bathyamaryllis*, the genus *Vijaya* was so poorly known that he could not have realised the close relationship of his species to the species that Walker (1904) described. We (Lowry & Stoddart, 2002) have examined Walker's material and redescribed the species based on new material from the Andaman Sea. This has shown several generic level differences between these species. *Vijaya* has a ventrally tapered eye and a unique acutely produced anteroventral corner on coxa 4; it does not have the proximally ball-shaped peduncular article 1 of antenna 1 that characterizes *Bathyamaryllis* and *Devo*. *Pseudamaryllis* has reniform eyes, a callynophore in the female and subparallel anterior and posterior margins on coxa 4.

*Vijaya*ines typically live in the deep sea; *Vijaya* is the only member of the group that lives in shallow tropical waters.

The female of *Vijaya tenuipes* has oostegites on gnathopod 1 to pereopod 5; it is the only amaryllid species known to have an oostegite on gnathopod 1. The only other lysianassoid we know to have such an array of oostegites is *Eurythenes gryllus*.

Distribution. Northern Indian Ocean and Andaman Sea; shallow water to 68 m depth (see Fig. 77).

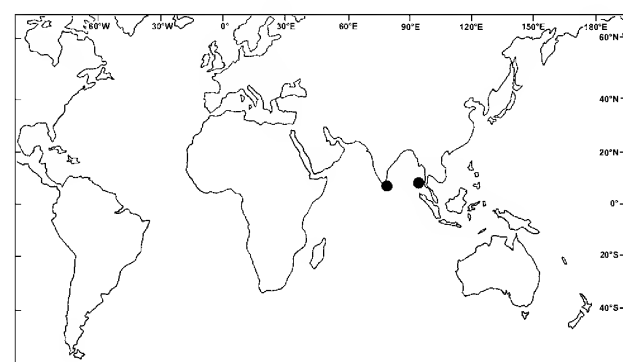


Figure 77. Distribution of genus *Vijaya*.

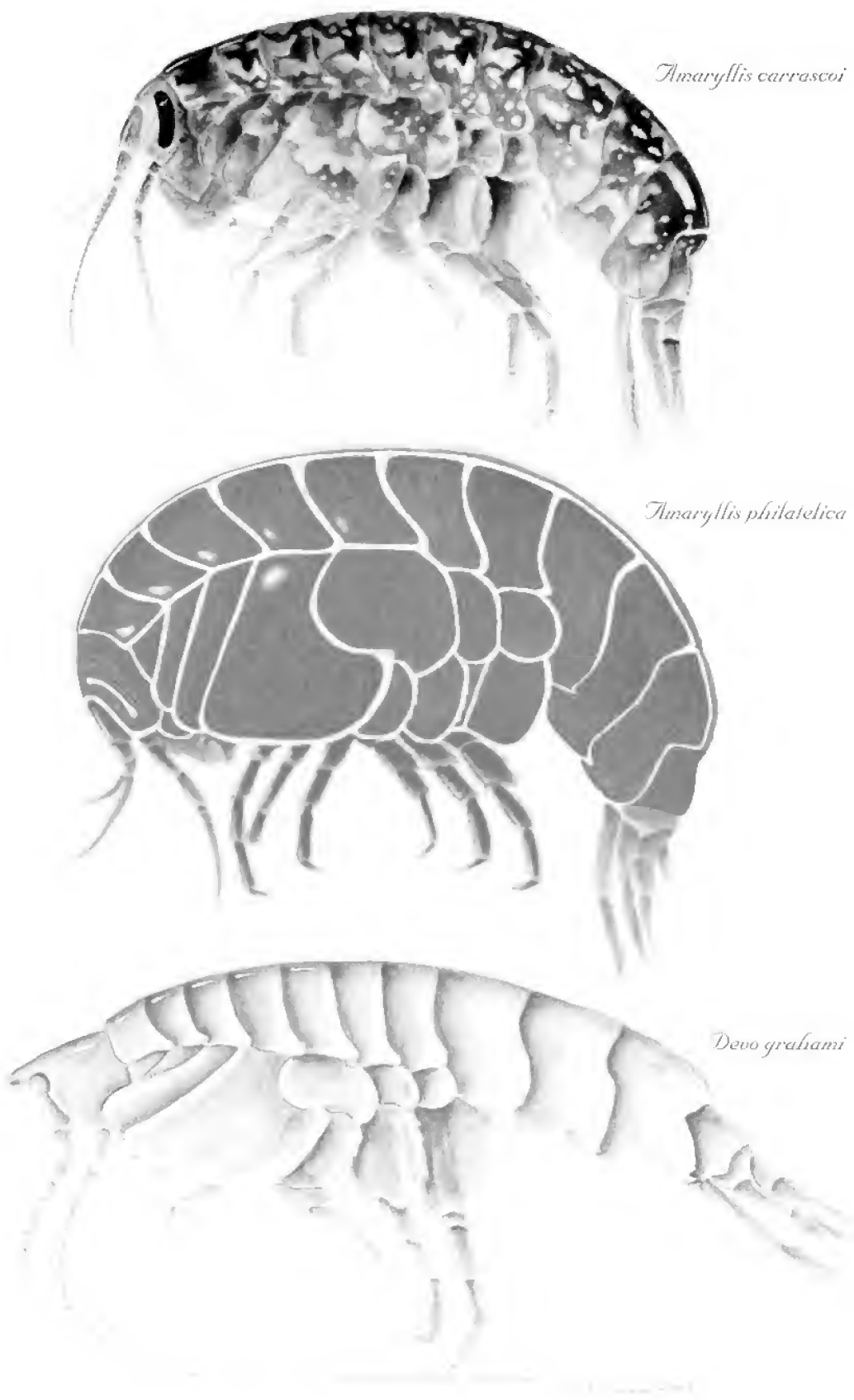


Plate 1. Watercolours by Sharne Wiedland, from photographs of living specimens, showing the diversity of colour in amaryllidids. These figures show the camouflage pattern of *Amaryllis carrascoi* n.sp. (a, upper), the warning colours of *Amaryllis philatelica* n.sp. (b, middle) and the lack of colour in the deep-sea species *Devo grahami* n.sp. (c, lower)

ACKNOWLEDGMENTS. We thank Gary Poore (Museum of Victoria) and Wolfgang Zeidler (South Australian Museum) for the loan of large amounts of material; Ken Graham (NSW State Fisheries) for material collected by the FRV *Kapala*; Stephen Keable, Kate Dempsey and Rachael Peart for illustrations; and Roger Springthorpe for making the plates. Parts of this project were supported by grants from the Australian Research Council and the Australian Biological Resources Study.

References

Alonso, G.M., 1987. Estudios sistemáticos de tres Lysianassidae (Amphipoda, Gammaridea) de la Argentina. *Physis Sección A: Oceanos y sus Organismos* 45(108): 1–10.

Andres, H.G., 1981. Lysianassidae aus dem Abyssal des Roten Meeres. Bearbeitung der Köderfänge von FS "Sonne"—MESEDA I (1977) (Crustacea: Amphipoda; Gammaridea). *Senckenbergiana Biologica* 61(5/6): 429–443.

Barnard, J.L., 1958. Index to the families, genera, and species of the gammaridean Amphipoda (Crustacea). *Allan Hancock Foundation Publications, Occasional Paper* 19: 1–145.

Barnard, J.L., 1964. Revision of some families, genera and species of gammaridean Amphipoda. *Crustaceana* 7(1): 49–74.

Barnard, J.L., 1969. The families and genera of marine gammaridean Amphipoda. *United States National Museum Bulletin* 271: 1–535.

Barnard, J.L., 1972. Gammaridean Amphipoda of Australia, Part I. *Smithsonian Contributions to Zoology* 103: 1–333.

Barnard, J.L., 1974. Gammaridean Amphipoda of Australia, Part II. *Smithsonian Contributions to Zoology* 139: 1–148.

Barnard, J.L., & G.S. Karaman, 1991. The families and genera of marine gammaridean Amphipoda (except marine gammaroids). *Records of the Australian Museum, Supplement* 13(2): 419–866.

Barnard, K.H., 1916. Contributions to the crustacean fauna of South Africa. 5—The Amphipoda. *Annals of the South African Museum* 15: 105–302, pls 26–28.

Barnard, K.H., 1925. Contributions to the crustacean fauna of South Africa. No. 8. Further additions to the list of Amphipoda. *Annals of the South African Museum* 20: 319–380, pl. 34.

Barnard, K.H., 1932. Amphipoda. *Discovery Reports* 5: 1–326, pl. 1.

Barnard, K.H., 1937. Amphipoda. *Scientific Reports of the John Murray Expedition* 4(6): 131–201.

Barnard, K.H., 1940. Contributions to the crustacean fauna of South Africa. 12. Further additions to the Tanaidacea, Isopoda, and Amphipoda, together with keys for the identification of the hitherto recorded marine and fresh-water species. *Annals of the South African Museum* 32: 381–543.

Bonnier, J., 1896. Résultats Scientifiques de la Campagne du «Caudan» dans la Golfe de Gascogne—Août—Septembre 1895. Edriophthalmes. *Annales de l'Université de Lyon* 26: 527–689, pls. 28–40.

Chevreux, E., 1903. Campagnes Scientifique de S.A. le Prince Albert 1er de Monaco. Note préliminaire sur les amphipodes de la famille des Lysianassidae recueillis par la Princesse-Alice dans les eaux profondes de l'Atlantique et de la Méditerranée. *Bulletin de la Société Zoologique de France* 28: 81–97.

Chevreux, E., 1911. Diagnoses d'amphipodes nouveaux provenant des campagnes de la Princesse-Alice dans l'Atlantique nord (suite). *Bulletin de l'Institut Océanographique, Monaco* 204: 1–13.

Chevreux, E., 1935. Amphipodes provenant des campagnes du Prince Albert 1er de Monaco. *Résultats des Campagnes Scientifiques Accomplies sur son Yacht par Albert 1er Prince Souverain de Monaco* 90: 1–214, pls 1–16.

Chilton, C., 1885. Notes on a few Australian Edriophthalmata. *Proceedings of the Linnean Society of New South Wales* 9(4): 1035–1044, pls 46, 47.

Chilton, C., 1906. Report of some Crustacea dredged off the coast of Auckland. *Transactions of the New Zealand Institute* 38: 265–268.

Chilton, C., 1912. The Amphipoda of the Scottish National Antarctic Expedition. *Transactions of the Royal Society of Edinburgh* 48: 455–520, pls 1, 2.

Chilton, C., 1921. Report on the Amphipoda obtained by the F.I.S. "Endeavour" in Australian seas. *Biological Results of the Fishing Experiments carried on by the F.I.S. "Endeavour", 1909–14* 5(2): 33–92.

Dallwitz, M.J., T.A. Paine & E.J. Zurcher, 1993 onwards. *User's Guide to the DELTA System: A General System for Processing Taxonomic Descriptions*. 4th edition. <http://biodiversity.uno.edu/delta/>

Dallwitz, M.J., T.A. Paine & E.J. Zurcher, 1998. Interactive keys. In *Information Technology, Plant Pathology and Biodiversity*, ed. P. Bridge, P. Jeffries, D.R. Morse and P.R. Scott, pp. 201–212. Wallingford: CAB International.

Day, J.H., J.G. Field & M.J. Penrith, 1970. The benthic fauna and fishes of False Bay, South Africa. *Transactions of the Royal Society of South Africa* 39(1): 1–108.

Debelius, H., 1999. *Crustacea Guide of the World*. (English Edition). Frankfurt: IKAN, 321 pp.

Della Valle, A., 1893. Gammarini del Golfo di Napoli. *Fauna und Flora des Golfs von Neapel* 20: 1–948, pls. 1–61.

Edgar, G.J., 1997. *Australian Marine Life—The Plants and Animals of Temperate Waters*. Kew: Reed Books, 544 pp.

Gonzalez, E., 1991. Actual state of gammaridean amphipoda taxonomy and catalogue of species from Chile. *Hydrobiologia* 223: 47–68.

Griffiths, C.L., 1973. The Amphipoda of southern Africa. Part 1. The Gammaridea and Caprellidea of southern Moçambique. *Annals of the South African Museum* 60(10): 265–306.

Griffiths, C.L., 1974a. The Amphipoda of southern Africa. Part 2. The Gammaridea and Caprellidea of South West Africa south of 20°S. *Annals of the South African Museum* 62(6): 169–208.

Griffiths, C.L., 1974b. The Amphipoda of southern Africa. Part 3. The Gammaridea and Caprellidea of Natal. *Annals of the South African Museum* 62(7): 209–264.

Griffiths, C.L., 1974c. The Amphipoda of southern Africa. Part 4. The Gammaridea and Caprellidea of the Cape Province east of Cape Agulhas. *Annals of the South African Museum* 65(9): 251–336.

Griffiths, C.L., 1975. The Amphipoda of southern Africa. Part 5. The Gammaridea and Caprellidea of the Cape Province west of Cape Agulhas. *Annals of the South African Museum* 67(5): 91–181.

Griffiths, C.L., 1976. *Guide to the Benthic Marine Amphipods of Southern Africa*. Cape Town: Trustees, South African Museum, 106 pp.

Griffiths, C.L., 1977. The South African Museum's Meiring Naude cruises. Part 6. Amphipoda. *Annals of the South African Museum* 74(4): 105–123.

Grindley, J.R., & B.F. Kensley, 1966. Benthonic marine fauna obtained off the Orange River mouth by the diamond dredger Emerson-K. *Cimbebasia* 16: 1–14.

Guiler, E.R., 1952. A list of the Crustacea of Tasmania. *Records of the Queen Victoria Museum, Launceston* 3(3): 15–44.

Gurjanova, E., 1962. [Amphipods of the northern part of the Pacific Ocean (Amphipoda—Gammaridea) Part 1]. *Opredeliteli po Faune SSSR Akademii Nauk SSSR* 74: 1–440 (in Russian).

Hale, H.M., 1929. *The Crustaceans of South Australia. Part II*. Pp. 201–381. Adelaide: H. Weir, Government Printer.

Haswell, W.A., 1879. On Australian Amphipoda. *Proceedings of the Linnean Society of New South Wales* 4(3): 245–279, pls. 7–12.

Haswell, W.A., 1880. Preliminary report on the Australian Amphipoda. *Annals and Magazine of Natural History, Series 5*, 5: 30–34.

Haswell, W.A., 1882. *Catalogue of the Australian Stalk- and Sessile-eyed Crustacea*. Sydney: Australian Museum, 324 pp, 4 pls.

Hutchings, P., J.T. Van Der Velde & S.J. Keable, 1989. Baseline survey of the benthic macrofauna of Twofold Bay, N.S.W., with a discussion of the marine species introduced into the Bay. *Proceedings of the Linnean Society of New South Wales* 110(4): 339–367.

Hutton, F.W., 1904. *Index Faunae Novae Zealandiae*. London: P. Dulau and Co., 372 pp.

Karacsonyi, T., 1997. Brilliant fleas of the sea. *Australian Geographic* 45: 29.

Kensley, B.F., & M.J. Penrith, 1977. Biological survey of Sandris. 1. Introduction and faunal list. *Madoqua* 10(3): 181–190.

Lawson, G.S., P.A. Tyler & C.M. Young, 1993. Attraction of deep-sea amphipods to macrophyte food falls. *Journal of Experimental Marine Biology and Ecology* 169: 33–39.

Ledoyer, M., 1978. Amphipodes gammariens (Crustacea) des biotopes cavitaires organogènes récifaux de l'île Maurice (Océan Indien). *The Mauritian Institute Bulletin* 8(3): 197–332.

Ledoyer, M., 1979. Les gammariens de la pente externe du Grand Récif de Tuléar (Madagascar) (Crustacea Amphipoda). *Memorie del Museo Civico di Storia Naturale, Verona. 2nd Serie, Sezione Scienze della Vita* 2: 1–150.

Ledoyer, M., 1986. Crustacés Amphipodes Gammariens. Familles des Haustoriidae à Vitjazianidae. *Faune de Madagascar* 59(2): 599–1112.

Lowry, J.K., & S. Bullock, 1976. Catalogue of the marine gammaridean Amphipoda of the Southern Ocean. *The Royal Society of New Zealand Bulletin* 16: 1–187.

Lowry, J.K., & H.E. Stoddart, 1987. A new South American genus and species in the amaryllidid group of lysianassoid Amphipoda. *Journal of Natural History* 21: 1303–1309.

Lowry, J.K., & H.E. Stoddart, 1993. Crustacea Amphipoda: Lysianassoids from Philippine and Indonesian waters. In *Résultats des Campagnes MUSORSTOM*, ed. A. Crosnier, volume 10. *Mémoires du Muséum National d'Histoire Naturelle, Paris* 156: 55–109.

Lowry, J.K., & H.E. Stoddart, 1994. Crustacea Amphipoda: Lysianassoids from the tropical western South Pacific Ocean. In *Résultats des Campagnes MUSORSTOM*, ed. A. Crosnier, volume 12. *Mémoires du Muséum National d'Histoire Naturelle, Paris* 161: 127–223.

Lowry, J.K., & H.E. Stoddart, 2002. First records of lysianassoid amphipods (Crustacea) from the Andaman Sea. In *Biodiversity of Crustacea of the Andaman Sea. Proceedings of the International Workshop on the Crustacea in the Andaman Sea, Phuket Marine Biological Center, 29 November–20 December 1998*, ed. N.L. Bruce, M. Berggren & S. Bussawarit. Phuket Marine Biological Center Special Publication 23(1): 165–188.

Lyons, J., & A.A. Myers, 1991. Amphipoda Gammaridea from coral rubble in the Gulf of Aqaba, Red Sea: families Dexaminidae, Eusiridae, Isaeidae, Ischyroceridae, Leucothoidae, Liljeborgiidae and Lysianassidae. *Journal of Natural History* 25: 597–621.

Pirlot, J.M., 1933. Les amphipodes de l'expédition du Siboga. Deuxième partie: Les amphipodes gammarides, II:—Les amphipodes de la mer profonde. 1 (Lysianassidae, Stegocephalidae, Stenothoidae, Pleustidae, Lepechinellidae). *Siboga-Expedition, Monograph* 33c: 114–167.

Pirlot, J.M., 1939. Amphipoda. Résultats scientifiques des croisières du navire-école Belge «Mercator». *Mémoires du Musée Royal d'Histoire Naturelle de Belgique*, ser. 2, 15: 47–80.

Poore, A.G.B. & J.K. Lowry, 1997. New amphithoid amphipods from Port Jackson, New South Wales, Australia (Crustacea: Amphipoda: Ampithoidae). *Invertebrate Taxonomy* 11: 897–941.

Poore, G.C.B., S.F. Rainer, R.B. Spies & E. Ward, 1975. The zoobenthos program in Port Phillip Bay, 1969–73. *Fisheries and Wildlife Paper, Victoria* 7: 1–78.

Ren, X., 1998. [A new genus and two new species of the family Lysianassidae (Crustacea: Amphipoda) from Nansha Islands, South China Sea]. *Studies on Marine Fauna and Flora of the Nansha Islands and Neighbouring Waters* 3: 156–165. (in Chinese and English)

Schellenberg, A., 1926. Amphipoda 3: Die Gammariden der Deutschen Tiefsee-Expedition. *Wissenschaftliche Ergebnisse der Deutschen Tiefsee-Expedition auf dem Dampfer "Valdivia" 1898–1899* 23(5): 193–243, pl. 5.

Schellenberg, A., 1931. Gammariden und Caprelliden des Magellangebietes, Südgeorgiens und der Westantarktis. *Further Zoological Results of the Swedish Antarctic Expedition 1901–1903* 2(6): 1–290, pl. 1.

Sergeev, V.N., S.M. Clarke & S.A. Shepherd, 1988. Motile macroepifauna of the seagrasses, *Amphibolis* and *Posidonia*, and unvegetated sandy substrata in Holdfast Bay, South Australia. *Transactions of the Royal Society of South Australia* 112: 97–108.

Sheard, K., 1937. A catalogue of Australian Gammaridea. *Transactions of the Royal Society of South Australia* 61: 17–29.

Springthorpe, R.T., & J.K. Lowry, 1994. Catalogue of crustacean type specimens in the Australian Museum: Malacostraca. *Technical Reports of the Australian Museum* 11: 1–134.

Stebbing, T.R.R., 1888. Report on the Amphipoda collected by H.M.S. Challenger during the years 1873–1876. *Report on the Scientific Results of the Voyage of H.M.S. Challenger during the years 1873–76, Zoology*, 29: 1–1737, pls. 1–210.

Stebbing, T.R.R., 1906. Amphipoda. I. Gammaridea. *Das Tierreich* 21: 1–806.

Stebbing, T.R.R., 1908. South African Crustacea. (Part IV). *Annals of the South African Museum* 6: 1–96, pls. 1–15.

Stebbing, T.R.R., 1910a. Scientific results of the trawling expedition of H.M.C.S. "Thetis". Crustacea. Part V. Amphipoda. *Memoirs of the Australian Museum* 4: 565–658, pls. 47–60.

Stebbing, T.R.R., 1910b. General catalogue of South African Crustacea (Part V. of S.A. Crustacea, for the Marine Investigations in South Africa). *Annals of the South African Museum* 6: 281–593, pls. 15–22.

Stephensen, K., 1923. Crustacea Malacostraca, V: (Amphipoda, I). *Danish Ingolf-Expedition* 3(8): 1–100.

Thomson, G.M., 1902. Some recent additions to and notes on the crustacean fauna of New Zealand. *Annals and Magazine of Natural History, Series 7*, 10: 462–465.

Thurston, M.H., & E. Allen, 1969. Type material of the families Lysianassidae, Stegocephalidae, Ampeliscidae and Haustoriidae (Crustacea: Amphipoda) in the collections of the British Museum (Natural History). *Bulletin of the British Museum (Natural History) (Zoology)* 17: 347–388.

Walker, A.O., 1904. Report on the Amphipoda collected by Professor Herdman, at Ceylon, in 1902. *Ceylon Pearl Oyster Fisheries—1904. Supplementary Reports* 17: 229–300, pls. 1–8.

Walker, A.O., 1909. Amphipoda Gammaridea from the Indian Ocean, British East Africa, and the Red Sea. *Transactions of the Linnean Society of London, Series 2, Zoology* 12(4): 323–344, pls. 42–43.

Whitelegge, T., 1889. List of the marine and fresh-water invertebrate fauna of Port Jackson and the neighbourhood. *Journal and Proceedings of the Royal Society of New South Wales* 23: 163–323.

Index

Amaryllididae	131	<i>kamata, Amaryllis</i>	147
Amaryllidinae	132	<i>kapala, Bathymaryllis</i>	200
<i>Amaryllis</i>	132	<i>keablei, Amaryllis</i>	150
<i>andresi, Pseudamaryllis</i>	210	<i>kimbla, Bamarooka</i>	189
<i>anomala, Bamarooka</i>	176	<i>macrophthalma, Amaryllis</i>	152
<i>Bamarooka</i>	175	<i>migo, Amaryllis</i>	157
<i>Bathyamaryllis</i>	199	<i>moona, Amaryllis</i>	160
<i>bathycephala, Bamarooka</i>	179	<i>olinda, Amaryllis</i>	163
<i>brevicornis, Amaryllis</i>	134	<i>philatelica, Amaryllis</i>	166
<i>carrascoi, Amaryllis</i>	137	<i>Pseudamaryllis</i>	210
<i>croca, Amaryllis</i>	143	<i>quokka, Amaryllis</i>	169
<i>Devo</i>	201	<i>spencerensis, Amaryllis</i>	173
<i>dianae, Amaryllis</i>	143	<i>tropicalis, Bamarooka</i>	192
<i>dinjerra, Bamarooka</i>	182	<i>Vijaya</i>	210
<i>dubuc, Devo</i>	204	<i>Vijayiinae</i>	199
<i>endota, Bamarooka</i>	185	<i>wonga, Wonga</i>	196
<i>Erikus</i>	195	<i>Wonga</i>	195
<i>grahami, Devo</i>	204		

The Tumbarumba Basaltic Gem Field, New South Wales: In Relation to Sapphire-Ruby Deposits of Eastern Australia

F.L. SUTHERLAND¹, I.T. GRAHAM¹, R.E. POGSON¹, D. SCHWARZ², G.B. WEBB¹,
R.R. COENRAADS³, C.M. FANNING⁴, J.D. HOLLIS¹ AND T.C. ALLEN¹

¹ Geodiversity Research Centre, Australian Museum, 6 College Street, Sydney NSW 2010, Australia

² Gübelin Gemmological Laboratory, Maihofstrasse 102, CH-6000, Lucerne, Switzerland

³ Gemmological Association of Australia (NSW Division), 24 Wentworth Avenue, Sydney NSW 2000, Australia

⁴ PRISE, Research School of Earth Sciences, Australian National University, Canberra ACT 0200, Australia

lins@austmus.gov.au

ABSTRACT. Tumbarumba gemfield in the Snowy Mountains basalt province, NSW, yields corundums, zircons and garnet, corroded by magmatic effects and abraded by alluvial transport. Sub-basaltic contours suggest present drainage profiles mimic Miocene sub-basaltic leads. Six types of corundum were identified. Blue, green, yellow (BGY) zoned sapphires (80%) contain ferrocolumbite as a main mineral inclusion and exhibit variable $\text{Fe}_2\text{O}_3/\text{TiO}_2$ and low $\text{Cr}_2\text{O}_3/\text{Ga}_2\text{O}_3$ (<1). Two sub-types differ in colour absorption spectra, one being unusual in lacking the typical $\text{Fe}^{2+}-\text{Fe}^{3+}$ charge transfer effects found in such sapphires. Related trapiche-like corundums (5%) show higher $\text{Cr}_2\text{O}_3/\text{Ga}_2\text{O}_3$, possibly due to Fe-Ti oxide exsolution. Vari-coloured, diffuse-zoned and pale blue sapphires (10%) have higher $\text{Cr}_2\text{O}_3/\text{Ga}_2\text{O}_3$ and colour absorption characteristics intermediate between BGY sapphires and pink to red corundums with elevated $\text{Cr}_2\text{O}_3/\text{Ga}_2\text{O}_3$. The BGY and trapiche-like sapphires are considered magmatic, the intermediate sapphires magmatic-metasomatic (possibly through interactions with Cr-bearing serpentinite bodies) and the pink to red corundums metamorphic in origin. Zircons include low- to high-U types. The latter show {100}-{110} prism combinations (unusual in eastern Australian zircons) and suggest incompatible element enriched parental melts. The magmatic sapphires and zircons (U-Pb age 23 Ma) crystallised in deep evolved salic melts, before transport in basalt. Magmatic-metasomatic sapphires contain zircon inclusions with both older inherited U-Pb ages (up to 903 Ma) and younger magmatic U-Pb ages (27–22 Ma). Basalts represent little evolved undersaturated melts (basanites and alkali basalts), and minor near-saturated transitional melts (olivine basalts). Most generated from garnet peridotite sources, but some from spinel peridotite sources. Mantle normalised incompatible multi-element patterns suggest Oceanic Island Basalt (OIB) melts interacted with amphibole (+ apatite) veined mantle. A sapphire and zircon-bearing basalt, also carries kaersutitic amphibole, apatite, alkali feldspar, titanian mica and titanian magnetite xenocrysts from a veined metasomatised source. Olivine micro-dolerite in a plug resembles the Cainozoic basalts in freshness, but its distinct trace element pattern and Early Devonian K-Ar age (400 Ma) indicate an earlier unmetasomatised spinel peridotite source. The Tumbarumba field evolved through explosive gem-bearing basaltic activity between 27–15 Ma and peaked in basalt lava activity. Interactions of basaltic melts with amphibole-rich mantle, serpentinite bodies and metamorphic corundum deposits combined to generate multi-modal gem suites.

SUTHERLAND, F.L., I.T. GRAHAM, R.E. POGSON, D. SCHWARZ, G.B. WEBB, R.R. COENRAADS, C.M. FANNING, J.D. HOLLIS & T.C. ALLEN, 2002. The Tumbarumba Basaltic Gem Field, New South Wales: in relation to sapphire-ruby deposits of eastern Australia. *Records of the Australian Museum* 54(2): 215–248.

35°30'
148°30'

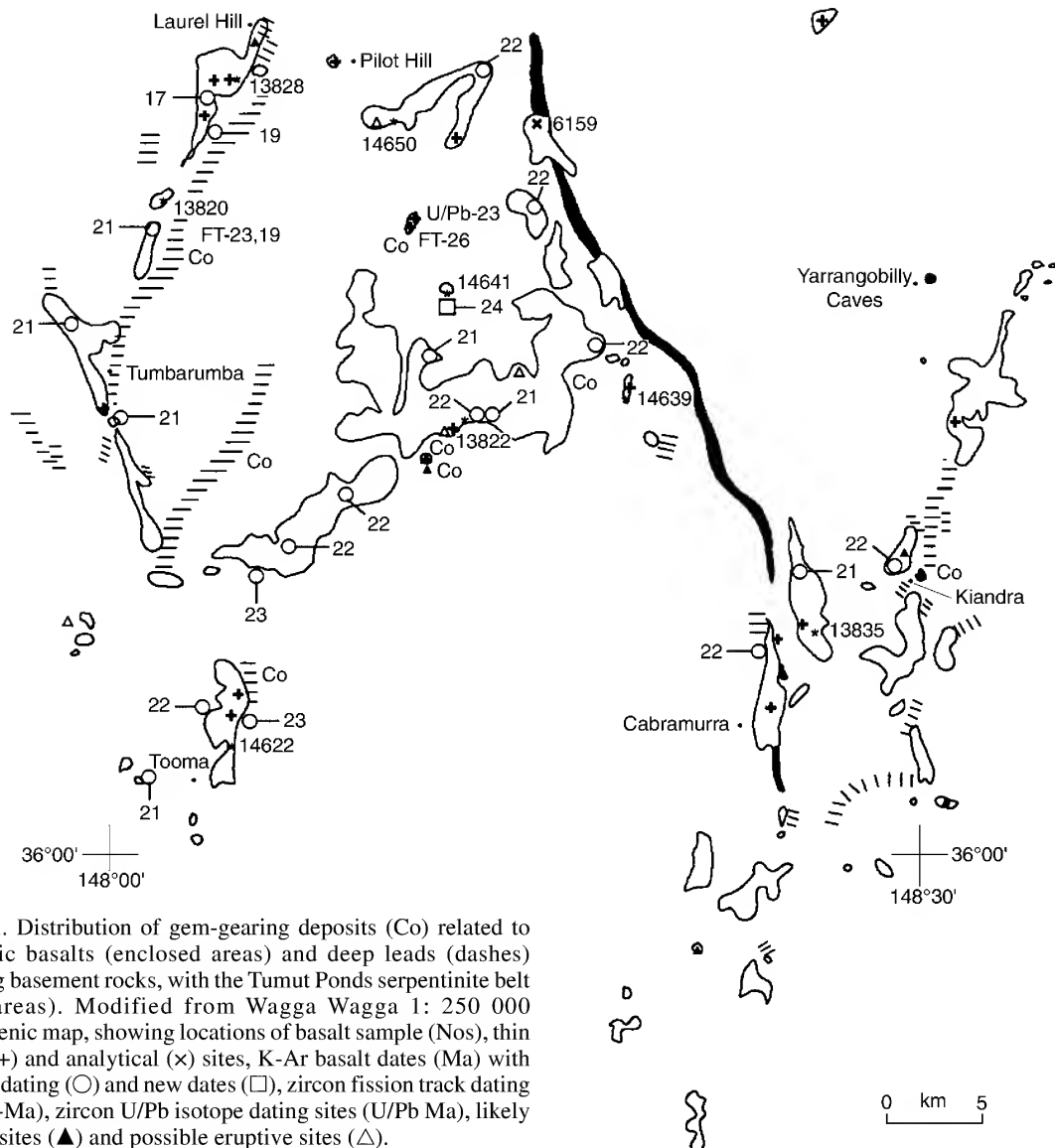


Figure 1. Distribution of gem-gearing deposits (Co) related to Cainozoic basalts (enclosed areas) and deep leads (dashes) overlying basement rocks, with the Tumut Ponds serpentinite belt (filled areas). Modified from Wagga Wagga 1: 250 000 metallogenic map, showing locations of basalt sample (Nos), thin section (+) and analytical (x) sites, K-Ar basalt dates (Ma) with previous dating (○) and new dates (□), zircon fission track dating sites (FT-Ma), zircon U/Pb isotope dating sites (U/Pb Ma), likely eruptive sites (▲) and possible eruptive sites (△).

Eastern Australia is a prime source of gem corundums derived from basaltic eruptives and the larger fields supply sapphires to international markets (Coldham, 1985; Mumme, 1988; Oliver & Townsend, 1993; Sutherland, 1996; Hughes, 1997; Neville & Gnielinski, 1998). Detailed studies of gem corundum associations and their volcanic host relationships concentrate on the larger commercial fields in New England, New South Wales (Coenraads, 1990a,b, 1994; Sutherland *et al.*, 1993; Pecover, 1993, 1996; Oakes *et al.*, 1996), and in central and northern Queensland (Stephenson, 1990; Krosch & Cooper, 1991a,b; Robertson & Sutherland, 1992; Pecover, 1996; Neville & Gnielinski, 1999). Recent studies of gem corundums from a medium-sized basaltic field (Barrington, NSW) firmly established that both magmatic and metamorphic corundum suites co-exist, with the latter suite including pink sapphires and rubies of potential commercial viability (Sutherland & Coenraads, 1996; Sutherland *et al.*, 1998c). In addition, the precise origin of magmatic sapphires, common in eastern Australian suites, is under review (Guo *et al.*, 1996a; Sutherland *et al.*, 1998a; Upton *et al.*, 1999). The Tumbarumba-Kiandra gem field in southern New South Wales includes both sapphire and ruby (MacNevin & Holmes, 1980). Moreover, the provider

eruptives are restricted in age (26–18 Ma; Wellman & McDougall, 1974; Young & McDougall, 1993; Sutherland, 1996) so that the volcanic evolution of the field is less complex than in the larger commercial sapphire fields and the long-lived (60–5 Ma) Barrington bimodal corundum field. The current detailed study of the Tumbarumba basaltic gem field aims to further clarify two aspects of gem corundum/basalt relationships:

- 1 better definition of eastern Australian multi-modal corundum suites,
- 2 better understanding of eastern Australian magmatic sapphire origin.

The Tumbarumba gemfield lies within the Snowy Mountains basalt province (34.8–36.2°S 147.9–149.7°E; Wellman & McDougall, 1974). The lava field erupted c. 24 km³ of alkali basalts from 23–18 Ma (Duncan & McDougall, 1989; Knutson & Brown, 1989; Young & McDougall, 1993). The area is covered by the Wagga Wagga (SI 55-15), Canberra (SI 55-16) and Tallangata (SJ 55-3) 1:250 000 Geological Series Sheets. The gemstones are found in sub-basaltic leads and later alluvial redistributions along the present-day drainage, principally along Tumbarumba Creek, Buddong Creek,

Paddy's River and near Kiandra (Fig. 1). These leads and river courses were extensively worked for gold and corundums and zircons were often recovered in the process (Clarke, 1860; Liversidge, 1888; Curran, 1897; Andrews, 1901; Gill & Sharp, 1957; Willis, 1972; Degeling, 1982). An unusual specimen of basalt containing both sapphire and zircon xenocrysts from the Tumbarumba area was drawn to Australian Museum attention in 1993 (K.G. McQueen and P.J. Brown, Geology Dept. University of Canberra). This specimen (Fig. 2a) confirmed a basaltic matrix for these gem minerals and prompted more detailed study of the gemfield and its basalts.

Fieldwork for this study was undertaken between late January–early February and early April 1997 (F.L. Sutherland, I.T. Graham & R.E. Pogson) and was assisted in the Yarrangobilly 1:100 000 Sheet area (R.S. Abell, AGSO, Canberra). Gem concentrates were recovered from three main locations; upper Tumbarumba Creek (S.A. Miller's Property); Upper Buddong Creek (Parsons Gully) and upper Paddy's River (Ruby Creek). A parcel of sapphires from Tumbarumba Creek was purchased by the Australian Museum from P.J. Brown and family, Albion Park Rail, NSW in 1996 to facilitate the study. Additional sapphires and rubies from Tumbarumba Creek were loaned for study by P.W. Millsteed, Geology Department, University of Canberra. Basalts for detailed study were collected along these drainages and in the Cabramurra–Kiandra–Talbingo areas. Gemmological properties of the corundums were investigated at the Gemini Laboratory, Australian Museum (G.B. Webb) and trace element contents and colour absorption spectra were studied through the Gübelin Gemmological Laboratory, Lucerne, Switzerland (D. Schwarz). Corundum mineral inclusions were analysed at the University of New South Wales (R.R. Coenraads) and dated using the Sensitive High Resolution Ion Micro-Probe (SHRIMP) facility, Research School of Earth Sciences, Australian National University (C.M. Fanning and P.D. Kinny). Zircons were dated through fission track analysis (Geotrack International, Melbourne) and garnets were analysed at the electron microprobe facility (EMP), Macquarie University. Basalts were dated and major elements analysed at AMDEL laboratories, South Australia, with an additional date made at the K-Ar dating facility at CSIRO, Sydney, while basalts were analysed for trace elements at the Geochemical Laboratory, University of Queensland.

Geological setting. The Tumbarumba–Kiandra deep leads and basalts (Fig. 1) occupy a dissected landscape developed in underlying Palaeozoic Lachlan Fold Belt and its granitic intrusions (Degeling, 1982; Scheibner & Basden, 1996). Metamorphic assemblages and granitic rocks found with the folded basement rocks have been described by Vallance (1953, 1954a,b). The main gem field and western basaltic leads lie within the Wagga–Omeo terrain along an anticlinal zone and are mostly entrenched within the mid-Silurian Green Hills granite. There is minor overlap across the enclosing Ordovician flysch sequences and the Tumut Ponds Serpentinite Belt to the west (Stuart-Smith, 1990; Graham, 2000). The Tumut Ponds serpentinitic slivers form a distinctive feature, along the NW–SSE trending Gilmore Suture and are probably related in age to the 400 Ma Coolac ophiolitic belt (Graham *et al.*, 1996). The eastern basalts largely overlie the Goonumbla segment on the western boundary of the Molong–Monaro Terrain. This forms a synclinal zone composed of Early Silurian island arc volcanic rocks and pre-accretionary sedimentary sequences and Late Devonian shelf deposits that

include massive limestones. However, basalts in the Round Mountain lead that passes through Cabramurra probably erupted within the Green Hills granitic body west of the Gilmore Suture. The basalts farther east in the Kiandra lead probably largely erupted within the Goonumbla subterrain.

The deep leads that include gem-bearing alluvial deposits and basaltic infillings are dominated by approximately north–south trending drainage directions (Degeling, 1982). However, different interpretations exist for the direction of the original deep lead river flows; Andrews (1901) considered northerly flows were involved, while Gill & Sharp (1957) suggested the deep lead drainage was southerly, until tectonic uplifts reversed the drainages, ponding rivers to form overlying lacustrine deposits. Detailed landscape reconstruction based on extensive geochronology of the basalts (Young & McDougall, 1993) demonstrated that the major topographic features were in place by the Mid-Tertiary and that modern stream profiles are closely similar to the palaeodrainage under the basalts. Recent studies of the denudation history of the Snowy Mountains, based on apatite fission track thermochronology, suggest possible accelerated denudation from Cainozoic uplift, but the specific ages of uplift are uncertain (Kohn *et al.*, 1999).

The basaltic eruptions that introduced gem corundum, zircon and garnet into the deep leads and later alluvial deposits were mostly confined valley fills with only wider overtopping of leads in places. Subsequent erosion since the Early Miocene has left the basaltic infills as small plateaus, discontinuous elongated strips and peaks and has established a new drainage divide (Gill & Sharp, 1957; Young & McDougall, 1993). The gem minerals were incorporated from the underlying lithosphere into ascending, relatively primitive basaltic melts. Many basalts erupted from their mantle sources, without prolonged residence time (see O'Reilly, 1989), although olivine–spinel–clinopyroxene assemblages (Mackenzie & White, 1970) suggest some crystal fractionation at depth took place en route (see also Fig. 4b).

Seismic studies suggest a depth to mantle of ~50 km in the region (Scheibner & Basden, 1996; Zielhuis & van der Hilst, 1996). Other studies suggest a shallower crust–mantle transition at ~30 km depth (O'Reilly *et al.*, 1997). Examples of Jurassic lower crust–upper mantle assemblages beneath the Snowy Mountains are recorded in xenolith suites in basaltic breccia pipes, at Delegate (O'Reilly *et al.*, 1988; White & Chappell, 1989). Isotopic dating on these xenoliths suggests granulitic facies metamorphism in the region at ~390 Ma after mafic intrusion and granitic melting (Chen *et al.*, 1998). However, precise depths of present crust–mantle lithology remain uncertain as modelling depends on assumed geotherms (Sutherland *et al.*, 1998b). The deep structure of the Australian continent, based on surface wave tomography, shows the Tumbarumba region lies over a zone of slow shear velocity in the mantle, extending to over 200 km depth (Simons *et al.*, 1999). These slow mantle anomalies may reflect present elevated thermal zones among other possibilities, but their exact nature and status relative to Australian lithosphere at 20 Ma is conjectural.

Gem minerals

The gem minerals in heavy mineral suites include resorbed corundum (sapphire, ruby), zircon, garnet and rare pale green orthopyroxene. These, with opaque spinels and ilmenite, are derived from basaltic sources. Rutile, cassiterite, dravite tourmaline, yellow to green monazite, biotite, topaz, small euhedral zircons and gold probably

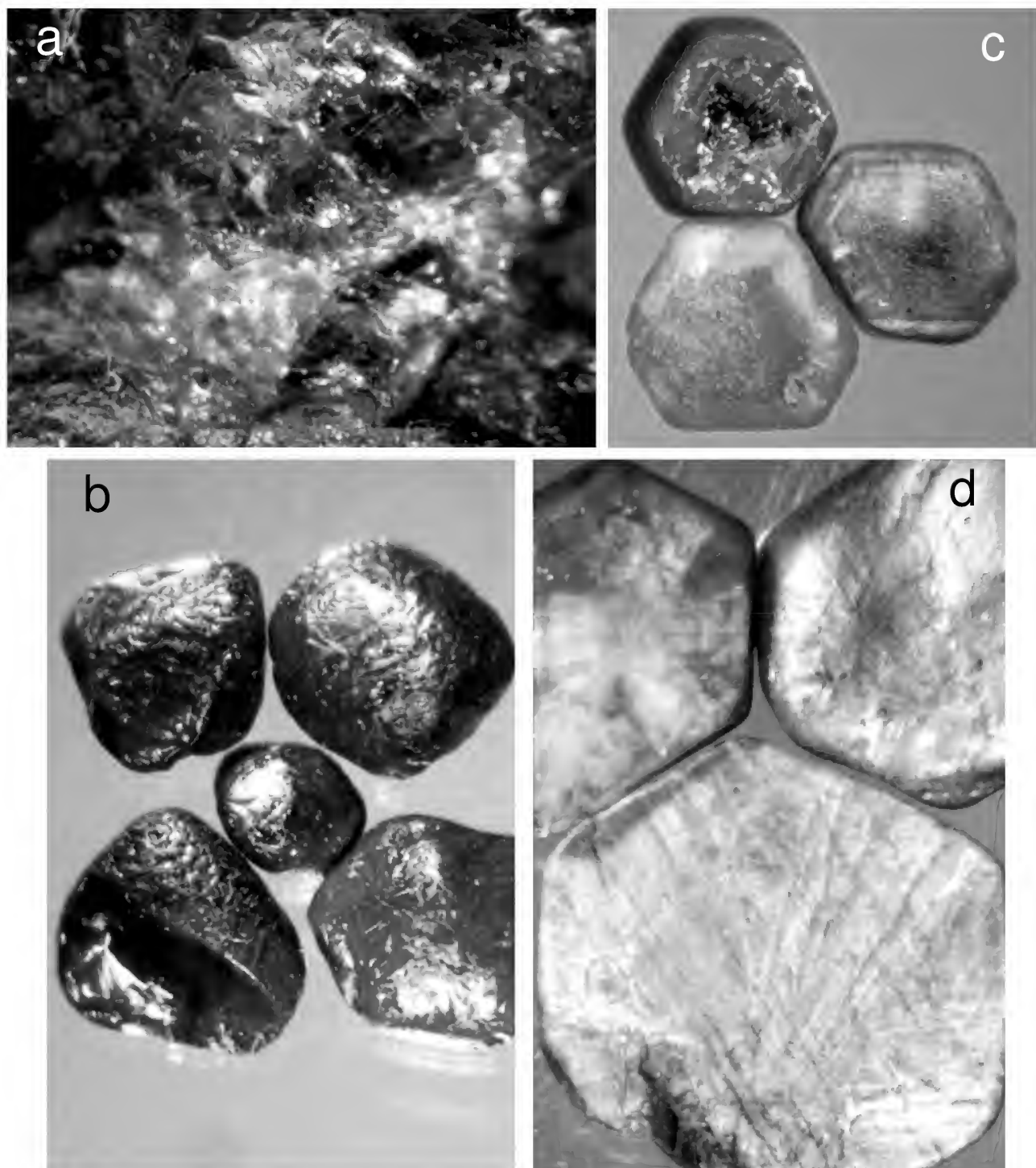


Figure 2. Gemstones, Tumbarumba field, photography G. Webb. a—Zircon xenocryst in basalt matrix, Ruby Creek. The crystal is 3 mm across. b—Strongly corroded blue sapphires, Tumbarumba Creek. Crystals to 6 mm across. c—Zoned “agate” sapphires, Tumbarumba Creek. Crystals to 6 mm across. d—Trapiche-like sapphires, with radiating silk zones, Tumbarumba Creek. Crystals to 11 mm across. e—Diffuse-zoned, vari-coloured sapphire crystals, Tumbarumba Creek. Crystals to 7 mm across. f—Pink to red corundums, Tumbarumba Creek. Crystals to 11 mm across.

come from granitic and associated vein rocks, while sillimanite crystals and serpentinitic fragments come from metamorphic sources. Diamonds were recorded with sapphires and rubies in the Tooma deep lead (Willis, 1972).

Corundums. Around one thousand corundum crystals, grains and fragments were examined by binocular

microscope to sort them into different crystal groups and colours. Grains ranged up to 11 mm in size. All crystals showed magmatic corrosion (Fig. 2b-d) and small, pitted abrasions due to mechanical transport. Rare crystals show relics of dark rinds, typical of spinel reaction rims found on basaltic sapphires elsewhere (Stephenson, 1990). Main groups observed (Fig. 2b-d) were:

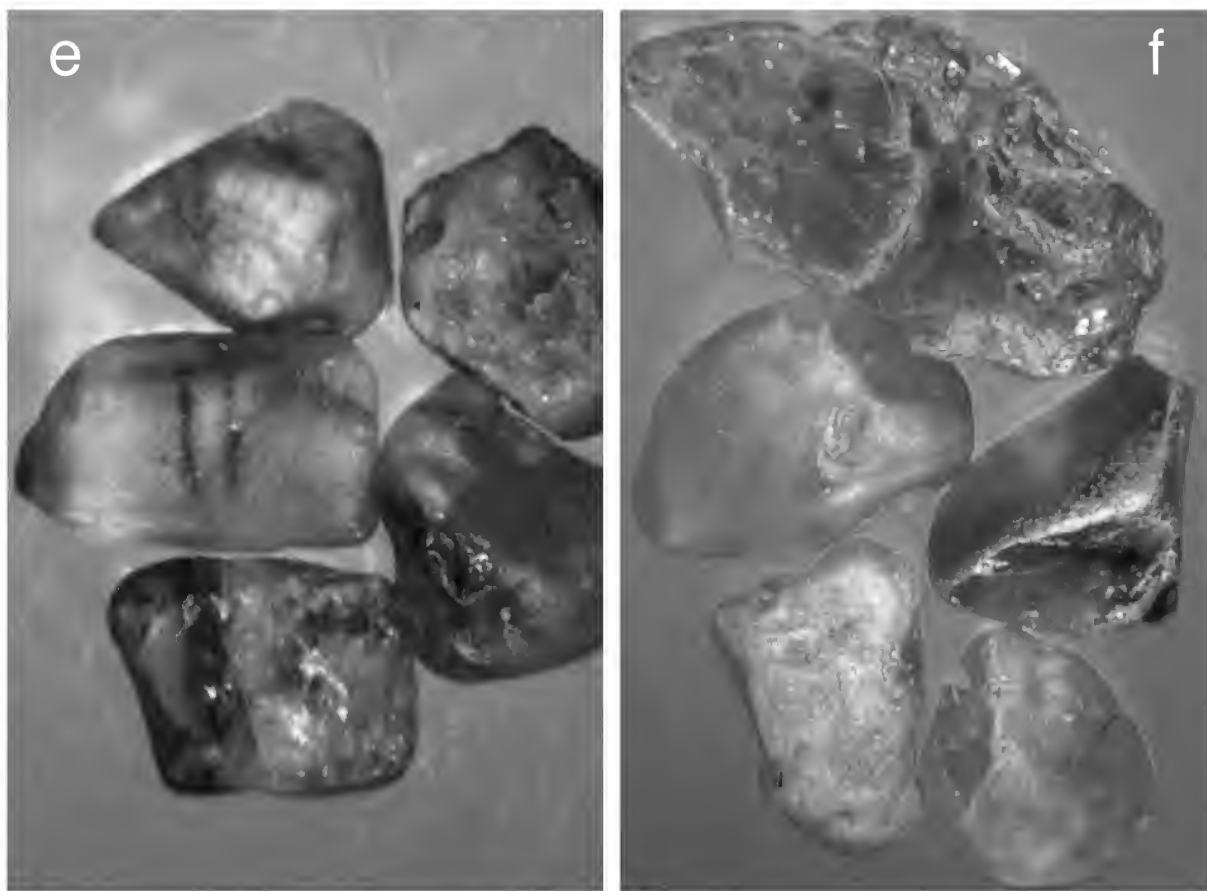


Figure 2, continued.

- Group 1 Strong blue transparent crystal fragments, with pronounced blue/green pleochroism.
- Group 2 Strong blue crystal fragments; some with yellow colour bands or yellow cores.
- Group 3 So called "agate" sapphires; many with dark blue cores, composed of milky hexagonal outer banding.
- Group 4 Particoloured blue, green crystal fragments with diffuse colour zoning.
- Group 5 Large, milky blue crystal fragments with green and bronze (silk-rich) colour zoning.
- Group 6 Coarse, opaque crystal fragments with silk radiating from a central core, in a trapiche-like pattern.
- Group 7 Small transparent, particoloured light blue and green (\pm yellow) crystals and part crystals with an elongated barrel shape, showing a diffuse pale pink core.
- Group 8 Small pale blue crystal fragments with undifferentiated pinkish or mauve zones.
- Group 9 Pink to red crystal fragments and crystals; in one example, hexagonal colour zoning of pale pink and milky bands was observed.

Groups 1–5 resemble typical representatives of the Blue-Green-Yellow (BGY) suite of corundums from basaltic regions (Sutherland *et al.*, 1998a) and make up 80% of the Tumbarumba sample. Group 6 (5%) are corundums distinctive because of their strong silk structure, but typically accompany BGY suite corundums elsewhere. Group 7 (10%) is noted for more complete crystals and is distinctive in appearance compared to the fragments found in the other groups. Groups 8–9 (5%) include types that resemble the fancy coloured sapphire and ruby corundum suite from basaltic regions (Sutherland *et al.*, 1998c).

Group 9, which includes ruby, was limited to seven studied grains. One was light pink, three were bright pink, two were purple red and one red. Small rounded remnant crystal faces were visible on each grain; in one case (light pink) the bi-pyramidal crystal shape was observed. Grains ranged from 5–11 mm in length. They exhibited a medium red fluorescence when exposed to Long Wave Ultra-Violet Light but were inert under Short Wave Ultra-Violet Light. Polysynthetic twin planes were evident as well as crystals containing healing fractures, fluid inclusions and 2- and 3-phase inclusions, with some subsequent iron-staining. The red crystal was internally clear and showed a ruby spectrum using a diffraction grating spectroscope—a couplet in the red, absorption in the yellow-green and three lines in the blue. All pink crystals showed a couplet in the red, due to chromium.

Trace elements. Electron Micro-Probe (EMP) analyses of inclusion-bearing sapphires showed Fe as the main substituting element (up to 1 wt% Total FeO), with lesser Ti and in some cases minor Cr as other substitutions in the Al_2O_3 lattice (see Table 1). Rarely, sapphires contain detectable Nb, Si, Mn or Ca. To investigate the distributions of these elements and their role as colouring agents in Tumbarumba corundums, 72 crystals (CORTUM 1–72) were analysed for Fe, Ti, Cr and V by "chemical fingerprinting". This involved element analysis of main components and minor constituents with the aim of defining groups ("populations"), e.g., gemstones originating from a specific genetic environment or a specific geographic region and identification of individuals by objective and reproducible methods. This employed Energy-dispersive X-ray fluorescence (EDXRF) using a Spectrace 5000 EDXRF system, in a method developed between the University of Basel

(W.B. Stern) and the Gübelin Gemmological Laboratory (D. Schwarz). This method is a useful tool for investigating geological affinities of natural corundums (Stern, 1984; Sutherland *et al.*, 1998c; Schwarz *et al.*, 2000; Schwarz & Stern, 2000). The main chromophores for corundum are Fe and Ti, \pm Cr, while V is generally below the detection limit of the method (\pm 0.005 wt% V_2O_3) and has little input into Tumbarumba corundums apart from one group.

In trace element variations, the corundums fall into five main types (Table 2).

- Type 1 Typical blue, green, yellow corundums (Groups 1–5) that show high Fe, variable Ti, noticeable Ga and negligible Cr and V contents.
- Type 2 Trapiche-like, silk structured sapphires (Group 6) that show similar trace element ranges to the BGY sapphires, but modified by abundant Ti and Fe exsolution effects.
- Type 3 Blue, green, pink diffuse zoned corundums (Group 7) that also show high Fe, low-moderate Ti, but have noticeable Ga and Cr Contents.
- Type 4 Paler blue to white zoned sapphires (Group 8) that show relatively low Fe, moderate to high Ti, quite low Ga, but have noticeable Cr and V contents.
- Type 5 Dark pink to purple red ruby (Group 9) with significant Cr, but which includes low and high Fe variants that also differ in Ti, Ga and V contents.

The most useful trace element discriminant for separating corundums of magmatic and metamorphic origin (Schwarz *et al.*, 2000) are correlation diagrams that plot Cr_2O_3/Ga_2O_3 against Fe_2O_3/Cr_2O_3 or Fe_2O_3/TiO_2 (Fig. 3a,b). Magmatic corundums in general show higher Ga and lower Cr contents than metamorphic corundums, apart from some Ga-enriched metasomatic corundums. Metasomatic corundums can be distinguished using a correlation diagram that plots TiO_2/Ga_2O_3 against Fe_2O_3/Cr_2O_3 (Fig. 5) where they give Fe_2O_3/Cr_2O_3 ratios between 20–110. Magmatic corundums typically give Cr_2O_3/Ga_2O_3 ratios below 1 and Fe_2O_3/Cr_2O_3 ratios between 70–800. Most of the blue, green and yellow zoned colour groups from Tumbarumba (Cr_2O_3/Ga_2O_3 0.10–0.50; Fe_2O_3/Cr_2O_3 >100; Fe_2O_3/TiO_2 4–80) fall in the magmatic field, which is typical for many eastern Australian sapphire suites. “Trapiche-like” Type 2 corundums, however, show intermediate Ga_2O_3/Cr_2O_3 (0.35–2.0), extend to Fe_2O_3/Cr_2O_3 <100 and have relatively restricted Fe_2O_3/TiO_2 (9–35). The pale blue, green and pink hues Type

Table 1. Ferrocolumbite inclusion and sapphire analyses, sapphire (S2), Tumbarumba gem field.

wt% oxide	crystal 1	crystal 2	crystal 3	host sapphire
TiO_2	4.43	4.56	4.12	0.01
Al_2O_3	0.04	0.06	0.03	99.49
Cr_2O_3	0.00	0.00	0.02	
FeO	12.84	12.65	12.75	0.97
MnO	5.41	5.59	5.76	
MgO	0.88	0.91	0.88	
CaO	0.03	0.04	0.02	
ZrO_2	1.23	1.44	0.96	
Nb_2O_5	73.18	72.33	72.93	0.07
Ta_2O_5	1.71	1.20	1.59	
ThO_2			0.11	SiO_2 0.01
total	99.75	98.78	99.17	100.55
cations	(based on 6 oxygens, and partitioning of FeO to FeO/Fe_2O_3)			
Ti	0.1843	0.1908	0.1725	
Al	0.0025	0.0037	0.0017	
Cr	0.0000	0.0000	0.0011	
Fe^{2+}	0.5942	0.5623	0.5712	
Fe^{3+}	0.0000	0.0260	0.0219	
Mn	0.2535	0.2635	0.2714	
Mg	0.0722	0.0754	0.0732	
Ca	0.0015	0.0024	0.0011	
Zr	0.0330	0.0391	0.0259	
Nb	1.8304	1.8186	1.8345	
Ta	0.0257	0.0182	0.0241	
Th	0.0000	0.0000	0.0014	
total	2.9973	3.0000	3.0000	

1 $(Fe_{0.59} Mn_{0.25} Mg_{0.07})_{0.91} (Nb_{1.83} Ta_{0.03} Ti_{0.18} Zr_{0.03})_{2.07} O_6$

2 $(Fe_{0.59} Mn_{0.26} Mg_{0.08})_{0.93} (Nb_{1.82} Ta_{0.02} Ti_{0.19} Zr_{0.04})_{2.07} O_6$

3 $(Fe_{0.59} Mn_{0.27} Mg_{0.07})_{0.93} (Nb_{1.83} Ta_{0.02} Ti_{0.17} Zr_{0.03})_{2.05} O_6$

Analyst: R.R. Coenraads.

3 corundums show trace element contents intermediate to those of the typical magmatic and metamorphic types, with some overlap in Cr_2O_3/Ga_2O_3 ratios (0.15–30). This makes their precise assignments uncertain. In contrast, rare Tumbarumba pale blue, mauve to pink Type 4 and pink-red Type 5 corundums extend to higher Cr_2O_3/Ga_2O_3 typical of metamorphic ratios (1–25), but trend to lower Fe_2O_3/TiO_2

Table 2. Geochemical trace element ranges (wt%), Tumbarumba corundums.

type	description	Fe_2O_3	TiO_2	Ga_2O_3	Cr_2O_3	V_2O_3
Type 1A*	blue, green \pm yellow, white, colour zoned	1–2	0.02–0.15	0.02–0.035	<0.005	<0.01
Type 1B*	blue, green \pm yellow, white, colour zoned	1.0–2.1	0.01–0.35	0.020–0.040	<0.01	<0.01
Type 2	opaque, blue, dark trapiche-like silk	1–2	0.08–0.21	0.015–0.030	<0.01–0.03	<0.01–0.015
Type 3	blue, green, pink, diffuse zoned	0.8–1.5	0.01–0.22	0.015–0.025	0.01–0.04	<0.01–0.015
Type 4	blue, light blue, white colour zoned	0.40–0.65	0.07–0.24	0.01–0.025	0.015–0.035	0.01–0.03
Type 5	dark pink, purple red					
	low Fe	0.06	0.1	0.02	0.25	0.02
	high Fe	0.7	0.05	0.005	0.15	<0.005

* Type 1A and 1B show different Fe colour absorption patterns (see text).

Type 1A (15 specimens, CORTUM 13,23,27,30,31,36,37,38,48,56,64,65,66,67,68)

Type 1B (14 specimens, CORTUM 10,12,21,22,39,40,41,42,43,50,60,69,71,72)

Type 2 (8 specimens, CORTUM 15,16,17,18,19,57,58,59)

Type 3 (19 specimens, CORTUM 4,5,6,7,8,9,11,14,20,24,32,33,34,51,52,53,54,55,63)

Type 4 (6 specimens, CORTUM 1,2,3,25,46,70)

Type 5 (2 specimens, CORTUM 44,45)

(1–10). The pale blue sapphires have relatively low $\text{Cr}_2\text{O}_3/\text{Ga}_2\text{O}_3$ values (1–3) compared to the ruby values (>10).

Colour absorption spectra. Polished corundums were studied with a Perkin Elmer Lambda 9 spectrophotometer at the Gübelin Gem Lab. Ultraviolet-visible-near infrared spectra (UV-vis-NIR, 280–880 nm range) absorption behaviour was recorded from selected stones, with polarised spectra being taken on crystals orientated normal to the c -axis (D. Schwarz analyst).

The BGY “magmatic” (Type 1) group shows two distinct sub-groups in their absorption spectra.

Type 1A spectra are combination spectra dominated by the Fe^{3+} -line groups 375 and 475 nm. This basic absorption spectrum becomes superimposed by intense absorption bands, assigned to Fe^{2+} - Ti^{4+} charge transfer processes (maxima around 600 nm, with polarisation $\perp c > \parallel c$, and ~700 nm, with

polarisation $\parallel c = \perp$ to c). There is also Fe^{2+} - Fe^{3+} pair absorption (maximum ~870–880 nm, with polarisation $\perp c > \parallel c$). These spectra are typical for BGY sapphires elsewhere (Sutherland *et al.*, 1998c; Schwarz *et al.*, 2000).

In contrast, Type 1B spectra do not show the typical absorption bands in the NIR region related to Fe^{2+} - Fe^{3+} charge transfer transitions (Fig. 6a). This unusual combination of chemical and absorption features does not seem to have been previously described in the literature.

The trapiche-like (Type 2) sapphires are almost opaque, so that absorption spectra could not be recorded. This also applies to some of the more opaque (Type 1) sapphires.

The blue, green, pink (Type 3) sapphires show quite unusual absorption behaviour in the UV-vis-NIR range (Fig. 6b). Strong Fe^{3+} -line groups are representative at 375 and 475 nm and are accompanied by pronounced absorption bands ~550 nm and in the NIR. The latter are related to

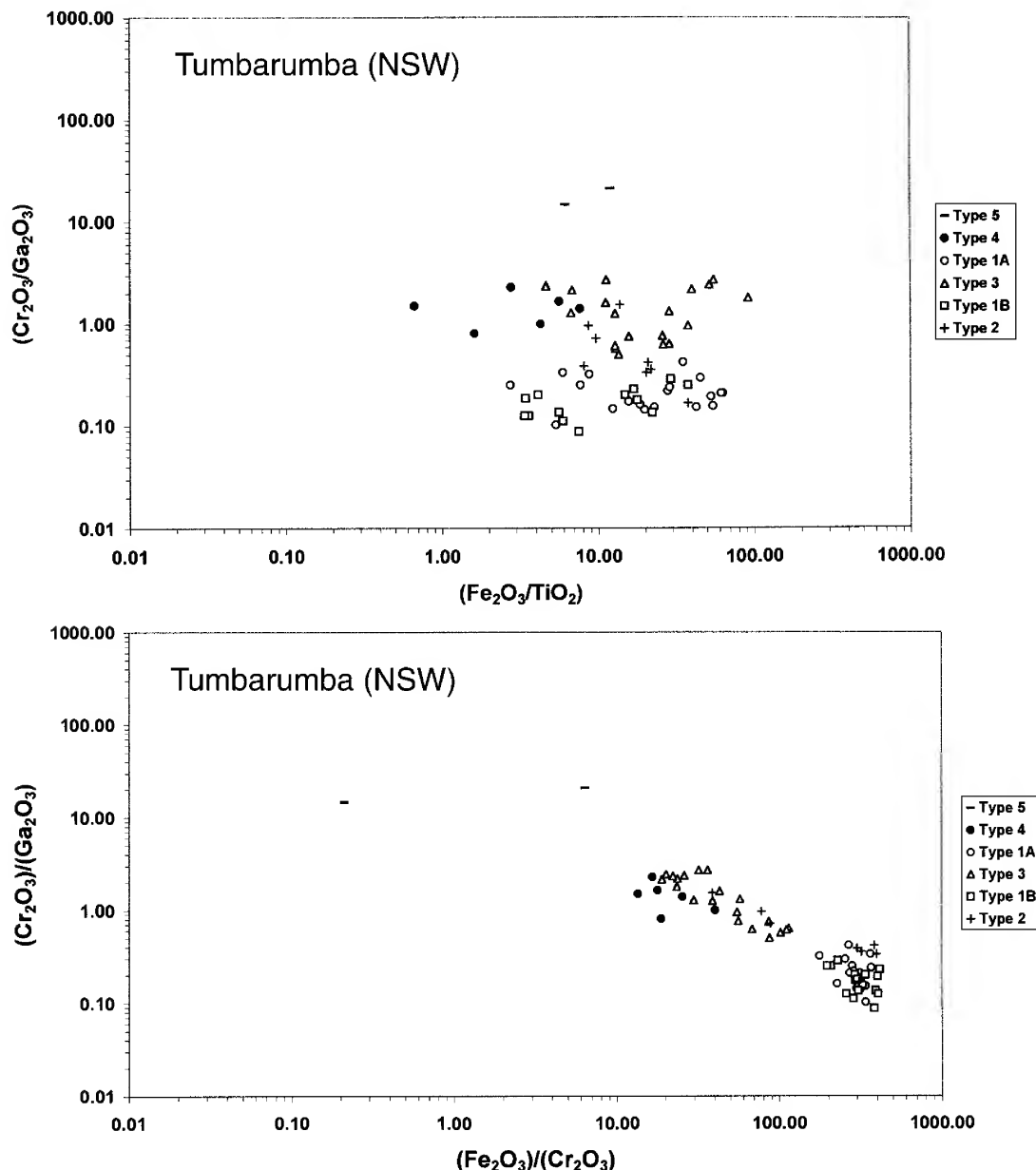


Figure 3. Chemical ratio variation diagrams, Tumbarumba corundums. Type 1A (\circ), Type 1B (\square), Type 2 (+), Type 3 (\triangle), Type 4 (\bullet), Type 5 (—). a— $\text{Cr}_2\text{O}_3/\text{Ga}_2\text{O}_3$ against $\text{Fe}_2\text{O}_3/\text{Cr}_2\text{O}_3$. b— $\text{Cr}_2\text{O}_3/\text{Ga}_2\text{O}_3$ against $\text{Fe}_2\text{O}_3/\text{TiO}_2$.

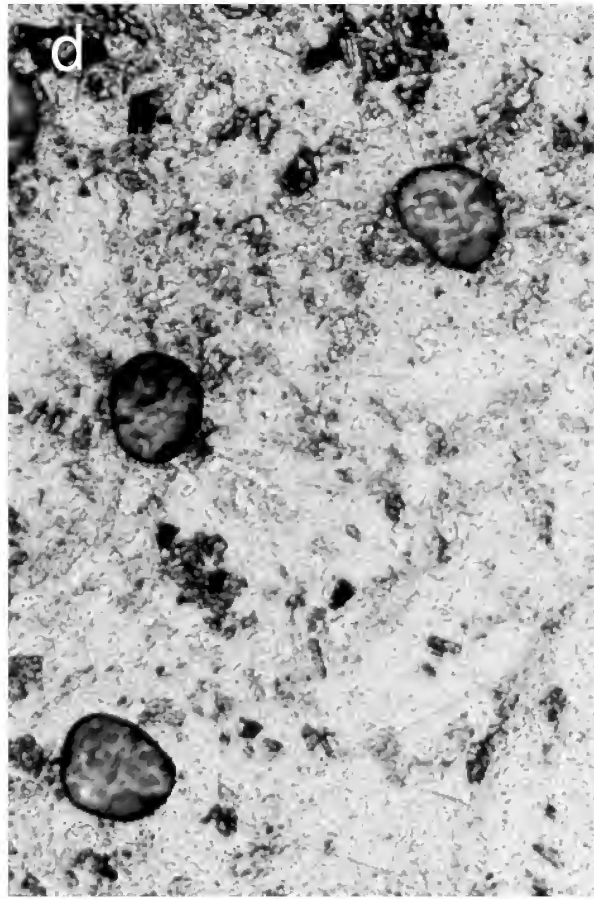
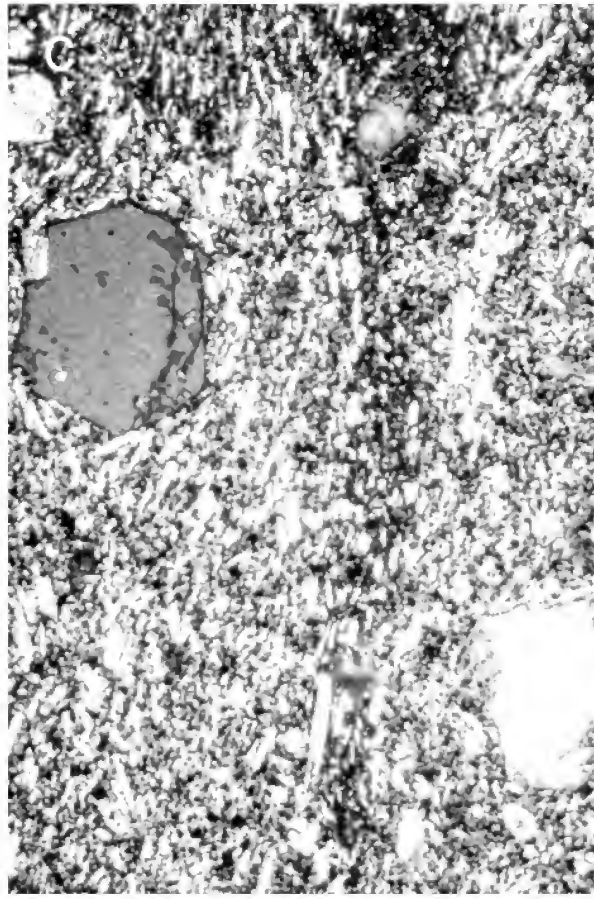
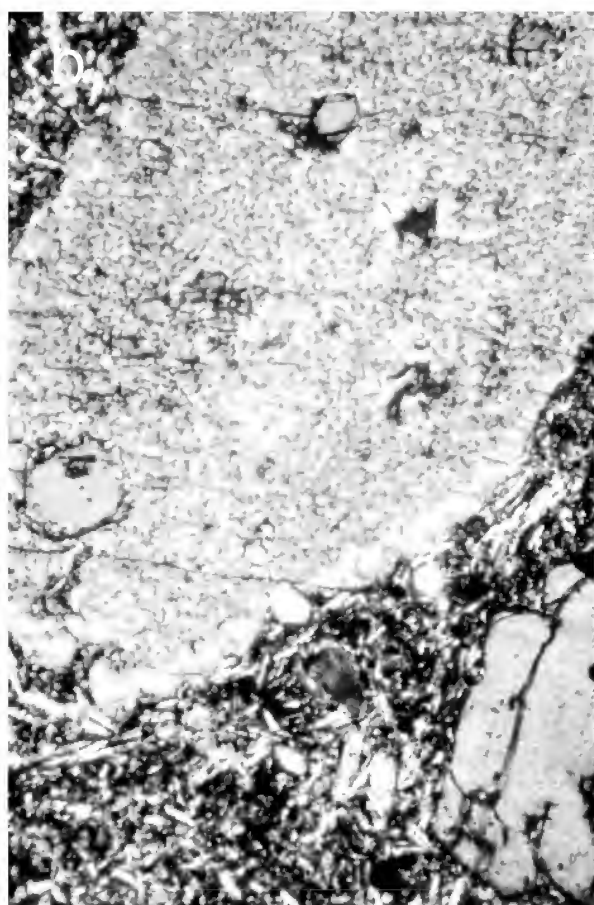
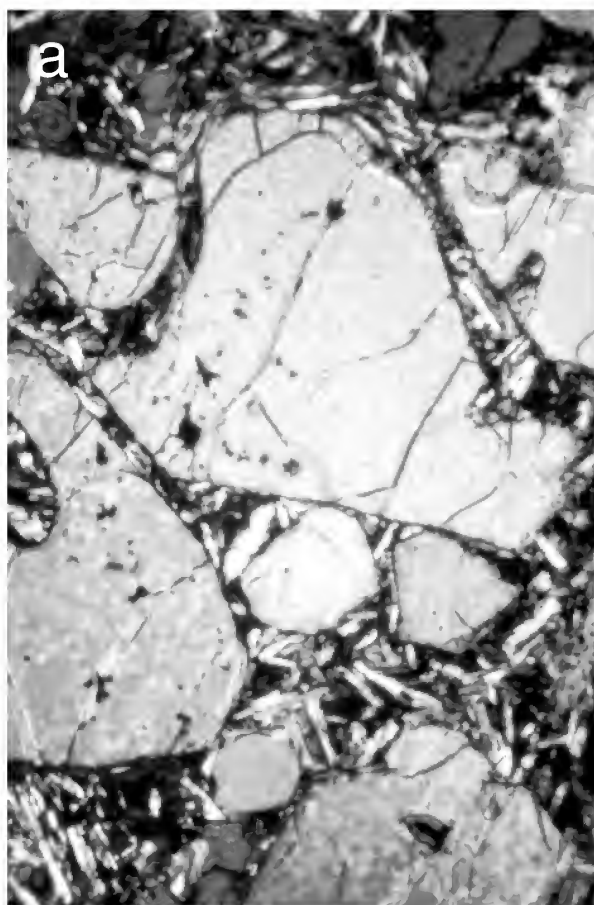




Figure 4. Photomicrographs of Tumbarumba basalts (F.O.V. = Field of View width). a—Olivine phyric alkali basalt, Yorkers Creek (DR14639). F.O.V. 2.5 mm. b—Augite xenocryst, with included olivine and reacted sieved interior, and overgrowth rim, Tooma (DR14662). Field of view (F.O.V.) width 1.25 mm. c—Olivine and augite microporphyritic, flow-banded basanite, Jimmies Hill (DR14641). F.O.V. 2.5 mm. d—Feldspathic (sodian plagioclase) segregation, with rounded vesicles, in alkali basalt, Laurel Hill (DR13828). F.O.V. 3.75 mm. e—Olivine micro-dolerite, Ruby Creek (DR13822). F.O.V. 2.5 mm. f—Kaersutite, biotite and apatite xenocrysts in transitional hawaiite, Ruby Creek (D48682). F.O.V. 3.75 mm.

Fe^{2+} - Fe^{3+} charge transfer transitions and the absorption in the 500–600 nm range is caused by Cr^{3+} as well as by Fe^{2+} - Ti^{4+} charge transfer transitions. This absorption may be more intense than the Fe absorption.

The paler blue “metamorphic” (Type 4) sapphires show absorption spectra that lack pronounced features. Normally a rising “background” absorption towards the UV-region is present. Cr^{3+} and Fe^{2+} - Ti^{4+} charge transfer absorption bands are only weakly developed, as are Fe^{3+} -line groups. The Fe^{2+} - Fe^{3+} charge transfer absorption in the NIR as typically seen in magmatic sapphires is absent.

The pink to red “metamorphic” (Type 5) corundums provide absorption spectra dominated by Cr^{3+} bands. The low-Fe ruby shows an almost pure Cr^{3+} absorption pattern, whereas the spectrum of the high-Fe ruby has an intense absorption shoulder in the UV at ~ 320 nm (related to Fe) and a distinct Fe^{3+} line group at 375 nm.

Mineral inclusions. Exsolved iron and titanium oxides, commonly aligned along crystal directions, prevail in many of the sapphire groups. Some sapphires contain discrete syngenetic or protogenetic crystals and several were sliced and polished to expose such inclusions for analysis. Determinations used a automated Cameca SX 50 CAMEBAX Electron Micro-Probe (EMP), equipped with 4 wave length-dispersive spectrometers (WDS) and an energy-dispersive

spectrometer (EDS) attachment, in the Material Sciences Facility, University of New South Wales, Sydney. Operating conditions included an accelerating voltage of 15kV, a sample current of 20nA, PAPS software for processing raw counts and an ASTIMEX standard block.

The main syngenetic mineral analysed was ferrocolumbite, in euhedral, elongate opaque crystals. Three separate crystals within a sapphire (S3) showed a narrow compositional range (Table 1), approximating $(\text{Fe}_{0.59} \text{Mn}_{0.26} \text{Mg}_{0.07})_{0.92} (\text{Nb}_{1.83} \text{Ta}_{0.03} \text{Ti}_{0.18} \text{Zr}_{0.03})_{2.06} \text{O}_6$. This composition is typical of ferrocolumbite inclusions in basaltic “magmatic” sapphire suites (Guo *et al.*, 1996a; Sutherland *et al.*, 1998a). It is low in Ta and in this respect matches ferrocolumbite inclusions in Jizerská Louka, Czech Republic sapphires (Malíková, 1999). Orange inclusions in the edge of another sapphire (S2) contain high TiO_2 (84–85 wt%), with variable amounts of Al_2O_3 (6–7%), BaO (3–4%), P_2O_5 (2–3%) and FeO (2–3%). The main mineral present matches anatase, with some Fe-oxide, when examined by laser Raman spectroscopy (M. Garland, Geology Department, University of Toronto, pers. comm. 1999) and the Ba, Al and P may represent a gorceixite-like phase. These inclusions may mark breakdown and metasomatic alteration of original rutile. Other orange-red grains, associated with tension-like fractures, have subhedral shape and form a granular mass with a rough surface. The

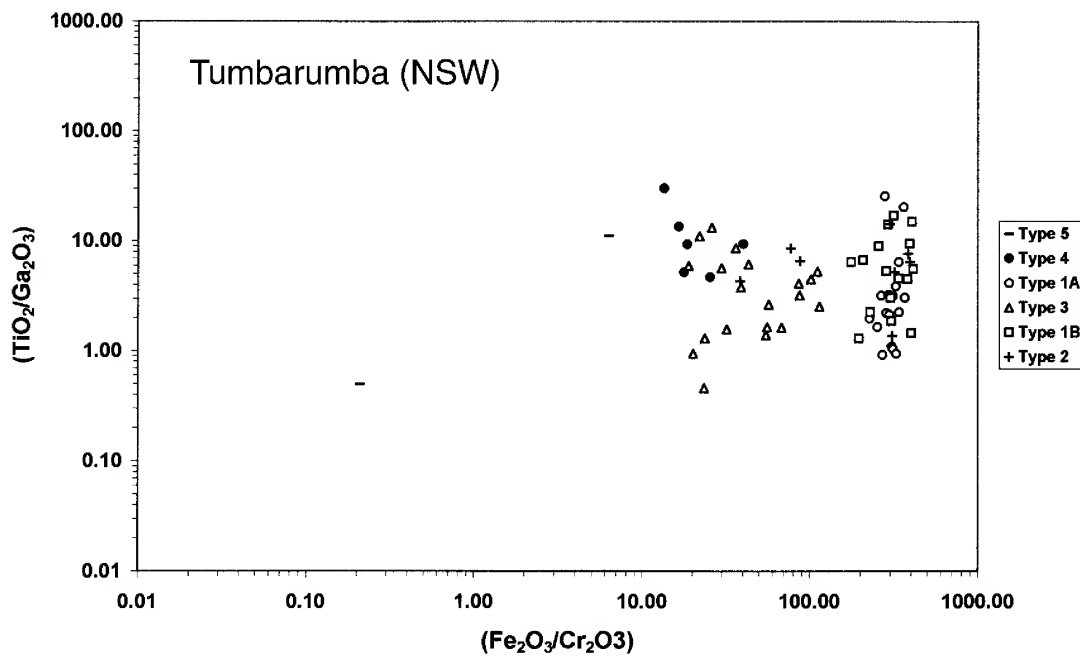


Figure 5. Chemical ratio variation diagram, Tumbarumba corundums. Types as for Fig. 3. $\text{TiO}_2/\text{Ga}_2\text{O}_3$ against $\text{Fe}_2\text{O}_3/\text{Cr}_2\text{O}_3$.

granular mass takes poor polish and shows low reflectivity. It is Fe-rich and may represent a primary iron oxide, altered by fluids invading along the surrounding cracks. A small inclusion of feldspathic glass was also identified by EDS and has a composition approaching anorthoclase.

Other analysed inclusions include ferrocolumbite (CORTUM 11, 20, 46), ilmenorutile (CORTUM 28), zircon (CORTUM 46, 63) and thorian monazite (CORTUM 46). Ferrocolumbite compositions (7 analyses) range between 71–75% Nb_2O_5 , 11–17% FeO, 1.5–8% MnO, 3–5% TiO_2 , <0.5–2% Ta_2O_5 , 1–2% ZrO_2 , 0–2% SiO_2 , 0.5–1.5% MgO and 0–1% Al_2O_3 . Ferrocolumbites in Type 1 sapphires are enriched in FeO compared to MnO in ferrocolumbite in a Type 3 sapphire. Ilmenorutile (2 analyses) contains between 41–44% Nb_2O_5 , 24–32% TiO_2 , 13–18% FeO, 2–4% Ta_2O_5 , 1–2% SiO_2 and some Zr substitution for Nb. Zircons in Type 3 sapphires (2 analyses) contain minor FeO and TiO_2 (up to 4%) and traces of HfO_2 , ThO_2 , UO_3 and Sc_2O_3 (<0.5%). Thorian monazite in Type 3 sapphires (2 analyses) contains 24–25% Ce_2O_3 , 21–23% ThO_2 , 11–13% La_2O_3 , 10–11% Nd_2O_3 and minor UO_3 , Sm_2O_3 , Gd_2O_3 and Pr_2O_3 (<4%).

Zircon megacrysts. Zircons range up to 8 mm long and show a variety of colours and crystal habits. Three main groups were separated from concentrates examined under the binocular microscope, viz:

- darker orange brown and red grains
- colourless to pale yellow grains
- brightly polished pale grains.

The darker grains dominate the Parsons Gully and Ruby Creek samples, while the paler and brightly polished grains are more prevalent within the Tumbarumba Creek samples. The zircon in basalt is a euhedral prismatic orange-brown crystal, 3 mm across, with fractured surface (Fig. 2a).

Crystal features. Surface and crystallographic features of the zircon suites were studied in detail (J.D. Hollis). Strong magmatic resorption and mechanical abrasion are common

on the larger crystals, particularly in the Tumbarumba Creek and Parsons Gully suites. Many resorbed zircons exhibit surface "slits". These typically develop by later etching within a regolith to form baddeleyite (ZrO_2) rinds, which erode off leaving elongate indentations. The abrasive wear on the large crystals is typical of zircons that travel at least 20–30 km from their release site in high energy, large river systems, based on Victorian studies. However, small zircons (<2 mm fraction) show lesser abrasion, with some crystals (<0.5 mm) being practically unabraded, suggesting a degree of protection from abrasion. The zircon suites exhibit very high proportions of resorbed crystals, peaking in size distribution in the >2 mm + range. The relatively low proportion of smaller crystals reflects a typical resorption pattern where small zircons were largely dissolved.

Only the Ruby Creek suite preserves zircons with sufficient crystal characteristics to separate them into different groups. Three groups are recognised, with notation after Dana (1932):

- 1 Orange-red zircons; with forms largely 1st order pyramids {111} and prisms {110}, with minor 2nd order prisms {100}. Some crystals range into 2nd order prisms {100}, combined with major or minor development of 1st order pyramids {111} and ditetragonal pyramids {311}
- 2 Mauve zircons; with 1st order pyramids {111} and prisms {110} ± minor 2nd order prisms {100}.
- 3 Paler highly resorbed zircons; with 1st order pyramids {111} and prisms {110} ± ditetragonal pyramids {311} and 2nd order prisms {100}.

In general, Tumbarumba zircons predominantly exhibit 1st order prism forms ranging into 1st and 2nd order prism combinations. Ditetragonal pyramids tend to develop mostly with the prism combinations. The Tumbarumba suites are relatively unusual among eastern Australian basaltic suites with their lack of pure 2nd order prism crystals, and in this aspect they are closest to Boat Harbour, Tasmania, zircons in their morphology (Hollis & Sutherland, 1985).

Geochemistry. Detailed analyses of zircons were not made, but U contents were measured during fission track dating of the three main zircon groups (Table 3). The darker coloured groups yielded moderate U contents (95–879 ppm, av. 387 ppm), the pale coloured group generally had higher U (36–1433 ppm, av. 486 ppm), while the bright polished group was low in U (37–130 ppm, av. 103 ppm). This suggests separate zircon sources for the groups, in keeping with differences in fission track ages. An orange brown crystal used for U-Pb isotope dating (Table 4), showed high U (1744 ppm) and Th (6050 ppm) with low U/Th ratio (0.29).

Garnet. Bright pink, transparent garnet grains are abundant as broken fragments in the gem concentrates. They form small, magmatically corroded grains and rare composite aggregates up to 5 mm across. They resemble the pink corundums in the concentrates and without detailed inspection are sometimes mistaken for them. Crystal faces are rarely preserved and some grains are coated with a fusion crust of dark Fe and Mn oxide material.

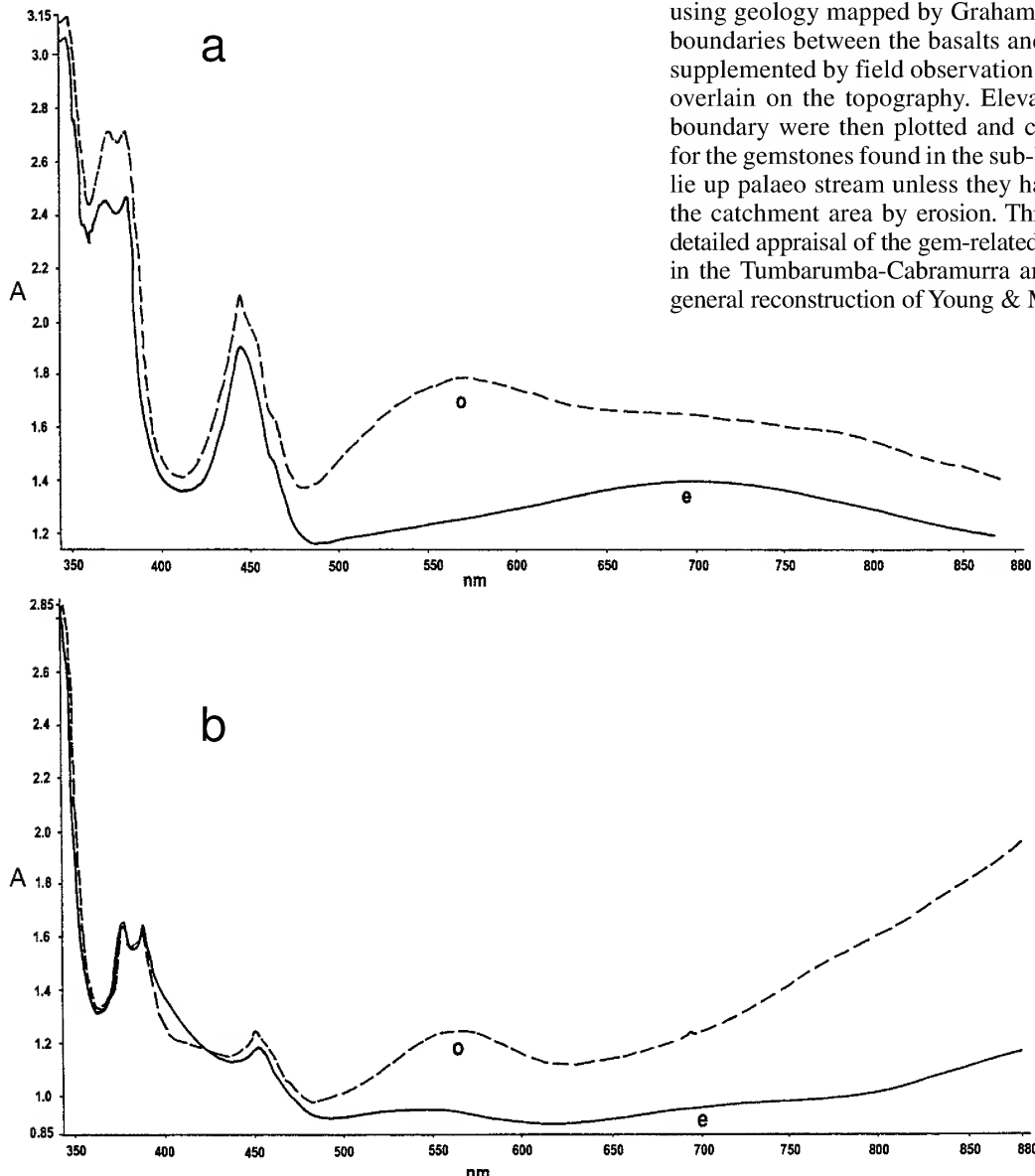


Figure 6. Representative colour absorption spectra (amplitude, A, plotted against wavelength in nm), unusual corundum types: a—Type 1b sapphire, ordinary ray (dashed line) and extraordinary ray (solid line). Blue green sapphire (CORTUM 50). b—Type 3 sapphire, with o- and e-rays as in Fig. 6a. Blue sapphire (CORTUM 08).

Geochemistry. The crystals and a composite garnet microxenolith were polished and analysed by EMP (Table 5). Representative analyses show that the garnets are manganese-bearing almandines ($\text{al}_{68-75} \text{ py}_{12-20} \text{ sp}_{4-15} \text{ an}_{3-4}$). The microxenolithic garnetites contain minor accessory minerals including quartz, calcite and muscovite. The garnet composition and accessory phases suggest derivation from a metamorphic crustal assemblage before incorporation into basalt melt.

Sub-basaltic drainage

The gem minerals represent minor alluvial components within sub- and inter-basaltic lead systems. To better understand their origin, pre-basaltic drainage channels were analysed along the lines used in previous studies in the Central Volcanic Province in New South Wales (Coenraads, 1990a,b). The sub-basaltic topography was analysed at a scale of 1:25 000 (on the Yarrangobilly, Ravine, Cabramurra, Tumbarumba, Tooma, Batlow and Courabyra map sheets) using geology mapped by Graham (2000). The geological boundaries between the basalts and older basement rocks, supplemented by field observation of direct contacts, were overlain on the topography. Elevations for each mapped boundary were then plotted and contoured. Source rocks for the gemstones found in the sub-basaltic deep leads must lie up palaeo stream unless they have been removed from the catchment area by erosion. This study allows for more detailed appraisal of the gem-related palaeodrainage systems in the Tumbarumba-Cabramurra area than in the previous general reconstruction of Young & McDougall (1993).

Table 3. Zircon fission track results, Tumbarumba-Cabramurra area.

number of grains	Ns	Ni	Na	ratio	RHOs	RHOi	age (Ma) \pm error	U ppm (av.)
Parsons Gully, Buddong Creek (sub-basaltic lead)								
dark red grains: 4	283	534	100	0.525	3.23E+06	6.09E+06	26.0 \pm 1.1	149–505 (av. 290)
Tumbarumba Creek, Miller's property (sub-basaltic lead)								
dark red grains: 8	154	215	69	0.760	3.533E+06	4.933E+06	22.8 \pm 1.0	95–819 (av. 361)
pale grains: 8	237	312	77	0.770	4.902E+06	6.439E+06	23.6 \pm 0.9	153–1433 (av. 486)
bright polished grains: 9	52	83	100	0.610	8.193E+05	1.322E+06	18.6 \pm 1.2	37–161 (av. 103)

Determinations from Geotrack Reports No. 30 (Buddong Creek, compiled by P.F. Green & I.R. Duddy, 1985) and No. 655 (Tumbarumba Creek, compiled by P.F. Green, 1997). Standard (RHOD) and induced track RHOi densities were measured on external detector faces and fossil track densities (RHOs) on internal mineral surfaces. Ages were calculated using a Zeta of 87.9 (Buddong Creek) and 87.7 \pm 0.8 (Tumbarumba Creek) for dosimeter glass U3. Ns is the number of spontaneous tracks, Ni the number of induced tracks and Na area of units of counted tracks. RHOD (cm⁻²) is 1.119E+06 (Buddong Creek) and 6.858E+05 (Tumbarumba Creek). Ages represent pooled ages and errors are quoted as $\pm 1\sigma$.

Yarrangobilly 1:100 000 synthesis. The detailed analyses of basaltic leads from the seven 1:25 000 map sheets were combined at 1:100 000 scale (Yarrangobilly Sheet 8526) to provide an overview of the sub-basaltic palaeochannels and their catchments (Fig. 7).

The highest regions of this area lie along the Great Dividing Range (Cabramurra 1:25 000 Sheet, 35°55'S 148°25'E) at elevations still exceeding 1600 masl. Flat topped basalt hills and abandoned gold diggings preserve sections of Miocene palaeochannels that once flowed from the palaeohighs south of Cabramurra. Substantial palaeochannels descending to the north include the Cabramurra (1560 to 1320 masl, with over 80 m thickness of basalt), Kiandra-Dunn's (1500 to <1400 masl, with basalt >190 m thick at Dunn's Hill) and Section (1480 to 1240 masl) palaeochannels. Since then, this palaeohigh has been deeply dissected by the Tumut River and its tributaries draining to the south and west, and the Yarrangobilly River and its tributaries draining to the north and west. The present divide here runs east of Cabramurra and west of Kiandra north towards Yarrangobilly.

Another prominent palaeohigh existed around the Granite Mountain area (Courabyra 1:25 000 Sheet, 100E 456N) and still remains at >1400 masl. Several palaeochannels drain radially away from this high land. The Rutherford (from 1240 masl) and Buddong (from 1180 masl) palaeochannels descend northeasterly from the Burra Ridge palaeohigh before joining up (at ~900 masl, with basalt up to 200 m thick). The Honeysuckle palaeodrainage trends northward (from 1120 to 1000 masl) towards the Rutherford-Buddong palaeochannel. Several palaeochannels drained southward from the palaeohigh including Sparks Plain, Granite, Bull & Damper and Paddy's palaeochannels (from >1300 to <550 masl, with basalt up to 180 m thick). The first named channels joined the continuation of Paddy's channel as the

main outlet. The largest area of basalt was ponded within the tributary channel junctions with Paddy's channel. This basalt mass is less severely dissected than other basalt infillings in the region. The relatively flat area of basalt forms the swampy headwaters to several present day drainages that flow radially off this basalt plateau.

The north-south trending Burra Ridge palaeohigh (Tumbarumba 1:25 000 Sheet, 010E 480N) still exceeds 1200 masl. This separates Paddy's palaeochannel from Tumbarumba palaeochannel, which continues as the major southerly palaeochannel after this junction. Tumbarumba palaeochannel is traceable over 50 km (descending from 1000 to 440 masl, with basalt up to 80 m thick). The present topography is now largely inverted by well-developed lateral stream activity and the infilling channel remnants are now largely visible as a series of linear flat-topped remnant basalt mesas. The straight sections of this course appear to be fault controlled (Wagga 1:250 000 Geological Sheet).

The palaeodrainage reconstruction as presented here applies to drainages largely in place before initial damming and sealing by the earliest lava flows. As lavas progressively filled the channels they would affect stream courses and some lavas would overtop the lower adjacent divides. The main overtopping took place in upper Paddy's drainage where several courses had interfluves bevelled into relatively subdued palaeotopography. Potential overtopping from the Rutherford infilling also exists towards the adjacent Buddong tributary channel, west through Pilot Hill towards the distant Tumbarumba channel and south towards Paddy's channel. An example of diversion from a well-established channel may be represented in the lower Tumbarumba channel where the highest basalt flow in the infilling north of Tooma petrographically resembles basalts overlying lead deposits to the west and south of Tooma.

Table 4. Reconnaissance U-Pb isotope dating, zircon megacryst, Tumbarumba gemfield.

grain colour	U (ppm)	Th (ppm)	$^{206}\text{Pb}/^{238}\text{U} \pm 1\sigma$	age $\pm 1\sigma$ (Ma)	Pb*	% cPb
B2 orange brown	1744	6050	0.00362 \pm 18	23.3 \pm 1.2	12	2.4

$^{206}\text{Pb}/^{238}\text{U}$ refers to radiogenic ^{206}Pb which was estimated by correcting the measured $^{207}\text{Pb}/^{206}\text{Pb}$ in each case by the amount required to yield concordant Pb/U ages, using an assumed common $^{207}\text{Pb}/^{206}\text{Pb}$ of 0.9618 (Broken Hill ore Pb). Pb* refers to the total radiogenic Pb as measured (in ppm). %c Pb refers to the percentage of common (non radiogenic) ^{206}Pb in the total measured ^{206}Pb . Analyst P.D. Kinny, SHRIMP facility, Australian National University.

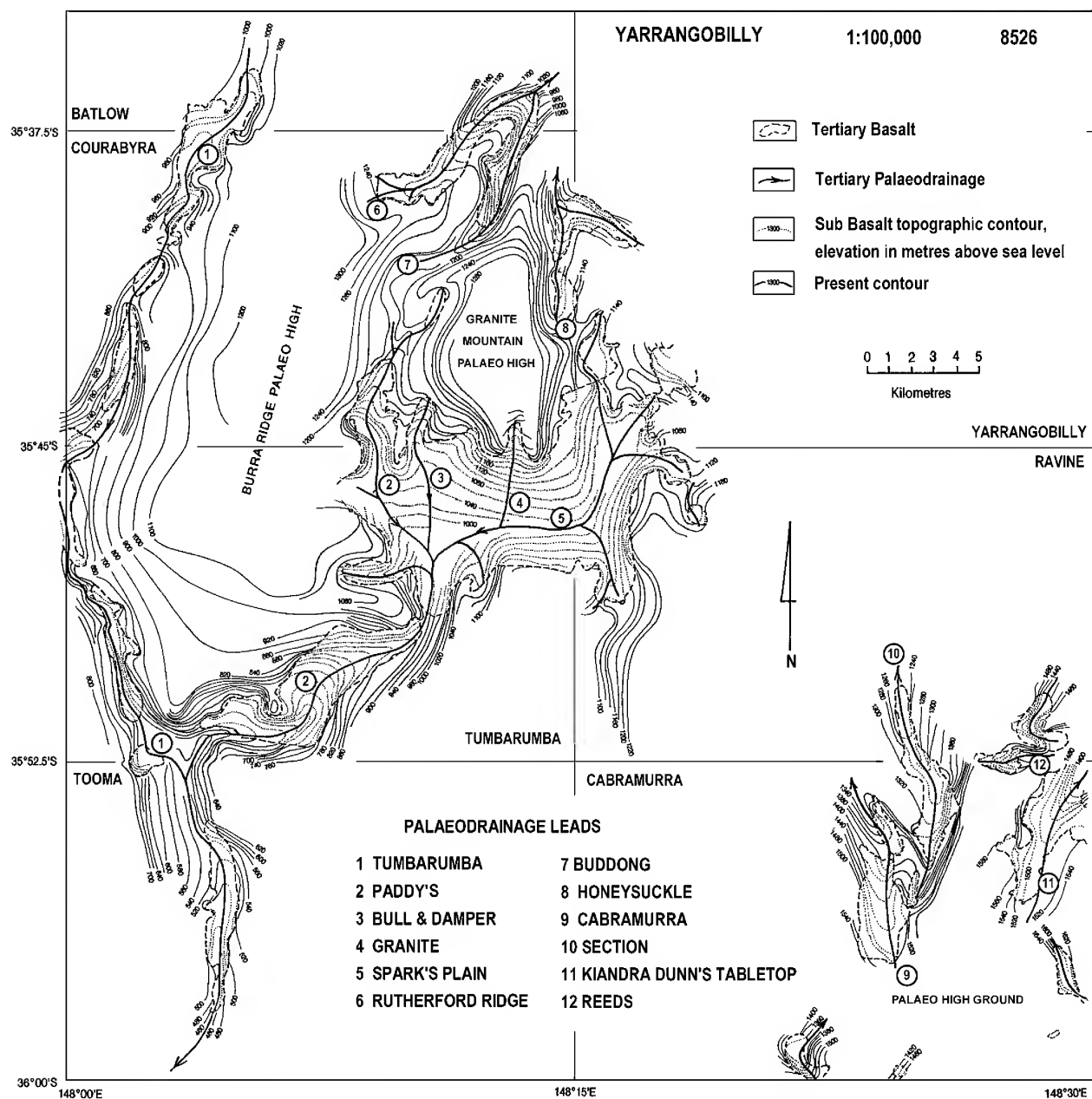


Figure 7. Sub-basaltic paleodrainage related to basalt lava exposures, Tumbarumba-Kiandra region (Yarrangobilly 1:100 000 sheet). Palaeochannels (thick lines) showing direction of drainage flow (arrows) are based on sub-basaltic contours (thin lines) shown at 400 m contour intervals.

Basalts

Basalts infill two main drainage areas, which mark separate eruptive foci (Figs. 1, 7). Western basalts, with largely southerly trending thalwegs, extend from Laurel Hill, Rutherford Ridge and Bago Range through Tumbarumba and Bago Plains to Tooma. Eastern basalts, with largely northerly trending thalwegs, extend from 25 km south of Cabramurra through Cabramurra and Kiandra towards Yarrangobilly Caves.

Distribution. The western basalts form dissected strips within a 140 km² area. Eruptive sources probably underlie Laurel Hill (dykes in flow, 2 km S of Laurel Hill), Rutherford Ridge and Bago Range (topographic basalt highs) and near Ruby Creek (basalt dyke ? and volcaniclastic beds). Basalt flows from Bago Range (>1300 m elevation)

and Rutherford Ridge (>1260 m) descend to Bago Plains and join Laurel Hill (>1000 m) and Tumbarumba (>550 m) flows at Paddy's River, to continue to Tooma (>440 m). Basalts are 80 m thick east of Rutherford Ridge, 180 m at Bago Plains, 170 m at Paddy's River and under 80 m in the Laurel Hill-Tumbarumba-Tooma lead. Up to four flows are observed in exposed sections. Columnar cooling joints are well developed on Tumbarumba-Batlow Road (Courabyra 1:25 000 Sheet 965563), at Paddy's Falls (lower flow), in Tumbarumba Basalt Quarry (upper part) and on Tumbarumba-Tooma Road near Tooma (lowest flow in sequence, passing into sub-horizontal platy jointing). Flow contacts are exposed overlying weathered granite at Laurel Hill, protruding into dark siltstones 4 km S of Laurel Hill and in the three-flow Tooma sequence where flows successively overlie weathered granite, interbasaltic quartz

grits and clays and then a weathered amygdaloidal flow top. Deep lead deposits containing rounded quartz and dacitic metavolcanic fragments were observed under flows extending from 3 km S of Laurel Hill as far as 5 km S of Tooma. Drill holes to 70 m depth west of Tumbarumba intersected two flows with intervening sands and silts and underlying carbonaceous siltstones and weathered granite. The cores (R. Condon, pers. comm. 1997) suggest local undulating pre-basaltic topography.

The eastern basalts form elongate remnants aligned along two major infills each up to 30–35 km long and 20 km across (Gill & Sharp, 1957). Eruptive sources were suggested 12 km S of Cabramurra (plug), 3 km ENE of Cabramurra (dyke) and 11 km S of Kiandra (plug) and 2.1 km SW of Kiandra (plug; Mackenzie & White, 1970). Flow sequences reach 30–100 m thick and up to 4 flows were recognised in the section west of Cabramurra. Well-developed cooling columns are present at several localities (Lafeber 1956; Gill & Sharp, 1957). These columnar basalts are subject to spontaneous cracking within columns due to hydrothermal alteration effects imposed within the lava during cooling (Lafeber, 1956). Flow contacts were well-exposed at Kiandra, where compact basalt overlies lacustrine and fluvial sediments of a deep lead (Andrews, 1901). The basalts were considered to be the source of alluvial sapphires rather than redistribution from the underlying deep lead as was previously suggested by Curran (1897).

Petrology. Some 30 basalts from the Tumbarumba-Kiandra region (samples DR13808–13836; 14638–14669) were thin sectioned for examination by petrological microscope. The main mineralogy includes olivine, clinopyroxene, plagioclase feldspar and opaque iron oxides with associated minor alkali feldspar, feldspathoid(s), apatite, biotite, chlorite, hornblende, zeolite, carbonate, clay, goethite and opal-chalcedony. Many rocks have porphyritic, micro-porphyritic or glomeroporphyritic textures and fluidal flow textures appear in some rocks (Fig. 4a–c). Approximate estimates of phenocrysts and groundmass phases and extent of alteration in the rock are listed in Table 6. Olivine largely alters to chlorite, magnetite and goethite, but “iddingsite” and siderite alteration was noted in a quenched basalt (Barron, 1987). Clinopyroxene is largely augite, zoned to titanian augite, and plagioclase ranges from calcian to sodian

compositions (An_{70–35}). Opaque oxides include ferrian and titanian spinels and ilmenite. Analcime is an alteration phase in more undersaturated rocks and nepheline- and analcime-bearing basanites, some with late-stage phonolitic globules composed of sanidine, nepheline, clinopyroxene and magnetite are described from the Kiandra-Cabramurra area (Lafeber, 1956; Mackenzie & White, 1970). A range of crustal and mantle xenoliths appear in some flows, e.g., a flow on Elliot Way, 20 km W of Tumbarumba (Tumbarumba 1:25 000 Sheet 120389) contains sporadic fragments of Palaeozoic quartzites, granites and pyroxenite-gabbro and mantle lherzolites and pyroxenites.

Pyroclastic and altered volcaniclastic sediments and regoliths were sampled and sectioned from the Tumbarumba-Tooma area during investigations by the NSW Department of Mineral Resources in 1984–1987 (G. Oakes, S.R. Lishmund, L.M. Barron data; Barron, 1987). A lithic volcanic mudstone at a basalt flow base near Ruby Creek (Tumbarumba 1:25 000 Sheet 619 579) contained clasts of highly vesicular basalt, olivine and pyroxene-phyric basalt and microlitic basalt as well as fragments of olivine, feldspar, spinel and pyroxene in a red fine-grained muddy matrix. Red multi-generation peaty fragmental rock exposed in fresh cuts at Permanent Creek contained iron-stained lithic fragments, including altered basalt (?), feldspar, augite (?) and olivine (?) set in a clay matrix. A micaceous muddy reworked volcaniclastic deposit underlies basalt (Tooma 1:25 000 Sheet 975 230) within the Tooma lead (Barron, 1987). It includes material derived from granite, micas that are well separated and unbent and local high contamination by reworked (?) airfall crystal/vitric rhyolitic tuff. These basal (?) and interbedded volcaniclastic sediments and pyroclastics in the basalt sequences suggest explosive phases during eruption of the basaltic lavas. The presence of rhyolitic tuff is further considered in the Discussion section on evolution of the Tumbarumba gemfield (Early Miocene activity, 24–18 Ma).

The survey of basalt types shows a dominance of alkali-olivine basalts and basanites based on petrographic assemblages. Phryic rocks commonly include olivine-dominant, olivine and augite-dominant and olivine, augite and plagioclase-dominant types. In some sequences lower flows are more strongly olivine-phyric (DR14639), in others, upper flows are olivine-phyric (DR13828). Olivine

Table 5. Garnet xenocryst and microxenolith analyses, Tumbarumba gem field.

wt % oxide	xenocryst range	average (3 grains)	xenolith range	average (3 grains)	xenocryst range	xenolith range
SiO ₂	37.96–38.34	38.12	37.01–37.59	37.24	al 68.7–74.6	al 73.5–74.5
TiO ₂	0.00–0.06	0.03	0.01–0.02	0.02		
Al ₂ O ₃	20.94–21.08	21.02	20.63–20.78	20.72	py 17.2–19.4	sp 12.1–14.7
Cr ₂ O ₃	0.01–0.04	0.03	0.01–0.05	0.03		
MgO	4.17–4.81	4.49	1.91–2.48	2.14	sp 4.0–8.9	py 7.9–8.5
CaO	1.10–1.44	1.24	1.07–1.09	1.08		
MnO	1.69–3.89	3.08	6.15–6.25	6.20	an 3.1–4.1	an 3.0–3.2
FeO	31.99–33.93	32.66	33.26–33.89	33.48		
NiO	0.01–0.08	0.05	0.00–0.00	0.00	u 0.0–0.1	u 0.0–0.2
Na ₂ O	0.00–0.03	0.02	0.00–0.03	0.01		
total	100.19–100.93	100.68	100.32–100.92	100.60	gr 0.0–0.0	gr 0.0–0.0

Electron microprobe analyses, Cameca CAMEBAX unit, CSIRO, Sydney. Abbreviations: al-almandine, py-pyrope, sp-spessartine, an-andradite, u-uvarovite, gr-grossular. Analyst: B.J. Barron.

Table 6. Summary of basalt characteristics, Tumbarumba-Snowy Mountains Region.

~%	phenocryst minerals (modal)					ground mass ~%	alteration degree	R.L. (m)	section number	loc.
	oliv.	aug.	plag.	qtz.	composites					
<i>west of Tumbarumba: Ruby Creek (RC), Yorkers Creek (YC)</i>										
40	•					60	minor	1220	14639	YC
25	•	•				75	major	1000	13823	RC
MD	•	•	•				minor	950	13822	RC
<i>south of Tumbarumba: Tumbarumba basalt quarry (TB), Tooma (TO)</i>										
15	•			•		85	major	610	14646	TB
15	•	•		•		85	minor	460	14662	TO
15	•	•	•	•	•	85	minor	480	14664	TO
15	•	•	•	•	•	85	minor	550	14669	TO
<i>northeast of Tumbarumba: Jimmies Road (JR), Rutherford Ridge (RR), Buddong Creek, (BC), Pilot Hill (PH), Parson's Gully (PG)</i>										
40	•	•	•	•		60	major	1200	13819	PG
20	•	•			•	80	minor	1220	13817	PG
5	•	•			•	95	negligible	1360	14641	JR
30	•	•			•	70	negligible	1275	14650	RR
25	•	•	•	•	•	75	negligible	1100	14652	BC
30	•	•			•	70	major	1150	14653	PH
40	•	•			•	60	major	1150	14655	PH
<i>north of Tumbarumba: Miller's Property (MP), Laurel Hill (LH)</i>										
10	•	•			•	90	minor	860	13820	MP
20	•	•			•	80	minor	990	13833	LH
30	•		•		•	70	minor	990	13826	LH
20	•	•			•	80	minor	1060	13830	LH
30	•	•			•	70	minor	1000	13828	LH
<i>Snowy Mountains Region: Yarrangobilly (YB), Cabramurra (CA), Talbingo Ruby Creek (TR), Kiandra (KI)</i>										
20	•		•			80	minor	1150	Y13	YB
30	•	•	•		•	70	minor	1200	Y26	YB
5			•			95	minor	>1000	DR1	YB
20	•		•		•	80	major	1290	13813	TR
30	•		•			70	major	1522	13810	KI
30	•	•			•	70	minor	1325	13834	CA
40	•	•			•	60	minor	1540	13832	CA
10	•	•			•	90	major	>1400	13811	KI
30	•				•	70	minor	1325	13835	CA
25	•	•	•			75	minor	1390	13836	CA

Thin section numbers are Australian Museum DR registration numbers, except for Y13, Y26 and DR1 (R.A. Osborne, University of Sydney). Abbreviations: MD, micro-dolerite; oliv., olivine; aug., augite; plag., plagioclase; qtz., quartz.

and augite glomeroporphyritic and micro-glomeroporphyritic basalts are found in most sequences. The phenocrystic basalts contrast with more uniformly textured olivine basalts. Basalts with predominant sodian plagioclase, typical of hawaiite-mugearite associations are generally absent, although microlitic plagioclase of An₄₀ is recorded in a quenched basalt (Bartron, 1987). Basalts with low Ca pyroxenes or black iron-oxide charged glassy mesostases denoting distinct tholeiitic affinities were not observed. However, rare basalts show transitional characteristics, including absence of titanian colour enrichments in pyroxenes and/or presence of an opaline mesostasis. In some sections flows become less mafic and more feldspathic up through the sequences, but this is not a consistent feature throughout the sequence, suggesting the presence of eruptive cycles.

An unusual texture is present in alkali-olivine basalt (DR13828) from a columnar jointed flow near Laurel Hill. Here, typical olivine, clinopyroxene, plagioclase, opaque oxide-bearing basalt (see Table 7C) is interspersed with feldspathic veinlets to > one cm across (Fig. 4d). These

segregations largely consist of sodian plagioclase passing into albite, with subsidiary magnesian fayalite and augitic clinopyroxene. They commonly contain a central vesicle or a few small vesicles and resemble micro-miarolitic structures. The veinlets are sub-horizontal within the columns and expand in thickness towards the column margins.

Olivine micro-dolerite from the Ruby Creek plug (DR13822) has a coarser texture in which calcic plagioclase forms 50% of the rock in prismatic subhedral grains ranging up to 1.5 mm long (Fig. 4e). Augite (30%) forms subophitic to ophitic intergrowths with plagioclase. Some clinopyroxene completely encloses khaki-brown primary amphibole inclusions. Olivine (15%) forms euhedral to subhedral ovoid grains and aggregates between plagioclase laths and is partly replaced by fine-grained chlorite and magnetite. Opaque angular and irregular grains of ferrian oxides and minor mesostasis and carbonate form the remainder.

Some basalt fragments found within gem-bearing alluvial deposits represent a different basalt than those observed in local basalt flows within the catchment. This includes the sapphire-zircon bearing basalt from Ruby Creek, which also

Table 7A. Major elements and CIPW norms, Tumbarumba-Cabramurra basalts.

oxide	DR	DR	DR	DR	DR	DR	DR	DR	IG	SL	SL
wt%	14639	13822	13835	14650	13820	14662	13828	14641	159	61	63
SiO ₂	44.1	47.2	44.9	43.1	43.7	43.6	44.8	45.3	46.15	43.70	43.60
TiO ₂	1.54	1.08	1.93	1.97	2.53	2.11	2.31	2.68	1.77	2.47	2.42
Al ₂ O ₃	11.9	17.1	14.4	14.4	14.7	14.5	15.0	17.0	14.96	14.20	16.10
Fe ₂ O ₃	2.48	1.93	2.32	2.26	2.28	2.28	2.52	2.34	3.43	3.20	5.30
FeO	8.93	6.96	8.35	8.13	8.21	8.21	9.07	8.42	7.32	7.90	5.30
MnO	0.19	0.16	0.17	0.17	0.18	0.17	0.17	0.19	0.17	0.15	0.15
MgO	16.80	9.61	10.30	9.71	9.55	9.28	8.81	6.27	10.08	10.70	7.75
CaO	7.93	11.90	9.62	10.90	10.00	10.10	9.01	9.13	8.79	9.80	8.06
Na ₂ O	2.47	2.48	3.89	4.10	3.32	3.97	3.47	3.89	2.85	3.00	3.30
K ₂ O	0.96	0.12	1.43	1.54	1.56	1.63	1.33	1.71	0.69	1.26	1.35
P ₂ O ₅	0.56	0.07	1.10	1.40	1.42	1.41	1.16	0.94	0.66	1.20	1.50
L.O.I.	0.70	1.10	0.49	1.50	1.39	1.45	1.00	0.80	2.99	2.90	4.50
total	98.56	99.71	98.90	98.19	98.84	98.71	98.65	98.67	99.86	100.48	99.33
Mg#	0.77	0.71	0.69	0.68	0.68	0.67	0.63	0.57	0.67	0.68	0.62
Mg# = Mg ²⁺ /Mg ²⁺ + Fe ²⁺											
CIPW Norms (anhydrous norms calculated using Fe ₂ O ₃ /FeO + Fe ₂ O ₃ = 0.2)											
Or	5.74	0.71	8.51	9.23	9.37	9.81	7.97	10.23	4.21	7.63	8.41
Ab	14.98	21.11	14.88	7.51	14.99	11.98	21.13	20.15	24.88	15.64	26.28
An	18.76	35.39	17.72	16.57	20.94	17.25	21.72	24.16	26.81	22.09	26.50
Ne	3.34		9.89	15.00	7.35	12.05	4.67	7.13		5.63	1.72
Di	13.85	18.96	18.59	23.37	16.14	19.69	12.88	12.59	10.84	15.87	4.32
Hy		0.61							4.78		
Ol	34.42	17.39	19.84	17.00	18.69	17.52	19.73	14.01	20.37	22.49	21.13
Mt	3.64	2.82	3.39	3.32	3.36	3.37	3.70	3.43	2.59	2.67	2.57
Il	2.96	2.06	3.69	3.79	4.89	4.08	4.45	5.15	3.47	4.81	4.85
Ap	1.34	0.17	2.62	3.36	3.42	3.40	2.78	2.25	1.61	2.91	3.75
An%	56	63	54	69	58	59	51	55	52	59	50
D.I.	24.16	21.8	33.3	31.7	31.7	33.8	33.8	37.5	29.10	28.9	36.4
Type (J&D)	Alkali ol basalt	Olivine basalt	Basanite	Basanite	Basanite	Basanite	Alkali ol basalt	Basanite	Olivine basalt	Basanite	Alkali ol basalt
Type (LM)	Basanite	Basalt	Basanite	Basanite	Basanite	Basanite	Basanite	Basanite	Basalt	Basanite	Basanite

An% = (An/[An+Ab])×100. D.I. differentiation index Σq or ab ne, lc; Type (J&D), basalt type, based on normative mineralogy after Johnson & Duggan (1989); Type (LM), basalt type, based on Total Alkali-Silica (TAS) diagram after Le Maitre (1989). IG 159 analysis by Macquarie University Laboratories, Sydney. SL61, SL62 analyses by NSW Mineral Resources Laboratories, Lidcombe, Sydney.

carries conspicuous xenocrysts, unobserved elsewhere in the Tumbarumba-Kiandra region (Fig. 2a).

The zircon-corundum-bearing basalt (DR48682) contains rare peridotite xenoliths up to 1.5 cm across and corroded xenocrysts of kaersutitic amphibole (5%), sparse apatite, and rare potassian anorthoclase, titanian biotite and titanian magnetite up to 5 mm across (Fig. 4f). The olivine in the peridotite is partly altered through oxidation of Fe, but is Mg-rich and is intergrown with aluminian diopside and kaersutitic amphibole. It may represent metasomatically altered lherzolite. The kaersutite shows khaki brown to pale yellow pleochroism and crystal cores mantled by narrow rims, with a reaction margin of fine-grained granular opaque iron oxide. Compositions vary between crystals (SiO₂ 39–41%, TiO₂ 4–6%, Al₂O₃ 14–16%, Fe₂O₃ 15–19%, MgO 8–9%, CaO 9–10%, Na₂O 1–2%, K₂O 1–2%), but core and rim compositions are generally similar. Larger crystals exhibit a crystallographic controlled prismatic phase (rhönite?), zeolite-replaced enclaves (barian phillipsite?) and intergrown apatite. Apatite xenocrysts have a cloudy pink grey colour and are also intergrown within heavily iron-oxide altered titanian biotite blades (up to 7 wt% TiO₂). The apatite resembles lherzolite mantle apatite described

by O'Reilly & Griffin (2000). The basalt groundmass is dominantly composed of plagioclase laths (~An₅₀) with accessory magnetite-ulvöspinel, some anorthoclase and feldspathic glass and rare small olivine crystals (~Fo_{70–80}). It approaches a transitional hawaiite in character.

Geochemistry. A range of fresh basalt types were selected for analysis after thin section examination (Tables 7A–C). Analyses were made at AMDEL Laboratories, Adelaide, using an alkaline fusion and Inductive Coupled Plasma (ICP) Mass Spectrometry for major elements ($\pm 5\%$ accuracy) and HF acid digest and ICP-MS for trace elements including rare earth elements (REE) ($\pm 10\%$ accuracy). Three unpublished analyses from other sources, with more limited trace element determinations, are also listed (I. Graham, Macquarie University Laboratory, Sydney; S. Lishmund, NSW Dept. Mineral Resources Laboratory, Sydney). Additional major element and restricted trace element analyses of Cabramurra-Kiandra basalts (Lafeber, 1956; Mackenzie & White, 1970; Knutson & Brown, 1989) were also considered in the overall synthesis.

Major element analyses (Table 7A) show a range of primary to slightly evolved basalts, based on Mg# (0.77–

Table 7B. Trace element analyses, Tumbarumba-Cabramurra basalts.

element (ppm)	14639	13822	13835	14650	13820	14662	13828	14641	159	61	63
Ni	550	160	260	190	195	200	165	62	245	258	170
Cr	460	350	410	250	250	290	240	60	350	283	199
Zn	115	83	110	120	120	115	125	120	74	95	88
Cu	105	91	60	74	75	70	66	64	56	98	66
V	170	220	180	180	200	170	190	220	162	197	174
Y	18	21.5	23	28	24.5	25	23.5	25.5	24	25	29
Sc	<5	15	25	15	15	20	25	25		24	25
Rb	14	9	21	30	16.5	22.5	13.5	19.5	10	15	22
Sr	650	160	1200	1700	1800	1700	1450	1250	884	1307	1386
Ba	280	<20	700	1000	850	950	550	700	437	639	865
Zr	110	60	170	170	180	190	170	220	218	233	296
Hf	4	7	3	7	3	4	3	15		<3	<3
Ga	15	16.5	19.5	19	20.5	23	18.5	20	14	20	18
Nb	57	2.5	120	175	80	135	22	150	57	81	104
Ta	5	6	7	6	7	9	7	8			
Th	4.6	0.5	11.5	19	10.5	13.5	6.5	7	5	7	9
U	0.9	0.1	2.2	3.1	2.3	2.8	1.4	1.3	1	<1	<1
La	39.5	3.6	89	120	110	125	83	67		100	109
Ce	59	8.5	120	160	155	170	120	110		138	164
Pr	7	1.65	11	18.5	15	15	12	14			
Nd	24.5	7.5	35.5	61	47	48.5	40.5	49		65	72
Sm	4.3	2.4	8	9	10	10	8.5	7.5			
Eu	1.60	1.05	2.6	3.3	3.4	3.3	2.9	2.8			
Gd	3.9	2.9	6	7	7.5	7.5	6.5	6			
Tb	0.56	0.51	0.85	0.96	1.05	1.05	0.91	0.84			
Dy	3.1	3.3	4.7	4.8	5.5	5.5	4.9	4.4			
Ho	0.7	0.84	0.81	1.05	0.89	0.91	0.83	0.96			
Er	1.55	1.95	2.2	2.3	2.3	2.4	2.2	2.2			
Tm	0.2	0.3	0.3	0.3	0.3	0.35	0.3	0.3			
Yb	1.35	1.95	1.85	2.0	1.85	1.95	1.80	2.0			
Lu	0.23	0.32	0.30	0.33	0.29	0.31	0.28	0.32			

0.57). Using CIPW norms and a Differentiation Index (DI) diagram (Johnson & Duggan, 1989), the rocks classify into basanites (<5% ne, >5%ab) and alkali olivine basalts (<5% ne, <5% hy). Using a Total Alkali ($\text{Na}_2\text{O} + \text{K}_2\text{O}$)—Silica (SiO_2) classification (TAS diagram; Le Maitre, 1989) most rocks are basanites with minor basalts. Quenched basalt from Ruby Hill (SL63) shows higher volatile content (4.5 wt%) than the other basalts (0.7–3.0 wt%) and is transitional

to hawaiite (An 50%). Ruby Creek micro-dolerite (DR13822) has highest SiO_2 (47.2%) and CaO (11.9%) and lowest K_2O (0.12%) and P_2O_5 (0.07%), which with low hy (0.6%) suggests transitional olivine basalts. This rock however proved Palaeozoic in age (see Table 9). Talbingo basalt (IG159) is also low in K_2O (0.69%) and P_2O_5 (0.66%) and with 4.8% hy approaches transitional olivine basalt. Some of the major analytical totals are slightly low. This

Table 7C. Locality data, analysed rocks, Tumbarumba-Cabramurra basalts.

DR14639	Coarse grained olivine-rich alkali basalt flow, Yorker's Creek, 1120 m R.L., Ravine 1:25 000 Sheet (GR 193 395)
DR13822	Coarse olivine basalt (micro-dolerite) plug (?), Ruby Creek, 950 m R.L., Tumbarumba 1:25 000 Sheet (GR 075 352)
DR13835	Basanite flow, Link Road, west of Ravine Junction, 1325 m R.L., Cabramurra 1: 25 000 Sheet (GR 274 287)
DR14650	Vesicular olivine-pyroxene phryic basanite, Rutherford Ridge, 1275 m R.L., Courabyra 1:25 000 Sheet (GR 060 539)
DR13820	Vesicular olivine-pyroxene phryic basanite, 0.7 km NE of Courabyra-Adelong road junction, 860 m R.L., Courabyra 1:25 000 Sheet (GR 947 507)
DR14662	Columnar olivine-pyroxene phryic basanite, lowest flow, Bald Hill, Tooma-Tumbarumba Road, 460 m R.L., Tooma 1:25 000 Sheet (GR 971 202)
DR13828	Columnar olivine alkali basalt flow, Laurel Hill camp, Adelong Road, 1000 m R.L., Courabyra 1:25 000 Sheet (GR 965 563) *
DR14641	Flow banded olivine-pyroxene phryic basanite, W side Jimmies Road, near Granite Mountain, 1360 m R.L., Courabyra 1:25 000 Sheet (GR 090 458)
IG159	Massive olivine basalt flow, near Talbingo, 1030 m R.L., Yarrangobilly 1:25 000 Sheet (GR 139 545)
SL61	Basanite flow, Ruby Creek, 1060 m R.L., Tumbarumba 1:25 000 Sheet (GR 096 374)
SL62	Olivine alkali basalt flow, above Ruby Creek, 1010 m R.L. Tumbarumba 1:25 000 Sheet (GR 073 359)

* DR13828 Main mineral phases, approximate compositions: Olivine ($\text{Fo}_{65-80} \text{Fa}_{20-35}$), augite-diopside ($\text{Wo}_{29-47} \text{En}_{23-45} \text{Fs}_{20-47}$), plagioclase ($\text{An}_{51-62} \text{Ab}_{34-41} \text{Or}_{2-6}$), anorthoclase ($\text{Ab}_{55-65} \text{Or}_{15-25} \text{An}_{15-20}$), ulvöspinel ($\text{Usp}_{69-72} \text{Mf}_{13-19} \text{Mt}_{3-11} \text{Hc}_{3-7} \text{Chr}_{0-2}$).

may reflect trace element enrichments as these rocks show relatively high Sr and Ba compared to other related eastern Australian basalts (see Knutson & Brown, 1989: table 3.6.1).

Trace elements analyses (Table 7B) show the primary basalts ($Mg\#$ 0.77–0.67) have relatively higher Ni (160–550 ppm) and Cr (250–460 ppm) than more evolved basalts ($Mg\#$ <0.67; Ni 62–170 ppm, Cr 60–240 ppm). The highest Zr content (296 ppm) is found in evolved basalt which borders on hawaiite (SL63). Most of the more primitive alkali basalts have relatively low K/Ba (14.2–17.0), Rb/Sr (0.01–0.02), K/Nb (73–162) and Zr/Nb (0.97–2.25). However olivine-rich Yorkers Creek basalt (DR14639) shows higher K/Ba (28.5), while near-transitional Talbingo basalt (IG159) shows lower K/Ba (13.1) and higher Zr/Nb (3.82) than in the typical range. Two basalts are significantly different in trace element ratios to the mainstream basalts. Laurel Hill alkali basalt (DR13828) is significantly low in Nb (22 ppm), resulting in high Zr/Nb (7.73) and K/Nb (502)

and low Nb/Ta (3.1). Ruby Creek micro-dolerite (DR13822) is exceptionally low in Sr, Rb, Ba, Zr, Nb and light to middle REE, leading to markedly high Zr/Nb (24.0), K/Nb (400), K/Ba (49.8) and Rb/Sr (0.06) and noticeably low Zr/Hf (8.6), Nb/Ta (0.32), La/Yb (1.8) and Ce/Y (0.40).

Incompatible element patterns for the basalts are compared using multi-element plots, normalised to primitive mantle values (Fig. 8). Normalising values are taken from Sun & McDonough (1989) to allow direct comparison with such plots from other eastern Australian basalt fields (O'Reilly & Zhang, 1995). Primary Tumbarumba-Cabramurra basanites and alkali basalts show highly differentiated patterns with marked depletions in Rb, K, Hf, Y and some heavier REE and enrichments in Th, Nb, Ta, P and light to middle REE (Fig. 8a,b). This type of pattern is attributed to the presence of amphibole and apatite in mantle sources, with their components entering into Oceanic Island Basalt (OIB)-like melts (O'Reilly & Zhang, 1995).

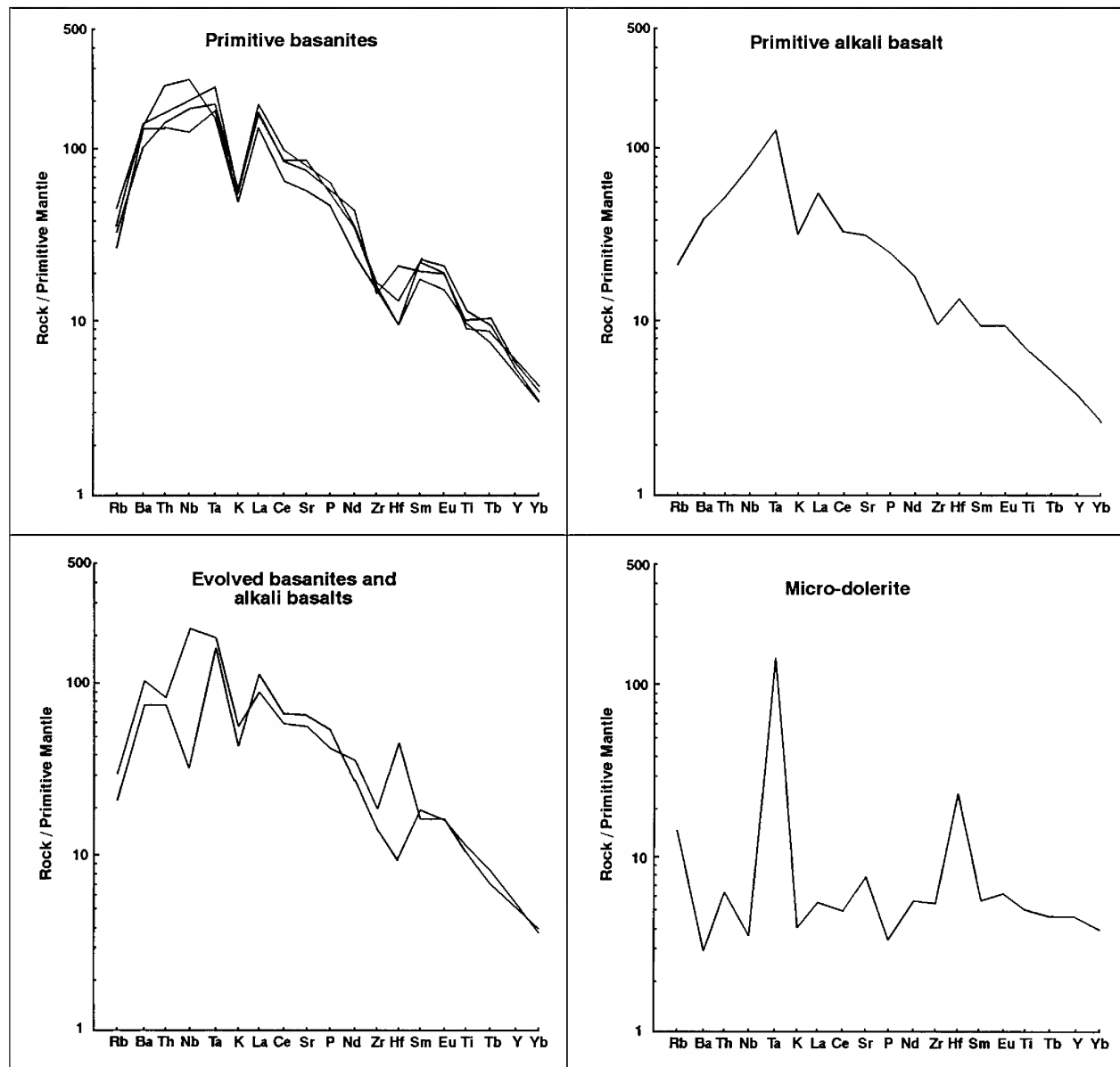


Figure 8. Normalised incompatible element plots, Tumbarumba basalts. a—primary-near primary basanites (DR13820, 13835, 14650, 14662); b—primary alkali basalt (DR14639); c—mildly evolved basanites and alkali basalt (DR13828, 14641); d—primary olivine micro-dolerite (DR13822).

Some variations in the patterns can be noted, e.g., for olivine-phyric alkali basalts (DR14639) and olivine and augite-phyric basanite (DR14650), where Hf is enriched relative to Zr. The evolved basanites and alkali basalts retain some characteristics of the more primitive patterns, but show additional variability (Fig. 8c). Jimmies Road basanite (DR14641) shows strong Hf enrichment and depletion in Th, while Laurel Hill alkali basalt (DR13828) shows marked Nb and Th depletion. The precise contributions of sources, fractionation and contamination in element variations in the alkaline lavas are uncertain, but all seem to carry strong imprints of amphibole (and apatite)-enriched sources and garnet-in residue partial melting.

Ruby Creek micro-dolerite (DR13822) exhibits a multi-element array that contrasts markedly with the other rocks (Fig. 8). It is strongly depleted in many incompatible elements such as Ba, Th, Nb, Zr, K and P and is enriched in a few elements, particularly Ta, Hf and to small extent Ba and Sr. This has high Mg# (0.71) and must derive from a very different garnet-free source to the amphibole-imprinted source for the other basalts. Basalts, with only limited trace element analyses (IG159, SL61, SL63) provide partial multi-element arrays that mostly conform to amphibole (apatite) source patterns, although relatively subdued in the Talbingo basalt (IG159).

Geochronology

Xenocrystic zircons in Tumbarumba basaltic corundum associations not only allow more complete dating beyond the radiometric basalt results, but also help to reinforce the basalt dating. Fission track dating of these basalt-released zircons provides “reset” ages corresponding to the eruptive event and has proved highly effective in establishing gemstone/basalt relationships in other eastern Australian fields (New England, Barrington, North Queensland; Sutherland *et al.*, 1993, 1999; Sutherland & Fanning, 2001). U-Pb isotope dating of these zircons and rare zircon inclusions in the sapphires helps to clarify sapphire/basalt melt formation, although precise mechanisms remain in contention (Coenraads *et al.*, 1990; Guo *et al.*, 1996a; Sutherland *et al.*, 1998a). Considerable K-Ar dating is already available for the basalts (21 dates; Young & McDougall, 1993) giving a solid framework to interpret the zircon dating, so that new basalt dating in this study was confined to isolated basalts of topographic interest.

Zircon fission track dating. Two zircon samples (Parsons Gully, Tumbarumba Creek) were dated by Geotrack International, Melbourne, using standard methods (Gleadow *et al.*, 1976; Green, 1981, 1985; Hurford & Green, 1983) and statistical smoothing and discrimination techniques (Galbraith, 1981, 1988). Dark red grains were selected from the Parson Gully sample and subsets of dark grains, pale grains and bright polished grains were selected from the Tumbarumba Creek sample.

The results (Table 3) suggest 3 or 4 possible pooled ages may be present within the zircon suites at the 1σ error level (26.0 ± 1.1 , 22.8 ± 0.9 , 23.6 ± 0.9 , 18.6 ± 1.2 Ma). However, the intermediate ages are within error and results at the 2σ level provide substantial overlap within error (26.0 ± 1.6 , 22.8 ± 1.3 , 23.6 ± 1.3 , 18.6 ± 1.7 Ma), so the age groups may not be separable. Nevertheless, the data shows a significant spread

in single grain fission track ages, so that the colour grouping may not accord strictly with age grouping. Therefore, the data was further analysed by a radial plot using statistical principles and methods outlined by Galbraith & Green (1990). The analysis (Geotrack Report #655, Australian Museum) gave estimated modal ages, with confidence limits (c.l.) for the following components.

- 1 26.6 Ma (29.3–24.2 95% c.l.); U 36–1070 (av. 311) ppm from 9 grains
- 2 21.6 Ma (23.4–19.8 95% c.l.); U 53–1433 (av. 510) ppm from 10 grains
- 3 15.6 Ma (19.0–12.8 95% c.l.); U 36–396 (av. 197) ppm from 6 grains
- 4 2.0 Ma (4.9–0.8 85% c.l.); U 95 ppm from 1 grain

The youngest age is represented by only a single grain and is not considered significant for the main “reset” zircon ages, as it may merely represent isolated local fire or lightning strike heating events. The three main episodes show some relative difference in av U contents, which reinforces the suggested age separations.

U-Pb isotope dating. This method investigated formation ages of zircon megacrysts and inclusions in sapphires in relation to the basaltic eruptions.

U-Pb zircon megacryst dating. A zircon megacryst from Parsons Gully (B2) was dated using a special treatment of the SHRIMP isotope data, needed to accommodate the geologically “young” age of these zircons (Coenraads *et al.*, 1990). The measured ^{207}Pb was used to estimate the proportion of non-radiogenic Pb present in the zircon. The resultant $^{206}\text{Pb}/^{238}\text{U}$ age (Table 4) when compared at 2σ uncertainty, (23.3 ± 1.7 Ma) lies within the 2σ error of fission track ages for similar zircons in the Parsons Gully—Tumbarumba Creek suites (26.0 ± 1.6 and 23.6 ± 1.3 Ma). The result implies zircon crystallisation was closely related in time to basaltic magmatic processes, assuming no Pb loss took place during heating from magmatic transportation.

U-Pb zircon in sapphire dating. SHRIMP analyses (based on techniques outlined in Sutherland & Fanning, 2001) for zircon inclusions in two Type 3 sapphires (C46, C63) are presented in Table 8. Six grains in C46 (U936–1578 ppm; Th 193–428 ppm; Th/U 0.18–0.46) gave an age range 392 ± 4 to 264 ± 3 Ma; this scatter in ages suggests these may represent inherited zircons from the Palaeozoic fold belt. Three grains in C63 also showed scatter in ages, 903 ± 10 to 22.6 ± 0.4 Ma, but each grain yielded coherent younger ages in the range 27.6 ± 0.3 to 22.6 ± 0.4 Ma. The younger results showed higher Th/U (0.73–1.74) than the older spread of ages (903–67 Ma; Th/U 0.34–0.64). The younger ages are geologically meaningful at the 2σ level (28 ± 0.4 – 23 ± 0.6 Ma) falling within the eruptive age range of zircon megacrysts and basalts from the region (28–16 Ma) and the older scattered ages may indicate inherited zircon within these grains.

Basalt K-Ar dating. Two basalts were dated in this study, using conventional K-Ar dating techniques (AMDEL Laboratories, Adelaide; CSIRO Laboratories, Sydney). One basalt (DR14641) represents an isolated high level flow cap on Jimmies Hill (1340 masl); the other (DR13822) an isolated plug in Ruby Creek (950 masl).

Table 8. Summary of SHRIMP U-Pb zircon results for Tumbarumba sapphires.

sample no. grain · spot	$^{204}\text{Pb}/^{206}\text{Pb}$	$f_{^{206}}$	$f_{^{206}}\%$	total $^{238}\text{U}/^{206}\text{Pb}$	\pm	total $^{207}\text{Pb}/^{206}\text{Pb}$	\pm	radiogenic $^{206}\text{Pb}/^{238}\text{U}$	\pm	age (Ma) $^{206}\text{Pb}/^{238}\text{U}$	\pm
C46											
1 · 1	0.000041	1.15E-02	1.15	19.96	0.240	0.0619	0.0007	0.0495	0.0006	311.6	3.7
2 · 1	0.000014	5.03E03	0.50	15.88	0.179	0.0588	0.0004	0.0627	0.0007	391.7	4.3
3 · 1	0.000100	1.77E-03	0.18	22.16	0.328	0.0535	0.0005	0.0451	0.0007	284.0	4.1
4 · 1	0.000015	2.61E-03	0.26	23.84	0.262	0.0537	0.0004	0.0418	0.0005	264.2	2.9
5 · 1	0.000010	0.00216	0.22	23.09	0.261	0.0536	0.0005	0.0432	0.0005	272.7	3.0
C63											
1 · 1	0.000835	1.35E-02	1.35	230.10	2.747	0.0572	0.0011	0.0043	0.0001	27.6	0.3
1 · 2	0.001057	1.01E-02	1.01	275.60	3.941	0.0544	0.0020	0.0036	0.0001	23.1	0.3
1 · 3	0.000040	0.00589	0.59	7.08	0.086	0.0723	0.0005	0.1404	0.0017	846.7	9.7
2 · 1	0.003739	0.0923	8.23	87.58	1.134	0.1124	0.0014	0.0105	0.0001	67.2	0.9
2 · 2	0.000567	0.00806	0.81	279.98	3.621	0.0529	0.0017	0.0035	0.0001	22.8	0.3
3 · 1	0.001894	0.01531	1.53	280.33	4.887	0.0586	0.0038	0.0035	0.0001	22.6	0.4
3 · 2	0.000011	1.26E-03	<0.01	6.66	0.080	0.0677	0.0004	0.1503	0.0018	902.7	10.2

Uncertainties given at the one σ level. $f_{^{206}}$ % denotes the percentage of ^{206}Pb that is common Pb

Correction for common Pb made using the measured $^{238}\text{U}/^{206}\text{Pb}$ and ^{207}Pb ratios following Tera & Wasserburg (1972) as outlined in Compston *et al.* (1992). **U, Th, Pb* contents (ppm)** (* = total radiogenic Pb).

C46: 1.1 U 936, Th 428, Th/U 0.48, Pb 34; 2.1 U 1048, Th 193, Th/U 0.18, Pb 49; 3.1 U 1191, Th 353, Th/U 0.30, Pb 40; 4.1 U 1081, Th 320, Th/U 0.30, Pb 33; 5.1 U 1139, Th 409, Th/U 0.36, Pb 37.

C63: 1.1 U 1454, Th 1227, Th/U 0.84, Pb 6; 1.2 U 861, Th 627, Th/U 0.73, Pb 3; 1.3 U 623, Th 212, Th/U 0.34, Pb 71; 2.1 U 867, Th 552, Th/U 0.64, Pb 7; 2.2 U 812, Th 1219, Th/U 1.50, Pb 3; 3.1 U 301, Th 524, Th/U 1.74, Pb 1; 3.2 U 573, Th 230, Th/U 0.40, Pb 72.

The results (Table 9) show that:

- 1 Jimmies Hill basalt at 23.7 ± 0.3 (2σ) Ma is the oldest dated Cainozoic lava and the related Bago Range basalt high point is the oldest preserved eruptive lava sequence.
- 2 The Ruby Creek olivine-microlite at 397 ± 9.5 (2σ) Ma is unrelated to the gemfield basalts, but is linked to the plagioclase-bearing intrusions of the Devonian ophiolitic belts (Graham *et al.*, 1996, 1998).

Discussion

The Tumbarumba basaltic gem field is notable for a diverse range of corundums, including ruby. However, good gem quality sapphires are scarce, while ruby is rare (Curran 1897; MacNevin & Holmes 1980; this study). Thus the field does not favour commercial prospects. Nevertheless, the corundum (and associated zircons) studied here have considerable scientific significance for the origin of these gem minerals in a wider context.

Corundum types. Tumbarumba corundums show a wide-range in colour, crystal and growth characteristics (Group 1–9). Colour combinations, inclusion mineralogy and chemical fingerprints demonstrate that many of these groups correspond to bimodal magmatic and metamorphic groups identified in some basalt fields (Barrington, West Pailin; Sutherland *et al.*, 1998c). Groups 1–5, in particular, show blue, green and yellow colour zoning, syngenetic inclusions (ferrocolumbite), trace element ratios ($\text{Cr}_2\text{O}_3/\text{Ga}_2\text{O}_3 < 1$) and related colour absorption spectra that typify BGY magmatic-origin corundums (Type 1 corundums). Groups 8–9, equally clearly, show the pastel colour range and passage through pink into red colours, with higher $\text{Cr}_2\text{O}_3/\text{Ga}_2\text{O}_3 (> 1)$ and

colour absorption spectra that typify metamorphic-origin corundums (Type 4–5 corundums). Tumbarumba metamorphic corundums, however, only partially overlap into the Barrington metamorphic field. The pale blue to mauve-pink colour range extends into lower $\text{Cr}_2\text{O}_3/\text{Ga}_2\text{O}_3$ and $\text{Fe}_2\text{O}_3/\text{TiO}_2$ ratios (Type 4 corundums). This type also shows more obvious colour zoning than Barrington examples. In fragments they can resemble outer parts of “agate” sapphires, but lack the intense blue cores found in those magmatic types. The strong pink, purple red, red range within the Tumbarumba metamorphic suite overlaps the Barrington field and shows higher Cr and Cr-controlled colour absorption spectra (Type 5 corundums). Tumbarumba ruby, however, extends into purer Cr, Fe-poor absorption spectra than observed at Barrington.

Overall, Tumbarumba corundum suites are not sharply bimodal, as they include suites (Groups 6 and 7) with intermediate trace element and colour absorption characteristics that smear the picture (15%). These intermediate groups include the BGY-like, “trapiche” exsolution (Type 2) sapphires, the vari-coloured diffuse zoned, well-crystallised (Type 3) sapphires and pale blue (Type 4) sapphires.

Corundum crystallisation. The predominant magmatic BGY sapphires have differing interpretations for their formation in the literature, but two main models include:

- 1 Crystallisation through a hybrid meeting of carbonatitic and silicic melts at mid-crustal levels and $T \sim 400^\circ\text{C}$ (Guo *et al.*, 1996a).
- 2 Crystallisation in syenitic melts generated under deeper crustal to shallow mantle conditions at $T \sim 680$ – 900°C , in the presence of hydrous phases such as amphiboles and mica (Australia, Sutherland *et al.*, 1998a; Scotland, Upton *et al.*, 1999). Such melt

compositions which would calculate normative corundum and zircon are designated as salic compositions (Le Maitre, 1989).

Some points against shallow level carbonatite-silicic melt mixing as a general process for BGY corundum formation are:

- i lack of syngenetic mineral inclusions such as carbonates that would reflect carbonatitic input.
- ii presence of Nb-bearing syngenetic mineral inclusions (ferrocolumbite, uranopyrochlore), which although found in carbonatites have compositional fields that more closely match these minerals in more silicic parageneses.
- iii finds of corundum-bearing xenoliths in basalts (Australia, Scotland) that have syenitic character.
- iv oxygen isotope values for corundums and associated minerals (Scotland) that suggest crystallisation in a magmatic reservoir at 800°C and which preclude an origin in crustal lithologies such as meta-sedimentary and evolved high level magmatic bodies.
- v corundum crystallisation in syenites (Scotland), which may involve fugitive loss of alkalis and carbonatitic residues from salic melts, rather than direct carbonatitic-silicic magmatic intermingling.
- vi general lack of silicic melts associated with eastern Australian basaltic gemfields.

Tumbarumba BGY magmatic sapphires (Type 1) conform with a salic paragenesis in the composition of observed inclusions (ferrocolumbite) and lack of carbonate inclusions expected for carbonatitic or some metamorphic/metasomatic paragenesis. The corundum, zircon, amphibole, feldspar megacryst assemblage in the Ruby Creek basalt also gives circumstantial support for an amphibole-related syenitic association. Some BGY sapphires show change in their crystallisation features during or after growth. Deep blue cores in many "agate-like" sapphires mark an early growth, probably at higher temperatures when corundum can accommodate greater Fe contents (Upton *et al.*, 1999). Intense blue colours were considered to largely mark Fe^{2+} -O- Fe^{3+} super-exchange rather than Fe^{2+} -O- Ti^{4+} charge transfer effects (Matson & Rossman, 1988; Upton *et al.*, 1999). However, this current and other studies indicate Fe^{2+} - Ti^{4+} charge transfer effects are comparable to or even higher in their intensity in Tumbarumba and other sapphire suites (see also Schwarz *et al.*, 2000). The outer "agate"-like milky and light blue growth zones indicate later Fe-depleted oscillatory crystallisation of corundum, due to changes in temperature, pressure, chemical composition or reduction-oxidation effects.

Metamorphic-type Tumbarumba corundums (Types 4 and 5) resemble the Barrington fancy coloured sapphire-ruby suite in some general crystal characteristics. However they lack abundant co-existing mineral phases to better define their parental association and only partially overlap the Barrington metamorphic geochemistry (Figs. 3, 5). Barrington metamorphic corundums crystallised at 780–940°C (based on sapphirine-spinel geothermometry; Sutherland & Coenraads, 1996) and similar temperatures may apply at Tumbarumba. The trace element differences, however preclude any definite correlation and their crystallisation at Tumbarumba involved a chemistry more

depleted in Fe relative to Ti and slightly depleted in Cr relative to Ga. The light blue (Type 4) sapphires plot separately to the pink-red (Type 5) corundums in chemical variation diagrams (Figs. 3, 5) suggesting different metamorphic parameters for their origins. Type 4 sapphires, in fact, plot within the field for metasomatic sapphires from Madagascar (Schwarz *et al.*, 2000), which raises the possibility for a metasomatic-metamorphic origin.

The enigmatic vari-coloured Tumbarumba intermediate sapphires (Type 3) pose problems for genetic origin. Their Fe, Ti and Ga ranges match "magmatic" sapphires, but Cr is unusually high for such sapphires. Consequently, their absorption spectra show prominent Cr^{3+} - Fe^{2+} - Ti^{4+} absorption.

- 1 They may be magmatic in origin, but represent special types associated with Cr-enriched melts (hence higher Cr/Ga). Growth banding typical in magmatic types (Type 1) may not be a completely reliable criterion at Tumbarumba in assigning origin, as it also appears within an apparent metamorphic type (Type 4). Cr-bearing serpentinites near Tumbarumba provide a potential Cr-enriching interactor at depth.
- 2 They may be metamorphic in origin, but represent special metasomatic types associated with Ga-enriched fluids (hence lower Cr/Ga). Such metasomatic corundums occur in some skarn deposits (Schwarz *et al.*, 1996). The presence of granitic intrusions, massive limestones and skarns in the Silurian sequence east of the Gilmore Suture provides potential support for such metasomatic processes near Tumbarumba. However, known exposures seem geographically separated from the gem field, unless the sequences extend westward below the serpentinite belt bounding the field.

Relatively high Ga can occur in metasomatic sapphires (Schwarz *et al.*, 1996) but these show lower Fe and Cr contents and their inclusions are more in line with metamorphic corundums (e.g., calcite, phlogopite/biotite, apatite). Magmatic crystallisation from evolving salic melts that interacted with a Cr-bearing source (serpentinite?) seems the most likely origin for this unusual type.

The trapiche-like sapphires (Type 2) exhibit pronounced exsolution due to cooling after crystal growth. Zones of silk radiate from central cores cutting across earlier growth zones and intersect prism faces in hexagonal sections. These sapphires differ from trapiche sapphires described by Schmetzler *et al.* (1996), where the radial arms contain phlogopite inclusions rather than exsolved rutile-hematite inclusions, and also differ from trapiche rubies, which form by a change in growth mechanism (Sunagawa *et al.*, 1999). The Tumbarumba examples resemble trapiche-like sapphires found elsewhere in eastern Australia (Sweeny, 1996; Neville & Gnielinski, 1998; authors' observations) and in Scotland (Upton *et al.*, 1999), where zones intersect second order prism faces {1120}. $\text{Cr}_2\text{O}_3/\text{Ga}_2\text{O}_3$ ratios are mostly higher (except for CORTUM 58) than is typical for BGY corundums, requiring explanation. Trace element contents determined largely on clearer zones away from the heavily included silk zones would sample corundum from which Fe and Ti had migrated into the crystal-controlled exsolution zones. Gallium, with stable trivalent

Table 9. Summary new whole rock K-Ar dating, Tumbarumba-Cabramurra basalts.

sample number	Status	Ref.	%K#	$^{40}\text{Ar}^*(\times 10^{-10} \text{ moles/g})$	$^{40}\text{Ar}^*/^{40}\text{Ar}_{\text{total}}$	age $\pm 1\sigma$
DR14641	A	1	1.51	0.62433	08.894	23.7 \pm 0.2
DR13822	A	2	0.11	0.84825	0.5985	397.4 \pm 6.7

DR14641 Basanite, Jimmies Road, Granite Mountain (35°43.5'S 148°12.3'E)

DR13822 Olivine micro-dolerite, Ruby Creek (35°49.4'S 148°11.5'E)

Status A: potassium-bearing phases are fresh. Ref. 1—AMDEL laboratories, A. Webb analyst. Ref. 2—CSIRO Division of Petroleum Research, H. Zwingmann analyst. # mean K value used in age calculations. * denotes radiogenic ^{40}Ar . Age in Ma with error limits given for the analytical certainly at one standard deviation.

Constants: $^{40}\text{K} = 0.01167$ atom%; $\lambda\beta = 4.962 \times 10^{-10} \text{ y}^{-1}$; $\lambda\varepsilon = 0.581 \times 10^{-10} \text{ y}^{-1}$

valency would probably follow Fe^{3+} into hematite, as supported by trace element data from Ambondromifehy, Madagascar magmatic sapphires where Fe and Ga show positive correlation with each other (Schwarz *et al.*, 2000). This would alter trace-element values in the residual zones. Alternatively, the trapiche-like structure typifying Type 2 corundums may be a composite phenomenon that developed in both Type 1 and Type 3 corundums, so that some corundums would range into higher Cr_2O_3 (CaO 0.03 wt%, CORTUM 15) and V_2O_3 (Ca 0.015 wt% V_2O_3 , CORTUM 19) contents. This alternative would suggest closely linked paragenesis for Type 1 and Type 3 corundums.

Zircon types. Tumbarumba zircons range from pale, anhedral low-U types into better crystallised types that show higher U contents. This is typical of zircon megacrysts from eastern Australian basalt fields, which exhibit wide variations in crystal and chemical features (Hollis & Sutherland, 1985; Robertson & Sutherland, 1992; Worden *et al.*, 1996; Sutherland, 1996; Sutherland & Fanning, 2001). The Tumbarumba zircons however, are notable for {110}-{100} prism combinations, a relatively rare feature in eastern Australian suites. This combination is common in Boat Harbour, Tasmania, zircons, but sapphire is relatively rare there. It also appears in a distinctive zircon suite within the Barrington, NSW, gemfield, but this suite is restricted in its abundance, geographical and temporal range compared to the other zircon suites in that field (Sutherland & Fanning, 2001).

Zircon crystallisation. The U-Pb isotope dating on a Tumbarumba zircon indicates crystallisation was probably related to basaltic magmatism. However, the strong resorption of megacrysts suggests this crystallisation was unrelated to the carrier basaltic melts. Zircon can crystallise in some mafic melts (SiO_2 48–60 wt%) and these zircons typically have high Th/U (up to 2.3; Heaman *et al.*, 1990). Tumbarumba zircons extend to high Th/U (3.47, Table 4), but inclusion studies on zircon megacrysts from elsewhere in Australia favour involvement of evolved salic melts similar to melts associated with corundum crystallisation (Coenraads, 1992). This is consistent with zircon (\pm corundum)—bearing syenitic xenoliths found in basalts elsewhere (Scotland, Upton *et al.*, 1999). The Tumbarumba zircons would develop in salic melts, where Zr-saturation was maintained essentially under non-peralkaline, metaluminous conditions (Watson, 1979; Linthout, 1984).

The morphology developed by Tumbarumba zircons would reflect a variety of factors including temperatures, melt composition and volatile content (see Speer, 1982). The {100} prism forms found in Tumbarumba zircons were initially equated with higher temperature, less evolved melts, with lower U, Th (Pupin & Turco, 1974; Pupin, 1980). However, later studies of zircon crystallisation showed that more complex interactions determined the final morphology of crystal growth. The relative growth of {100} and {110} prism forms are mainly controlled by zircon-supersaturation of the melt and may vary during zircon growth due to cooling effects (Vavra, 1990). In contrast, growth of steep pyramidal {211} forms are damped by adsorption of incompatible elements. The restrained presence of this form among Tumbarumba crystals suggests host melts with moderately high to high incompatible element concentrations.

The development of {100} and {110} prism combinations found at Tumbarumba may also reflect growth blocking, from U, Th adsorption and substitution of Zr^{4+} and Si^{4+} by Y (REE) $^{3+}$ + P^{5+} , favouring {110} expression (Benisek & Finger, 1993). Adsorption effects may also further control pyramidal forms, with {110} forms being adsorption-sensitive relative to {121} growth and {100} growth being favoured due to adsorption of H_2O inhibiting growth of {110} forms (Vavra, 1994). In contrast, {100} prism development depends largely on cooling rates.

Considering the multiplicity of factors involved in developing zircon crystal forms, only general characteristics of the Tumbarumba host melts can be construed here. The preponderance of {110} prism forms among the combined prism forms favours melts with high zircon-saturation and incompatible element levels, particularly enriched in U, Th relative to Zr. Development of {100} prisms and ditetragonal {311} pyramids among crystals suggest some melts involved lower zircon-saturation and incompatible element contents. The general absence of {100} prisms suggest crystallisation under slow cooling rates. These suppositions depict highly alkaline felsic melts evolving under late-stage, slowly cooling conditions. The Tumbarumba zircons converge in some features towards those of zircon inclusions found in Australian sapphires, which have dominant {110} prism forms and strong enrichments in elements such as U, Th, Hf and REE (Guo *et al.*, 1996a,b; Sutherland *et al.*, 1998a). Zircon megacrysts in eastern Australia with similar morphologies to Tumbarumba zircons (Boat Harbour, Barrington) contain 0.7–1.1 wt% Hf (Sutherland, 1996; Sutherland *et al.*, 1998a). This matches

the range for zircon found in syenitic xenoliths that lack corundum (0.6–1.1 wt% Hf, Scotland; Hinton & Upton, 1991). In comparison, zircons found in corundum-bearing xenoliths (Scotland, Thailand) contain 1.3–3.0 wt% Hf (Hinton & Upton, 1991; Sutherland *et al.*, 1998a). Thus, the zircon-crystallising melts at Tumbarumba were evolving towards corundum-crystallising conditions.

Distribution of gemstones. Zircons and corundums concentrate in relatively restricted sections of drainages descending through the basaltic infillings around Tumbarumba. Of eight main palaeochannels reconstructed under the eastern basalts (Fig. 7), the main gem deposits are confined to only three palaeochannels. The greatest concentrations were found in the present upper Buddong, Ruby Creek and Tumbarumba Creek drainage.

Gemstone delivery. Zircon fission track dating indicates gemstones were introduced early in the eruptive cycle (26 Ma), before substantial basaltic flows infilled the leads (19–24 Ma). However multiple deliveries (15–23 Ma) were interspersed with and followed the basaltic infilling. The time-space pattern of delivery suggests local pyroclastic eruptions were important providers. This would yield patchy sources from which hardy gemstones would be easily winnowed and concentrated into local drainages. Some sources would become re-exposed much later, after erosional removal of sealing basalt covers. Many gemstones not only exhibit magmatic corrosion from their eruptive delivery, but show significant abrasion and fragmentation from alluvial processes. The wear on zircons matches alluvial travel equivalent to over 30 km based on research into zircons traced back to their originating points in Victorian drainages (J.D. Hollis data). This raises the possibility of gemstone travel into the area from more distant outside sources, such as the Cabramurra-Kiandra uplands. However, such degrees of abrasion could result equally from continued recycling into fresh channels following disruptions to and erosion of earlier deposits, which may also involve changes in drainage fall and hydraulic forces. Recycling material two or three times would produce equivalent wear and reduce actual transport distances to under 20–25 km, well within the perimeter of the main gem field.

The best preserved zircon crystals were found at Ruby Creek. This suggests a local source, especially as pyroclastic and volcaniclastic horizons occur in the area. However, gemstones are scarce in Paddy's River to the west, so the source was not extensive. Gemstones in a Buddong Creek tributary include strongly abraded “early age” zircons (26 Ma) and shed from a small basaltic lead. This suggests derivation from a source that lay towards Rutherford Ridge in the north part of the basalt field. Gemstone deposits appear in Tumbarumba Creek 4 km south of its headwaters towards Laurel Hill and suggest a flanking rather than a northerly source. One possibility is that the gemstones were reworked from the high level deep lead deposits exposed on the west side, but this lead held little sapphire when under active mining (Curran, 1897). Alternatively, the gemstones may derive from an eastern source from poorly exposed lead or pyroclastic deposits that now lack basalt cover. The palaeodrainage reconstruction (Fig. 7) allows potential input for a lead diverted into the Tumbarumba drainage from Rutherford Ridge, skirting around the Storm Lookout palaeohigh via a basalt remnant at Pilot Hill.

The upper Tumbarumba Creek palaeodrainage includes complex leads formed at different levels and probably represents separate ages of channel disposition. The gemstones concentrate in young, low-level Quaternary deposits and show considerable wear, except for the brightly polished youngest pale, low-U zircons (<19 Ma). These zircons suggest some late-stage eruptive input, possibly from the nearby Laurel Hill centre. They probably entered the drainage after its basaltic infilling and are unlikely to herald a significant corundum contribution. Gemstones are recorded within Tumbarumba lead deposits (23–21 Ma) much farther south near Tooma. Whether this material travelled 30–40 km downstream from the upper Tumbarumba sources, arrived into the lead from the Ruby Creek source, via the lower Paddy's Lead (20–25 km), or even entered the lead from a nearer source (e.g., Mannus Creek tributary lead; Young & McDougall, 1993) is uncertain on present information.

Basalt petrogenesis. Basalts in the Snowy Mountain fields largely represent undersaturated, near-primary magmas based on Mg# and compatible element contents. Similar petrological ranges appear in some other southeastern Australian basaltic gemfields (Oberon, Barrington, Kandos, NSW; Weldborough, Tasmania), although some fields contain more olivine nephelinites (Morris, 1986; Sutherland *et al.*, 1989; O'Reilly & Zhang, 1995; Sutherland & Fanning, 2001). Other larger, or more diversely aged basaltic gemfields than the Snowy field (eastern Central Province, Southern Highlands, NSW; Hoy, Qld.) include a wider range of more evolved alkali to transitional basalts (Stephenson, 1989; Sutherland *et al.*, 1993; Coenraads, 1994; O'Reilly & Zhang, 1995). Primary and near-primary basanites and alkali to transitional olivine basalts dominate the Snowy basalts (over 70% of basalts analysed here compared to <20% at Oberon). Primary basanites, alkali and transitional basalts, as in the Snowy examples, represent a range in degrees of partial melting in mantle sources. Estimates based on complete partitioning of K₂O or P₂O₅ from the source into the melt (see Morris, 1986) are not used here due to uncertainties introduced by later work (Sun & McDonough, 1989; O'Reilly & Zhang, 1995) on precise modelling of mantle compositions, abundances of various elements and magmatic processes. However, they probably fall within the range of partial melting determined for similar melts elsewhere using incompatible element enrichment factors (basanite 4–6%, alkali basalts 6–11%, transitional basalts 7–12%; Beccaluva *et al.*, 1998; Zou *et al.*, 2000).

The primary basanites (13835, 14650, 13820, 14662) show high light REE to heavy REE ratios (La/Yb_N 34–46, using chondrite normalising factors after Sun & McDonough, 1989). This, and their high Ce/Y_N ratios (13–18) indicate melts derived from garnet peridotite mantle, with heavy REE and Y being retained in residual garnet. Similar ratios (La/Yb_N 26–39) were noted for alkaline melts generated from garnet lherzolite mantle (Beccaluva *et al.*, 1998) and these were significantly higher than ratios for melts derived from overlying spinel lherzolite mantle (La/Yb_N 3–24). Slightly evolved basanite (14641) and alkali basalt (13828) also show relatively high La/Yb_N (24–33) compatible with incomplete melting of a garnet peridotite source. In contrast, primary alkali basalt (14369) shows significantly lower La/Yb_N (21) and Ce/Y_N (8) and probably represents more complete garnet melting or perhaps even melting of spinel

peridotite mantle (alkali basalts, La/Yb_N 11–18; Beccaluva *et al.*, 1998).

Accessory mantle phases (amphibole, mica, apatite) influence incompatible element profiles of basaltic melts. Tumbarumba basalts show low $\text{K}_2\text{O}/\text{Na}_2\text{O}$ ratios (0.34–0.47) and low Rb/Sr (0.009–0.022) signifying titanian amphibole was a major donor over titanian mica to the alkali element budget in the melts (Wilkinson & Le Maitre, 1987). This is compatible with relative xenocryst abundance in the Ruby Creek basalt (kaersutite > apatite > mica). Titanian amphibole enrichment within the garnet peridotite source for Tumbarumba primary melts feeds into their high Ti/V ratios (64–75) which match ratios for mantle kaersutites (Ti/V 61–90; Wass, 1980). Alkali basalt (14639) sourced from garnet-poor mantle, however, shows lower Ti/V (54) indicating some amphibole depletion. An amphibole (+ apatite) imprint (depleted Rb, K, Zr and enriched Th, Nb, Ta, La and high P; O'Reilly & Zhang, 1995) typifies most of the basalts suggesting extensive amphibole in the underlying mantle. The lower Ba/Sr over Ba ratios (av. 0.00008) for Tumbarumba basalts compared to some other fields (e.g., Oberon, av. 0.00096) supports amphibole dominance over phlogopite as a main additional phase. This is also compatible with moderate Ba and Sr (cf Ba and Sr contents in vein amphibole and phlogopite in garnet lherzolite; Ionov & Hofmann, 1995) and high Ta and Nb enrichment and high light (La, Ce) and middle (Eu) REE enrichment over heavy REE, typical in amphibole-bearing mantle peridotites (McDonough & Frey, 1987; O'Reilly & Zhang, 1995; Eggins *et al.*, 1998). The amphibole imprint is less clear in some transitional olivine-basalts, probably due to dilution through higher degrees of partial melting of the source or even amphibole depletion by earlier melting in the source. Relative Nb depletion in one alkali basalt (13828) is anomalous, but this partly evolved, internally segregated rock incorporates a feldspathic, presumably Nb-poor, residue within its make up.

Primary olivine basalt (13822) differs markedly in its incompatible element pattern to other Tumbarumba patterns in its extremely flat light to heavy REE profile and very low La/Yb_N (1) and Ce/Y_N (1) values. Melting of spinel peridotite is favoured over an unusual garnet-free mantle assemblage. The rock is extremely low in $\text{K}_2\text{O}/\text{Na}_2\text{O}$ (0.05), moderately high in Rb/Sr (0.056) and low in Ti/V (29) suggesting a source impoverished in both amphibole and mica. The mantle-normalised incompatible element pattern is typical of enriched Mid-Ocean Ridge Basalt (MORB), with relatively flat profile, particularly if the variations in Ta and Hf ratios are often introduced in the analytical process (Sun & McDonough, 1989).

High Mg# alkaline melts with amphibole/apatite imprints, as in the Snowy lavas, were recently described elsewhere in eastern Australia as having HIMU-like trace element arrays (Barrington, NSW; Cooktown, Qld; Zhang *et al.*, 2001). These melts were attributed to lithospheric sources rather than asthenospheric sources of true HIMU (high radiogenic lead component) melts which show elevated $^{206}\text{Pb}/^{204}\text{Pb}$ isotope ratios. However, Snowy primary melts have key element ratios (Zr/Nb 1.0–2.3, La/Nb 0.69–1.38, Ba/Nb 4.9–10.6, Ba/Th 53–81, Rb/Nb 0.13–0.25, K/Nb 73–162, Ba/La 7.1–8.3) that show minimal overlap with values for Tasmanian-Southern Ocean HIMU-related basalts (Zr/Nb 3.1–4.6, La/Nb 0.54–0.62, Ba/Nb 5.0–7.2, Ba/Th 64–99, Rb/Nb 0.32–0.72,

K/Nb 111–261, Ba/La 9.3–12.6; Lanyon *et al.*, 1993). The Snowy melts resemble Barrington amphibole/apatite signature melts in these ratios (Sutherland & Fanning, 2001) suggesting HIMU-like is an inappropriate term for them.

Partial melting calculation. In order to refine a melting model for the Tumbarumba basalts, quantitative partial melting calculations were undertaken, using two methods: (a) major element mass balance; and (b) incompatible element modelling. Both methods require the estimation of primary magma compositions. Major element compositions of primary magmas were adjusted by mass balance mixing calculations, in which theoretical compositions of Mg-rich olivine (Fo_{89}) and clinopyroxene ($\text{En}_{45.5}\text{Fs}_{5.5}\text{Wo}_{49}$) were added to Tumbarumba basalt analyses to allow for effects of fractional crystallisation. For each basalt, increasing quantities of the two minerals were “mixed in”, until the modelled magma composition was appropriate for equilibration with Fo_{89} during partial melting. In determining the equilibrium compositions, a widely used $K_{\text{Mg/Fe}^{2+}}^{\text{ol/liq}}$ value of 0.3 was applied, following Roeder & Emslie (1970). Weight percentages of ol+cpx fractionation predicted by the models vary between 7% and 20%. Incompatible element contents for the primary magmas were obtained by “reversing” the effects of modelled olivine and clinopyroxene fractionation, using partition coefficients from the literature, and the fractionation equations of Shaw (1970).

The calculation of degrees of partial melting by major element mass balance entails: creating mantle modes for potential bulk mantle and mineral compositions; repeating these calculations using a primary magma composition as an extra phase, in order to find the degree of partial melting; and then comparing the results of each experiment, i.e. mode and mode+melt, to obtain the melting proportion of each mineral in the melting process. Satisfactory mass balance solutions are those resulting in squared residuals of <1. Tables 10 and 11 list melting calculations for Tumbarumba primary magmas, based on six possible mantle mineralogies, namely garnet and spinel lherzolites±phlogopite±kaersutite. Low clinopyroxene contents (5.2–12.5 wt%) combined with low garnet contents (2.1–11.5 wt%) may reflect the presence of metasomatic phases. The most accurate melting models are probably those which produce degrees of melting of >2–3 wt%, and in the order: basanite < alkali olivine basalt < olivine basalt. For some mantle types and bulk compositions (garnet, garnet-phlogopite [b], and garnet-amphibole lherzolite [a, b]), these conditions fail whilst for other types, solutions were not found for some or all primary magma compositions (garnet-phlogopite [b], spinel-phlogopite, and spinel-amphibole lherzolite). Both spinel and spinel-amphibole lherzolites returned feasible solutions; although the former (anhydrous) mantle type is unlikely on the basis of trace element evidence (see below). On the basis of absolute and relative degrees of melting (Table 11), the most feasible source type is garnet-phlogopite lherzolite (a), based on bulk mantle and mineral compositions cited by Comin-Chiaromonti *et al.* (1997). However, no unequivocal evidence is provided by these calculations to discount other modal mineralogies in the source region(s) of the Tumbarumba basalts. In particular, spinel-amphibole lherzolite is still a possible source, although lacking solutions for several primary magmas. It is conceivable that the magmas involved input from both phlogopite- and kaersutite-bearing lherzolites.

Table 10. Modal mineralogy and melting proportions of mantle types.

mantle assemblage		Olivine	Opx	Cpx	Garnet	Spinel	Kaersutite	Phlogopite
Spinel lherzolite	mode	58.06	25.96	12.45		3.53		
	melt prop	0.33	7.64	72.90		19.13		
	SD	0.30	5.10	4.85		0.49		
Garnet lherzolite	mode	59.80	21.10	7.60	11.50			
	melt prop	0.21	7.59	29.64	62.56			
	SD	0.19	4.90	4.30	1.64			
Spinel amphibole lherzolite (a)	mode	59.27	24.90	8.68		2.14	5.02	
	melt prop	1.08	14.36	17.43		3.23	63.90	
	SD	1.16	5.62	5.87		2.71	8.21	
Garnet amphibole lherzolite (a)	mode	59.70	20.22	6.46	9.53		4.09	
	melt prop	3.74	14.36	28.92	43.23		3.74	
	SD	0.66	5.62	0.61	1.06		0.66	
Garnet amphibole lherzolite (b)	mode	65.66	24.23	3.47	2.18		4.47	
	melt prop	1.59	6.86	13.68	24.37		53.50	
	SD	1.06	2.05	2.53	4.66		3.62	
Spinel phlogopite lherzolite	mode	58.18	25.18	12.33		3.27		1.05
	melt prop	11.00	13.17	52.42		12.97		10.44
	SD	15.52	18.59	24.98		3.34		5.78
Garnet phlogopite lherzolite (a)	mode	60.29	16.94	9.78	5.98		7.00	
	melt prop	1.14	3.08	25.55	13.36		56.87	
	SD	0.75	6.37	9.68	18.90		31.05	
Garnet phlogopite lherzolite (b)	mode	65.35	22.36	5.23	5.65		1.42	
	melt prop	0.89	0.89	26.19	68.33		3.71	
	SD	0.58	0.58	3.22	4.89		4.82	

Modal mineralogy of each mantle type is calculated using major element mass balance and also given are the melting proportions (and their standard deviations) which produce the degrees of partial melting listed in Table 11. All values in wt%. All mineral compositions are from McKenzie & O'Nions (1991), except that for amphibole, which is an average value for kaersutite xenocrysts from this study and those used in models GAL (b) and GPL (b), which are from Comin-Chiaromonti *et al.* (1997). In most models, the bulk mantle composition used is that of the bulk Earth (McKenzie & O'Nions, 1991). The only exceptions are models GAP(b) and GPP(b), which are based on an analysis of a garnet-phlogopite xenolith (Comin-Chiaromonti *et al.*, 1997). Suffix (a) stands for mantle based on the bulk Earth composition given by McKenzie & O'Nions (1991); and (b) for mantle compositions based on a garnet-phlogopite lherzolite from Comin-Chiaromonti *et al.* (1997).

Table 11. Degrees of partial melting for Tumbarumba primary magma compositions.

sample	garnet lherzolite	garnet-amphibole lherzolite (a)	garnet-amphibole lherzolite (b)	garnet-phlogopite lherzolite (a)	garnet-phlogopite lherzolite (b)	garnet-phlogopite lherzolite (b)	spinel lherzolite	spinel-amphibole lherzolite
14639	6.60	3.00	4.20	2.81	7.79	8.13	6.82	
13835	5.10	2.99	1.97	6.27	5.92	6.74	6.12	
14650	5.60	0.50	1.95	—	5.45	7.28	—	
13820	5.57	1.55	2.72	3.85	5.04	7.10	—	
14662	5.30	1.16	2.86	—	5.58	6.94	6.34	
13828	5.49	1.85	4.62	4.97	6.66	7.01	9.59	
14641	4.65	1.21	1.71	4.05	5.87	6.23	7.79	
159	4.86	1.80	2.29	4.60	6.23	6.49	—	
61	6.02	1.24	4.73	4.13	6.35	7.46	3.95	
63	4.50	2.14	1.41	3.53	8.14	6.04	—	
averages								
basanite alkali basalt	5.37	1.44	2.66	4.57	5.70	6.96	6.05	
basalt	5.53	2.33	3.41	3.77	7.53	7.06	8.21	
olivine basalt	4.86	1.80	2.29	4.60	6.23	6.49	—	
average basalt	5.36	2.20	3.13	3.98	7.20	6.92	—	

14639 alkali basalt, 13835 basanite, 14650 basanite, 13820 basanite, 14662 basanite, 13828 alkali basalt, 14641 basanite, 159 olivine basalt, 61 basanite, 63 alkali olivine basalt.

Degrees of partial melting are calculated by major element mass balance (see Table 10). All values in wt%.

Degrees of partial melting were estimated by analysing variations in the concentration of incompatible elements during the melting process. Melting curves (Fig. 9) were created for various mantle types, using the batch melting equations of Shaw (1970). Bulk mantle compositions and partition coefficients were obtained from the literature (see Fig. 9 caption), while the modes and melting proportions used were those formulated by major element analysis. These melting curves may be compared to the trace element contents of modelled primary magmas, as follows:

La/Yb vs Yb. When creating the curves a typical “enriched” or “primitive” mantle composition (Sun & McDonough, 1989) could not provide La/Yb ratios for reasonable degrees of melting. Therefore, a second set of curves was created, based on the composition of a cryptically metasomatised mantle xenolith from southeastern Australia (O'Reilly & Griffin, 1988). The latter curves predict approximately 10% melting of garnet lherzolite, or 5–8% melting of garnet-phlogopite and/or garnet-amphibole lherzolite. They also allow input into some alkali basaltic magmas of a 1–2% melt of modally metasoma-

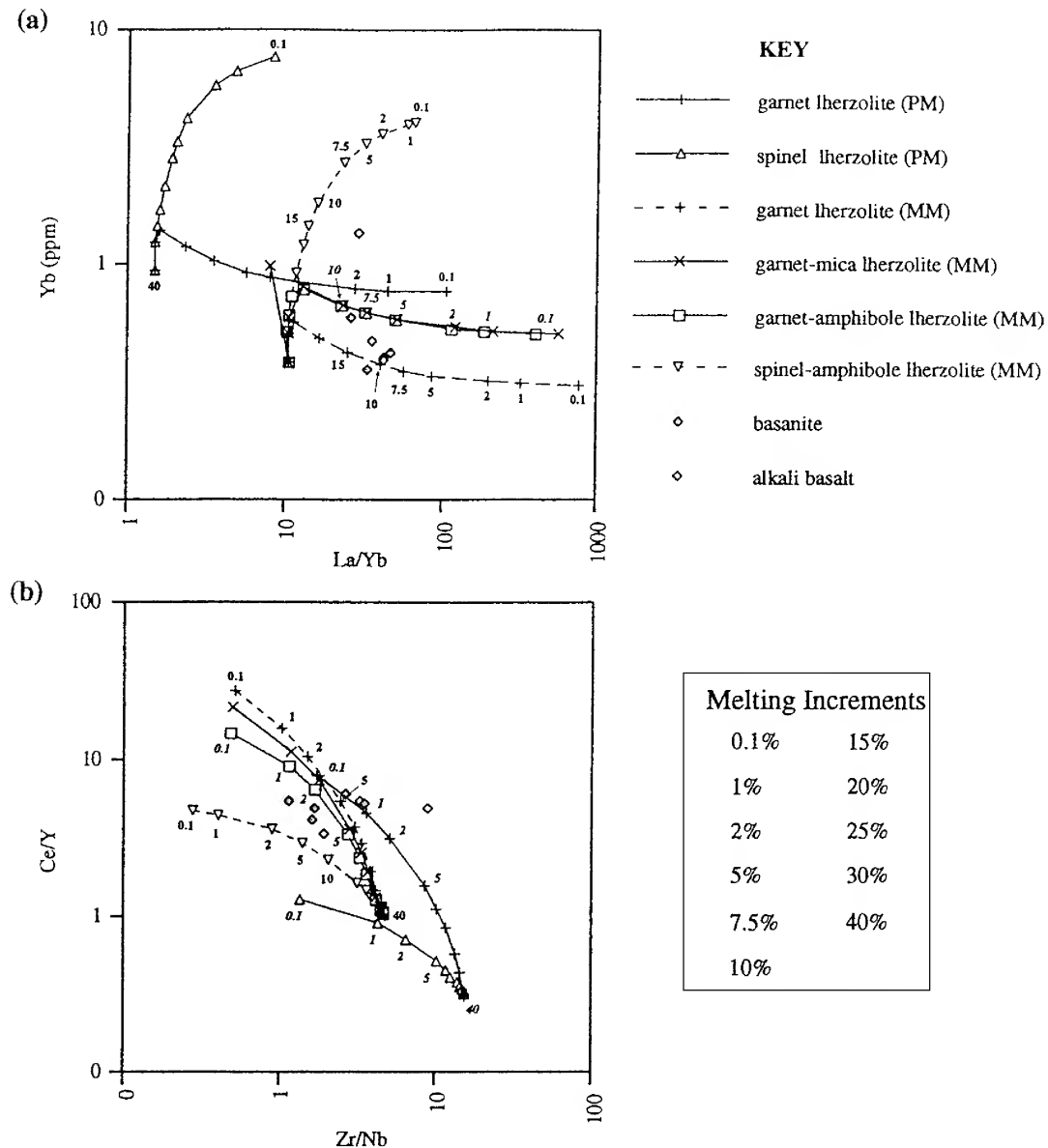


Figure 9. (a,b) Comparison between trace element concentrations in theoretical Tumbarumba primary magmas, and calculated curves for non-modal batch partial melting. See text for explanation. Each curve represents a different combination of mantle type and bulk trace element composition. PM = primitive mantle (Sun & McDonough, 1989); MM = metasomatised mantle (sample WGBM 15, O'Reilly & Griffin, 1988). Curve increments are listed in the Key, as well as being shown on the diagrams. The method for calculating trace element compositions of “primary” magmas is detailed in the text, with mineral/melt partition coefficients for olivine and cpx being obtained from: Ablay *et al.* (1998), Ewart & Chappell (1989), Kostopoulos & James (1992), McKenzie & O'Nions (1991), Nielsen (1998) and Panter *et al.* (1997). Source of partition coefficients used in the melting calculations are: all olivine, cpx, opx, garnet and spinel from Kostopoulos & James (1992), except for the REE (McKenzie & O'Nions 1991); all amphibole and kaersutite from Ionov *et al.* (1997), except REE for phlogopite (McKenzie & O'Nions, 1991).

tised spinel lherzolite. In general, basalts were produced by slightly higher degrees of melting than basanites.

Zr/Nb vs Ce/Y. These curves predict 3–7% melting of garnet lherzolite (metasomatised bulk composition), and/or 2–5% melting of modally metasomatised garnet lherzolite. Again they allow mixing with a 1–2% melt of metasomatised spinel lherzolite. The maximum degree of melting of garnet lherzolite based on the “primitive mantle” bulk composition is only 0.1–1%. Basanites are characterised by lower degrees of melting than alkali basalts.

These findings suggest the Tumbarumba source was dominated by cryptically and/or modally metasomatised, high LREE/HREE (HREE-poor) garnet lherzolite, with possible input of metasomatised spinel lherzolite. It is difficult to choose unequivocally between amphibole and mica as the main metasomatic phase; but on balance, based on the major element calculations, phlogopite seems the dominant phase. This, however, contradicts other evidence such as low Ba/Sr ratios, which suggests dominant amphibole. Again, this may mean the Tumbarumba magmas involved both phlogopite- and kaersutite-dominant mantle sources.

Comparison of the Tumbarumba primary magmas with experimental melts of hydrous mantle peridotites (Kushiro, 1990) permits estimation of the pressures and temperatures controlling partial melting, particularly using variations in the Si and Mg content of magmas (after Kushiro, 1990; Scarrow & Cox, 1995; Hoang & Flower, 1998; Allen, 1999). The results give the following average temperatures: basanite 1269°C; alkali basalt 1311°C; olivine basalt 1237°C. Average pressures/depths are: basanite 23.2 kb (75 km); alkali basalt 22.4 kb (73 km); olivine basalt 19.4 kb (64 km). These values indicate melting near the garnet–spinel transition (Sutherland *et al.*, 1998b) and the region where the “H₂O-undersaturated” solidus of Kushiro (1990) intersects the boundary of the phlogopite stability field (Hoang & Flower, 1998). They also suggest melting within or above the Low Velocity Zone in lithospheric mantle, which probably lies at >120 km below the Snowy region.

Evolution of Tumbarumba Gemfield. Dating of gem minerals and basalts suggests this gemfield mainly evolved over some 10 million years from Late Oligocene to Middle Miocene time (27–15 Ma).

Late Oligocene activity (27–24 Ma). Zircon and associated corundums were discharged explosively as xenocrysts in undersaturated volatile-rich basaltic melts. This activity centred in the northwest region. It followed initial low volume mantle melting, which crystallised zircon and corundum from evolved salic melts within the mantle/crust boundary. Two main potential mechanisms could generate magmatic zircon and corundum crystallisation under mantle conditions. One involves minor melting of amphibole (± garnet)-bearing mantle to provide relatively aluminous basaltic melts (Sutherland *et al.*, 1998a). These would fractionally crystallise, leaving residual liquids which then evolved towards salic compositions capable of crystallising zircon and corundum between 700–900°C and 0.7–1.1 Gpa. Alternatively, the salic melts formed with volatile fluxing and metasomatism of lithospheric mantle, yielding small fraction trachytic melts (Upton *et al.*, 1999). These evolved to peraluminous corundum-crystallising conditions,

between 700–970°C, perhaps involving fugitive alkali and carbonate loss.

The mantle-derived salic melts proposed here for crystallising Tumbarumba magmatic gemstones receive some support from alkaline, aluminous silica-rich glasses found in mantle xenoliths from basaltic fields, including eastern Australian examples. However, interpretation of these glasses has been a contentious subject. Some workers link them to melts derived from melting amphibole-bearing mantle (Schiano & Clocchiatti, 1994; O’Connor *et al.*, 1996). Others, however, equate them with mixing of introduced basaltic melts and siliceous melts produced by orthopyroxene reactions (Wilshire & McGuire, 1996; Neumann & Wulff-Pedersen, 1997), or with metasomatic reactions related to ephemeral alkali-rich carbonatites (Wiechert *et al.*, 1997; Coltorti *et al.*, 1999), or even with diffusion of sodium into partially molten peridotite (Lundstrom, 2000). Other workers consider they only represent localised *in situ* melting of mantle phases and were produced by high temperature (1010–1100°C) decompressive melting during rapid transport of xenoliths (Chazot *et al.*, 1996; Eggin *et al.*, 1998; Yaxley & Kamenetsky, 1999). Clearly a range of processes may be involved. Experimental work on more extreme silicic glass compositions (Draper & Green, 1997) suggested low degree melts of such compositions could co-exist and circulate within mantle assemblages, particularly harzburgitic mantle. However, phlogopite would be the main hydrous equilibrium phase, rather than amphibole, and this may not match Tumbarumba shallow mantle. Another study suggested that in eastern Australia carbonatitic melts produced amphibole, phlogopite and apatite metasomatism and this may release a fugitive alkaline, aluminous silicic melt (Yaxley *et al.*, 1998).

Several potential mechanisms thus exist for salic melt generation in the Tumbarumba mantle during initial Oligocene melting. A comparison of low-volume melt glasses in deeper garnet–spinel transitional peridotite (2.5 GPa) with those in shallower spinel peridotite (1 GPa) showed that at the lower pressure melts were more siliceous and alkaline in composition (Schiano *et al.*, 2000). On this basis, the salic gem-forming melts under Tumbarumba would probably crystallise in shallow spinel peridotite mantle at P < 1 GPa (i.e. <35 km depth).

Not all magmatic gemstone crystallisation at Tumbarumba need stem from the initial Late Oligocene melting. Low-volume melting conditions suitable for salic zircon and corundum formation may develop repeatedly around waxing and waning of episodic basaltic magmatism (Sutherland *et al.*, 1993; Sutherland *et al.*, 1998a; Sutherland & Fanning, 2001). Similarly, expulsion of the rarer metamorphic corundums and garnet could mark fortuitous intersections of basaltic magma with crustal metamorphic assemblages at any stage of eruptive activity.

The precursor mantle melting and explosive basaltic activity may have accompanied tectonic activity, which dammed and possibly reversed drainages, to give the sediments now preserved in deep leads (Gill & Sharp, 1957). This tectonism would follow conjectured faulting, tilting and downwarping proposed along the adjacent continental margin (Brown, 2000), which affects coastal basalts older than 28 Ma (Spry *et al.*, 1999). The timing of such tectonism, however, remains in debate (Young/Brown, 2000).

Early Miocene activity (24–18 Ma). Basaltic lava flow activity developed more fully after 24 Ma. Lavas emanating from the earlier regions of gem-bearing eruptions descended drainages flowing off the Granite Mountain palaeohigh, overtopping Paddy's palaeochannel and extending south to Tooma. Basanites and alkali basalts in these sequences indicate some 5–8% partial melting within the underlying metasomatised garnet peridotite mantle.

Lava flow activity became widespread across the Tumbarumba-Kiandra region by 22 Ma. This activity peaked, with near-saturated basalts being generated as degrees of partial melting in the mantle exceeded 10%. Melting rose into the overlying spinel peridotite mantle, with reduced imprints of amphibole and other hydrous phases. The rhyolitic tuff in the upper Tooma sequence (between 22.8–21.3 Ma) presents an enigmatic feature. It suggests local silicic activity, as the nearest known Early Miocene rhyolitic centres are minor bodies over 450 km north (Wingham; Sutherland, 1999), while larger central volcanoes lie over 600 km north (Nandewars, Tweed Shield; Duncan & McDougall, 1989).

Following this peak magmatism, western activity partly subsided, allowing an interlude of explosive gem-bearing activity, providing the second zircon fission track age peak (22–21 Ma). Further lava flow activity then topped up the Tumbarumba lead descending from Laurel Hill and western Paddy's lead to Tooma. Some eastern lava flow activity also took place, e.g., dyke and lower entrenched basanite flow, 8 km NE of Cabramurra. This later undersaturated magmatism marked relatively low degrees of partial mantle melting (around 4–6%).

Early-Middle Miocene activity (18–13 Ma). The late Tumbarumba magmatism seems to largely reflect explosive gemstone-bearing activity, marking the third zircon fission track age peak (16–15 Ma). This phase produced the magmatically polished and little abraded low U-zircons, which probably crystallised from less evolved alkaline melts. The unusual vari-coloured intermediate character corundums may belong here, as their more complete crystals suggest less re-working than for the other fragmentary corundum types. Minor alkaline melt pockets interacting with Cr-bearing wall rocks (serpentinite bodies?) may explain their origin, but their late development requires confirmatory age dating.

Overall synthesis (27–15 Ma). Some sapphires (Type 3) contain zircons with suspected inherited U-Pb ages (C46) which range up to the age of serpentinite bodies, suggesting formation later than, and possibly involving, those intrusions. Other sapphires (C63) contain zircons that provide ages comparable to the Miocene basaltic events and may indicate formation with that melting episode. Type 1 magmatic sapphires remain undated, lacking identified zircon. However, it is hoped to use the abundant ferrocolumbite inclusions as a dating technique in further investigations. Magmatic and metasomatic gemstone eruption (27–15 Ma) overlapped basaltic lava field magmatism (24–19 Ma). Lava fields, such as the Snowy field, have been equated to either sporadic diapiric mantle upwellings of OIB-related magmas, or to melting associated with long standing asthenospheric plumes (O'Reilly & Zhang, 1995; Zhang & O'Reilly, 1997; Sutherland, 1998). Distinction between short term mantle diapirs and longer term diapirs and

plumes is not always clear, as long term plume traces can exhibit discontinuous activity and involve both silicic central volcanoes and basalt lava fields (Sutherland, 1998; Sutherland & Fanning, 2001). If the Snowy field is plume-linked, then a migration in volcanism related to Australian plate motion should show up in adjacent lava fields.

During the Snowy field evolution, the Australian plate was moving northeasterly (0.63°/My from 30–20 Ma, 0.55°/My from 20–10 Ma; Sutherland, 1998). Comparison of the adjacent Snowy and Grabben Gullen basalt ages along this trend are shown in Figure 10. The Grabben Gullen basalt ages are adopted from Bishop *et al.* (1985), deleting the youngest ages which they discounted due to alteration effects. The ages suggest a shift between the two fields compatible with Australian motion (using an averaged 0.6°/My from 26–18 Ma). However Grabben Gullen dating is less complete than Snowy dating and lacks zircon fission track dating, while some uncertainties lie in Australia's precise plate motion because of differences in Indian and Pacific Ocean hotspot paths. Further testing of a mantle plume model needs to include the Oberon field, northeast of Grabben Gullen. However, only one basalt is dated there (18 Ma), although zircon fission track dating suggests activity extended beyond 27 Ma (F.L. Sutherland, unpublished data). Basalt fields with related migratory age are not obvious south of the Snowy field, so at best a migratory model would fit a short term (<20 Ma) mantle diapir. The thermal event peaked under Tumbarumba at 22 Ma, marked by maximum basalt generation and possible minor rhyolitic activity.

The post-eruptive evolution of the gemfield mainly reflects erosion. Since the Palaeogene, plateau surfaces, including the basaltic surfaces, were lowered by 2–5 m/My and major streams incised their courses by 5–18 m/My (max. 30 m/My), producing present profiles strikingly similar to pre-basaltic profile (Young & McDougall, 1993). The original gemstone deposits were eroded on exposure and now represent recycled heavy mineral concentrations in the recent drainage, within alluvial terraces and river beds.

Gemfield comparisons. Tumbarumba gemfield carries magmatically resorbed corundums and zircons that feature in many eastern Australian basaltic fields (Sutherland, 1996). Tumbarumba corundums, however show a particularly wide range of magmatic, metamorphic and metasomatic (?) types. Some of the sapphire types have unusual characteristics and there are two variants of ruby. This suite is more complex than other bimodal Australian suites (Barrington). Multi-modal suites are not confined to Tumbarumba, as similar intermediate character corundums also appear elsewhere (Swanbrook, New England, NSW; Myrniong, Victoria; Sutherland *et al.*, 1999) and large spreads in corundum characters are noted across some regions (Victoria—Birch & Henry, 1997).

Amphibole-endowed mantle features under several other basaltic gemfields besides Tumbarumba (e.g., New England—Wilkinson & Hensel, 1991; Barrington—Sutherland & Fanning, 2001). Such fields show closely similar incompatible element ranges and are summarised in Table 12. Other basaltic fields with minor gem deposits (e.g., Southern Highlands, Monaro) also include a proportion of basalts that indicate localised amphibole-mantle sources (O'Reilly & Zhang, 1995; Roach, 1999). Thus, ample titanian amphibole in mantle regions may be a

Table 12. Comparative key mantle-normalised incompatible element ranges, selected primary Na-rich basalts, eastern Australian sapphire fields.

basalt field no. analyses	Snowy ^a 6	Barrington ^b 10	Oberon ^c 7	New England ^d 3	Hoy, Qld ^e 3	NE Tas ^f 1
SiO ₂	43.1–46.2	41.4–46.5	43.2–45.7	44.0–44.7	42.0–44.9	44.6
MgO	9.3–16.8	9.0–12.3	8.8–12.9	8.0–9.5	9.6–12.4	8.7
K ₂ O/Na ₂ O	0.24–0.47	0.19–0.37	0.20–0.45	0.45–0.48	0.39–0.49	0.31
K _N	23–54	25–53	29–54	33–54	40–57	26
P _N	25–65	24–62	17–32	27–65	27–65	19
Zr _N	10–17	10–21	14–27	13–24	15–21	14
Nb _N	80–190	52–132	56–122	59–98	59–126	59
Rb _N	16–48	16–50	22–46	33–36	30–50	25
Th _N	59–141	35–188	—	24–71	24–94	30
Ta _N	122–220	49–195	—	—	—	—

^a this paper (4Bsn, 2AOB). ^b O'Reilly & Zhang (1995) and Sutherland & Fanning (2001) (3 Ne, 5Bsn, 2AOB). ^c Morris (1986) (5Bsn, 2AOB). ^d Coenraads (1994) (3AOB). ^e Sutherland & Robertson (unpublished data) (1Ne, 2AOB). ^f Sutherland *et al.* (1989) (1AOB). _N primitive mantle normalised values, based on Sun & McDonough (1989). Ne, Nepheline; Bsn, Basanite; AOB, Alkali Olivine Basalt.

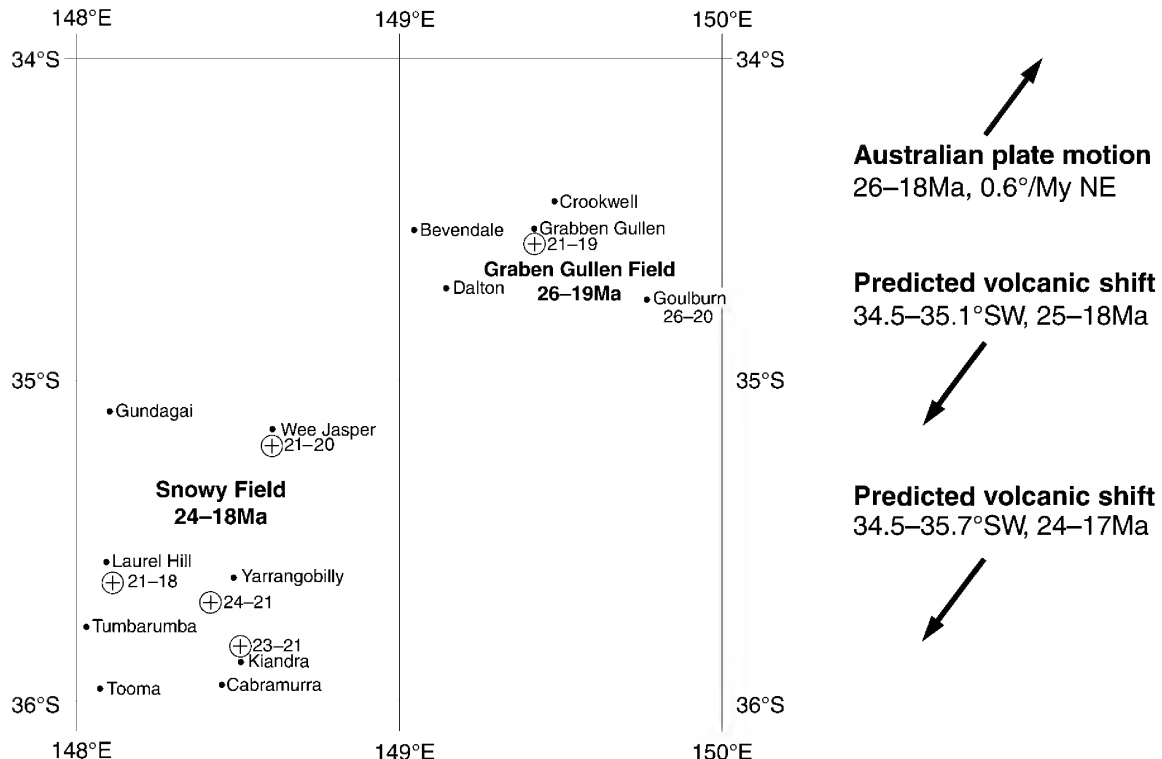


Figure 10. Comparative post-Eocene basalt ages, Southern Tablelands–Snowy Mountains region, New South Wales, Australia. Age data for Grabben Gullen field from Bishop *et al.* (1985) and for Snowy field from Wellman & McDougall (1974), Young & McDougall (1993) and this paper. The diagram sets out entries in approximate geographic relationship. \oplus indicates sapphire/zircon gemstone locality. Arrows indicate directions of plate motion and predicted volcanic shift.

factor in developing minor melts that crystallise zircon and corundum before mobile basaltic melts disrupt and carry up gem debris from their sources. Titanian mica may be more plentiful in some sources and contribute to the medium-K primary basalts found within several gemfields (Oberon—Morris, 1986; New England—Wilkinson & Hensel, 1991; Hoy—F.L. Sutherland & A.D. Robertson, unpublished data; Southern Highlands—O'Reilly & Zhang, 1995). Mixed mica-amphibole-enriched mantle sources for zircon and corundum crystallising melts, indeed, were proposed under Scottish basalt fields (Upton *et al.*, 1999).

Trace element ratios ($\text{Cr}_2\text{O}_3/\text{Ga}_2\text{O}_3$ vs $\text{Fe}_2\text{O}_3/\text{TiO}_2$) for Tumbarumba corundum suites (Fig. 3) can be compared with those from several eastern Australian basaltic fields (Sutherland & Schwarz, 2001). The magmatic Tumbarumba corundums occupy the usual BGY corundum envelope for many suites, although one variant lacks the typical strong Fe^{2+} – Fe^{3+} charge transfer colour absorption. The trapiche-like corundums range into higher $\text{Cr}_2\text{O}_3/\text{Ga}_2\text{O}_3$, but limited data on these “exsolution” corundums elsewhere restrict detailed comparisons. Metamorphic Tumbarumba corundums only show minor overlap with the Barrington

(higher $\text{Fe}_2\text{O}_3/\text{TiO}_2$) and Wellington (higher $\text{Cr}_2\text{O}_3/\text{Ga}_2\text{O}_3$) metamorphic envelopes. The high-Fe Tumbarumba ruby falls within and the low-Fe ruby just outside the Barrington envelope. The Wellington pink corundums are geochemically distinct and may derive from corundum-fassaite-garnet granulite assemblages, found as xenoliths in Jurassic breccia pipes (Sutherland & Schwarz, 2001).

Tumbarumba zircons display a moderate spread in crystal characteristics and fission track ages (27–16 Ma) compared to some other fields (e.g., New England, 81–6 Ma; Sutherland *et al.*, 1993). The unusual {100}–{110} prism combination probably reflects high incompatible element contents in highly evolved alkaline melts. Similar crystal forms in Boat Harbour, Tasmania, zircons (Hollis & Sutherland, 1995; Sutherland, 1996) differ in containing quartz inclusions, while corundum is a rare associate. The zircon-bearing Boat Harbour basalt sequence includes evolved alkaline lavas (Sutherland *et al.*, 1996), so that zircon crystallisation within crustal magma chambers remains a feasible process there. Tumbarumba basalts, however, lack extended fractionation, which favours zircon crystallisation from deep, low-volume, mantle-derived salic melts.

Many eastern Australian gemfields, including Tumbarumba, occupy granite-intruded basement rocks (e.g., Grabben Gullen, Oberon, Barrington, New England, NSW; Hoy, Lava Plains, Queensland; Victoria; NE Tasmania). This may just reflect abundant granite generation within the foldbelts, but could signal some genetic connection. A link between the gemfields and hydrous metasomatised mantle sources may involve slab subduction processes prior to granite emplacement as volcanic arc slivers are known along the Gilmore Suture (Scheibner & Basden, 1996). Metasomatised slabs would favour low-volume salic melt generation during initial basaltic thermal input. Ionov & Hofmann (1995) presented a model where vein titanian amphibole (and mica), enriched in Nb and Ta, develop in mantle peridotite above a subduction zone at depths of 50–90 km. Such metasomatic veinings would have different ages, depending on particular subduction/granite emplacement regimes within eastern Australia (Scheibner & Basden, 1996). This fits Sr isotopic studies of eastern Australian basalt fields, which suggest episodic, heterogeneous amphibole (+ mica + apatite) introductions within mantle source regions (O'Reilly & Griffin, 1984, 2000). The amphibole/mica-poor MORB source for the 400 Ma Ruby Creek micro-dolerite suggests amphibole metasomatism either post-dated or lay at deeper mantle levels at that time.

This Tumbarumba gemfield study shows:

- 1 Australian gem corundum suites not only extend to well-defined bimodal magmatic and metamorphic suites (Barrington), but also include polymodal suites of magmatic, magmatic “exsolution”, magmatic-metasomatic and metamorphic origins.
- 2 Australian magmatic BGY corundum and related zircon typically develop from minor salic melts associated with amphibole-enriched mantle below the host basaltic fields.
- 3 Some Cr-enriched metasomatic and metamorphic corundum suites may reflect interactions of basaltic melting events with local Cr-bearing serpentinite belts.

ACKNOWLEDGMENTS. Fieldwork and sampling in the Tumbarumba-Kiandra area was assisted by A. Spate and D. Costello, Tumut Office, NSW National Parks & Wildlife, who arranged collecting permits; by G. Martin, Tumbarumba, who provided information and access to his property and west Tumbarumba drilling program, as well as considerable hospitality; by R. Condon, Holdsworth, who supplied underground water drilling logs and core samples from west Tumbarumba; by J. Law, Tumbarumba Creek Caravan Park, who introduced local prospectors; by S.A. “Bluey” Miller, Adelong Road, for permission to sample on his land and for making his local gem collection available for inspection; by Dr H. Corbella, sabbatical visitor, University of Sydney, who assisted in the January–February 1997 trip; by M. Auybi who assisted in the April 1997 trip; by R. Abell, AGSO, Canberra, who aided the April work by providing radiometric maps and advice on basalt sites related to the Yarrangobilly 1:100 000 mapping projects. Dr L.M. Barron, G. Oakes and S.R. Lishmund provided field and analytical data from NSW Mineral Resources sources.

Further gem materials for the study came from P.J. Brown, Albion Park, who was instrumental in arranging purchase of a large parcel of sapphires collected by the family over 10 years and from K.G. McQueen, Cooperative Research Centre for Landscape Evolution and Mineral Exploration, University of Canberra, and P.W. Millsteed, Canberra, ACT.

Analytical aspects of the study were aided by Prof. W.B. Stern, University of Basel in his joint trace-element analytical gem program with D. Schwarz, Gübelin Gem Lab, Lucerne, Switzerland; by M. Garland, Geology Dept., University of Toronto, Canada who undertook laser Raman spectroscopy on sapphire inclusions; by C. Knockolds, Electron Microscope Unit, University of Sydney, who facilitated electron microprobe studies; and by K.J. Henley, AMDEL, Adelaide, who supervised basalt analyses. B.J. Barron, organised EMP analyses of garnet grains at CSIRO, Sydney.

Geochronology was organised through P.D. Kinny and M.C. Fanning (U-Pb isotope work), SHRIMP facility, Australian National University, ACT, through P. Green (zircon fission track), Geotrack International, Melbourne, and through B. Webb, AMDEL, and H. Zwingmann, CSIRO Petroleum, Sydney (K-Ar dating).

Preparation of the samples, script and diagrams was assisted by S. Folwell, R. Springthorpe, D. Colchester and S. Lindsey, Australian Museum; by R. Hungerford and L. Callan, Environmental Sciences, University of Technology, Sydney and K. Maynard, Sydney. The Australian Museum Trust provided funds for the project. K.G. McQueen read the script, while P.W. Carr, Geology Department, University of Wollongong, NSW and I.C. Roach, Department of Geology, Australian National University, Canberra, ACT provided valuable comments during reviews.

References

Ablay, G.J., M.R. Carroll, M.R. Palmer, J. Marti & S.J. Sparks, 1998. Basanite-phonolite lineages of the Teide-Pico Viejo volcanic complex, Teneriffe, Canary Islands. *Journal of Petrology* 39: 905–936.

Allen, T.C., 1999. Petrogenesis of the Jurassic Igneous Rocks of Southeastern Australia. *PhD thesis*, University of Sydney (unpubl.).

Andrews, E.C., 1901. Report on the Kiandra Lead. *New South Wales Geological Survey—Mineral Resources* 10, pp. 32.

Barron, L.M., 1987. Summary of petrology and chemistry of rocks from the Sapphire Project. *Geological Survey of New South Wales Department of Mineral Resources—Petrological Report* 87/9 (unpublished).

Beccaluva, L., F. Siena, M. Coltorti, A. Di Grande, A. Lo Giudice, G. Macciotta, R. Tassinari & C. Vaccaro, 1998. Nephelinitic to tholeiitic magma generation in a transitional tectonic setting: an integrated model for the Iblean volcanism, Sicily. *Journal of Petrology* 39: 1547–1576.

Benisek, A., & F. Finger, 1993. Factors controlling the development of prism faces in granite zircons: a microprobe study. *Contributions to Mineralogy and Petrology* 114: 441–451.

Birch, W.D., & D.A. Henry, 1997. *Gem Minerals of Victoria*. Special Publication No. 4 of the Mineralogical Society of Victoria, pp. 120. Melbourne: Royal Society of Victoria.

Bishop, P., R.W. Young & I. McDougall, 1985. Stream profile change and longterm landscape evolution: Early Miocene and modern rivers of the east Australian highland crest, central New South Wales, Australia. *Journal of Geology* 93: 455–474.

Brown, M.C., 2000. Cenozoic tectonics and landform evolution of the coast and adjacent highlands of southeast New South Wales. *Australian Journal of Earth Sciences* 47: 245–357.

Chazot, G., M.A. Menzies & B. Harte, 1996. Silicate glasses in spinel lherzolites from Yemen: origin and chemical composition. *Chemical Geology* 134: 159–179.

Chen, Y.D., S.Y. O'Reilly, W.L. Griffin & T.E. Krogh, 1998. Combined U-Pb dating and Sm-Nd studies on lower crustal and mantle xenoliths from the Delegate basaltic pipes, southeastern Australia. *Contributions to Mineralogy and Petrology* 30: 154–161.

Clarke, W.B., 1860. *Researches in the Southern Goldfields of New South Wales*, 2nd edn, vii, pp. 305. Sydney: Reading and Wellbank.

Coenraads, R.R., 1990a. Key areas for alluvial diamond and sapphire exploration in the New England gem fields, New South Wales, Australia. *Economic Geology* 85: 1186–1207.

Coenraads, R.R., 1990b. Palaeogeography of the Braemar deep-lead sapphire deposit, New South Wales. *Journal and Proceedings of the Royal Society of New South Wales* 123: 75–84.

Coenraads, R.R., 1992. Sapphires and rubies associated with volcanic provinces: inclusions and surface features shed light on their origin. *Australian Gemmologist* 18: 70–78.

Coenraads, R.R., 1994. Evaluation of potential sapphire source rocks within the catchments of Kings Plains Creek and Swan Brook, near Inverell, New South Wales. *Records of the Australian Museum* 46: 5–24.

Coenraads, R.R., F.L. Sutherland & P.D. Kinny, 1990. The origin of sapphires: U-Pb dating of zircon inclusions shed new light. *Mineralogical Magazine* 54: 1113–1122.

Coldham, T., 1985. Sapphires from Australia. *Gems & Gemology* 21(3): 130–146.

Coltorti, M., C. Bonadiman, R.W. Hinton, F. Siena & B.G.J. Upton, 1999. Carbonate metasomatism of the oceanic upper mantle: evidence from clinopyroxenes and glasses in ultramafic xenoliths of Grande Comore, Indian Ocean. *Journal of Petrology* 40: 133–165.

Comin-Chiaromonti, P., A. Cundari, E.M. Piccirillo, C.B. Gomes, F. Castorina, P. Censi, A. De Min, A. Marzoli, S. Speziale & V.F. Velazquez, 1997. Potassic and sodic igneous rocks from eastern Paraguay: their origin from the lithospheric mantle and genetic relationships with the associated Parana flood tholeiites. *Journal of Petrology* 38: 495–528.

Compston, W., I.S. Williams, J.L. Kirschvink, Z. Zhang & M.A. Guogu, 1992. Zircon ages for the Early Cambrian time-scale. *Journal of the Geological Society of London* 149: 171–184.

Curran, J.M., 1897. On the occurrence of Precious Stones in New South Wales and the Deposits in which they are found. *Journal and Proceedings of the Royal Society of New South Wales* 30: 214–285.

Dana, E.S., 1932. *A Textbook of Mineralogy*, 4th ed, pp. 851. Boston: F.H. Gilson Co.

Degeling, P.R., 1982. *Wagga Wagga 1:250 000 Metallogenic Map SI 55-15 (plus parts of SI 55-14, SJ 55-2, SJ 55-3) Mine Data Sheets and Metallogenic Study*. Pp. 451. Sydney: Geological Survey of New South Wales.

Draper, D.S., & T.H. Green, 1997. P-T phase relations of silicic, alkaline, aluminous mantle-xenolith glasses under anhydrous and C-O-H fluid-saturated conditions. *Journal of Petrology* 38: 1187–1221.

Duncan, R.A., & I. McDougall, 1989. Volcanic Time-Space Relationships. In: *Intraplate Volcanism in Eastern Australia and New Zealand*, ed. R.W. Johnson, pp. 43–54. Cambridge: Cambridge University Press.

Eggins, S.M., R.L. Rudnick & W.F. McDonough, 1998. The composition of peridotites and their minerals: a laser-ablation ICP-MS study. *Earth and Planetary Science Letters* 154: 53–71.

Ewart, A., & B.W. Chappell, 1989. Trace element geochemistry. In: *Intraplate Volcanism in Eastern Australia and New Zealand*, ed. R.W. Johnson, pp. 219–235. Cambridge: Cambridge University Press.

Galbraith, R.F., 1981. On statistical modes for fission track counts. *Mathematical Geology* 13: 471–488.

Galbraith, R.F., 1988. Graphical display of estimates having differing standard errors. *Technometrics* 30: 271–281.

Galbraith, R.F., & P.F. Green, 1990. Estimating the Component Ages in a Finite Mixture. *Nuclear Tracks Radiation Measurement* 17: 197–206.

Gill, E.D., & K.R. Sharp, 1957. The Tertiary rocks of the Snowy Mountains, eastern Australia. *Journal of the Geological Society of Australia* 4: 21–40.

Gleadow, A.J.W., A.J. Hurford & R.D. Quaife, 1976. Fission track dating of zircon: improved etching techniques. *Earth and Planetary Science Letters* 33: 169–187.

Graham, I.T., 2000. The Genesis and Tectonic Significance of Chromitite-bearing Serpentinites in Southern New South Wales, *PhD Thesis*, University of Technology, Sydney (unpubl.) 2 vols.

Graham, I.T., B.J. Franklin, B. Marshall & G. Caparelli, 1998. U/Pb and Nb/Sr geochronology of ophiolitic rocks from the Tumut serpentinite province, southern NSW. *Geological Society of Australia Abstracts Series* 49: 175.

Graham, I.T., B.J. Franklin, B. Marshall, E.C. Leitch & M. Fanning, 1996. Tectonic significance of 400 Ma zircon ages for ophiolitic rocks from the Lachlan Fold Belt, eastern Australia. *Geology* 24(12): 1111–1114.

Green, P.F., 1981. A new look at statistics in fission track dating. *Nuclear Tracks* 76: 148–150.

Green, P.F., 1985. A comparison of zeta calibration baselines in zircon, sphene and apatite. *Chemical Geology (Isotope Geoscience Section)* 58: 1–22.

Guo, J.F., S.Y. O'Reilly & W.L. Griffin, 1996a. Corundum from basaltic terrains: a mineral inclusion approach to the enigma. *Contributions to Mineralogy and Petrology* 122: 368–386.

Guo, J.F., S.Y. O'Reilly & W.L. Griffin, 1996b. Zircon inclusions in corundum megacrysts: I. Trace element geochemistry and clues to the origin of corundum megacrysts in alkali basalts. *Geochimica et Cosmochimica Acta* 60: 2347–2363.

Heaman, L.M., R. Bowins & J. Crocket, 1990. The chemical composition of igneous zircon suites: implications for geochemical tracer studies. *Geochimica et Cosmochimica Acta* 54: 1597–1607.

Hinton, R.W., & B.G.J. Upton, 1991. The chemistry of zircon: Variation within and between large crystals from syenite and alkali basalt xenoliths. *Geochimica et Cosmochimica Acta* 55: 3287–3302.

Hoang, N., & M. Flower, 1998. Petrogenesis of Cenozoic basalts from Vietnam: implication for origins of a “diffuse igneous province”. *Journal of Petrology* 39: 369–395.

Hollis, J.D., & F.L. Sutherland, 1985. Occurrences and origins of gem zircons in eastern Australia. *Records of the Australian Museum* 36: 299–311.

Hughes, R.W., 1997. Ruby & sapphire. Pp. 511. Boulder, Colorado: RWH Publishing.

Hurford, A.J., & P.F. Green, 1983. The Zeta age calibrations of fission-track dating. *Isotopic Geoscience* 1: 285–317.

Ionov, D.A., & A.W. Hofmann, 1995. Nb-Ta-rich mantle amphiboles and micas: implications for subduction related metasomatic trace element fractionations. *Earth and Planetary Science Letters* 131: 341–356.

Ionov, D.M., W.L. Griffin & S.Y. O'Reilly, 1997. Volatile-bearing minerals and lithophile trace elements in the upper mantle. *Chemical Geology* 141: 153–184.

Johnson, R.W. & M.B. Duggan, 1989. Rock classification and analytical databases. In: *Intraplate Volcanism in Eastern Australia and New Zealand*, ed. R.W. Johnson, pp. 12–13. Cambridge: Cambridge University Press.

Knutson, J., & M.C. Brown, 1989. Monaro, Snowy Mountains and South Coast. In: *Intraplate Volcanism in Eastern Australia and New Zealand*, ed. R.W. Johnson, pp. 130–131. Cambridge: Cambridge University Press.

Kohn, B.P., A.J.W. Gleadow & S.J.D. Cox, 1999. Denudation history of the Snowy Mountains: constraints from apatite fission track thermochronology. *Australian Journal of Earth Sciences* 46: 181–198.

Kostopoulos, D.K., & K.D. James, 1992. Parameterisation of the melting regime of the shallow upper mantle and the effects of variable lithospheric stretching on mantle model stratification and trace element concentrations in magmas. *Journal of Petrology* 27: 745–750.

Krosch, N.J., & W. Cooper, 1991a. Queensland sapphire. *Australian Gemmologist* 17(11): 460–464.

Krosch, N.J., & W. Cooper, 1991b. Queensland sapphire II. *Australian Gemmologist* 17(12): 511–515.

Kushiro, I., 1990. Partial melting of mantle wedge and evolution of island arc crust. *Journal of Geophysical Research* 95(B10): 15929–15939.

Lafeber, D., 1956. Columnar jointing and intracolumnar differentiation in basaltic rocks. *Verhandelingen. Koninklijke Nederlandse Geologisch Mijnbouwkundig Genootschap* 16: 241–245.

Lanyon, R., R. Varne & A.J. Crawford, 1993. Tasmanian Tertiary basalts, the Balleny plume, and opening of the Tasman Sea. *Geology* 21: 555–558.

Le Maitre, R.W., ed., 1989. *A Classification of IGNEOUS ROCKS and Glossary of Terms*, pp. 193 pp. Oxford: Blackwell, Scientific Publications.

Linthout, K., 1984. Alkali-zirconosilicates in peralkaline rocks. *Contributions to Mineralogy and Petrology* 86: 155–158.

Liversidge, A., 1888. *The Minerals of New South Wales, etc.*, pp. 326. London: Trübner & Co.

Lundstrom, C.C., 2000. Rapid diffusive infiltration of sodium into partially molten peridotite. *Nature* 403: 527–530.

Mackenzie, D.E., & A.J.R. White, 1970. Phonolite globules in basanite from Kiandra, Australia. *Lithos* 3: 309–317.

MacNevin, A.A., & G.G. Holmes, 1980. Gemstones. *New South Wales Geological Survey, Mineral Industry of New South Wales* 18, 119 pp.

Malíková, P., 1999. Origin of sapphires from the Jizerská Louka alluvial deposit in North Bohemia, Czech Republic, Europe. *Australian Gemmologist* 20(5): 202–206.

Matson, S.M., & G.R. Rossman, 1988. Fe^{2+} - Ti^{4+} charge transfer in stoichiometric Fe^{2+} , Ti^{4+} minerals. *Physics and Chemistry of Minerals* 16: 76–82.

McDonough, W.F., & F.A. Frey, 1987. Rare earth elements in upper mantle rocks. In: *Geochemistry and Mineralogy of the Rare Earth Elements, Reviews in Mineralogy*, ed. B.R. Lipin & G.A. McKay, vol 21, chapt 5, pp. 99–145. Washington DC: Mineralogical Society of America.

McKenzie, D., & R.K. O'Nions, 1991. Partial melt distributions from inversion of rare earth element concentrations. *Journal of Petrology* 32: 1021–1091.

Morris, P.A., 1986. Constraints on the origin of the mafic alkaline volcanics and included xenoliths from Oberon, New South Wales, Australia. *Contributions to Mineralogy and Petrology* 93: 207–214.

Mumme, I.A., 1988. *The World of Sapphires—Their Occurrence, Discrimination, Synthesis and Valuation*, pp. 189. Sydney: Mumme Publications.

Neumann, E.-R., & E. Wulff-Pedersen, 1997. The origin of highly silicic glass in mantle xenoliths from the Canary Islands. *Journal of Petrology* 39: 1413–1539.

Neville, B.J., & F. von Gnielinski, 1998. Australiens sapphire largestatten. In: *Rubin, Saphir, Korund*, pp. 70–75, Extra Lapis No. 15. München: Christian Weise Verlag.

Neville, B.J., & F. von Gnielinski, 1999. Gemstones. Sapphire and ruby in Australia. *Queensland Government Mining Journal* 100 (1171): 6–12.

Nielsen, R., 1998, 12 August. Geochemical earth reference model: trace element partitioning information. Internet address: <http://www-ep.es.llnl.gov/germ/partitioning.html>.

Oakes, G.M., L.M. Barron & S.R. Lishmund, 1996. Alkali basalt and associated volcaniclastic rocks as a source of sapphire in eastern Australia. *Australian Journal of Earth Sciences* 43: 289–298.

O'Connor, T.K., A.D. Edgar & F.E. Lloyd, 1996. Origin of glass in Quaternary Mantle Xenoliths from Meerfeldermaar, West Eifel, Germany: implications for enrichment in the lithospheric mantle. *The Canadian Mineralogist* 34: 187–200.

Oliver, J.G., & I.J. Townsend, 1993. *Gemstones in Australia*, pp. 72. Canberra: Australian Government Publishing Service.

O'Reilly, S.Y., 1989. Xenolith types distribution and transport. In: *Intraplate Volcanism in Eastern Australia and New Zealand*, ed. R.W. Johnson, pp. 249–253. Cambridge: Cambridge University Press.

O'Reilly, S.Y., & W.L. Griffin, 1984. Sr isotopic heterogeneity in primitive basaltic rocks, south-eastern Australia: correlation with mantle metasomatism. *Contributions to Mineralogy and Petrology* 87: 220–230.

O'Reilly, S.Y., & W.L. Griffin, 1988. Mantle metasomatism beneath western Victoria, Australia: I. Metasomatic processes in Cr-diopside Iherzolites. *Geochimica et Cosmochimica Acta* 52: 433–447.

O'Reilly, S.Y., & W.L. Griffin, 2000. Apatite in the mantle: implications for metasomatic processes and high heat production in Phanerozoic mantle. *Lithos* 43: 217–232.

O'Reilly, S.Y., W.L. Griffin & O. Gaul, 1997. Palaeogeothermal gradients in Australia. Key to 4-D lithosphere mapping, AGSO *Journal of Australian Geology and Geophysics* 17: 63–72.

O'Reilly, S.Y., W.L. Griffin & A. Stabel, 1988. Evolution of eastern Australian lithosphere: Isotopic evidence for magmatic and tectonic underplating. In: *Oceanic and continental Lithosphere: Similarities and differences*, ed. M.A. Menzies & K.G. Cox, pp. 89–108. Oxford: Journal of Petrology Special Volume, Oxford University Press.

O'Reilly, S.Y., & M. Zhang, 1995. Geochemical characteristics of lava-field basalts from eastern Australia and inferred sources: connections with the subcontinental lithospheric mantle? *Contributions to Mineralogy and Petrology* 121: 148–170.

Panter, K.S., P.R. Kyle & J.L. Smellie, 1997. Petrogenesis of a phonolite-trachyte succession at Mount Sidley, Marie Byrd Land, Antarctica. *Journal of Petrology* 38: 1225–1253.

Pecover, S.R., 1993. The geology and mining of the Strathdarr sapphire deposit, New England gemfields, northeastern New South Wales. In: *New England Orogen, eastern Australia*, ed. P.G. Flood & J. Aitchison, pp. 83–491. Armidale: Department of Geology and Geophysics, University of New England.

Pecover, S.R., 1996. Sapphire-producing Cretaceous/Tertiary volcano-fluvial deposits in eastern Australia. In: *Mesozoic 96. Mesozoic Geology of the Eastern Australia Plate Conference. Geological Society of Australia Extended Abstracts* 43: 442–449.

Pupin, J.P., 1980. Zircon and granite petrology. *Contributions to Mineralogy and Petrology* 73: 207–220.

Pupin, J.P., & G. Turco, 1974. Contrôle thermique du développement de la muscovite dans les granitoides et morphologie du zircon. *Compte Rendue de l'Academie des Sciences, Paris* 278 (D): 2719–2722.

Roach, I.C., 1999. The setting, structural control, geochemistry and mantle source of the Monaro Volcanic Province, southeastern New South Wales, Australia, *PhD thesis*, University of Canberra (unpubl.).

Robertson, A.D.C., & F.L. Sutherland, 1992. Possible origins and ages for sapphires and diamond from the central Queensland gemfields. In: *R.O. Chalmers Commemorative papers (Mineralogy, Meteoritics, Geology)*, ed. F.L. Sutherland, pp. 45–54. *Records of the Australian Museum, Supplement 15*.

Roeder, P.L., & R.F. Emslie, 1970. Olivine-liquid equilibrium. *Contributions to Mineralogy and Petrology* 29: 275–289.

Scarborough, J.H., & K.G. Cox, 1995. Basalts generated by decompressive adiabatic melting of a mantle plume: a case study from the Isle of Skye, NW Scotland. *Journal of Petrology* 36: 3–22.

Scheibner, E., & H. Basden, eds., 1996. Geology of New South Wales—Synthesis. Volume 1. Structural Framework. *Geological Survey of New South Wales, Memoir Geology* 13(1), pp. 295.

Schiano, P., & R. Clocchiatti, 1994. World wide occurrence of silica-rich melts in sub-continental and sub-oceanic mantle minerals. *Nature* 368: 621–624.

Schiano, P., R. Clocchiatti, B. Bourdon, K.W. Burton & B. Thellier, 2000. The composition of melt inclusions in minerals at the garnet-spinel transition zone. *Earth and Planetary Science Letters* 174: 375–383.

Schmetzler, K., H.A. Hänni, H.-J. Bernhardt & D. Schwarz, 1996. Trapiche rubies. *Gems & Gemology* 32 (winter issue): 242–250.

Schwarz, D., & W.B. Stern, 2000. Chemical fingerprinting as a tool for the characterization of gem corundums from different genetic environments. *Abstracts Volume [CD ROM], 31st International Geological Congress* 16–17 August, Rio de Janeiro, Brazil.

Schwarz, D., J. Kanis & K. Schmetzler, 2000. Sapphires from Ambondromifehy region, Antsiranana Province, northern Madagascar. *Gems & Gemology* 36(fall issue): 216–233.

Schwarz, D., E.J. Petsch & J. Kanis, 1996. Sapphires from the Andranondambo region, Madagascar. *Gems & Gemology* 32 (summer issue): 80–99.

Shaw D. M., 1970. Trace element fractionation during anatexis. *Geochimica et Cosmochimica Acta* 34: 237–243.

Simons, F.J., A. Zielhuis & R.D. van der Hilst, 1999. The deep structure of the Australian continent from surface wave tomography. *Lithos* 48: 17–43.

Speer, J.A., 1982. Zircon. In: *Reviews in Mineralogy*, vol. 5, Orthosilicates, chapt. 3, ed. P.H. Ribbe, pp. 67–112. Washington DC: Mineralogical Society of America.

Spry, M.J., D.L. Gibson & R.A. Eggleton, 1999. Tertiary evolution of the coastal lowlands and the Clyde River palaeovalley in southeast New South Wales. *Australian Journal of Earth Sciences* 46: 173–180.

Stephenson, P.J., 1989. Northern Queensland. In: *Intraplate Volcanism in Eastern Australia and New Zealand*, ed. R.W. Johnson, pp. 89–97. Cambridge: Cambridge University Press.

Stephenson, P.J., 1990. The geological context of sapphire occurrences in the Anakie region, central Queensland. *Geological Society of Australia Abstracts Series* 25: 232–233.

Stern, W.B., 1984. Zur simultan analyse von silicaten (Hauptkomponenten, Spuren) mittels energie-dispersiver Röntgenfluoreszenz-spektrometrie (EDS-XFA). *Fresenius Zeitschrift fuer Analytische Chemie* 2560: 1–9.

Stuart-Smith, P.G., 1990. The structure and tectonics of the Tumut region, N.S.W.: data record and summary of investigations 1986–1989. *Bureau of Mineral Resources, Australia, Record 1990/78*, pp. 41 (unpublished).

Sun, S.-S. & W.F. McDonough, 1989. Chemical and isotopic systematics of oceanic basalts; implications for mantle composition and processes. In: *Magmatism in the Ocean Basins*, ed. A.D. Saunders & M.J. Norry. *Geological Society of London Special Publication* 4(2): 313–346.

Sunagawa, I., H.-J. Bernhardt & K. Schmetzler, 1999. Texture formation and element partitioning in trapiche ruby. *Journal of Crystal Growth* 206: 322–330.

Sutherland, F.L., 1996. Alkaline rocks and gemstones, Australia: a review and synthesis. *Australian Journal of Earth Sciences* 43: 323–343.

Sutherland, F.L., 1998. Origin of north Queensland Cenozoic volcanism: Relationships to long lava flow basaltic fields, Australia. *Journal of Geophysical Research* 103(B11): 27347–27358.

Sutherland, F.L., 1999. Volcanism, geotherms, gemstones and lithosphere, since orogenesis, N.E. New South Wales: A Synthesis. In: *New England Orogen; Regional Geology, Tectonics and Metallogenesis*, ed. P.G. Flood, pp. 355–364. Armidale, NSW: Earth Sciences, University of New England.

Sutherland, F.L., & R.R. Coenraads, 1996. An unusual ruby-sapphire-spinel assemblage from the Tertiary Barrington volcanic province, New South Wales. *Mineralogical Magazine* 60: 623–638.

Sutherland, F.L., & C.M. Fanning, 2001. Gem-bearing basaltic volcanism, Barrington, New South Wales: Cenozoic evolution, based on basalt K-Ar ages and zircon fission track and U-Pb isotope dating. *Australian Journal of Earth Sciences* 48: 221–237.

Sutherland, F.L., & D. Schwarz, 2001. Origin of gem corundums from basaltic fields. *Australian Gemmologist* 21(1): 30–33.

Sutherland, F.L., A. Ewart, L.R. Raynor, J.D. Hollis & W.D. McDonough, 1989. Tertiary basalt magmas and the Tasmanian lithosphere. In: *Geology and Mineral Resources of Tasmania*, ed. C.F. Burritt & E.L. Martin. *Geological Society of Australia Special Publication* 15: 386–398.

Sutherland, F.L., D.F. Hendry, B.J. Barron, W.L. Matthews & J.D. Hollis, 1996. An unusual Tasmanian Tertiary basalt sequence, near Boat Harbour, Northwest Tasmania. *Records of the Australian Museum* 48: 131–161.

Sutherland, F.L., P.W.O. Hoskin, C.M. Fanning & R.R. Coenraads, 1998a. Models of corundum origin from alkali basaltic terrains: a reappraisal. *Contributions to Mineralogy and Petrology* 133: 356–372.

Sutherland, F.L., R.E. Pogson & B.J. Barron, 1998b. Discussion and Reply. Palaeogeothermal gradients in Australia: key to 4-D lithosphere mapping, S.Y. O'Reilly, W.L. Griffin & O. Gaul. *Australian Journal of Earth Sciences* 45: 817–821.

Sutherland, F.L., R.E. Pogson & J.D. Hollis, 1993. Growth of the central New England basaltic gemfields, New South Wales, based on zircon fission track dating. In *New England Orogen, Eastern Australia*, ed. P.G. Flood & J. Aitchison, pp. 483–491. Armidale, NSW: Department of Geology and Geophysics, University of New England.

Sutherland, F.L., D. Schwarz, R.R. Coenraads, G. Webb & T. Coldham, 1999. Origin of chromium-coloured gem corundums, Australia. In: *Abstracts. 17th International Gemmological Conference, Goa, India—1999*, pp. 37–39. Bombay: Forum of Indian Gemmologists for Scientific Studies.

Sutherland, F.L., D. Schwarz, E.A. Jobbins, R.R. Coenraads & G. Webb, 1998c. Distinctive gem corundum suites from discrete basalt fields: a comparative study of Barrington, Australia, and West Pailin, Cambodia, gemfields. *Journal of Gemmology* 26: 65–85.

Sweeny, B., 1996. Interesting gems from north-east Tasmania. *Australian Gemmologist* 19: 264–267.

Tera, F., & G.F. Wasserburg, 1972. U-Th-Pb systematics in lunar rocks. *Earth and Planetary Science Letters* 14: 281–304.

Upton, B.G.J., R.W. Hinton, P. Aspen, A. Finch & J.W. Valley, 1999. Megacryst and associated xenoliths: Evidence for migration of geochemically enriched melts in the upper mantle beneath Scotland. *Journal of Petrology* 40: 935–956.

Vallance, T.G., 1953. Studies in the metamorphic and plutonic geology of the Wantabadgery-Adelong-Tumbarumba district, N.S.W. Part I. Introduction and metamorphism of the sedimentary rocks. *Linnean Society of New South Wales—Proceedings* 78(3–4): 90–121.

Vallance, T.G., 1954a. Studies in the metamorphic and plutonic geology of the Wantabadgery-Adelong-Tumbarumba district, N.S.W. Part II. Intermediate basic rocks. *Linnean Society of New South Wales—Proceedings* 78(5–6): 181–196.

Vallance, T.G., 1954b. Studies in the metamorphic and plutonic geology of the Wantabadgery-Adelong-Tumbarumba district, N.S.W. Part III. The granitic rocks. *Linnean Society of New South Wales—Proceedings* 78(5–6): 197–220.

Vavra, G., 1990. On the kinematics of zircon growth and its petrological significance: a cathodoluminescence study. *Contributions to Mineralogy and Petrology* 106: 90–99.

Vavra, G., 1994. Systematics of internal zircon morphology in major Variscan granitoid types. *Contributions to Mineralogy and Petrology* 117: 31–344.

Wass, S.Y., 1980. Geochemistry and origin of xenolith-bearing and related alkali basaltic rocks from the Southern Highlands, New South Wales. *American Journal of Science* 280(A): 639–666.

Watson, E.B., 1979. Zircon saturation in felsic liquids: Experimental results and applications to trace element geochemistry. *Contributions to Mineralogy and Petrology* 70: 407–419.

Wellman, P., & I. McDougall, 1974. Potassium-argon ages of the Cainozoic volcanic rocks of New South Wales, Australia. *Journal of the Geological Society of Australia* 21: 247–272.

White, A.J.R., & B.W. Chappell, 1989. *Geology of the Numbat 1:100,000 Sheet (8624)*. Sydney: Geological Survey of New South Wales, Department of Minerals and Energy.

Wiechert, U., D.A. Ionov & K.H. Wedepohl, 1997. Spinel peridotite xenoliths from the Afsagin-Dush volcano, Darigana lava plateau, Mongolia: a record of partial melting and cryptic metasomatism in the upper mantle. *Contributions to Mineralogy and Petrology* 126: 345–364.

Wilkinson, J.F.G., & H.D. Hensel, 1991. An analcime mugearite-megacryst association from north eastern New South Wales: implications for high-pressure amphibole dominated fractionation of alkaline magmas. *Contributions to Mineralogy and Petrology* 127: 272–290.

Wilkinson, J.F.G., & R.W. Le Maitre, 1987. Upper mantle amphiboles and micas and TiO_2 , K_2O and P_2O_5 abundances and $100Mg/(Mg+Fe^{2+})$ ratios of common basalts and andesites: Implications for modal mantle metasomatism and undepleted mantle compositions. *Journal of Petrology* 28: 37–73.

Willis, J.L., 1972. Mining History of the Tumbarumba Gold Field. *Geological Survey of New South Wales Bulletin* 23, pp. 633 and 4 maps.

Wilshire, H.G., & A.V. McGuire, 1996. Magmatic infiltration and melting in the lower crust and upper mantle beneath the Cima volcanic field, California. *Contributions to Mineralogy and Petrology* 123: 358–374.

Worden, J.M., H. Baadsgaard, D.N. Cracknell & D. Krstic, 1996. Major extensional events recorded by zircon xenocrysts from the central Queensland gemfields. In *Mesozoic 96. Mesozoic Geology of the Eastern Australia Plate Conference. Geological Society of Australia Extended Abstracts* 43: 569–573.

Yaxley, G.M., D.H. Green & V. Kamenetsky, 1998. Carbonatite metasomatism in south eastern Australian lithosphere. *Journal of Petrology* 39: 1917–1930.

Yaxley, G.M., & V. Kamenetsky, 1999. In situ origin for glass in mantle xenoliths from south eastern Australia: insights from trace element compositions of glasses and metasomatic phases. *Earth and Planetary Science Letters* 172: 97–109.

Young, R.W., & M.C. Brown, 2000. Cenozoic tectonics and landform evolution of the coast and adjacent highlands of southeast New South Wales. Discussion [authored by Young]. Reply [authored by Brown]. *Australian Journal of Earth Sciences* 47: 823–826.

Young, R., & I. McDougall, 1993. Long-term landscape evolution: Early Miocene and modern rivers in southern New South Wales, Australia. *Journal of Petrology* 101: 35–49.

Zhang, M., P.J. Stephenson, S.Y. O'Reilly, M.T. McCulloch & M. Norman, 2001. Petrogenesis and geodynamic implications of late Cenozoic basalts in North Queensland, Australia: trace element and Sr-Nd-Pb isotope evidence. *Journal of Petrology* 42: 685–719.

Zhang, M., & S.Y. O'Reilly, 1997. Multiple sources for basaltic rocks from Dubbo, eastern Australia: geochemical evidence for plume-lithosphere mantle interaction. *Chemical Geology* 136: 33–54.

Zielhuis, A., & R.D. van der Hilst, 1996. Upper mantle shear velocity beneath eastern Australia from inversion of wave forms from SKIPPY portable arrays. *Geophysical Journal International* 127: 1–16.

Zou, H., A. Zindler, X. Xu & Q. Qi, 2000. Major, trace element, and Nd, Sr and Pb isotope studies of Cenozoic basalts in SE China: mantle sources, regional variations, and tectonic significance. *Chemical Geology* 171: 33–47.

Manuscript received 6 November 2000, revised 12 March 2001 and accepted 13 March 2001.

Associate Editor: G.E. Edgecombe.

The Dunbogan L6 Chondrite: A New Meteorite Fall from New South Wales, Australia

P.G. FLOOD¹, P.M. ASHLEY¹ AND R.E. POGSON²

¹ Earth Sciences, University of New England, Armidale NSW 2351, Australia

pflood@metz.une.edu.au

pashley@metz.une.edu.au

² Mineralogy and Petrology Section, Australian Museum, Sydney NSW 2010, Australia

rossp@austmus.gov.au

ABSTRACT. A meteorite crashed through the roof and ceiling of a house at Dunbogan on the north coast of New South Wales, Australia, on 14 December 1999, and 30 g of fragments were recovered. The fall was observed by a girl at Tinonee, 50 km to the SSW. The meteor was observed in the mid northern sky at about 22h00 East Australian DST (GMT + 11 hrs), moving in a SSE direction. In mid-flight the meteor broke into at least 3 fragments. Detailed mineralogical and petrological examination of the meteorite have revealed that it is comparable to an L6 ordinary chondrite with mean olivine composition Fa_{25} and pyroxene Fs_{21} .

FLOOD, P.G., P.M. ASHLEY & R.E. POGSON, 2002. The Dunbogan L6 Chondrite: a new meteorite fall from New South Wales, Australia. *Records of the Australian Museum* 54(2): 249–254.

At 22h05 East Australian DST (GMT + 11 hrs) on Tuesday, 14 December 1999, an object crashed at Dunbogan (c. 152°50'E, 31°40'S), leaving a 30 × 50 cm hole in the roofing tiles and timber-clad ceiling, coming to rest on the living-room floor of the home of Mr Paul Hancox (Fig. 1). The object, with calculated volume of 9 cm³ and weighing a minimum of about 30 grams, broke into several fragments on impact with the roof. The Australian Museum and the University of New England were each provided with one small fragment for study. The aerial fragmentation and later impact were not observed by the same person. No other persons reported rumbles or explosions. No other fragments have been located on the house roof or nearby. The name *Dunbogan* has been approved by the Meteorite Nomenclature Committee of the Meteoritical Society (Grossman & Zipfel, 2001).

Recoveries from observed meteorite falls are not common, and this is only the fourteenth such recovery from

Australia. Meteorite falls which cause structural damage to buildings are even more significant, because their rarity generates considerable scientific and popular interest. For these reasons it is important to document the meteorite involved.

The Fall

An eyewitness account by Elyse Smith, a girl residing at Tinonee, 50 km south of the impact site, reported observing a bright object “like a huge flamby ball crossing in a direction from the middle northern sky. After a few seconds it broke into one large fragment and two middle-sized bits with a lot of rubble fragments flying off”. It was observed falling over a period of several seconds. There were no other reports of sound effects or light trails, except when it hit the house. This account suggests that more fragments of the meteorite may have fallen to Earth than were recovered.

The Meteorite

The fragment provided to researchers at the University of New England was approximately 7 mm in diameter and about 2 mm thick. The specimen was catalogued as R77552 in the University of New England Earth Sciences Rock Collection and has since been transferred to the Australian Museum petrology collection and catalogued as a polished block mount DR16659. Another specimen, approximately 8 mm in diameter, 5 mm thick and 0.48 g in weight, loaned to the Australian Museum by Mr Hancox for specific gravity measurement, has been returned. A group of fragments totalling approximately 5 g, registered as DR16713 has been presented to the Australian Museum by Mr Hancox to satisfy requirements of the International Meteoritical Society.

A freshly-broken surface of the meteorite is pale grey-brown with scattered opaque grains and veinlets, but appears much darker in polished section. The UNE specimen is a dark brown colour in polished section, displaying a 1 mm thick, black glassy fusion crust on one side and dispersed metallic blobs throughout a brecciated groundmass (see Petrography and Chemistry). Individual pyroxene and olivine crystals which constitute the bulk of the grains rarely exceed 0.4 mm in diameter. The metallic blobs are up to 0.5 mm in diameter. The SG of the fragment examined by the Australian Museum was 3.48 ± 0.03 . Scanning Electron Microscopic examination of the UNE specimen clearly displayed the brecciated nature of the sample and the black glassy rim overlying an earlier melting surface which now displays quench textures.

Petrography and Mineral Chemistry

A polished block (approximately 30 mm² surface area) was prepared from the fragment mounted in resin. Petrographic observations of the main textural characteristics of the fragment in reflected light showed that it is probably chondritic. Abundant aggregates are irregular, angular to sub-rounded in outline and up to 2.5 mm across, in places with through-going fractures. No well-defined chondrules are apparent, but many apparent breccia clasts are sub-rounded (Fig. 2) and may represent variably recrystallised and broken chondrules. Certain clasts contain variably recrystallised chondrule material (e.g., relicts of "barred olivine"). The breccia is typically clast-supported and the amount of matrix interstitial to the clasts does not exceed 20 vol. % (Fig. 2). In general, clasts are composed of inequigranular aggregates of interlocking silicate grains (typically up to 0.8 mm across), with a few grains of a spinel phase, rare grains of a phosphate phase, and heterogeneously distributed metal and sulphide masses, commonly in composites. In-between the fragments, and locally forming apparent injection masses up to 0.2 mm wide into clasts, is a fine grained matrix, commonly showing a fine "emulsion" texture. The matrix appears to be composed of a mixture of finely comminuted silicate material, possible glass and tiny "droplets" of metal \pm sulphide (Fig. 3). This looks like eutectic melting in the heat affected zone of the meteorite. The amount of "emulsion-textured" material in the sample is 10 vol. %.

On one side of the meteorite fragment, there are relicts of a possible former glassy margin (fusion crust) (Figs. 4, 5). Adjacent to crystalline clast material, there is an inner zone up to 0.2 mm thick of quench-textured former glass which appears to grade into microbreccia matrix. This has

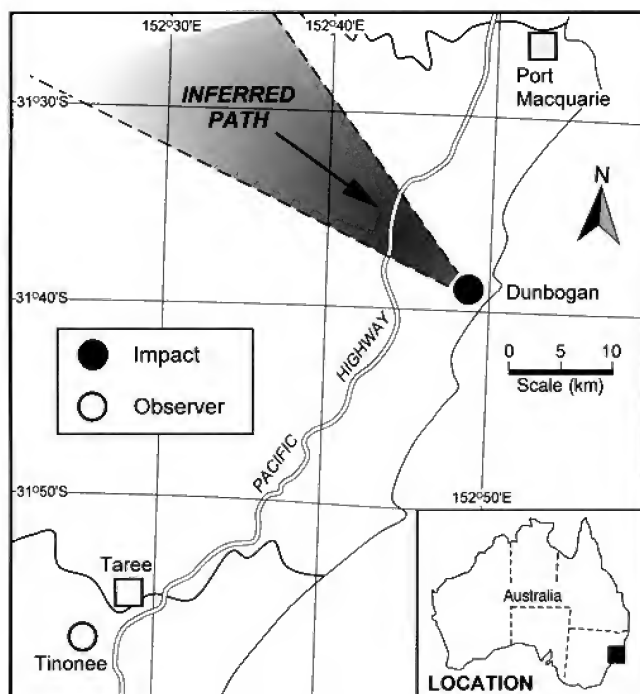


Figure 1. Estimated flight path of the fireball which resulted in the Dunbogan meteorite.

been subsequently bordered by an apparently homogeneous but vesicular glassy phase up to 0.1 mm thick. Similar fusion crust components were described by Genge & Grady (1999).

Examination under reflected light and using back-scattered electron (BSE) and secondary electron imagery (SEI) showed that the approximate mineral mode of the meteorite fragment was as follows: olivine and pyroxene each 40 vol. %, plagioclase 10 vol. %, sulphide phase 5 vol. %, metal phase(s) 3 vol. %, chromite and glass each about 1 vol. % and a tiny trace of a phosphate phase. These minerals were subsequently subjected to electron probe micro-analyses, with several grains of each phase being analysed and results listed in Table 1. Olivine and pyroxene are clear to pale brownish in colour from their internal reflections and have relatively constant compositions. Olivine averages Fa_{25} (with minor Mn, and locally detectable trace amounts of Al, Cr, Ni and Ca). The pyroxene is a Ca-poor type with an average composition of Fs_{21} (containing minor Ca and Mn, and trace amounts of Ti, Al, Cr, Ni and Na). Plagioclase appears to be largely interstitial to olivine and orthopyroxene (Figs. 5, 6) and has a rather consistent composition ranging between $\text{An}_{10-11}\text{Ab}_{84-85}\text{Or}_{4-5}$. The chromite forms individual anhedral grains up to 0.2 mm across, as well as local aggregates up to 0.3 mm across, in places attached to metal grains (Fig. 6). Chromite also occurs as scattered small inclusions in olivine and orthopyroxene; in the latter it may form oriented exsolution blebs. Compositionally, the spinel is a rather Fe-rich chromite, with minor Al, Ti, Mg, Mn, Zn and Ni (Table 1). Assuming stoichiometry, it has an approximate composition of $(\text{Fe}^{2+})_{0.89}\text{Mg}_{0.12}\text{Mn}_{0.02}\text{Zn}_{0.01})(\text{Cr}_{1.64}\text{Al}_{0.20}\text{Fe}^{3+}_{0.07}\text{Ti}_{0.05})\text{O}_4$.

The sulphide phase is slightly more abundant than the metal phase, and although the two are commonly closely associated, they can occur discretely. Both are found as isolated anhedral grains up to 0.5 mm across interstitial to silicates, as inclusions in silicates, as a fracture-filling component, and as a fine emulsion-like phase in the matrix

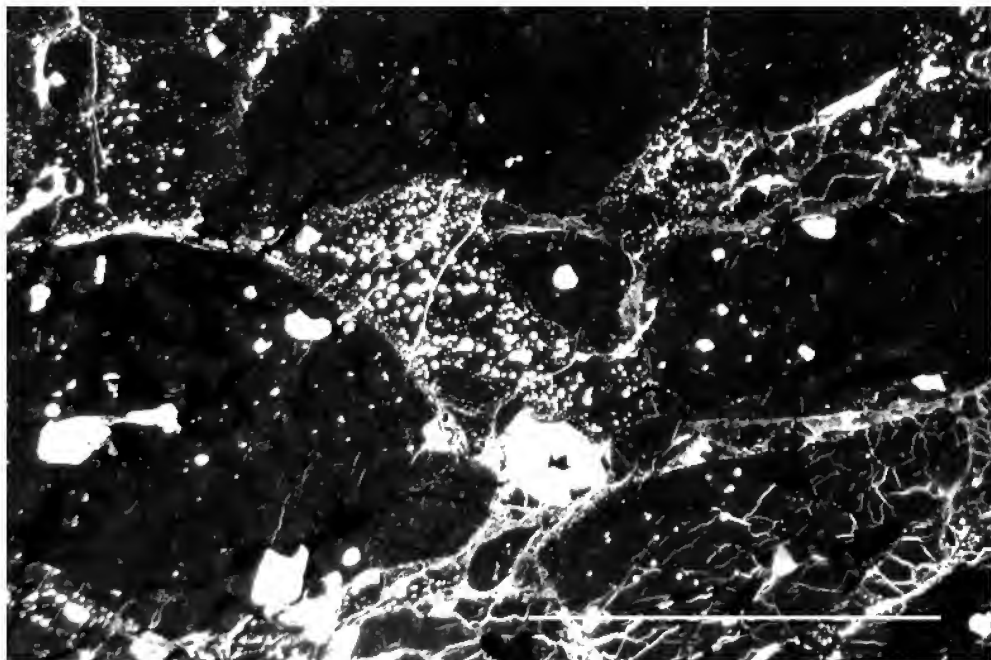


Figure 2. Photomicrograph showing chondrule texture (dark silicates, white sulphide and metal phases) and interstitial fine grained matrix with ‘‘emulsion’’ texture of metal/sulphide globules in silicate groundmass (?shock-melt vein). Note that the possible chondrules are locally strongly fractured. Scale bar 1 mm., plane polarised reflected light, oil immersion.

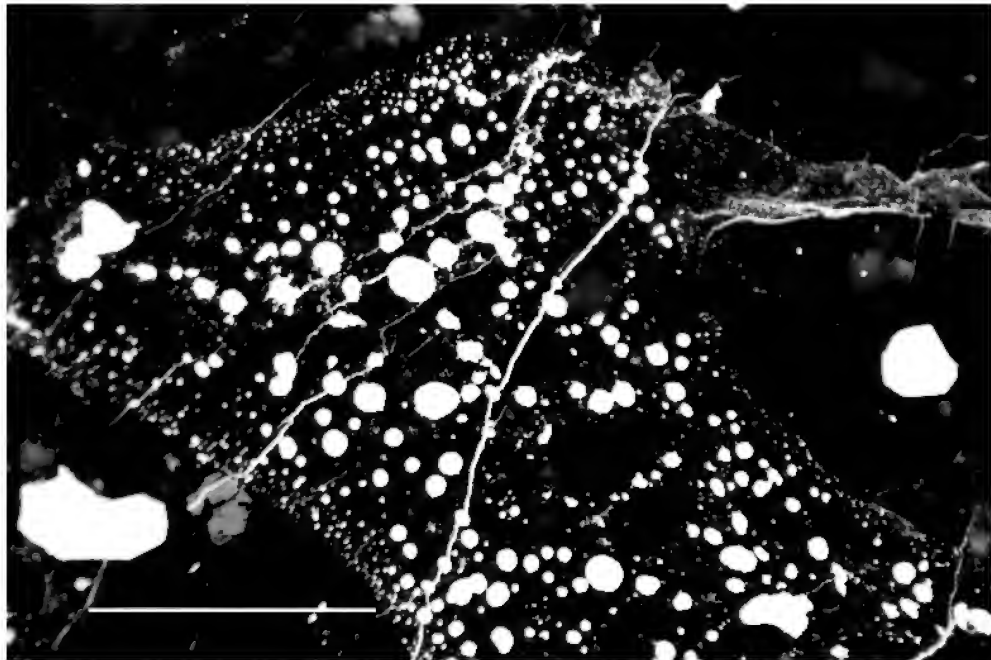


Figure 3. Photomicrograph showing enlarged detail from Fig. 2. Matrix interstitial to possible chondrule fragments contains abundant small white metal/sulphide droplets in a dark silicate groundmass, forming ‘‘emulsion’’ texture. Scale bar 0.25 mm. Plane polarised reflected light, oil immersion.

between the breccia clasts (Figs. 2, 3). Many composite masses of sulphide and metal phases show finely developed eutectoid textures (Fig. 7) indicative of having crystallised from a melt. Compositionally, the sulphide is a non-stoichiometric FeS-like phase, resembling pyrrhotite. It is strongly anisotropic under crossed polars and may contain minor to trace amounts of Ni, Co and Cu (Table 1). Under high-power examination and using X-ray mapping on the electron microprobe, it was observed that the metal phase is heterogeneous, with two constituents of slightly varying reflectivity and varying Fe and Ni contents. There is a range

from Fe-rich to a phase approaching Fe_3Ni . Minor Co is present, with its content being highest in the most Fe-rich phase (Table 1). The metallic material, consists of both kamacite and taenite. Rare anhedral grains of a phosphate phase up to 0.05 mm across, enclosed in silicates, were noted during BSE scanning. A single analysis of this phase (Table 1) demonstrated that it was a Ca-rich orthophosphate, with minor Fe and Mg. No F or Cl was detected and the stoichiometry was inconsistent for apatite; the phase is merrillite (cf. Dowty, 1977) and has a composition similar to that reported by Bevan *et al.* (1988) and Cooney *et al.* (1999).

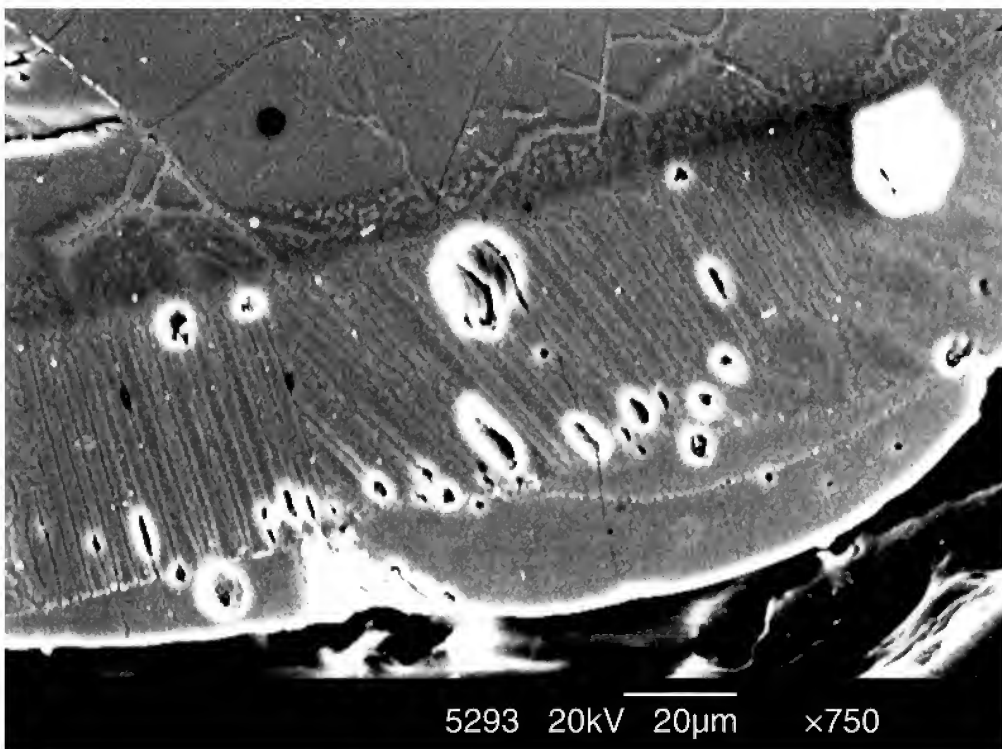


Figure 4. Secondary electron image of fusion crust of meteorite (lower right-hand area of Fig. 5) showing crystalline silicate material at top, bordered by a zone of crystallised glass (now containing bladed crystallites) plus one grain of metal phase (white), and with a thin rim of homogeneous glass at bottom of image. Scale bar 20 μ m.

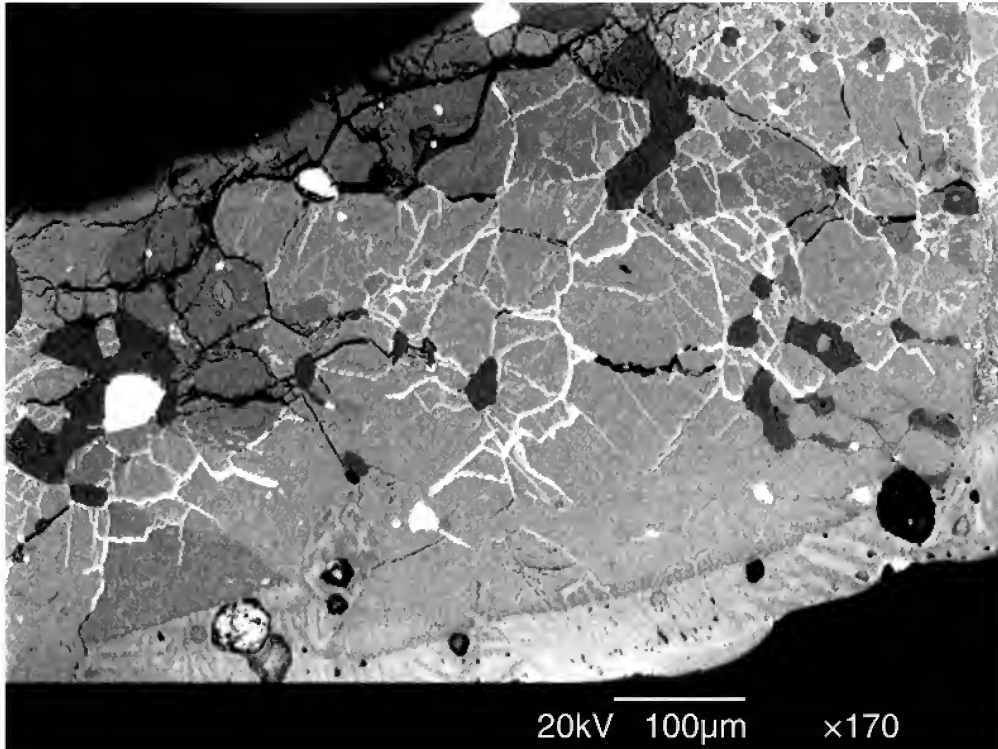


Figure 5. Back-scattered electron image of portion of the meteorite showing a granular crystalline aggregate of olivine (medium grey), pyroxene (slightly darker grey), plagioclase (black) and metal phase (white). There is a compound rim (fusion crust) of crystallised glass, partly bordered by a thin zone of homogeneous glass towards the bottom of the image. Note how the metal phase has invaded along silicate grain boundaries. Scale bar 100 μ m.

In the quench-textured zone (fusion crust) rimming part of the meteorite fragment, two bladed phases are evident on SEI scans (Fig. 4). Analyses of these phases indicated

that they do not conform to stoichiometric minerals perhaps because of electron beam overlap onto adjacent phases. One phase is olivine-like, but contains higher Si, Al, Cr, Ca and

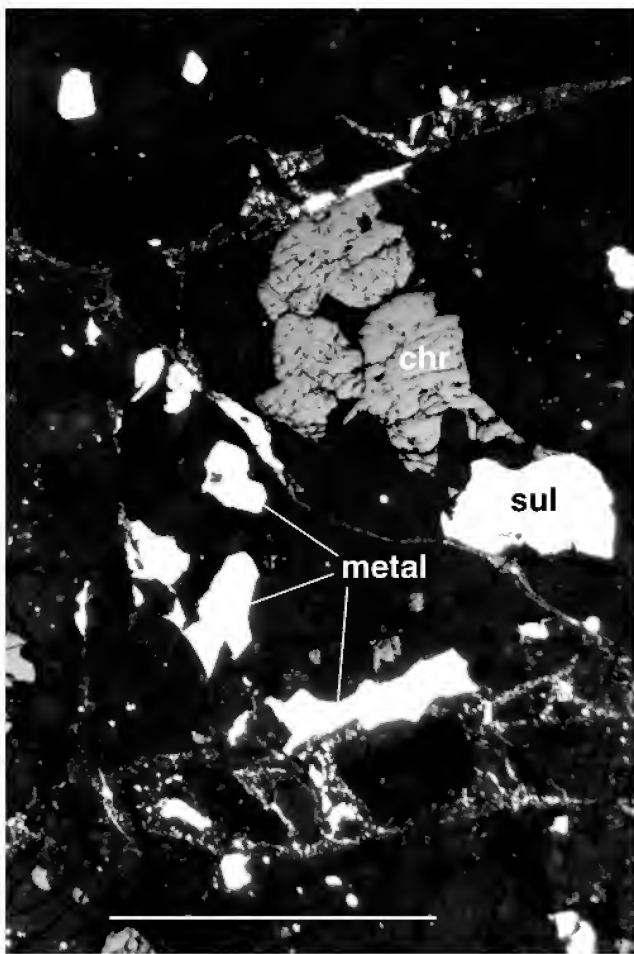


Figure 6. Portion of chondrule showing intergrowth of olivine and pyroxene (dark grey), with plagioclase (black), chromite (chr), troilite (sul) and metal phase. Scale bar 1 mm. Plane polarised reflected light, oil immersion.

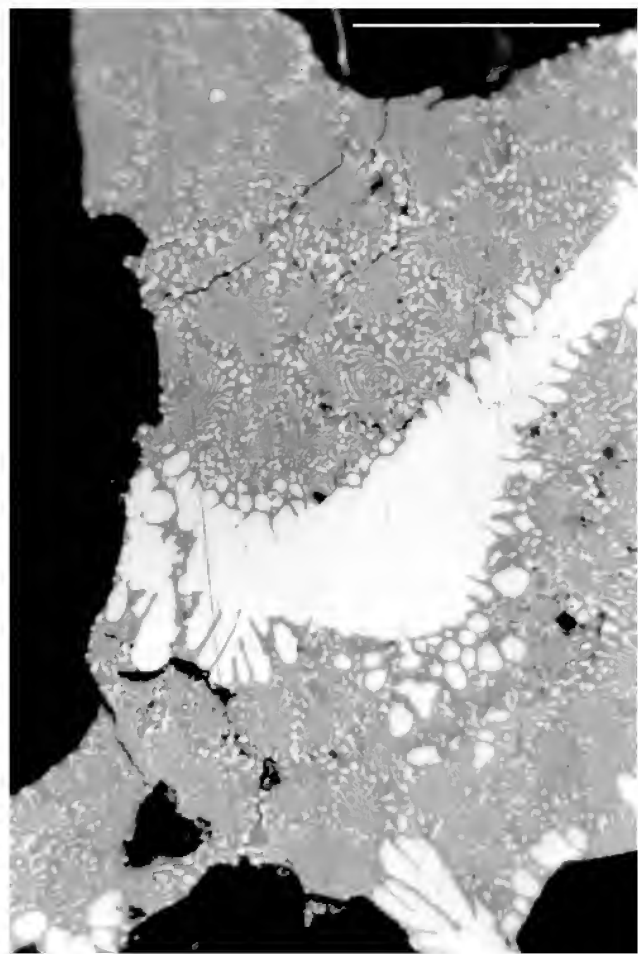


Figure 7. Detail of composite sulphide-metal grain showing eutectoid textures (indicative of crystallisation from a melt) between metal phase (white) and troilite (grey). Scale bar 0.1 mm. Plane polarised reflected light, oil immersion.

lower Fe and Mg than analysed olivines. The other phase is more heterogeneous and may contain the components of olivine, orthopyroxene, plagioclase and sulphide. Analyses of the thin rim of apparently homogeneous glass could give an indication of the bulk composition of the meteorite. However, it is clear that the amount of Fe, Ni and S in this glass is insufficient to balance what is obviously present in the bulk of the meteorite. It is possible that when melting during atmospheric passage formed the fusion crust, the sulphide-metal phase became mobile and infiltrated into fractures and along grain boundaries in adjacent crystalline material (e.g., Fig. 5).

Discussion

Classification of the meteorite. From the observed textures in the meteorite, the sample represents a chondritic type, based on the preservation of chondrule outlines (e.g., Fig. 2). However, the chondrules have been strongly recrystallised, as well as being subject to fracturing and brecciation. The presence of planar fractures in olivine and interconnected melt veins suggest an S4 shock stage (moderately shocked) of Stöffler *et al.* (1991). The compositions of

olivine (average Fa_{25}) and Ca-poor pyroxene (average Fs_{21}) are consistent with the meteorite belonging to the L-group of ordinary chondrites of Van Schmus & Wood (1967) and Dodd (1981). Forty EDS analyses of olivine grains showed a narrow variation within $\pm \text{Fa}_{1.8}$ of the mean for 90% of the analyses, indicating an equilibrated chondrite. Sodic plagioclase is common in equilibrated ordinary chondrites of moderate to extensive recrystallisation, especially for petrologic type 6 (Nakamura & Motomura, 1999). The Wo content of Ca-poor pyroxene is a key quantitative parameter for distinguishing petrologic types, and determined values (Wo 1.5–1.6), indicate an L6 classification (Scott *et al.*, 1986).

The recrystallised textural characteristics, the olivine and pyroxene compositions, presence of sodic plagioclase and metal phases including Fe-rich and significantly Ni-rich types, are most consistent with the meteorite being of petrologic type 6 (Van Schmus & Wood, 1967). The L6 group is the most common type of chondritic meteorite seen to fall and the Dunboghan sample displays strong textural and mineralogical similarities to other L6 examples (e.g., Bevan *et al.*, 1992). Up to 1992, 55 L6 chondrites from Australia had been documented, representing 19.9% of known Australian meteorites and four out of 13 observed falls (Bevan, 1992).

Table 1. Mineral chemistry of phases in the Dunbogian L6 chondrite. Analyses by P. Garlick and P. Ashley, University of New England, using a JEOL JSM5800LV SEM/Oxford Link Isis EDS, at 20kV and 34 nA, with a 100 second count time; *n.d.* = not detected; *In chromite, Fe_2O_3 and FeO are calculated assuming stoichiometry. In other analyses total Fe is expressed as ΣFeO .

	Olivine mean n=4 (range)	Pyroxene mean n=4 (range)	Plagioclase mean n=3 (range)	Chromite mean n=3 (range)
SiO_2	38.0 (37.8–38.3)	54.7 (54.4–55.0)	66.8 (66.2–67.3)	<i>n.d.</i>
TiO_2	<i>n.d.</i>	0.12 (0.11–0.12)	<i>n.d.</i>	1.80 (1.08–2.46)
Al_2O_3	0.06 (0.03–0.12)	0.12 (0.08–0.15)	20.1 (19.9–20.3)	4.70 (3.64–6.47)
Cr_2O_3	0.03 (0.03–0.07)	0.19 (0.13–0.24)	<i>n.d.</i>	57.7 (56.0–58.8)
Fe_2O_3^*				2.53 (0.61–4.25)
FeO^*				29.7 (28.4–31.4)
ΣFeO	22.7 (22.2–23.2)	13.8 (13.4–13.7)	0.42 (0.30–0.53)	
MnO	0.44 (0.40–0.47)	0.60 (0.57–0.65)	<i>n.d.</i>	0.76 (0.64–0.87)
MgO	38.6 (38.3–38.7)	29.3 (28.9–29.5)	0.25 (0.24–0.28)	2.24 (1.77–2.60)
NiO	0.04 (0.03–0.15)	0.08 (0.03–0.16)	<i>n.d.</i>	0.12 (0.03–0.31)
ZnO	<i>n.d.</i>	<i>n.d.</i>	<i>n.d.</i>	0.50 (0.34–0.59)
CaO	0.05 (0.03–0.09)	0.78 (0.71–0.90)	2.07 (2.03–2.14)	<i>n.d.</i>
Na_2O	<i>n.d.</i>	0.16 (0.16)	9.41 (8.83–10.2)	<i>n.d.</i>
K_2O	<i>n.d.</i>	<i>n.d.</i>	0.79 (0.70–0.94)	<i>n.d.</i>
BaO	<i>n.d.</i>	<i>n.d.</i>	0.06 (0.05–0.13)	<i>n.d.</i>
total	99.9	99.8	99.8	100.0
	$\text{Fa}_{25.1}$ (24.5–25.6)	$\text{Fs}_{20.9}$ (20.2–21.2)	$\text{An}_{10.6}\text{Ab}_{84.9}\text{Or}_{4.5}$	
	metal range n=4	sulphide range n=2	phosphate	
Fe	72.3–93.4	59.6–60.5	FeO	1.01
Co	0.21–1.63	0.06–0.07	MgO	3.15
Ni	4.32–25.9	0.03–2.24	CaO	49.0
Mn	0.03–0.03	<i>n.d.</i>	P_2O_5	46.8
Cu	0.03–0.17	0.03–0.11	Total	99.9
Cr	0.03–0.05	<i>n.d.</i>		
S	0.05–0.12	37.9–39.8		

ACKNOWLEDGMENTS. A special thanks to Mr Paul Hancox of Dunbogian for supplying the specimen for study and for depositing reference specimens in the Australian Museum collection. Miss Elyse Smith of Tinonee provided details about the meteorite fall. Mr Peter Garlick of the Electron Microscope Facility at the University of New England is thanked for his assistance with the sample analysis. Mr David Keith prepared the polished section of the meteorite. Sue Lindsay of the Australian Museum Electron Microscopy Unit assisted with preliminary SEM and EDS studies. The authors thank Dr Ray Binns and an anonymous reviewer for valuable comments and suggestions for improving the manuscript.

References

Bevan, A.W.R., 1992. Australian meteorites. *Records of the Australian Museum, Supplement* 15: 1–27.

Bevan, A.W.R., B. Griffin, R.E. Pogson & F.L. Sutherland, 1992. Tabbita: an L6c chondrite from New South Wales, Australia. *Meteoritics* 27(1): 97–98.

Bevan, A.W.R., K.J. McNamara & J.C. Barton, 1988. The Binningup H5 chondrite: a new fall from Western Australia. *Meteoritics* 23: 29–33.

Cooney, T.F., E.R.D. Scott, A.N. Krot, S.K. Sharma & A. Yamaguchi, 1999. Vibrational spectroscopic study of minerals in the Martian meteorite ALH84001. *American Mineralogist* 84: 1569–1576.

Dodd, R.T., 1981. *Meteorites, A Petrologic-chemical Synthesis*. Cambridge University Press, pp. 368.

Dowty, E., 1977. Phosphate in Angra de Reis: structure and composition of the $\text{Ca}_3(\text{PO}_4)_2$ minerals. *Earth and Planetary Science Letters* 35: 347–351.

Genge, M.J., & M.M. Grady, 1999. The fusion crusts of stony meteorites: implications for the atmospheric reprocessing of extraterrestrial materials. *Meteoritics & Planetary Science* 34(3): 341–356.

Grossman, J., & J. Zipfel, 2001. *The Meteoritical Bulletin* (85), p. 4. Meteoritical Society.

Nakamura, Y., & Y. Motomura, 1999. Sodic plagioclase thermometry of type 6 ordinary chondrites: implications for the thermal histories of parent bodies. *Meteoritics & Planetary Science* 34(5): 763–771.

Scott, E.R.D., G.J.F. Taylor & K. Keil, 1986. Accretion, metamorphism and brecciation of ordinary chondrites: evidence from petrologic studies of meteorites from Roosevelt County, New Mexico. Proceedings of the Seventeenth Lunar and Planetary Science Conference, November 1986, Part 1, *Journal of Geophysical Research* 91(813): E115–E123.

Stoffler, D., K. Keil & E.R.D. Scott, 1991. Shock metamorphism of ordinary chondrites. *Geochimica et Cosmochimica Acta* 55: 3845–3867.

Van Schmus, W.R., & D.A. Wood, 1967. A chemical-petrologic classification for the chondritic meteorites. *Geochimica et Cosmochimica Acta* 31: 747–765.

Manuscript received 6 July 2000, revised 26 June 2001 and accepted 29 June 2001.

Associate Editor: F.L. Sutherland.

Errata

http://www.amonline.net.au/pdf/publications/1307_complete.pdf
http://www.amonline.net.au/pdf/publications/1314_complete.pdf

In two papers published during 2000 in *Records of the Australian Museum* (52: 1–40, 52: 187–222) reference was made to a work co-authored by Blakemore and Kingston and published in 1997 in *Journal of Natural History* (31: 1683–1708). Blakemore and Kingston (1997) described the genus *Nexogaster* and the five new Tasmanian earthworm species *Hickmaniella gogi*, *Anisochaeta simpsonorum*, *Nexogaster sexies*, *N. pilus*, and *Megascolides maestus*. The correct citation for the source publication and the correct authority for *M. maestus* is “Blakemore & Kingston, 1997”—this should replace “Blakemore, 1997c” on p. 2 and “Blakemore, 1997a” on pp. 197, 198, 213 and 216 of volume 52 of the *Records of the Australian Museum*.

INSTRUCTIONS TO AUTHORS

Manuscripts must be submitted to the Editor. Authors will then liaise with a nominated Associate Editor until a work is accepted, rejected or withdrawn. All manuscripts are refereed externally.

Only those manuscripts that meet the following requirements will be considered for publication.

Submit three hard copies and one electronic file. Attach a **cover sheet** showing: the title; the name, address and contact details of each author; the author responsible for checking proofs; a suggested running head of less than 40 character-spaces; the number of figures, tables and appendices; and total word count. Manuscripts must be complete when submitted.

Electronic copy is stripped and reconstructed during production, so authors should avoid excessive layout or textual embellishments; a single font should be used throughout (Times or Times New Roman are preferred). **Tables** and **figures** should be numbered and referred to in numerical order in the text.

All copy is manipulated within a Windows (not Mac) environment using Microsoft and Adobe software. Electronic submissions should be entirely readable using the latest version of Microsoft Word. Avoid using uncommon fonts. The submitted manuscript should be printed from the most recent version of electronic copy.

A manuscript should be prepared using recent issues as a guide. There should be a **title** (series titles should not be used), **author(s)** with their institutional and e-mail addresses, an **abstract** (should be intelligible by itself, informative not indicative), **introduction** (should open with a few lines for general, non-specialist readers), **materials and methods**, **results** (usually subdivided with primary, secondary and sometimes tertiary-level headings), **discussion**, **acknowledgments** and **references**. If appropriate, an appendix may be added after references. An index may be called for if a paper is very large (>55,000 words) and contains many indexable elements.

In the **titles** of zoological works the higher classification of the group dealt with should be indicated. Except for common **abbreviations**, definitions should be given in the materials and methods section. Sentences should not begin with abbreviations or numerals. Metric units must be used except when citing original specimen data. It is desirable to include **geo-spatial coordinates**; when reference is made to them, authors must ensure that their format precludes ambiguity, in particular, avoid formats that confuse arcminutes and arcseconds. If known, authors should indicate how geo-spatial coordinates are derived, for example, from GPS, map, gazetteer, sextant, or label.

Label and specimen data should, as a minimum requirement, indicate where specimens are deposited. Original specimen data—especially that of type material—is preferred over interpreted data. If open to interpretation, cite original data between quotation marks or use “[sic]”.

Rules of the most recent edition of the International Code of Zoological Nomenclature must be followed; authors must put a very strong case if Recommendations are not followed. Authorities, including date, should be given when a specific name is first mentioned except where **nomenclature** follows an accepted standard (in which case that standard should then be cited). When new taxa are introduced in works having **multiple authors**, the identity of the author(s) responsible for the new name(s) and for satisfying the criteria of availability, should be made clear in accordance with recommendations in Chapter XI of the Code (1999). In the view of the Editorial Committee, a scientific name with more than two authors is unwieldy and should be avoided. **Keys** are desirable; they must be dichotomous and not serially indented. **Synonyms** should be of the short form: taxon author, year, pages and figures. A period and dash must separate taxon and author except in the case of reference to the original description. Proposed type material should be explicitly designated and, unless institutional procedure prohibits it, registered by number in an institutional collection.

Authors should retain **original artwork** until it is called for. Previously published illustrations will generally not be accepted. Artwork may be submitted either as hard copy or as **digital images**. The author, figure number and orientation must be clearly marked on each piece of artwork. Extra costs resulting from **colour** production are charged to the author. All artwork must (a) be rectangular or square and scalable to a width of 83 mm (one text column) or 172 mm (both text columns) and any depth up to 229 mm (the number of lines in a caption limits depth); (b) have **lettering** similar to 14 point upper case normal Helvetica in final print; and (c) have **scale bars**, the lengths of which should be given in the caption.

Hard copy submissions must meet the following requirements: (a) they must be no larger than A4; (b) the dimension of artwork should not be less than the desired final size; (c) **halftones** and **line-drawings** must be mounted separately; (d) lettering, scales and edges—especially of halftone artwork—must be sharp and straight; (e) photographic **negatives** can be used in production, but *positive* images are, of course, required by referees.

Halftone, colour or black and white line images may be submitted electronically once a work has been accepted for publication; all such images must be presented in a file format, such as TIFF, suitable for *Adobe Photoshop* version 5.0 or later. Halftone and colour images must be at a minimum **resolution** of 300 dpi (not higher than 400 dpi) at final size and all labelling must be sharp. Black and white line images must be at a minimum resolution of 1200 dpi at final size.

When reference is made to **figures** in the present work use Fig. or Figs., when in another work use fig. or figs.; the same rule applies to tables. Figures should be numbered and referred to in numerical order in the text.

Authors should refer to recent issues of the *Records of the Australian Museum* to determine the correct format for listing **references** and to *The Chicago Manual of Style* to resolve other matters of style.

Certain **anthropological manuscripts** (both text and images) may deal with culturally sensitive material. Responsibility rests with authors to ensure that approvals from the appropriate person or persons have been obtained prior to submission of the manuscript.

Stratigraphic practice should follow the *International Stratigraphic Guide* (second edition) and *Field Geologist's Guide to Lithostratigraphic Nomenclature in Australia*.

The Editor and Publisher reserve the right to modify manuscripts to improve communication between author and reader. Authors may make essential corrections only to final **proofs**. No corrections can be accepted less than six weeks prior to publication without cost to the author(s). All proofs should be returned as soon as possible. There are no page **charges**. Authors of a paper in the *Records* receive a total of 50 free **offprints**. Authors of a *Supplement* or *Technical Report* receive a total of 25 free offprints. Additional offprints may be ordered at cost.

All authors must agree to publication and certify that the research described has adhered to the Australian Museum's *Guidelines for Research Practice* (www.amonline.net.au/about/research_ethics.htm)—or those of their home institution providing they cover the same issues, especially with respect to authorship and acknowledgment. Agreement can be registered by signing and returning the Editor's letter that confirms our receipt of a submitted manuscript. While under consideration, a manuscript may not be submitted elsewhere.

More information and examples are available at our website: www.amonline.net.au/publications/

CONTENTS

The Amaryllididae of Australia (Crustacea: Amphipoda: Lysianassoidea)	129
..... J.K. LOWRY & H.E. STODDART	
The Tumbarumba Basaltic Gem Field, New South Wales: in relation to sapphire-ruby deposits of eastern Australia	
..... F.L. SUTHERLAND, I.T. GRAHAM, R.E. POGSON, D. SCHWARZ, G.B. WEBB, R.R. COENRAADS, C.M. FANNING, J.D. HOLLIS & T.C. ALLEN	215
The Dunboggan L6 Chondrite: a new meteorite fall from New South Wales, Australia	
..... P.G. FLOOD, P.M. ASHLEY & R.E. POGSON	249
Errata	255

